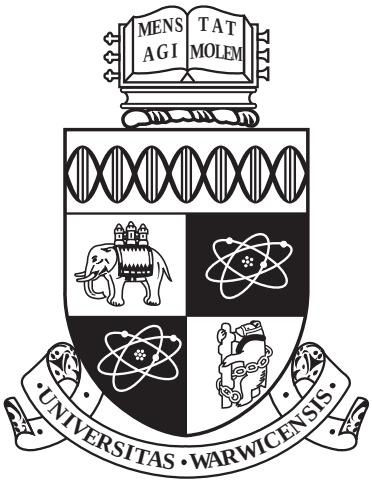

The kinematics, dynamics and statistics of three-wave interactions in models of geophysical flow

by

Jamie Harris

Thesis

Submitted to the University of Warwick

for the degree of

Doctor of Philosophy in Mathematics and Complexity Science

Complexity Science Doctoral Training Centre

January 2013

THE UNIVERSITY OF
WARWICK

Contents

Acknowledgments

I am indebted to all the assistance, guidance and personal council provided by my two supervisors, Miguel Bustamante and Colm Connaughton. Without doubt, this thesis would never have been finished without their assistance. I would like to extend my thanks to EPSRC for the funding they provide, and to each and every member of the Complexity Science DTC.

Declarations

Most of the work as it appears in Chapter 4 can be found in the reference [Harris et al., 2012a]. While the majority of the mathematical content in the publication was derived by the lead author, credit must be given to Miguel Bustamante for the derivation of the novel one-dimensional particle interpretation given towards the end of the chapter. Material that formed the basis of this chapter was then edited collaboratively for publication.

Chapter 5 appears as it does in its original state, with all of the mathematical content and numerical analysis derived by the author. A reduced version of the first half of this chapter, as edited by the collaborating authors, can be found in [Harris et al., 2012]. This includes an alternative derivation of the quasi-resonant solution set, but omits any proof for the bounds placed on the resonance broadening.

Abstract

We study the dynamics, kinematics and statistics of resonant and quasi-resonant three-wave interactions appearing in models of geophysical flow. In these dispersive wave systems, the phenomenon of nonlinear resonance broadening plays a significant role across all three different branches of wave turbulence theory: from the statistical, to the discrete, and even the mesoscopic, formed as an intermediate regime between the two. The principal aim of this thesis is to understand the processes by which resonance broadening can induce a transition between each of these three different regimes. Beginning with the discrete case, we study two variants of the isolated triad: one with a constant additive forcing term; and the other in the presence of detuning. We provide a detailed analysis of both of these systems, covering their integrability and boundedness properties, showing that for almost all initial conditions the motion remains quasi-periodic and periodic respectively. Interestingly, we show that moderate amounts of detuning can actually promote energy exchange, increase the period and in rare instances cease to be periodic at all; each of these statements are contrary to what was previously thought. This motivates a more detailed study into the kinematics of resonance broadening. By analysing how the set of quasi-resonant modes develops under increased broadening, we show that a percolation-like transition exists, independent of the dispersion relationship used. At critical levels of broadening, we see the emergence of a single quasi-resonant cluster that begins to dominate the entire system. We argue that the formation of this cluster provides a way of characterising the turbulent state of the system, distinguishing between the discrete and statistical regimes. Through direct numerical simulation of the Charney-Hasegawa-Mima equation, we then assess whether this view is truly representative of the underlying dynamics. Here we find that the generation of quasi-resonantly excited modes can be detected through the statistical measures of total correlation and mutual information. We conclude by suggesting that these techniques have an incredible potential to infer the signature of both resonant and quasi-resonant clusters in fully realised turbulent systems, and yet are also subtle enough to detect qualitative changes in the underlying dynamics between different interacting modes.

Chapter 1

Introduction

Systems of nonlinearly interacting dispersive waves are ubiquitous in nature. They appear across a vast array of different scientific disciplines, covering everything from applications in engineering [Kundu and Bauer, 2006; Graff, 1975], interfaces between stratified fluids [Dyachenko et al., 2003; Craik, 1988], Rossby waves in geophysical fluid dynamics [Pedlosky, 1987], Alfvén waves in the turbulence of solar winds [Galtier et al., 2002], and even drift waves in magnetically confined plasmas [Horton and Hasegawa, 1994]. Intimately connected with the phenomenon of dispersive wave propagation is that of nonlinear resonance. In each of these systems, waves are characterised by both a wave vector, k, and a nonlinear frequency given in terms of this wave vector, which we denote $\omega(k)$. Their dispersive name comes from the fact each of these waves travel with different phase velocities, and so act to disperse energy throughout the spatially extended system. Whey they interact, which they do because of the nonlinearity present in the underlying evolutionary equations, they exchange energy. What we generally find is that when this nonlinearity is weak, there are select groups of modes that seem to preferentially exchange energy, but only among themselves. Energy exchange between these modes appears orders stronger than the surrounding background fluctuations of the rest of the system. We find that these clusters of waves satisfy certain resonance conditions, dependent on the wave number and frequency. If the system exhibits quadratic nonlinearity, then three-wave interactions dominate, and these resonance conditions appear in the form

$$\begin{cases} k_3 = k_1 + k_2, \\ \omega(k_3) = \omega(k_1) + \omega(k_2). \end{cases} \tag{1.1}$$

At its heart, the concept is cunningly seductive. It promises that we can take a system, which is an inherently complex, infinite-dimensional nonlinear prob-

lem and reduce it down so that the dynamics of the problem can be captured by a finite-dimensional set of resonant modes. The majority of clusters that appear in most physical examples are typically small [Kartashova and L'vov, 2008], with the systems of ordinary differential equations that govern them relatively straightforward to calculate. What adds to their appeal, is that the form of these equations are completely generic across a host of different problems; they appear in a different manner of systems used to describe different kinds of mode coupling, from their inception in nonlinear optics [Armstrong et al., 1962], electronics [Manley and Rowe, 1956], and geophysical fluid dynamics [Gill, 1974; Connaughton et al., 2010]. The smallest of these clusters, the resonant triad, which is formed by the interaction of just three waves, is completely integrable with an explicit solution known in terms of elliptic functions [Bustamante and Kartashova, 2009b]. It is by no means unsurprising then that these factors have spurred on considerable research into the categorisation and analysis of all the different types of resonant cluster that are available. They have been enumerated for a variety of different systems [Kartashova and Mayrhofer, 2007], numerical algorithms have been developed to solve various resonance conditions [Kartashova and Kartashov, 2007; Kartashova, 1998], their integrability properties assessed [Bustamante and Kartashova, 2011], and even a graphical language has been built to describe them [Kartashova, 2009]. All of this comes now comes under what is now known as Discrete Wave Turbulence [Kartashova et al., 2010; Kartashova, 2009], and blossomed from the very appealing idea that in some way, discrete and regular dynamics can still persist among the chaotic and seemingly random ensemble of weakly interacting waves.

There is another slightly more prevalent and well-established description of wave turbulence however. The problem is that general collections of modes in dispersive wave systems are not resilient to perturbation. Even if we take one mode, the introduction of another causes the growth of a third, which in turn allows for the successive generation of other modes through further three-wave interactions that form a cascade-like effect. Rapidly, we can go from a situation where only a few modes are populated with energy, to where this energy has dispersed throughout the entire system. As the size of the problem grows, so do the number of degrees of freedom, and so the underlying dynamics become more random in nature. In this situation, a statistical description of the system becomes more appropriate, which is perfectly encapsulated by the theory of Statistical Wave Turbulence [Nazarenko, 2011; Newell and Rumpf, 2011]. In most physically relevant contexts, external forcing is applied to modes at large scales, which acts as a source of energy for the system. Resonant interactions then redistribute this energy throughout the system, along with other

conserved quantities, until it dissipated at small scales. Kinetic equations can then be derived, which describe how this ensemble evolves in time. One of the most celebrated aspects of this theory, is that these equations admit power-law stationary solutions, $k^{-\alpha}$, known as the Kolmogorov-Zakharov energy spectra [Zakharov et al., 1992]. Furthermore, in the continuous limit when the domain is unbounded, this theory is known to be asymptotically exact in the weakly nonlinear limit. In this case, the wave vectors characterising each mode are continuous.

The problem is that neither of these two descriptions of turbulence are actually complete in their own right. When the domain of our system is bounded, such as we find when studying wave systems defined with periodic boundary conditions, each of the wave vectors now becomes discrete. This is completely necessary when considering any numerical studies of wave turbulence, but has the unfortunate consequence of invalidating some of the key assumptions underpinning statistical wave turbulence theory. There are now instances, however, when both statistical and discrete turbulent regimes can mutually co-exist. We see that while the majority of the system appears random, certain discrete, organised and persistent structures emerge formed by independent clusters of resonant modes [Kartashova, 2006]. This intermediate regime has been labelled as mesoscopic wave turbulence, and is induced through the phenomenon of nonlinear resonance broadening [Zakharov et al., 2005; L'vov and Nazarenko, 2010; Nazarenko, 2007]. The discreteness of the system acts to apply a linear correction term to the frequency of each wave, which is dependent on its amplitude [Whitham, 1974]. For small amplitudes, this broadening is likewise small, and resonant triads remain isolated. However, by increasing the amplitude and hence nonlinearity of the system, we can reach the point where this broadening can overcome the lattice spacing between the wave vectors for each mode. This allows for the generation of quasi-resonant interactions, which we account for by allowing some degree of frequency mismatch, Ω, in the resonance conditions above,

$$\begin{cases} k_3 = k_1 + k_2, \\ |\omega(k_3) - \omega(k_1) - \omega(k_2)| \leq \Omega. \end{cases} \tag{1.2}$$

Each of the two pre-existing turbulent regimes can therefore be classified according to the strength of this resonance broadening alone. We see that for a small degree of broadening, clusters of modes remain isolated and so the theory discrete wave turbulence becomes applicable. However, when the broadening is sufficiently large, all the modes become effectively part of one large quasi-resonant structure, and so statistical wave turbulence theory becomes the more appropriate description for the system. Finally, mesoscopic turbulence is the intermediate stage

between these two regimes, consisting of both relatively small, isolated clusters, and the highly connected, pervasive statistical component formed via quasi-resonant interactions. It is now widely accepted that no theoretical description of dispersive wave systems can be complete without considering the influence of quasi-resonant interactions [Bustamante and Hayat, 2012; Janssen, 2003].

The outline of the thesis flows in a way that is in keeping with this transition from the discrete to the statistical regimes of turbulence. After a precursory introduction into the fundamentals of discrete wave turbulence, we begin by studying two variants on the isolated triad. These consist of first the detuned triad. While the isolated triad has been extensively studied, this system has been seemingly overlooked. We will show that it is integrable and that an explicit solution for the amplitudes and individual phases can be found. The most novel part of this work is a detailed numerical study into the effect of detuning. We we will show that in the limit of large detuning, the period of oscillations and variability in the amplitudes vanish. This falls in line with what is expected from our discussion of discrete wave turbulence, that in the presence of weak nonlinearity, resonant interactions should exchange energy far more effectively than non-resonant ones. However, what happens for intermediate degrees of detuning is far less clear. We will show that for certain initial conditions, detuning can have the unexpected effect of promoting greater energy exchange between modes and lengthen the period of oscillations. A similar effect is noted in the example that follows on the forced triad. Here we apply a constant forcing term to the unstable mode in the triad and ask whether the system remains integrable. We prove that it in general the energy in the system remains generally bounded, except for a specific set of initial conditions that is independent on the strength of the forcing term. Even though an explicit solution can no longer be computed, we will show that the system admits a novel one-dimensional particle representation that can be exploited to reveal the existence of periodic and quasi-periodic orbits for a general set of initial conditions.

We will argue that each of these relatively simple, low dimensional systems serve to illustrate some key points when dealing with larger scale systems. This novel effect of detuning, for instance, motivates a more careful consideration of resonance broadening in general, which we will approach in Chapter 5. Here we consider a kinematic overview of the wave system by analytically solving the broadened resonance conditions given in equation (1.2) for the Charney-Hasegawa-Mima (CHM) equation. We will show that the naïve interpretation that broadening only serves to 'thicken' the resonant manifold is actually completely misleading. In fact, we will show that it is entirely possible to characterise analytically the quasi-resonant set

of modes interacting with a given mode. By doing so we show that a finite, critical value of detuning does emerge from this analysis, at which point the curve bounding this solution set diverges. We therefore consider how the set of quasi-resonant clusters varies as a function of the broadening parameter, Ω. We will show that a percolation-like transition occurs for a critical value of broadening Ω^*, at which point one singular, large cluster begins to form. The existence of this critical point we will argue has important consequences in terms of the classification of the three different types of turbulent regime mentioned above.

Up to this point, we have only considered a kinematic representation of the effects nonlinear broadening. The final chapter attempts to address this issue by using the information theoretical ideas of total correlation and mutual information to infer correlations between quasi-resonantly interacting modes. Using the energy contained within an isolated triad to regulate the amount of broadening, we will show that we can use these techniques to capture the onset and generation of quasi-resonantly excited modes. Furthermore, we will show that the signature of a resonant clusters does actually persist despite the presence of large nonlinearity. More importantly, however, we will show that exactly resonant clusters need not form the most correlated sets of modes in the system. Here, quasi-resonant triads can appear at least as influential to the dynamics of the entire wave system. We view this as only adding weight to the continually mounting evidence that quasi-resonant interactions form a crucial part in the evolution of dispersive wave systems. Above anything else, the thesis in general should convince the reader of that.

Chapter 2

Resonance, Integrability and the Charney-Hasegawa-Mima Equation

The phenomena of dispersive wave propagation nonlinear resonances are prevalent in a wide variety of different physical systems. Depending on one's approach, studying them encompasses a range of different scientific disciplines, which to name but a few includes: Hamiltonian systems; integrability of finite dimensional systems; the inverse scattering transform and integration of nonlinear PDEs; stability analysis; and, classical problems of existence and smoothness to certain Cauchy initial value problems. In this sense it compounds any attempts to write a concise, yet informative, introduction to the topic that would prove sufficient for the following chapters. The majority of the thesis, however, can be classified according to two broad areas. These are the integrability of small finite dimensional Hamiltonian systems, consisting of single isolated triads of resonantly interacting waves, and the second area, which attempts to offer a kinematic overview of the entire wave system that incorporates the addition of quasi-resonant interactions.

Between each of these topics lies the concept of resonance. Using the Charney-Hasegawa-Mima (CHM) equation as our archetypal dispersive wave system, we will show that it admits selective groups of waves that preferentially exchange energy only among themselves. These clusters of modes are characterised by satisfying certain resonance conditions, which we will motivate using a perturbative style analysis based on the method of multiple time-scales. We will show that this technique allows us to derive the dynamics of each cluster, and by doing so, acts as a starting point in considering the dynamical properties of the most basic resonant clusters, such as the

isolated triad, kite and butterfly. This forms the basis of what is known as discrete wave turbulence. However, we will also argue that a more complete understanding of wave coupling in dispersive systems requires the introduction of quasi-resonant interactions. This is required for the percolation-like analysis on the kinematics of nonlinear resonance broadening towards the end of the thesis.

The final two sections of this chapter deal with the related concepts of integrability and Hamiltonian systems. We know that both the CHM equation and finite-dimensional systems of resonant clusters admit Hamiltonian representations. However, it is the non-canonical representation of the infinite dimensional CHM equation that can be exploited to reveal certain integrability properties of smaller clusters of modes. It allows for the systematic construction of a Lax pair, and so in turn, a sufficient number of conservation laws to prove integrability of the detuned triad, which we will consider in the following chapter. The significance of finding a Lax pair will be highlighted in the context of the determining integrability of both finite and infinite dimensional nonlinear systems. Finally, we will discuss Jacobi's last multiplier theorem, also known as the $(N-2)$-integrability theorem, which we will later use for guaranteeing integrability of the forced triad under a restricted class of initial conditions.

2.1 The role of resonant interactions

As we have mentioned in the introduction, dispersive waves form a pivotal role in a host of different spatially extended physical systems, appearing across a range of varied scientific disciplines. Such systems are called dispersive since whenever we consider just the linear part of their evolution equation alone, they often admit harmonic solutions of the form $\psi(\mathbf{x},t) = \Re\{A_k \exp(i(\mathbf{x}\cdot k - \omega(k)t))\}$, with nonlinear frequency $\omega(k)$ written in terms of the wave vector $k \in \mathbb{R}^2$ [L'vov and Nazarenko, 2010]. For finite sized systems, each of these waves then becomes categorised by a discrete wave vector instead, with form dictated by the boundary conditions. As we have already discussed, the nonlinearity present in these dispersive wave systems forces these modes to interact and couple together, exchanging energy as they do so. It is those sets of modes that satisfy the resonance conditions given in equation (1.1), that should do this the most effectively. In principle, provided that the nonlinearity is sufficiently weak, these modes should remain relatively isolated from the rest of the system, evolving independently. This idea forms the basis of what is known as Discrete Wave Turbulence, which throughout this section we will now briefly summarise.

Methodology does exist for tackling the dynamics of these systems of resonant clusters. Say for the moment that our dispersive wave system admits a canonical Hamiltonian structure [Bustamante and Kartashova, 2009b; L'vov and Nazarenko, 2010]:

$$i\frac{\mathrm{d}a_k}{\mathrm{d}t} = \frac{\partial \mathcal{H}}{\partial a_k^*}. \tag{2.1}$$

We note that non-canonical Hamiltonian systems will be considered in the latter half of this chapter. The standard approach then relies on finding pairwise canonical coordinates $\{a_k, a_k^*\}$, which are typically the Fourier coefficients of the dependent variables, and then expanding the resulting Hamiltonian in terms grouped by powers of a_k and a_k^* combined,

$$\mathcal{H} = \mathcal{H}_2 + \mathcal{H}_3 + \mathcal{H}_4 + \dots. \tag{2.2}$$

The first of these terms gives the linear evolution of each mode, while the following terms related to the nonlinear coupling of three and four-waves respectively. When the amplitudes are small, the influence of each of these higher order terms diminishes. We can therefore truncate this Hamiltonian accordingly. For this thesis, we will consider systems where only three wave interactions are prominent. This gives a Hamiltonian of the form

$$\mathcal{H} = \sum_k \omega(k) a_k a_k^* + \frac{1}{2}\sum_{k_1,k_2,k_3} V_{23}^1 a_1^* a_2 a_3 \delta_{23}^1 + \text{c.c.}, \tag{2.3}$$

where V_{23}^1 describes the three-wave interaction coefficient, and δ_{23}^1 is the shorthand notation for the Kronecker delta symbol, $\delta(k_1 + k_2 - k_3)$. The corresponding equations of motion are therefore,

$$i\frac{\mathrm{d}a_k}{\mathrm{d}t} = \omega(k)a_k + \sum_{k_1,k_2}\left[\frac{1}{2}V_{12}^k a_1 a_2 \delta_{12}^k + {V_{k2}^1}^* a_1 a_2^* \delta_{k2}^1\right]. \tag{2.4}$$

We will consider just one such dispersive wave system throughout this thesis, that governed by the CHM equation. It serves as an ideal way to introduce the various concepts at the core of discrete wave turbulence, and yet is not so restrictive as to suggest that the techniques elaborated upon in this section cannot be applied to other problems.

2.1.1 The Charney-Hasegawa-Mima equation

The CHM equation is the archetypal model for quasi-geostrophic flow used throughout this thesis. It is simple enough to be in some ways mathematically tractable, and

while it is two-dimensional, it still accounts for what could be considered typically three-dimensional effects such as vortex tube stretching, or compression. Perhaps more importantly, by introducing a background vorticity, it admits the existence of plane wave solutions, called Rossby waves [Rossby, 1939]. These are thought to be crucial in determining the large scale evolution of geophysical flows, exerting influence over the atmospheric circulation between different regions and the formation of global circulation patterns [Ding et al., 2010; Lachlan-Cope and Connolley, 2006]. Since the CHM equation can effectively capture other meteorological features in addition to Rossby waves, such as the formation of blocking regimes [Charney and DeVore, 1979], it is an ideal candidate for both theoretical and numerical analysis. From the perspective of this thesis, it offers the perfect setting to understand the role of resonant and quasi-resonant interactions in models of geophysical flows, especially in the context of understanding the different types of wave turbulence theory.

We shall simply state the form of the CHM equation here, as it is written in [Pedlosky, 1987]. For those looking for a more complete derivation, consult either this reference or the more concise version given in [Swaters, 1999]. The CHM equation states that the scalar streamfunction $\psi(x, y, t)$, or geopotential height, must evolve according to

$$\frac{\partial}{\partial t}\left(\Delta\psi - F\psi\right) + \partial\left(\psi, \Delta\psi\right) + \beta\frac{\partial\psi}{\partial x} = 0. \tag{2.5}$$

In effect, it is used to describe the leading order, large scale dynamics of an incompressible, shallow layer of fluid on a rotating sphere. It has been derived independently in two different contexts related to drift waves in magnetically confined plasmas [Hasegawa and Mima, 1978], and that of geophysical fluid dynamics presented here [Charney, 1948]. Within this second context, it appears as a first-order approximation to the shallow-water equations on the beta-plane. It is therefore a localised approximation, restricted to the plane $(x, y) \in \mathbb{R}^2$, with a background vorticity gradient introduced via the term $\beta\partial_x\psi$. In this sense, we have that x denotes the zonal, east-west direction while y corresponds to the meridional, north-south direction.

The first term in the CHM equation captures the effect of vortex tube stretching. Here the parameter F is simply proportional to the inverse of the square of the Rossby deformation radius. The last term left unaccounted for is the Jacobian denoted by $\partial\left(\psi, \Delta\psi\right)$. This introduces a quadratic nonlinearity to the equation that accounts for the nonlinear advection of vorticity. It is defined for any two

differentiable, scalar functions $f(x, y)$ and $g(x, y)$, by

$$\partial(f, g) = \frac{\partial f}{\partial x}\frac{\partial g}{\partial y} - \frac{\partial f}{\partial y}\frac{\partial g}{\partial x}. \tag{2.6}$$

Sometimes the CHM equation is referred to as the quasi-geostropic potential vorticity equation in association with the shallow-water equations [Swaters, 1999]. This stems from the fact that the potential vorticity, $q = \Delta\psi - F\psi + \beta y$, must be conserved [Lynch, 2003]. However, to keep things clear throughout the thesis, it will only be referred to as the CHM equation.

Explicit solutions to the CHM equation do exist. These include the compactly supported, travelling dipole vortex solutions called modons [Lerichev and Reznik, 1976], which were initially thought to be the two-dimensional analogue of solitons. Unfortunately, this was not the case and an inverse scattering procedure, if it even exists, has yet to be found for the CHM equation. Recently it has been found that other more exotic solutions can be constructed through the use of an appropriate Bäcklund transformation [Xiao-Rui and Yong, 2010]. Rossby waves are the other type of explicit solution. These are harmonic solutions of the form $\psi = A(k)\cos(k_x x + k_y y - \omega(k)t)$, with $k \in \mathbb{R}^2$, that have the anisotropic dispersion relationship,

$$\omega(k) = -\frac{\beta k_x}{k^2 + F}. \tag{2.7}$$

Because of the chirality induced by the earth's rotation, Rossby waves are characterised by the fact that they must propagate in a westwardly direction. An example of a numerically simulated solution of the CHM equation is included in figure (2.1).

2.1.2 The dynamics of resonant clusters

Even though a single Rossby wave is a solution to the CHM equation, a linear superposition will not be. If we now perturb this single Rossby wave by adding another. This perturbation would rapidly lead to the generation of other modes, in a cascade-like effect, where additional waves are generated through successive three-wave interactions. This is because of the quadratic nonlinearity present in the Jacobian term, which allows the creation of a third wave with wavenumber, k, that is a sum of the other two. If, however, the nonlinearity is weak, then we observe that energy exchange between modes is effectively restricted to groups of modes that are in resonance. This is what we will now demonstrate, using a special perturbative technique, based on isolating the fast and slow time-scales. It will allow us to derive both the necessary resonance conditions, and the equations of motion

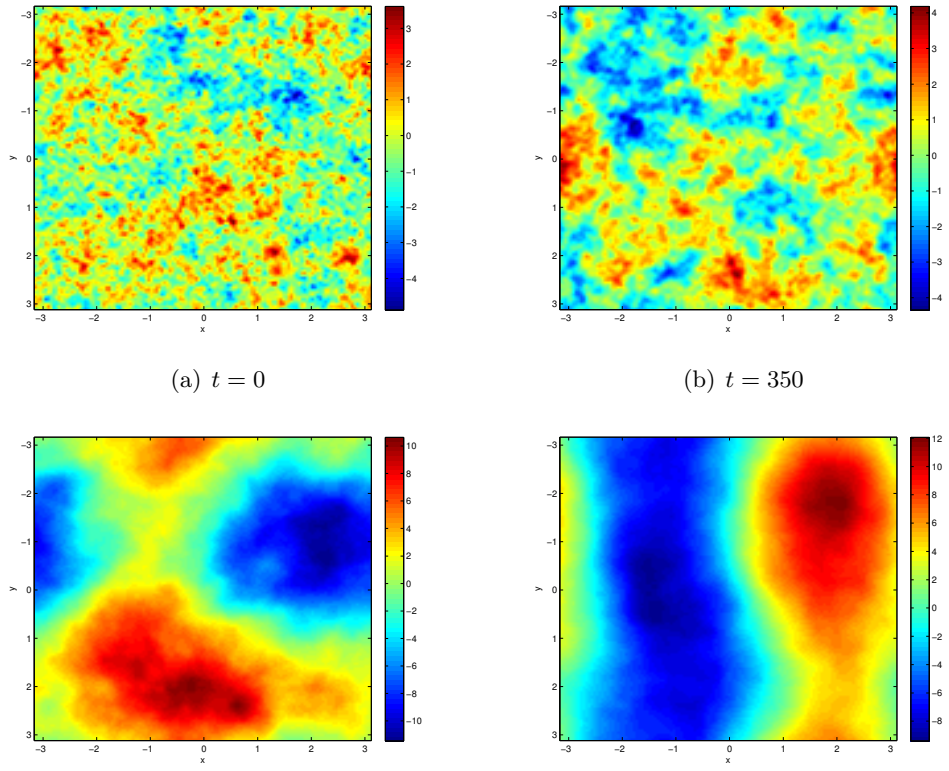

(a) $t = 0$ (b) $t = 350$

(c) $t = 700$ (d) $t = 1000$

Figure 2.1: Direct numerical simulation of the CHM equation on the torus, starting from a random distribution of energy among modes. A hyper-viscosity term is introduced to dissipate energy away from the system at small scales.

governing each mode forming part of a resonant cluster. At first glance, this process offers a great deal. It provides a way of representing complex, infinite dimensional PDE problems in terms of a collection of possibly disjoint, low-dimensional systems of ODEs. However, there are some key issues with this representation that we will show throughout the course of this thesis.

Method of multiple time-scales

Let us consider the case when the nonlinearity is weak, corresponding to the case when $\beta >> 1$. We proceed as suggested in [Pedlosky, 1987], by introducing the fast and slow time variables, $\bar{t} = \beta t$ and t, respectively. Since we have now cast the problem in terms of two different time scales, the chain rule implies that we must replace any time derivative in the CHM equation accordingly,

$$\frac{\partial}{\partial t} \to \frac{\partial}{\partial t} + \beta \frac{\partial}{\partial \bar{t}}.$$

We now have that

$$\frac{\partial}{\partial \bar{t}}(\Delta\psi - F\psi) + \frac{\partial \psi}{\partial x} = -\frac{1}{\beta}\left[\partial\left(\psi, \Delta\psi\right) + \frac{\partial}{\partial t}(\Delta\psi - F\psi)\right]. \tag{2.8}$$

Written in this form, we have separated the each side according to the small parameter $1/\beta$. Expanding our solution in terms of this small parameter gives

$$\psi(x, y, t, \bar{t}) = \psi_0(x, y, t, \bar{t}) + \frac{1}{\beta}\psi_1(x, y, t, \bar{t}) + ... \tag{2.9}$$

The idea is that the introduction of two time-scales avoids both the creation of an infinite response in the wave amplitudes when the resonance conditions are met, and the development of secular growth terms if we were to naively approach this perturbative method in terms of one time variable alone.

Let us now substitute our series expansion into the modified CHM equation (2.8). Equating different orders of the parameter $1/\beta$, we see that to zeroth order, ψ_0 must satisfy the linear PDE given by

$$\frac{\partial}{\partial \bar{t}}(\Delta\psi_0 - F\psi_0) + \frac{\partial \psi_0}{\partial x} = 0. \tag{2.10}$$

If we now restrict our attention to the domain to the torus, $\Omega = \mathbb{T}^2$, this has general

solution given in terms of

$$\psi_0(x, y, t, \bar{t}) = \sum_k A(k, t) \mathrm{e}^{i(k_x x + k_y y - \omega_k \bar{t})}. \tag{2.11}$$

However, for every term in this series, its complex conjugate is also a perfectly valid solution. Since the stream function must be real-valued, we must impose the additional requirement that for each wavenumber k,

$$A(-k, t) = A(k, t)^*. \tag{2.12}$$

Using this constraint, we see that by pairwise grouping each term corresponding to k and its negative value, the zeroth order solution is simply a linear superposition of Rossby waves.

If we now substitute this leading order solution back into equation (2.8), we see that ψ_1 must satisfy the equation,

$$\frac{\partial}{\partial \bar{t}}(\Delta\psi_1 - F\psi_1) + \frac{\partial}{\partial x}\psi_1 = -\partial\left(\psi_0, \Delta\psi_0\right) - \frac{\partial}{\partial t}(\Delta\psi_0 - F\psi_0). \tag{2.13}$$

Expanding the Jacobian term fully, this is found to be equivalent to

$$\begin{aligned} \frac{\partial}{\partial \bar{t}}(\Delta\psi_1 - F\psi_1) + \frac{\partial \psi_1}{\partial x} = & \sum_{k_1, k_2} B(k_1, k_2) A(k_1, t) A(k_2, t) \mathrm{e}^{i(\theta(k_1, t) + \theta(k_2, t))} \\ & + \sum_{k_1} (k_1^2 + F) \frac{\partial A(k_1, t)}{\partial t} \mathrm{e}^{i\theta(k_1, t)}, \end{aligned} \tag{2.14}$$

where for notational brevity we have defined

$$\theta(k, \bar{t}) = k_x x + k_y y - \omega(k)\bar{t}. \tag{2.15}$$

together with the interaction coefficient

$$B(k_1, k_2) = \frac{1}{2}(k_1 \times k_2)_Z \left(k_1^2 - k_2^2\right). \tag{2.16}$$

For those unfamiliar with the notation, we have that

$$(k_1 \times k_2)_Z = k_{1x} k_{2y} - k_{1y} k_{2x}. \tag{2.17}$$

The structure of this interaction coefficient suggests that that two waves do not interact if either they are either the same wavelength or have parallel wave vectors.

Conditions for resonance

The idea now is to determine the evolution of the amplitudes, $A(k,t)$, in the slow time variable, t, that eliminate the appearance of secular growth terms at first order. This can be done in a systematic way by asking that for any choice of test function, ϕ, when averaging over space and the fast time variable, $\bar{t}$, we get

$$\lim_{T\to\infty}\frac{1}{T}\int_0^T\int_{\mathbb{T}^2}\phi\mathcal{L}\psi_1\,\mathrm{d}x\,\mathrm{d}y\,\mathrm{d}\bar{t}=0, \tag{2.18}$$

for the differential operator $\mathcal{L}$ defined by

$$\mathcal{L}\phi=\frac{\partial}{\partial\bar{t}}\left(\Delta\phi-F\phi\right)+\frac{\partial\phi}{\partial x}. \tag{2.19}$$

Using integration by parts, we see that this operator is in fact skew-adjoint:

$$\lim_{T\to\infty}\frac{1}{T}\int_0^T\int_{\mathbb{T}^2}\phi\mathcal{L}\psi_1\,\mathrm{d}x\,\mathrm{d}y\,\mathrm{d}\bar{t}=\lim_{T\to\infty}\frac{1}{T}\int_0^T\int_{\mathbb{T}^2}\psi_1\mathcal{L}^*\phi\,\mathrm{d}x\,\mathrm{d}y\,\mathrm{d}\bar{t}, \tag{2.20}$$

where the adjoint operator is given simply by $\mathcal{L}^*=-\mathcal{L}$. Choosing any test function in the kernel of the adjoint means that both of these two limits evaluate to zero, which we know consists of functions of the form $\phi=\mathrm{e}^{\pm\theta(k,\bar{t})}$ for arbitrary k. If we now substitute this into equation (2.18) and integrate, we are left with the following system of ordinary differential equations given in terms of the slow time variable, t:

$$\frac{\mathrm{d}A_k}{\mathrm{d}t}=-\sum_{k_1,k_2}\frac{B(k_1,k_2)}{k^2+F}A(k_1)A(k_2)\delta\left(k_1+k_2-k\right)\delta\left(\omega(k_1)+\omega(k_2)-\omega(k)\right). \tag{2.21}$$

The crucial element of this result is that it suggests that initially over a time $\bar{t}=O(\beta)$, the dynamics of our wave system are dominated by three-wave interactions satisfying the resonance conditions

$$\begin{cases}\omega(k_3)=\omega(k_1)+\omega(k_2),\\ \quad k_3=k_1+k_2.\end{cases} \tag{2.22}$$

In other words, the lowest order amplitudes are affected by an $O(1)$ amount from modes with whom they share resonance, while non-resonant modes should appear as modest background fluctuations with influence $O(1/\beta)$ [Pedlosky, 1987]. This result forms the basis of much of the work behind discrete wave turbulence theory [Kartashova, 2009]: if the non-linearity is weak, then it is sensible to truncate the full system of modes to those being either resonant, or close to resonance, to a collec-

tion of possibly disjoint finite-dimensional systems formed by resonantly interacting clusters of modes. Initially, these systems should faithfully capture the dynamics of the full wave system. However, it is worth keeping in mind that resonant interactions alone do not form the complete description of how waves interact. In fact, it is now considered that quasi-resonant interactions are essential to building a complete description of turbulent behaviour in dispersive wave systems. This we will consider in more detail in Chapter 5.

2.1.3 Examples of some typical, small resonant clusters

Once we assume that interactions in weakly nonlinear wave systems are dominated by clusters of resonant interacting waves, the next step is to begin to classify each of these clusters according to their dynamical behaviour and theoretical properties. There is now an extensive wealth of literature devoted to the classification of these clusters, analysing their Hamiltonian structure and discerning whether or not they are integrable [Bustamante and Kartashova, 2011; Kartashova and L'vov, 2008; Bustamante and Kartashova, 2009b]. Throughout the course of this thesis, we will even add to this process by analysing two different variants of a known integrable system, the isolated triad. In particular, we will assess how the integrable structure is influenced by the presence of constant forcing in one chapter, and detuning in another. Here, we will only briefly review the three most prevalent types of resonant cluster: the isolated triad, the kite and the butterfly.

The process for calculating these resonant clusters is relatively straightforward. For discrete wave systems, one possibly way is to simply enumerate all possible triplets, (k_1, k_2, k_3) that satisfy the resonance conditions given by equation (2.22) within some predefined cut-off in wave number space. Since the solution must be real, we say that wavenumbers that differ only in sign are equivalent, and in fact represent the same mode. The next step is then to test whether there are triplets that share a common wave number, and if so, connect these triads together to form even larger clusters and so on. This process defines an underlying graph structure that forms a kinematic representation of our wave system. We will discuss this representation in far greater detail in the later chapter on resonance broadening. However, we will note that there are some far more sophisticated methods available, based on some advanced concepts in number theory. These work on existing methods for solving Diophantine equations, an example being the resonance conditions given above, such as the q-class decomposition method [Kartashova and Kartashov, 2007] for the power-law dispersion relationship, or methods based on the analysis of quadratic forms for the CHM equation studied here [Bustamante and Hayat, 2012].

The isolated triad

The isolated triad is by far the simplest primary cluster, consisting of just three modes k_1, k_2 and k_3 that satisfy the resonance conditions given in equation (2.22). Enumerating each combination of these three modes, including their negative values, and substituting them into equation (2.21), gives the following system:

$$\begin{cases} \dot{A}_1 = T(k_1, k_2, k_3) A_2^* A_3, \\ \dot{A}_2 = T(k_2, k_1, k_3) A_1^* A_3, \\ \dot{A}_3 = -T(k_3, k_1, k_2) A_1 A_2, \end{cases} \tag{2.23}$$

together with their complex conjugates, which we have written in terms of general interaction coefficient $T(k_1, k_2, k_3)$. For the CHM equation, this coefficient is given by

$$T(k_1, k_2, k_3) = \frac{(k_2 \times k_3)_Z (k_2^2 - k_3^2)}{k_1^2 + F}. \tag{2.24}$$

The integrability of this system is well-established, with solutions known in terms of Jacobi elliptic functions, spanning across multiple different fields of study, including optics [Armstrong et al., 1962], electronics [Jurkus and Robson, 1960], and of course, fluid mechanics [Bretherton, 1964]. Following recent work on the effect of the dynamical phase [Bustamante and Kartashova, 2011], their evolution is pretty much completely understood. Constructing these solutions requires finding a number of functionally independent conservation laws, which we will discuss in more detail throughout the rest of this chapter. Two of these, however, are defined as the energy and enstrophy, which for each member of a triad corresponding to the CHM equation are defined, respectively, as [Pedlosky, 1987]:

$$E_j = (k_j^2 + F)|A_j|^2, \tag{2.25}$$

$$V_j = (k_j^2 + F) E_j, \tag{2.26}$$

for $j = 1, 2, 3$. What is perhaps surprising, is that it can be shown that both the *total* energy and enstrophy are conserved properties for the full wave system and any arbitrary resonant cluster as well. This means that on the advective time scale, to first order, energy and enstrophy must remain confined to each resonant cluster.

As noted in the reference above, it is possible to write each of these conservation statements in the form,

$$\frac{1}{k_2^2 - k_3^2} \frac{\partial E_1}{\partial t} = \frac{1}{k_3^2 - k_1^2} \frac{\partial E_2}{\partial t} = \frac{1}{k_1^2 - k_2^2} \frac{\partial E_3}{\partial t}. \tag{2.27}$$

This means that since each member of the triad can be ordered according to scale, for instance $k_1^2 < k_3^2 < k_2^2$, that the flow of energy must always be passed from one mode, in this case k_3, and then shared with the remaining two. We can see this since if $\partial_t E_3 < 0$, then both the remaining two gradients must be positive. Similarly, we see that energy must flow from k_1 and k_2, and then back into k_3. In this instance, we call the k_3 mode the active one, and the remaining two passive modes [Kartashova and L'vov, 2008]. In terms of a more general discussion, we can instead use the Hasselmann criterion for nonlinear instability [Hasselmann, 1967]. This stipulates that the mode with the intermediate frequency, such as $\omega(k_3)$ for example, is unstable, while the remaining two are neutral. We can therefore interchangeably use active and unstable, or passive and neutral, to mean equivalent things.

Canonical transformation of variables

There is a fundamental problem with how the dynamical system for the isolated triad is currently written. The problem is that it remains context specific; we need to the form of the interaction coefficient to calculate each factor, thus limiting the scope of any analysis conducted on this system as applied to other wave systems. The idea is to introduce a change of variables that makes the study of the dynamics of resonant clusters completely generic. We can in fact exploit the concept of active and passive modes to do this consistently.

While the transformation can be generalised to other wave systems, for the CHM equation, we introduce a linear transformation $B_j = \lambda_j A_j$, $j = 1, 2, 3$, where each $\lambda_j \in \mathbb{R}$ is constant. We need only in fact define one of these constants,

$$\lambda_1^2 = s_2 s_3 \frac{(k_2^2 + F)(k_3^2 + F)}{(k_1^2 - k_2^2)(k_1^2 - k_3^2)}, \tag{2.28}$$

and remark that the remaining two can be calculated by permuting the indices. The three additional constants, $s_j \in \{+1, -1\}$, represent the choice of sign required to ensure that each λ_j is real-valued. We simply take $s_1 = \operatorname{sgn}\left(k_2^2 - k_3^2\right)$, $s_2 = \operatorname{sgn}\left(k_1^2 - k_3^2\right)$ and $s_3 = \operatorname{sgn}\left(k_1^2 - k_2^2\right)$. The resulting system reads,

$$\begin{cases} \dot{B}_1 = (k_2 \times k_1)_Z s_1 B_2^* B_3, \\ \dot{B}_2 = (k_1 \times k_2)_Z s_2 B_1^* B_3, \\ \dot{B}_3 = (k_2 \times k_1)_Z s_3 B_1 B_2. \end{cases} \tag{2.29}$$

There are now six possible cases to consider, depending on the all the possible ways we can order the three wave vectors according to magnitude. The process is tedious

and so we spare the details. Suffice to say, by relabelling variables, and taking the complex conjugates where necessary, it is always possible to reduce this system to the canonical form

$$\begin{cases} \dot{B}_1 = ZB_2^* B_3, \\ \dot{B}_2 = ZB_1^* B_3, \\ \dot{B}_3 = -ZB_1 B_2, \end{cases} \tag{2.30}$$

such that the mode B_3 always corresponds to the unstable/active mode.

Kites and butterflies

A kite consists of two triads connected via two modes. We label these two different triads as a and b, with corresponding variables B_{ja}, B_{jb}, $j = 1, 2, 3$. There are four different types of kite depending on the position of the two active modes, one from each triad, that are present in the cluster [Bustamante and Kartashova, 2009b]. Let us suppose that each triad in the kite shares both its passive modes, $B_{1a} = B_{1b}$ and $B_{2a} = B_{2b}$, then the dynamics of a PP-PP kite are given by the system,

$$\begin{cases} \dot{B}_{1a} = B_{2a}^* \left(Z_a B_{3a} + Z_b B_{3b} \right), \\ \dot{B}_{2a} = B_{1a}^* \left(Z_a B_{3a} + Z_b B_{3b} \right), \\ \dot{B}_{3a} = -Z_a B_{1a} B_{2a}, \ \dot{B}_{3b} = -Z_b B_{1a} B_{2a}. \end{cases} \tag{2.31}$$

A butterfly on the other hand consists of just two triads, connected by one common mode. This time there are three different types of butterflies corresponding to the three different ways the two different triads can share one active/passive mode [Kartashova and L'vov, 2008; Bustamante and Kartashova, 2009b]. Let us say that they both share the active mode $B_{3a} = B_{3b}$, then the dynamics of an AA-butterfly are given by

$$\begin{cases} \dot{B}_{1a} = Z_a B_{2a}^* B_{3a}, \ \dot{B}_{1b} = Z_b B_{2b}^* B_{3a}, \\ \dot{B}_{2a} = Z_a B_{1a}^* B_{3a}, \ \dot{B}_{2b} = Z_b B_{1b}^* B_{3a}, \\ \dot{B}_{3a} = -Z_a B_{1a} B_{2a} - Z_b B_{1b} B_{2b}. \end{cases} \tag{2.32}$$

It is worth noting that while the integrability of the kite follows relatively trivially, the same cannot be said for any of the three types of butterfly. In all but the rarest of trivial cases, butterflies are generally not integrable [Bustamante and Kartashova, 2009b].

Generally speaking, clusters consisting of modes numbering more than seven are generally rare. We have calculated the distribution of cluster sizes for the CHM equation with parameter $F = 0$, defined in the rectangular box $|k_x|, |k_y| \leq 512$,

Cluster Size	Number of Clusters
3	1302
5	95
7	4
11	2
13	4
15	2
23	2
25	2
27	2
33	2
55	2

Table 2.1: Distribution of cluster sizes and their frequency for the CHM equation. Here, we taken $F = 0$ and specified a cut-off wave number such that $|k_x|$, $|k_y| \leq 512$. Note that most clusters occur in pairs due to the symmetry property of the dispersion relationship.

which can be seen in table (2.1). Due to the symmetry properties of the dispersion relationship we know that if (k_1, k_2, k_3) forms a resonant triad then other solutions can be found under the transformations $(k_{jx}, k_{jy}) \to (-k_{jx}, k_{jy})$, $(k_{jx}, k_{jy}) \to (k_{jx}, -k_{jy})$ and $k_j \to -k_j$, for $j = 1, 2, 3$. Even after we discard copies of modes that are the complex conjugates of others, most clusters will still occur in pairs, which can be identified from the table. We see that approximately 98.4% of the clusters available consist of either isolated triads or butterflies. Since the dynamical systems governing these clusters are relatively simple, and explicitly integrable in the case of the isolated triad, the appeal is that each one can be integrated separately and when combined should provide an accurate representation of the evolution for the entire wave system. This approach of reducing an infinite-dimensional system to one described by a few isolated, low dimensional ODEs is called the Clipping Method [Bustamante and Kartashova, 2009b].

As part of the entire taxonomy of grouping and classifying different resonant clusters, we note that a concise graphical representation has been developed, that uniquely defines not only the number of modes in a cluster, but the number of triads and the connections between them. This representation is called an NR-diagram [Kartashova, 2009]. We make this remark only for a sense of completeness; most, if not all, small clusters have been analysed theoretically and numerically, when an explicit solution cannot be found. They have been enumerated and their underlying network structure has been analysed for a variety of different dispersion

relationships [Kartashova, 2007]; and a whole language, in terms of this graphical representation, has been developed to describe them. What people now realise as missing from this picture, is any discussion on quasi-resonant interactions. These are now thought crucial to the understanding of the the different types of turbulent regime: from the discrete, to the statistical, and an intermediate stage known as the mesoscopic.

2.1.4 Introducing quasi-resonant interactions

While the method of multiple time-scales was effective in deriving conditions for resonance, and equations of motion for the evolution of clusters of resonantly interacting waves, it says little about the prominence of clusters that are near resonance. In fact, it now considered that any complete theory of wave interactions and turbulence should take into account the effect of quasi-resonant interactions [Bustamante and Hayat, 2012]. Such interactions have been proposed both as crucial in the generation of freak waves [Janssen, 2003; Mori and Janssen, 2006], and are found to play a role in the generation of zonal jets induced by a modulational instability [Connaughton et al., 2010]. The problem with the perturbative approach taken above, is that in reality the level of nonlinearity is always finite and not infinitesimally small. As a consequence, rather than the distinct separation of time-scales mentioned above, the time-scales between non-resonant and resonant interactions can become comparable [Bustamante and Hayat, 2012]. For geophysical systems, different types of forcing, either through heating or the effect of topography can also induce some degree of resonance broadening [Dehai, 1998].

A slightly more heuristic method for deriving the interaction equations of both resonant and quasi-resonant interactions are as follows. For simplicity, let us consider that our domain is the torus, $\Omega = \mathbb{T}^2$. We therefore know that we can represent the stream function, $\psi(x, y, t)$, for the CHM equation in terms of its Fourier series, with coefficients given by

$$\psi_n = \frac{1}{(2\pi)^2} \iint_{\mathbb{T}^2} \psi(x, y) \mathrm{e}^{-i\, n\cdot(x,y)}\, \mathrm{d}\, x \mathrm{d} y.$$

Each coefficient evolves according to the equation

$$\frac{\partial \psi_k}{\partial t} + i\omega(k)\psi_k = \frac{1}{2} \sum_{k_1+k_2=k} T(k, k_1, k_2)\psi_{k_1}\psi_{k_2}, \tag{2.33}$$

where the interaction coefficient, $T(k, k_1, k_2)$, is defined according to equation (2.24). Because of our choice of domain, each wavenumber is now discrete: we know that

each wavenumber k must occupy the regular lattice

$$(2\pi n_x/L_x, 2\pi n_y/L_y),\ n_x, n_y \in \mathbb{Z},$$

where L_x and L_y are the lengths of the sides in our bi-periodic, rectangular domain. If we now make the substitution $\phi_k = \mathrm{e}^{i\omega(k)t}\psi_k$, we derive the interaction form of the dynamical system written above:

$$\frac{\partial \phi_k}{\partial t} = \frac{1}{2}\sum_{k_1+k_2=k} T(k,k_1,k_2)\phi_{k_1}\phi_{k_2}\mathrm{e}^{i\,\Delta\omega(k,k_1,k_2)t}, \tag{2.34}$$

where $\Delta\omega(k,k_1,k_2) = \omega(k) - \omega(k_1) - \omega(k_2)$ represents the finite resonance width. It is clear that in the context of the CHM equation, the variables ϕ_k can be identified as Rossby waves.

We can readily identify the first resonance condition $k = k_1 + k_2$, and so this system admits three-wave interactions only. The second resonance condition takes a little more reasoning: using the Riemann-Lebesgue lemma [Gradshteĭn et al., 2007], integrating the right-hand-side over time, we see that three-wave interactions with large resonance width should contribute little to the dynamics. This can be interpreted on an intuitive level by noting that fast oscillations should average to zero.

Much can be said for making this limiting argument more precise however. In fact careful scrutiny of this limiting argument has led to recent discussion on the validity and self-consistency behind the the derivation of the kinetic equation, which broadly speaking defines the evolution of the statistical ensemble of interacting waves [Lvov et al., 2011]. In this reference it is argued that quasi-resonant interactions can potentially offer a way to address this discrepancy, as well as issues explain slower than expected evolutionary rates for certain approximate stationary states. This approach has also been applied to the study of Fermi-Pasta-Ulam chains [Gershgorin et al., 2007] and that of acoustic turbulence [L'vov et al., 1997]. We will briefly touch upon the theory of statistical wave turbulence in the upcoming chapter on the kinematics of nonlinear resonance broadening. Here we simply state the results found within these references: for Hamiltonian system of the form given in equation (2.3) with canonical variables $\{a_k, a_k^*\}$, except defined over a continuous and not discrete set of wavenumbers $k \in \mathbb{R}^n$, the generalised kinetic equation describing the evolution of the wave action $n_k =< a_k a_k^* >$ reads,

$$\frac{\mathrm{d}n_k}{\mathrm{d}t} = 4\int \left|V^k_{k_1,k_2}\right|^2 f_{k12}\delta(k-k_1-k_2)\mathcal{L}(\omega(k)-\omega(k_1)-\omega(k_2))\mathrm{d}k_1\mathrm{d}k_2 - perms. \tag{2.35}$$

Here, the additional terms we have omitted can be accounted for by simply permuting the indices of the above expression, and have been removed for clarity. The coefficient f_{k12} is quadratic in the wave action for each member in the triad and is given by

$$f_{k12} = n_{k_1} n_{k_2} - n_k(n_{k_1} + n_{k_2}).$$

We see that the only part of the generalised kinetic equation that is context specific is the interaction coefficient, $V^k_{k_1,k_2}$.

What is crucial about this equation in terms of the limiting argument described above is the form of the "broadened" delta-function $\mathcal{L}(\Delta\omega)$. Here, it is defined simply as

$$\mathcal{L}(\Delta\omega(k, k_1, k_2)) = \frac{\Omega_{k12}}{\Delta\omega^2 + \Omega^2_{k12}}, \tag{2.36}$$

where Ω_{k12} describes the total broadening of each particular resonance. In the limit when this total broadening is small, we still recover that

$$\lim_{\Omega_{k12}\to 0} \mathcal{L}(\Delta\omega_{k12}) = \pi\delta(\Delta\omega_{k12}),$$

which is precisely what we expect both the Riemann-Lebesgue to tell us, and allows us to recover the standard exactly resonant version of the kinetic equation. Importantly, we note that the total resonance broadening is clearly wavenumber dependent, and not actually applied uniformly across each triad. In fact, an analytical value of this parameter has been proposed [L'vov et al., 1997], and is simply given by

$$\Omega_{k12} = \gamma_k + \gamma_{k_1} + \gamma_{k_2}, \tag{2.37}$$

where each γ_k can be found by evaluating the right-hand-side of equation (2.35), keeping only the terms proportional to the wave action n_k. It is argued that by doing so, the resonance broadening appears to act as a nonlinear dampening effect applied to the evolution of each mode.

Computing the value of this total resonance broadening practically, however, is another matter; the value of Ω_{k12} now appears implicitly within its own definition, found in the integrand of each γ_k. To make matters considerably more tractable for the analysis in the upcoming chapters, we consider only a constant level of total broadening applied to each set of quasi-resonant interactions, modifying equation (2.22) to get

$$\begin{cases} |\omega(k_1) + \omega(k_2) - \omega(k_3)| \leq \Omega, \\ k_3 = k_1 + k_2. \end{cases} \tag{2.38}$$

for some constant total broadening $\Omega > 0$. Solutions to these quasi-resonance conditions can be computed explicitly for the CHM dispersion relationship, as we will discover in chapter 5. These solutions are in no way trivial or predictable. We will show that the total resonance broadening must in fact be bounded for all possible interactions, with bounds that can be computed explicitly. When we set $\Omega = 0$, the corresponding set of exactly resonant solutions forms a one-dimensional, closed curve in wave number space. However, increasing the amount of broadening does not simply result in a 'thickening' of this manifold. Instead, we show that a critical value of detuning does exist at which point the continuous, closed curve bounding the solution set of quasi-resonant modes diverges. Analysis of this critical point leads to the idea that the network of quasi-resonant modes formed by these solving these conditions undergoes a percolation-like transition. Existence of this percolation threshold suggests a novel approach to characterising the turbulent state of the wave system.

2.2 Hamiltonian fluid dynamics

The majority of this thesis deals with Hamiltonian systems of some description; whether they be the finite dimensional, canonical ones governing the dynamics of resonant clusters, or the infinite-dimensional, non-canonical representation of the CHM equation. The Hamiltonian description provides an invaluable tool to understanding the various different concepts of fluid mechanics in general. It provides a structured and clear method by which we can derive asymptotic approximations, study stability theorems and undertake perturbation style analysis, as well as provide a freedom in the choice of variables [Lynch, 2002; Salmon, 1988]. Crucially, however, is that Hamiltonian mechanics provides a clear and concise connection between symmetries and invariants of the system, as well as a means of generating conservation laws through degeneracy of the Hamiltonian formulation [Shepherd, 1990]. As we will see in the following section, invariants of the dynamics are fundamental to many different concepts of integrability, especially in the classical context of the Liouville integrability of Hamiltonian systems.

We begin this section by talking about the more familiar concept of finite dimensional Hamiltonian systems in canonical form. This includes a brief review of the least action principle, or Hamilton's principle, and the intimate connection between Hamiltonian and Lagrangian mechanics. The problem is that this canonical formulation is too restrictive; it has often been remarked that the fixation with the canonical form has unduly held back progress in Hamiltonian fluid dynamics,

especially when considered with the advances made in other fields where the generalisation of Hamiltonian systems had already been applied to quantum mechanics [Shepherd, 1990]. This motivates a more generalised, or abstract, notion of what makes a Hamiltonian system. This is called the symplectic formulation, and induces what is known as a Poisson bracket. In this more abstract language, Hamiltonian systems can therefore be classified according to its phase space, and two additional objects, which are the scalar Hamiltonian and this Poisson bracket [Lynch, 2002; Bihlo, 2011]. We then need only check that this symplectic structure satisfies certain algebraic properties alone, rather than being constrained to think only in terms of the canonical equations of motion. Moreover, the advantage is that each of these concepts have a natural analogue in the continuum limit, where we can discuss what it means for certain partial differential equations to be Hamiltonian. Returning to the archetypal example in this thesis of the CHM equation, we will show that this in fact admits a Hamiltonian structure. Using this formalism, we will show that the CHM equation admits an infinite hierarchy of conservation laws, similar to the two-dimensional Euler equation, due to the degeneracy of this symplectic structure. Finally, we discuss why spectrally truncating the CHM equation destroys this non-canonical Hamiltonian structure, and what this means in terms of the Hamiltonian representation of resonant and quasi-resonant clusters of modes.

2.2.1 Hamilton's equations and the canonical form

Consider an N-dimensional system, described by a discrete set of generalised coordinates, q_n, $n = 1, 2, \ldots, N$, each evolving in time. The evolution of this system is given by Hamilton's equations of motion, which are derived by considering solutions that minimise the action

$$S[q] = \int_{t_0}^{t_1} L(q_n, \dot{q}_n, t)\ \mathrm{d}t. \tag{2.39}$$

This is called Hamilton's principle, and the associated variational problem yields what are known as the Euler-Lagrange equations,

$$\frac{\partial L}{\partial q_n} - \frac{\mathrm{d}}{\mathrm{d}t}\left(\frac{\partial L}{\partial \dot{q}_n}\right) = 0,\ \forall n = 1, 2, \ldots, N. \tag{2.40}$$

The elegance of this result, and why physically it is so appealing, is that all we require is knowledge of the Lagrangian, $L(q, \dot{q}_n, t)$, to completely determine the evolution of our system. Calculating this Lagrangian is typically straightforward, provided we have the correct physical intuition, and is given simply as the difference between the

kinetic and potential energies, respectively.

Since the body of this section deals with Hamiltonian mechanics, the question to then ask is how the two representations are related. This is made clear once we define the generalised momenta, $p_n = p_n(q, \dot{q}, t)$, by

$$p_n = \frac{\partial L(q, \dot{q}, t)}{\partial \dot{q}}, \tag{2.41}$$

for $n = 1, 2, \ldots, N$. In principle, it is possible to solve these equations to calculate $\dot{q}_n$ as functions of the generalised positions and momenta, provided the Lagrangian is non-singular [Lynch, 2002]. Fortunately, this is generally true for most physical systems, which allows us to define the Hamiltonian through the Legendre transformation,

$$H(q, p, t) = \sum_{n=1}^{N} \dot{q}_n p_n - L(q, \dot{q}, t). \tag{2.42}$$

It is now trivial to show that the Euler-Lagrange equations are entirely equivalent to the canonical form of Hamilton's equations, by substituting this expression for the Hamiltonian into the action given by equation (2.39) and considering an equivalent variation problem. The resulting analysis gives the canonical form of Hamilton's equations,

$$\dot{q}_n = \frac{\partial H}{\partial p_n}, \; \dot{p}_n = -\frac{\partial H}{\partial q_n}. \tag{2.43}$$

We have therefore written what was effectively a $2N$-dimensional, second order system of ODEs described by the Euler-Lagrange equations, into a first order one. At first, it is not immediately obvious why this is beneficial, especially when working in finite dimensions. However, in infinite-dimensional systems, it is often difficult to formulate a least action principle, let alone begin even attempt to solve the corresponding Euler-Lagrange equations [Swaters, 1999]. This motivates the definition of a more abstract notion of what it means for a system to be Hamiltonian, which we will now consider.

2.2.2 General Hamiltonian systems

For a system to be considered Hamiltonian, it need not be restricted to the canonical form of Hamilton's equations described above. Poisson brackets allow us to neatly generalise what is meant for a system to be Hamiltonian, even when applied to infinite dimensional phase spaces. Given a smooth manifold, $\mathcal{M}$, and the space of smooth scalar functions defined on this manifold, $C^\infty(\mathcal{M})$, a Poisson bracket is a

bilinear map,

$$\{\cdot,\cdot\} : C^\infty(\mathcal{M}) \times C^\infty(\mathcal{M}) \to C^\infty(\mathcal{M}),$$

which for any $F, G, Q \in C^\infty(\mathcal{M})$ satisfies the following [Karasözen, 2004; Swaters, 1999]:

(i) Skew-symmetry, or $\{F, G\} = -\{G, F\}$.

(ii) Leibniz rule, or $\{FG, Q\} = F\{G, Q\} + \{F, Q\}G$.

(iii) Jacobi identity, whereby $\{F, \{G, Q\}\} + \{G, \{Q, F\}\} + \{Q, \{F, G\}\} = 0$.

Often we see, as in the last of these references, the additional property of self-Poisson commutation, namely $\{F, F\} = 0$. It is relatively trivial to see that this is in fact implied by the skew-symmetry property and so need only be given implicitly.

This Poisson bracket then defines what is called a Poisson structure on the manifold $\mathcal{M}$. If locally this manifold has coordinates $x = (x_1, \ldots, x_N)$, then the Poisson bracket for two smooth functions $F(x), G(x) \in C^\infty(\mathcal{M})$ is given by

$$\{F, G\} = \sum_{i=1}^{N} \{x_i, x_j\} \frac{\partial F}{\partial x_i} \frac{\partial G}{\partial x_j}. \tag{2.44}$$

When written in this form, the structure functions $\{x_i, x_j\}$ naturally define what is called a Poisson operator, $\mathbf{J}$, a skew-symmetric (anti-Hermitian) matrix which we define accordingly, $J_{ij} := \{x_i, x_j\}$ for each $i, j = 1, \ldots, N$. The skew-symmetry it inherits directly from the corresponding Poisson bracket property we have listed above. In a similar fashion, we can prove that it must also satisfy an analogue of the Jacobi identity [Abramov and Majda, 2003]:

$$\sum_{l=1}^{N} \left(J_{pl}\partial_l J_{qr} + J_{rl}\partial_l J_{pq} + J_{ql}\partial_l J_{rp} \right), \ \forall p, q, r \leq N. \tag{2.45}$$

Using the Poisson operator, $\mathbf{J}$, the Poisson brackets given by equation (2.44) can now be written concisely as

$$\{F, G\} = \left\langle \frac{\partial F}{\partial x}, \mathbf{J} \frac{\partial G}{\partial x} \right\rangle, \tag{2.46}$$

which we have written in terms of the standard inner product defined on $\mathbb{R}^N$.

For any given smooth function H, our Hamiltonian vector field X_H takes the form [Karasözen, 2004]:

$$X_H = \sum_{i,j=1}^{N} J_{ij} \frac{\partial H}{\partial x_j} \frac{\partial}{\partial x_i}. \tag{2.47}$$

We can therefore write the total time derivative of any function, assuming they are not explicitly time-dependent, simply as

$$\frac{\mathrm{d}F}{\mathrm{d}t} = X_H(F) = \{F, H\}. \tag{2.48}$$

As a consequence we see that any function is an invariant of motion if and only if it Poisson commutes with the Hamiltonian. Since, the Hamiltonian trivially commutes with itself, it must therefore be likewise invariant as well. This also means that Hamilton's equations now become

$$\dot{x} = \{x, H\}, \tag{2.49}$$

or equivalently,

$$\dot{x} = \mathbf{J} \frac{\partial H}{\partial x}. \tag{2.50}$$

We have therefore motivated two equivalent definitions of what it means for a system to be Hamiltonian. Both require the definition of a smooth manifold, $\mathcal{M}$, together with a function called the Hamiltonian, $H : \mathcal{M} \to \mathbb{R}$, which must necessarily be conserved by the dynamics. We can then either define a Poisson operator $\mathbf{J}$ that is both skew-symmetric and satisfies the Jacobi identity, or take the alternate approach and define a bilinear map called a Poisson bracket, that satisfies the three key properties listed above.

Let us for a moment return to the canonical form of Hamilton's equations (2.43) derived in the previous section, writing a combined vector of canonical position and momenta given as $\mathbf{z} = [q_1, q_2, \ldots, q_N, p_1, p_2, \ldots, p_N]^T$. Hamilton's canonical equations of motion are then

$$\dot{\mathbf{z}} = \mathbf{J_c} \frac{\partial H}{\partial \mathbf{z}}, \tag{2.51}$$

with Poisson operator defined according to

$$\mathbf{J_c} = \begin{bmatrix} \mathbf{0} & \mathbf{I} \\ -\mathbf{I} & \mathbf{0} \end{bmatrix}. \tag{2.52}$$

Written in block form, we have that $\mathbf{0}$ and $\mathbf{I}$ represent the $N \times N$ zero and identity matrices respectively. One can readily verify in this instance that $\mathbf{J_c}$ is both skew-

symmetric and satisfies the Jacobi identity. What is perhaps less obvious is that this operator also transforms as a rank-2 covariant tensor [Morrison, 1998]. We can see this by considering any general, time-dependent change of coordinates $\bar{z}_i = \bar{z}_i(z)$, along with transformed Hamiltonian $\bar{H}(\bar{z}) = H(z)$. If we now differentiate each of these new variables we find that

$$\dot{\bar{z}}_l = \frac{\partial \bar{z}_l}{\partial z_i}\dot{z}_i = \frac{\partial \bar{z}_l}{\partial z_i} J_c^{ij} \frac{\partial H}{\partial z_j} = \left[\frac{\partial \bar{z}_l}{\partial z_i} J_c^{ij} \frac{\partial \bar{z}_m}{\partial z_j}\right] \frac{\partial \bar{H}}{\partial \bar{z}_m}. \tag{2.53}$$

Defining the new operator

$$\bar{J}^{lm} = \frac{\partial \bar{z}_l}{\partial z_i} J_c^{ij} \frac{\partial \bar{z}_m}{\partial z_j}, \tag{2.54}$$

we recover the same structure written in equation (2.50), suggesting that this new symplectic representation is covariant under general coordinate transformations.

As we have just seen, our general description of a Hamiltonian system provides a certain transparency when dealing with variable transformations that means we avoid the unnecessary task of finding the canonical position and momenta. Furthermore, this assertion is given additional weight courtesy of Darboux's theorem, which tells us that if $\mathbf{J}$ is non-singular, then there exists at least locally, a transformation of variables where $\mathbf{J}$ can always be written in the canonical form [Salmon, 1988]. In fact, if it is invertible then $\mathbf{J}$ defines as symplectic structure on $\mathcal{M}$ if and only if its inverse is both skew-symmetric and satisfies the Jacobi identity [Karasözen, 2004], meaning that Poisson and symplectic manifolds are not to be confused as being one and the same. Darboux's theorem therefore allows us to classify Hamiltonian systems as non-canonical whenever $\mathbf{J}$ is singular, and canonical otherwise.

Degeneracy of the Poisson operator in fact allows for the creation of certain invariants, that unlike Noether's theorem, do not appear from some underlying symmetry of our system. Let us suppose that it is possible to find a function, $C(x)$, that Poisson commutes with every element in our set of admissible functions. Immediately we see that such a function would be a constant of motion, since it must necessarily commute with the Hamiltonian. Extending this analysis, we see that by exploiting the properties of inner products found in the definition given by equation (2.46), we must also have that

$$\frac{\partial C}{\partial x} \in \ker(\mathbf{J}).$$

It follows that if J is invertible, then it must have a trivial kernel, and so the set of such functions $C(x)$ must be equally trivial. If however, this operator is singular, then this set is non-empty, and has dimension equal to the co-rank of the operator

J. We call these functions Casimirs. While not a topic in this thesis, we remark that degeneracy of this type is important in the analysis of Hamiltonian fluid dynamics: aside from being used to create invariants of seen here, it is considered a crucial property behind much of the work on the stability of steady-state solutions [Swaters, 1999].

As a final remark we consider an important type of Poisson structure, given when the structure functions J_{ij} are linear,

$$J_{ij}(x) = \sum_{k=1}^{N} c_{ij}^{k} x_k. \tag{2.55}$$

Here, c_{ij}^{k} form the structure constants associated with an N-dimensional Lie algebra [McLachlan, 1993; Morrison, 1998]. Brackets with a Poisson operator of this form are called Lie-Poisson brackets and so corresponds to what is called a Lie-Poisson structure. Cited examples detailed in the references above include Euler's equations of a rigid body and the two-dimensional Euler equations governing inviscid flow. These are intrinsically connected with two examples considered in this thesis: that of the equations governing the evolution of a resonant triad and of course, the CHM equation.

2.2.3 Hamiltonian formulation for the CHM equation

It is perhaps difficult to pinpoint the exact moment the non-canonical Hamiltonian description was formalised in the context of fluid dynamics. Many of the systems studied in continuum mechanics, such as the two-dimensional Euler equations, are naturally expressed in terms of their Eulerian variables. While a suitable variational principle follows naturally using the Lagrangian description, as shown in [Virasoro, 1981], the same cannot be argued when Eulerian variables are used. A solution is available, but involves introducing Clebsch potentials at the cost of convenience and clarity [Seliger and Whitham, 1968]. Applying the approach outline in the preceding section, moving from the Lagrangian to Hamiltonian description, therefore fails to work when we want to work with the more familiar Eulerian description. We can sidestep these issues by simply defining what it means for a system to be Hamiltonian as we did in the abstract definition given above. While it has been suggested that this was first done for ideal magnetohydrodynamics in [Morrison and Greene, 1980; Swaters, 1999], we know that the as a major step to proving integrability of the Korteweg-de Vries equation, it was first formulated in terms of an infinite-dimensional, non-canonical Hamiltonian system [Gardner, 1971; Zakharov

and Faddeev, 1971]. This was almost a decade earlier than the work by Morrison and Greene. A number of standard references then followed that made concrete this Hamiltonian formulation for a system of PDEs, such as [Benjamin, 1984] and [Morrison, 1982]. An excellent review of historical context behind the Hamiltonian formulation of the CHM equation can be found in [Swaters, 1999], with only the briefest summary of this material given above.

Put simply, a system of partial differential equations written in terms of dependent variables $u(x,t) = (u_1(x,t), u_2(x,t), \ldots, u_N(x,t))^T$ and defined on a spatial domain $x \in \Omega \subseteq \mathbb{R}^m$, is said to be Hamiltonian if it can be expressed in the form

$$\frac{\partial u}{\partial t} = \mathbf{J}\frac{\delta H}{\delta u}, \tag{2.56}$$

where $H[u]$ is a conserved functional called the Hamiltonian. Additionally, for any two smooth, arbitrary functionals $F[u]$ and $G[u]$, the Poisson bracket defined by

$$\{F, G\} = \left\langle \frac{\delta F}{\delta u}, \mathbf{J}\frac{\delta G}{\delta u} \right\rangle, \tag{2.57}$$

must satisfy the three properties detailed in section (2.2.2). Here, $\mathbf{J}$ could be a matrix of possible pseudo-differential operators, while typically the $L^2(\Omega)$ inner product used, as in for example,

$$\{F, G\} = \int_\Omega \left(\frac{\delta F}{\delta u}\right)^T \mathbf{J}\frac{\delta G}{\delta u}\, \mathrm{d}x. \tag{2.58}$$

In the transition from the discrete to the continuous case, we note that any function has now become a functional, which means that any derivative must be replaced by its corresponding variational, or Fréchet, derivative. This means that for a functional of the form

$$F[u] = \int_\Omega \mathcal{F}(u)\, \mathrm{d}x, \tag{2.59}$$

where $\mathcal{F}(u)$ is called the density, the variational derivative $\frac{\delta F}{\delta u}(u)$ is defined by

$$\lim_{\epsilon \to 0} \frac{\partial}{\partial \epsilon} F[u + \epsilon \delta u] = \left\langle \frac{\delta F}{\delta u}, \delta u \right\rangle, \tag{2.60}$$

where any variations δu vanish at the boundaries of Ω.

The Hamiltonian structure for the CHM equation in the plane was first proposed by [Weinstein, 1983]. Through a simple modification of the Hamiltonian it can readily be extended to account for arbitrary domains $\Omega \subseteq \mathbb{R}^2$, whose boundaries consist of a finite union of smooth, simply connected curves $\{\partial\Omega_i\}_{i=1}^n$. This is

acceptable provided we stipulate that there can be no normal flow of mass across the boundary, which is equivalent to asking that the stream function on each section of the boundary, with $\psi|_{\partial\Omega_i} = \lambda_i$. As stated in [Swaters, 1999], with these boundary conditions the CHM equation can be cast into Hamiltonian form given by equation (2.56), with Hamiltonian,

$$H = \frac{1}{2}\int_\Omega \nabla\psi \cdot \nabla\psi + F\psi^2 \, \mathrm{d}x - \sum_{i=1}^{n} \lambda_i \oint_{\partial\Omega_i} \mathbf{n}_i \cdot \nabla\psi \, \mathrm{d}s, \tag{2.61}$$

together with the operator,

$$J(\,\cdot\,) = -\partial(q, \,\cdot\,). \tag{2.62}$$

Here the variable q is simply the total vorticity,

$$q = \Delta\psi - F\psi + \beta y. \tag{2.63}$$

We know that the Hamiltonian must be conserved, comprising of a first term, which is simply an expression that the sum of kinetic and potential energies is constant, and a second term, which is a restatement of Kelvin's Circulation Theorem.

In a perhaps unexpected connection with the classical notion of integrable systems, the Lie-Poisson structure presented here actually forms part of what is a Lax pair for the CHM equation. While this is discussed in greater detail in the following section, finding a Lax pair is thought to be central to the inverse scattering transform used in the method of solving certain non-linear, integrable PDEs. This Lax pair was first suggested as a natural extension to the one known for the two-dimensional Euler equation in [Li, 2001, 2003]. However, knowledge of the existence of a Lax pair does not necessarily imply that the CHM equation is integrable, or that a solution can be calculated explicitly. While progress has been limited in this area, to date we have seen this work develop such that an ergodic representation of the eigenfunctions associated to the operator $\mathbf{J}$ is known [Li, 2005], as well as being used to construct novel, explicit solutions for the two-dimensional Euler equation using a Darboux transformation method [Sen-Yue and Yi-Shen, 2006]. Perhaps the key issue, especially with any in terms of numerical validation, is that one must be careful when naively truncating any infinite-dimensional Hamiltonian structure into its finite dimensional counterpart; indeed, truncating the number of modes in the CHM equation invalidates both the Jacobi identity and isospectral representation. This is crucial, especially with regards to this thesis, since it means that any low-dimensional representation, say where we consider clusters of resonant and quasi-resonant modes, do not necessarily inherit the same Lax pair and Hamiltonian

structure of the parent equation. This has major implications for the integrability of the dynamics of these reduced systems.

2.2.4 Hamiltonian description of resonant and quasi-resonant clusters

Since we are primarily interested in discrete wave turbulence, let us now restrict our attention to bi-periodic domain $\Omega = \mathbb{T}^2$. Since the Hamiltonian structure introduced above applies to a general class of domains, this is perfectly acceptable provided we define the new periodic variable, $q = \Delta\psi - F\psi$, which is known as the relative vorticity. This allows us to reformulate the problem as infinite-dimensional, discrete Hamiltonian system by expressing q in terms of its Fourier series, with coefficients

$$q_n = \frac{1}{(2\pi)^2} \iint_{\mathbb{T}^2} q(x,y) \mathrm{e}^{-i\, n\cdot(x,y)}\, \mathrm{d}x\mathrm{d}y.$$

Additionally, with this new domain, we can remove the circulation terms at the boundary from the Hamiltonian. Once written in interaction form, $\phi_n = \mathrm{e}^{i\,\omega_n t} q_n$, in these new variables we uncover the Hamiltonian system

$$\dot{\phi}_n = \left(\mathbf{J} \frac{\partial H}{\partial \phi} \right)_n, \; n \in \mathbb{Z}^2, \tag{2.64}$$

with the reduced Hamiltonian, which is simply the total energy,

$$H = \frac{1}{2} \sum_m \frac{\phi_m \phi_{-m}}{m^2 + F}, \tag{2.65}$$

together with skew-symmetric operator

$$J^{mn} = -(m \times n)\, \mathrm{e}^{i\,\delta(m,n)t} \phi_{m+n}, \tag{2.66}$$

and where we have defined the resonance width $\delta(m,n) = \omega(m) + \omega(n) - \omega(m+n)$. Even though the Poisson structure is now time-dependent, it can still be shown to satisfy the Jacobi identity in a fairly straightforward manner.

The temptation now would be to simply truncate the Hamiltonian given above to some desired set of modes, such as those we know to be resonant or expect to dominate the evolution of the system. From the discussion in the previous section, the hope would be that the effect of such a truncation would preserve the non-canonical Hamiltonian structure and simultaneously provide the basis for constructing a Lax pair for the reduced set of modes. However, in all but the rarest of

circumstances, this both invalidates Jacobi's identity and the compatibility condition for the Lax pair.

The consequences of breaking this Hamiltonian structure also has a profound effect any conserved quantities the system may have. For instance, we know that the Hamiltonian structure for the CHM equation is singular; we can see that the operator $\mathbf{J}$ has a non-trivial kernel since it must contain arbitrary functions of the form $F(q + \beta y)$. What this means is that the CHM equation must also admit non-trivial Casimir invariants that are solutions to the equation

$$\mathbf{J}\frac{\delta C}{\delta q} = 0. \tag{2.67}$$

Integrating this equation, we see that any functional of the form

$$C[q] = \iint_{\mathbb{T}^2} \mathcal{C}(q + \beta y)\, \mathrm{d}x\mathrm{d}y \tag{2.68}$$

satisfies these conditions for arbitrary density $\mathcal{C}(q + \beta y)$, that is periodic at the boundaries. This periodicity is absolutely essential, since if we were to differentiate the Casimir directly, we would find that

$$\frac{\mathrm{d}C}{\mathrm{d}t} = \oint_{\partial\mathbb{T}^2} \mathcal{C}(q + \beta y)\frac{\partial \psi}{\partial s}\, \mathrm{d}s. \tag{2.69}$$

This periodicity guarantees that this integral along the boundary vanishes. If without loss of generality, we assume that our periodic box has sides of equal length 2π, then we could for example take the infinite set of invariants,

$$C_n = \iint_{\mathbb{T}^2} \cos\left(\frac{n}{\beta}(q + \beta y)\right)\, \mathrm{d}x\mathrm{d}y,\ n \in \mathbb{N}. \tag{2.70}$$

Truncating the Hamiltonian invalidates the Jacobi identity, which means that only the Hamiltonian and enstrophy remain conserved and we lose each of the Casimir invariants listed above. There are however finite mode truncations of the two-dimensional Euler equations, for example, that preserve this Hamiltonian structure [Zeitlin, 1991]. For instance, the sine-bracket approximation adopted in this reference takes the form,

$$J_{mn} = \frac{1}{\epsilon}\sin\left(\epsilon m \times n\right) q_{m+n \bmod N}, \tag{2.71}$$

which is only accurate to first order in $\epsilon := 2\pi/N$, where N is the number of modes in our system. There is still debate over whether these higher order invariants have any statistical significance in determining the long term evolution of geophysical

flows [Abramov and Majda, 2003].

We have already noted that there are two additional quadratic invariants, the energy and enstrophy, that apply to both the full wave system and arbitrarily sized, exactly resonant clusters. Perhaps surprisingly, it was proposed that it is possible to construct an additional cubic invariant, sometimes called the 'zonostrophy' [Nazarenko and Quinn, 2009], that is actually an exact invariant of the kinetic equation [Balk et al., 1991; Balk, 1991]. As such it is adiabatic, or approximate, and not actually a conserved by the full underlying dynamics given by equation (2.64). Moreover, it has been proven that this adiabatic, cubic invariant can never be turned into an exact invariant through the introduction of higher order terms [Balk and van Heerden, 2006].

We have established therefore that reduced mode approximations, such as those consisting of clusters of resonant and quasi-resonant modes, do not generally inherit the same non-canonical Hamiltonian structure as the CHM equation. This is generally true for all but the isolated triad, which exhibits both a non-canonical Hamiltonian structure and Lax pair representation. The second of these we will exploit in the following chapter, while the first follows naturally from other systems with similar evolutionary equations, such as Euler's equations for motion of a rigid body [Shepherd, 1990], or the simple mechanical example of a swinging spring [Lynch, 2001, 2002]. Exactly resonant clusters when written in general form do however admit a canonical Hamiltonian representation [Bustamante and Kartashova, 2009b]. For instance, we have that for the isolated triad

$$H_T = \Im \left\{ Z B_1 B_2 B_3^* \right\}, \tag{2.72}$$

while for a kite and butterfly we might, respectively, have

$$H_K = \Im \left\{ B_{1a} B_{2a} (Z_a B_{3a}^* + Z_b B_{3b}^*) \right\}, \tag{2.73}$$

$$H_B = \Im \left\{ B_1 (Z_a B_{2a} B_{3a}^* + Z_b B_{2b} B_{3b}^*) \right\}, \tag{2.74}$$

depending the connectivity between different modes in each triad. The corresponding canonical equations of motion for each system are then given by

$$i \dot{B}_j = \frac{\partial H}{\partial B_j^*}, \tag{2.75}$$

together with their complex conjugates, so that the canonical operator $\mathbf{J}$ has been scaled by a constant factor of i. Adding any detuning to these system so as to make any one of the triads quasi-resonant, makes the Hamiltonian explicitly time-

dependent by introducing a factor $e^{i\delta t}$, for resonance width δ. While the canonical equations of motion still hold, the Hamiltonian is no longer conserved, and so no longer agrees with the definition of what it means for a system to be Hamiltonian as found in the preceding sections. This issue is encountered when attempting to find an explicit solution for the detuned triad in the following chapter: however, in this case we find that the the now time-dependent Hamiltonian can be modified to include a quadratic term so as to create a new cubic constant of motion. For general wave systems, we need to resort to the unscaled equations of motion that still include their interaction coefficients, and derive the canonical Hamiltonian form in the original variables instead [L'vov and Nazarenko, 2010]. This means that while it may still be possible to find on cubic conservation law related to the canonical Hamiltonian form, the problem is now context specific.

2.3 Integrability of finite and infinite-dimensional dynamical systems

One major concept used throughout this thesis is that of integrability. On its own, the term 'integrability' is ambiguous; there are a multitude of different definitions surrounding what it means for either a finite or infinite dimensional system to be integrable. In terms of finite dimensional systems, when we talk of integrability we will principally mean that a solution can be obtained by quadratures. This itself has no formal definition, but typically means that an explicit or closed-form solution can be found through a process of reduction, eliminating variables by solving a finite number of algebraic equations and integrating directly what remains. Typically, these algebraic equations relate to conserved properties of the system, such as energy for example, or by exploiting certain symmetries of the system. As we have mentioned before this is not the only concept of integrability, but this idea of obtaining a solution we can write explicitly remains a common theme running through each one. For instance, we say that a finite, or infinite dimensional, nonlinear system is C-integrable if through a change of variables it can be made linear [Kartashova and Shabat, 2005]. Once a system is linearised, it is then relatively trivial to compute a solution explicitly. Perhaps unsurprisingly, the notion of C-integrability is very closely connected with the other major topic of this thesis - resonance. Poincaré's theory of normal forms proves that any non-resonant vector field can be reduced to linear form by constructing an appropriate diffeomorphism [Arnol'd and Levi, 1988] using a formal power series representation. Here, a slightly different concept of resonance is used applied to the eigenvalues for the first order

term of this diffeomorphism.

The true worth of Poincaré's theorem, and others like it, lies in its utilitarian appeal. It demonstrates precisely how we can construct this diffeomorphism, and in doing so it provides a systematic approach to integrating our problem explicitly. In a similar vein, in the section we will introduce three other integrability theorems that will be of practical significance in the upcoming chapters, especially with regards to showing the integrability of relatively small clusters of interacting modes. We have already seen how resonant clusters of these modes underpin much of the theory behind discrete and statistical wave turbulence. It is understandable then that to date, there has been an extensive body of work in classifying whether comparatively small, Hamiltonian systems of resonant modes are integrable [Bustamante and Kartashova, 2009b]. Central to much of this work lies the idea that certain conserved quantities of the system act to restrict the flow to lower dimensional manifolds, and thus reduce the system. If we know enough functionally independent conservation laws, we can reduce the problem to one or two dimensions, for cases where we know it to be explicitly solvable. This systematic approach is accredited to Jacobi, where he showed that for N-dimensional system, knowledge of $N-2$ functionally independent conservation laws plus a what is now known as a Jacobi multiplier, can be used to construct the integrating function for the final reduced two-dimensional system [Boole, 1959]. Proof of this theorem is constructive and demonstrates how to compute the integrating factor explicitly. Jacobi's theorem is a fundamental result that we will exploit in two following chapters regarding proof for integrability of the detuned triad and the forced triad, and is worthy of the attention given below. For a review on its application to the integrability of resonant clusters, see [Bustamante and Kartashova, 2011].

Since the majority of work underpinning this thesis deals with Hamiltonian systems, it would be amiss not to consider the classical notion of integrability as introduced by Liouville. Here, we will only briefly review the concept of Liouville integrability, demonstrating why we favour Jacobi's approach instead, especially in the treatment of small dimensional systems. We conclude this section by briefly considering the ambiguity behind what it means for certain PDEs, or infinite dimensional systems, to be completely integrable. While formally this topic is never addressed in this thesis, some of the techniques used in this field are readily applicable to the study of finite dimensional systems. Particularly, we will discuss how rewriting a system using a Lax Pair formalism allows one to indirectly prove integrability by providing a way to systematically construct conservation laws that can then be used in conjunction with Jacobi's theorem detailed above.

2.3.1 Jacobi's Last Multiplier

For a domain Ω contained in $\mathbb{R}^N$ let us consider the N-dimensional, autonomous system of ordinary differential equations given by

$$\begin{cases} \dot{x}_1 = X_1\left(x_1, x_2, \ldots . x_N\right), \\ \dot{x}_2 = X_2\left(x_1, x_2, \ldots . x_N\right), \\ \quad \vdots \\ \dot{x}_N = X_N\left(x_1, x_2, \ldots . x_N\right), \end{cases} \tag{2.76}$$

where each scalar function X_i, $i = 1, \ldots, N$ is continuously differentiable in Ω. For compactness, we often write $\dot{x} = X(x)$, where each term is implicitly treated as a vector. We define a conservation law for this system as any scalar function $f(x_i, t)$ that satisfies

$$\frac{\mathrm{d}}{\mathrm{d}t} f(x_i, t) = \sum_{k=1}^{N} \frac{\partial f}{\partial x_k} X_k + \frac{\partial f}{\partial t} = 0. \tag{2.77}$$

From this definition we readily identify two different types of conversation law: those that depend explicitly on time, and those that do not. To distinguish between the two, the terminology often used in the literature is to define the first of these as a *dynamical invariant*, while reserving the term *conservation law* for those that remain time-independent [Bustamante and Kartashova, 2009b]. We see that each conservation law has the effect of defining the invariant manifold to which the motion is confined. The manifold corresponding to each conservation law therefore fibres the phase space, with the motion restricted to the intersection of each of these level sets. The role of the dynamical invariant therefore describes the evolution of the system on this level manifold.

We say that a set of conservation laws, f_k are functionally independent if at arbitrary points in the phase space, we have that their gradients ∇f_k are linearly independent. With each conservation law acting to restrict the motion of the system, the question is then precisely how many invariants are required before the system is integrable by quadratures. Clearly, if system (2.76) admits N independent invariants, it must be integrable. In fact, knowledge of $N - 1$ independent conservation laws allows us to construct a final dynamical invariant that must be functionally independent of the others. The system is therefore integrable, and the two statements are precisely equivalent. This dynamical invariant can be constructed relatively simply in practice. For instance, say that we label our $N - 1$ conservation laws

$f_k(x_1, x_2, \ldots, x_N)$, and define the function $g : \mathbb{R}^N \to \mathbb{R}^{N-1}$ by

$$g(x_1, x_2, \ldots, x_N) = (f_1(x_1, \ldots, x_N), f_2(x_1, \ldots, x_N), \ldots, f_{N-1}(x_1, \ldots, x_N)) .$$

We clearly see that g must be constant along each trajectory of the system, so $g = g(x_1(0), \ldots, x_N(0)) = c$, say, where c is constant. If we now apply the Implicit Function Theorem at this initial point, we obtain a continuously differentiable function $h : U \to V$, and two open sets U and V, with $x_1(0) \in U$ and $(x_2(0), \ldots, x_N(0)) \in V$, such that

$$g(x_1, h_1(x_1), \ldots, h_{N-1}(x_1)) = c$$

for $x_1 \in U$. For sufficiently small time t_1, this enables us to write each variable as a function of x_1 alone: $x_k(t) = h_{k-1}(x_1(t))$ for $k = 2, \ldots, N$ and for all $t \in [0, t_1]$. We can analytically continue h at t_1, and then along the remainder of the trajectory since we know that g is constant under the flow. Functional independence of the family of conservation laws guarantees that we can apply the Implicit Function Theorem at any point in the phase space. Finally, we would have reduced system (2.76) to what is effectively a one-dimensional manifold governed by

$$\frac{\mathrm{d}x_1}{\mathrm{d}t} = X_1(x_1, h(x_1)).$$

Our dynamical invariant is then given simply by the integral

$$I = \int^{x_1(t)} \frac{\mathrm{d}u}{X_1(u, h(u))} - t.$$

We can in fact go one further, proving integrability in the case when we have $N - 2$ conservation laws, plus an additional quantity known as the Jacobi multiplier. For a wide class of one and two-dimensional problems, integrating factors are used as a way to uncover explicit solutions for these systems. The Jacobi multiplier generalises this concept of an integrating factor but applied to higher dimensional systems [Berrone and Giacomini, 2003]. Using this reference it can be defined accordingly: a continuously differentiable function, or in fact density, $\rho(x_1, \ldots, x_N)$ defined on an open set $\Omega_0 \subseteq \Omega$ is said to be a *Jacobi multiplier* of system (2.76) in Ω_0 when ρ solves (in Ω_0) the linear first order PDE

$$\sum_{k=1}^{N} \frac{\partial}{\partial x_k} (\rho X_k) = \mathrm{div}(\rho X) = 0. \tag{2.78}$$

We immediately see that for divergence free vector fields, this multiplier is simply the constant $\rho = 1$.

As we have alluded to in the definition, we could equally view ρ as a density associated with some invariant measure. This is based on the highly regarded, seminal work of Poincare on his analysis of the three-body problem [Barrow-Green, 1997]. Here, he formalised the concept of an invariant integral, that is, a conservation law which takes the form

$$\int_{\phi(A;t)} \rho(x)\, \mathrm{d}x,\ A \subset \Omega_0,$$

where $\phi(x;t)$ is the flow corresponding to the vector field X. We have that this integral is conserved by the dynamics, meaning $\rho(x)$ is the density of the invariant measure

$$\mu(A) := \int_A \rho(x)\, \mathrm{d}x,$$

if and only if $\rho(x)$ satisfies the definition of a Jacobi multiplier given above. Moreover, we see that as a consequence of this theorem, by introducing the transformation of variables $y = G(x)$, we find that for any $A \subset \Omega_0$,

$$\int_{\phi(A;t)} \rho(x)\, \mathrm{d}x = \int_{G(\phi(A;t))} \left(\rho \circ G^{-1}\right)(y) |\det(DG^{-1})(y)|\, \mathrm{d}y$$

must likewise be invariant. Since $G(\phi(x;t))$ corresponds to the new flow under this transformation of variables, we have that

$$\hat{\rho}(y) = \left(\rho \circ G^{-1}\right)(y) |\det(DG^{-1})(y)| \tag{2.79}$$

must be a Jacobi multiplier for our system written in terms of the new variable y.

Let us now consider the three-dimensional case where we have precisely one conservation law, $\phi(x_1, x_2, x_3) = C$, and one Jacobi multiplier $\rho(x_1, x_2, x_3)$. A similar account is given in the two references [Berrone and Giacomini, 2003] and [Boole, 1959], which we will now briefly summarise. Suppose momentarily that our system was in fact two-dimensional,

$$\frac{\mathrm{d}x_1}{X_1(x_1, x_2)} = \frac{\mathrm{d}x_2}{X_2(x_1, x_2)}.$$

For any function $\psi(x_1, x_2)$ to be invariant, it would necessarily mean that

$$\frac{\partial \psi}{\partial x_1} = \mu(x_1, x_2) X_2,\ \frac{\partial \psi}{\partial x_2} = -\mu(x_1, x_2) X_1, \tag{2.80}$$

where the function μ is called the integrating factor for this system. A general solution to this pair of equations is then simply

$$\psi(x_1, x_2) = \int \mu X_2 \, \mathrm{d}x_1 - \int \left(\mu X_2 + \frac{\partial}{\partial x_2} \int \mu X_1 \, \mathrm{d}x_1 \right) \mathrm{d}x_2 + \text{const.}$$

As shown in the second of the references detailed above, if we are prudent in our choice of integrating factor μ, we can calculate a closed-form solution for ψ even for arbitrary choices of the functions X_1 and X_2.

Returning to our three-dimensional system, we can use our knowledge of one conservation law, together with the Jacobi multiplier, to systematically reduce the system to a two-dimensional manifold and then construct this integrating factor explicitly. Using the Implicit Function Theorem as above allows us to write $x_3 = F(x_1, x_2, C)$, whereby we derive the two relationships

$$\frac{\partial F}{\partial x_i} = -\frac{\partial \phi}{\partial x_i} \Big/ \frac{\partial \phi}{\partial x_3}, \; i = 1, 2.$$

We therefore have the two-dimensional system

$$\frac{\mathrm{d}x_1}{X_1(x_1, x_2, F(x_1, x_2, C))} = \frac{\mathrm{d}x_2}{X_2(x_1, x_2, F(x_1, x_2, C))}.$$

If we were to now differentiate equation (2.80), we would see that any integrating factor of this reduced system must satisfy

$$\left(\frac{\partial}{\partial x_1}(\mu X_1) + \frac{\partial}{\partial x_3}(\mu X_1) \frac{\partial F}{\partial x_1} \right) + \left(\frac{\partial}{\partial x_2}(\mu X_2) + \frac{\partial}{\partial x_3}(\mu X_2) \frac{\partial F}{\partial x_2} \right) = 0.$$

Substituting the two relationships given above, and with some simple application of the product rule for derivatives we find that

$$\frac{\partial}{\partial x_1} \left(\frac{\partial \phi}{\partial x_3} \mu X_1 \right) + \frac{\partial}{\partial x_2} \left(\frac{\partial \phi}{\partial x_3} \mu X_2 \right) - \frac{\partial}{\partial x_3} \left(\mu \left(\frac{\partial \phi}{\partial x_1} X_1 + \frac{\partial \phi}{\partial x_2} X_2 \right) \right) = 0.$$

However, knowing that ϕ is invariant, we obtain

$$\frac{\partial \phi}{\partial x_1} X_1 + \frac{\partial \phi}{\partial x_2} X_2 + \frac{\partial \phi}{\partial x_3} X_3 = 0,$$

and so this statement is precisely equivalent to saying that $\rho = \mu \frac{\partial \phi}{\partial x_3}$ must be a Jacobi multiplier for this reduced system. Conversely, using prior knowledge of this

multiplier ρ, we can construct an integrating factor for this final system by setting

$$\mu = \rho \left[\frac{\partial \phi}{\partial x_3} \right]^{-1}. \tag{2.81}$$

We remark that because of the way in which ϕ is used to construct this final integrating factor, it is often called *Jacobi's last multiplier*. Using induction we can then generalise this result to account for higher dimensional systems. This leads to the following theorem courtesy of Jacobi, which we write as it appears in [Boole, 1959]:

Theorem (Jacobi): If a system of $N-2$ functionally independent conservation laws f_1, f_2, ..., f_{N-2} of system (2.76) be so reduced by elimination that the variable x_1 shall not appear in f_2, the variables x_1, x_2 shall not appear in f_3 and so on; then the integrating factor for that first differential equation between x_{N-1} and x_N will be given by the formula

$$\mu = \rho \left[\frac{\partial f_1}{\partial x_1} \frac{\partial f_2}{\partial x_2} \cdots \frac{\partial f_{N-2}}{\partial x_{N-2}} \right]^{-1} \tag{2.82}$$

in which ρ represents a Jacobi multiplier of system (2.76).

As we have seen, the proof of this theorem provides a constructive method by which in theory, an explicit solution to system (2.76) can be obtained by quadratures. This does not mean, however, that the actual calculations involved in deriving this solution are in any way trivial. As we will see, even for the relatively simple example in the following chapters on the detuned and forced triad, proving integrability and finding these solutions explicitly are quite separate matters.

2.3.2 Liouville Integrability

Liouville integrability, as it is now known, is the classical concept of integrability as applied to finite-dimensional Hamiltonian systems. We say that a $2N$-dimensional Hamiltonian system is Liouville integrable if it possesses N functionally independent conserved quantities f_i, $i = 1, \ldots, N$, which are involution [Babelon et al., 2003]. By involution we mean that each invariant Poisson commutes with each and every other conserved quantity: for any i and j we have that

$$\{f_i, f_j\} = 0. \tag{2.83}$$

We know that for this integrable system, the phase spaced can be deconstructed into connected components formed by common level surfaces corresponding to each of these conserved quantities. This is called the Liouville foliation for this integrable system [Bolsinov and Fomenko, 2004].

Let us now assume that the flow is complete, and we choose one common level set of this foliation, which is compact and connected, then it is possible to prove that a solution for this Hamiltonian system can be obtained by quadratures [Babelon et al., 2003; Bolsinov and Fomenko, 2004]. This theorem was first accredited to Liouville. Specifically, it says that this level set is diffeomorphic to the N-dimensional torus, and that in a neighbourhood U of this torus, the Liouville foliation is trivially the direct product $U = D^N \times T^N$, between an N-dimensional torus and disc. What is crucial, however, is that it guarantees within this neighbourhood there is a canonical change of co-ordinates s_i, φ_i, $i = 1, \ldots, N$, called the action-angle variables where each of the action variables, s_i, is constant. We therefore have that

$$\dot{s}_j = 0, \ \dot{\varphi}_j = \frac{\partial H}{\partial s_j}, \tag{2.84}$$

which can be integrated trivially to see that each angle φ_j depends linearly on time only. It is worth noting that Liouville's theorem only guarantees that a solution can be obtained locally. An amended version of this theorem was developed later by Arnold that guarantees complete integrability across the entire phase space [Arnol'd et al., 1989]. Unsurprisingly, this global version is called the Liouville-Arnold theorem.

For Hamiltonian systems, we see that Liouville's theorem guarantees integrability, but does so requiring only half as many invariants as there are degrees of freedom. Compare this with Jacobi's theorem, where the best we could hope for is two less than the total dimensionality of the system. This seems especially striking considering that the majority of this thesis deals with Hamiltonian systems, namely those formed by resonant clusters of interacting waves. While Liouville's theorem states that an action-angle representation does exist, for realistic problems, the map defining these variables is often near impossible to find. For small systems, which roughly speaking we count as less than ten in this thesis, the discrepancy between the number of conservation laws required in each case diminishes. This is especially so when we consider that order reduction methods can be applied to these resonant clusters, where certain variables become 'slave' to others. Often these systems are no longer in canonical form, even though they remain Hamiltonian. This is where Jacobi's theorem comes into its own, and marries neatly with the actual systematic

approach used to solve these systems explicitly.

2.3.3 Lax Pair Representation

We have already seen the definition of a Hamiltonian system can be naturally extended to the infinite dimensional case, which we demonstrated in terms of a non-canonical formulation of the CHM equation. Applying periodic boundary conditions and taking the Fourier transform, this system admits an equivalent non-canonical representation with coordinates written in terms of each Fourier coefficient. We also demonstrated some examples of typically small, exactly resonant clusters which admit a canonical Hamiltonian representation. Here we are free to use any of the definitions of integrability covered above to determine the behaviour of these finite dimensional systems. What is now unclear, however, is what these concepts of integrability mean when the dimensionality is no longer finite. Indeed, if we have infinite degrees of freedom, simply counting the number of conservation laws seems absurd. In contrast to Hamiltonian systems, it seems at first that many of the ideas behind what makes a system integrable cannot be readily transferred to the infinite dimensional case.

Many of the issues surrounding what it means for an infinite dimensional system to be completely integrable were resolved with the introduction of what is known as the Inverse Scattering Transform [Beals and Sattinger, 1991]. Thought of as a nonlinear generalisation of the Fourier Transform, the problem is effectively linearised, being completely determined by the evolution of the scattering data, which is governed by a finite dimensional and linear system of ordinary differential equations. The scattering map that transforms the field into the scattering data is completely invertible, and so a solution can be recovered once we have determined the evolution of the scattering data. In essence, what we have described here sounds very familiar to the concept of C-integrability introduced earlier. This procedure was first applied by Kruskal et al. in application to the Korteweg-de Vries equation [Miura et al., 1968], where the associated linear problem was shown to be given by the one-dimensional Schrodinger equation. However, formalising what it meant for the KdV equation to be completely integrable came later. This came in two steps: first it was shown that the KdV equation possesses a canonical Hamiltonian structure, which can then be used to construct an infinite hierarchy of invariants that are in involution [Gardner, 1971]; and finally, this Hamiltonian structure was used to show that the scattering map in fact defines a transformation which reduces the problem to its action-angle variables [Zakharov and Faddeev, 1971]. As such, an explicit solution for the KdV equation can be obtained. This procedure laid the

foundations for the study of other exactly solvable models, such as the nonlinear Schrodinger equation, the Toda lattice and Sine-Gordon equation.

Central to this approach is the discovery of a Lax Pair for the problem in question. We define a Lax Pair as a pair of one-parameter, once differentiable operators $L(t)$ and $A(t)$, mapping a Hilbert space onto itself, which satisfy compatibility relation

$$L_t = [A, L]. \tag{2.85}$$

Here, the operator $[\cdot, \cdot]$ denotes the commutator. P. D. Lax showed that $L(t)$ is smoothly unitarily equivalent to $L(0)$ if and only if there exists an anti-Hermitian operator $A(t)$, which together with $L(t)$ forms a Lax Pair [Lax, 1968]. By definition, smoothly unitarily equivalent means there is a family of unitary once differentiable operators $g(t)$, with $g(0) = \mathrm{Id}$, such that $L(t) = g(t)L(0)g^{-1}(t)$. Since $L(t)$ and $L(0)$ are equivalent, it means that there eigenvalues must be identical, and so constant for all $t \geq 0$. The proof of this result is constructive as it gives $g(t)$ explicitly in terms of the solution to the initial value problem $g_t(t) = A(t)g(t)$, $g(0) = \mathrm{Id}$.

For the KdV equation, $L(t)$ is simply the Schrodinger operator

$$L(t) = \frac{\mathrm{d}^2}{\mathrm{d}x^2} + u(t). \tag{2.86}$$

The scattering data is then given simply by the eigenvalues of this operator, which are invariant, the normalising coefficients, and the reflection coefficients. Once we have determined the evolution of the eigenfunctions associated with each eigenvalue, the solution is obtained by performing the inverse scattering procedure as defined above.

The process underlying the inverse scattering transform is not actually of chief concern in this thesis; the systems we will mainly deal with are of finite dimension, and depend on time only only. Even though the CHM equation does admit a Lax Pair representation, and is Hamiltonian, we will never attempt to ascertain whether this implies that this equation is completely integrable as done with the KdV equation above. Indeed, it has already been established that existence of a Lax Pair does not necessary imply integrability of the type described above, as shown in [Chandre and Eilbeck, 2002]. What is significant is the isospectral property itself. In the following chapter on the detuned triad, we will show how determining a Lax Pair for this system provides a systematic approach to determining conservation laws for this system. Once this is done, we will show that integrability does in fact follow trivially, using Jacobi's $(N-2)$-integrability theorem.

It is worth noting that once a system is completely integrable in the Liouville

sense, and we have found the canonical transformation defining the action-angle variables, then it is fairly trivial to construct a Lax Pair for this system [Bolsinov and Fomenko, 2004]. In effect this is the converse of the statement that existence of a Lax Pair does not imply integrability. However, the knowledge of the Lax Pair is now redundant if we already know that the system is exactly solvable.

Chapter 3

The Detuned Triad

We have seen how a perturbation style analysis gives rise to clusters of resonantly interacting modes thought crucial to the underlying dynamics of most dispersive wave systems. These networks of interacting modes form the basis of discrete wave turbulence theory; the idea that for some suitable low level nonlinearity, reduced ODE systems of resonant modes effectively capture the dynamical behaviour of the entire wave system. This will be elaborated on further in later chapters when we start to consider the effect of resonance broadening, and how this categorises the system into three different turbulent regimes: the discrete, the statistical, and an intermixing of the two known as the mesoscopic. The transition between these regimes may be loosely connected with the idea that we increase the degrees of freedom in our system as we move from the regular discrete regime, towards a system exhibiting randomness well captured by some underlying statistical process. As we have discussed in the introduction and preliminary chapters, this transition marks the main theme of the thesis, and so where better to start than by considering the simplest cluster of interacting modes - the isolated triad.

In their most generalised form, after suitable re-scalings of the wave amplitudes, the interaction equations can always be reduced to the form:

$$\begin{cases} \dot{B}_1 = Z\mathrm{e}^{-i\delta t}B_2^*B_3, \\ \dot{B}_2 = Z\mathrm{e}^{-i\delta t}B_1^*B_3, \\ \dot{B}_3 = -Z\mathrm{e}^{i\delta t}B_1B_2, \end{cases} \tag{3.1}$$

where B_1, B_2 and B_3 are the re-scaled complex amplitudes of the modes dependent on time only. The real parameter $\delta = \omega_3 - \omega_1 - \omega_2$ corresponds to some finite resonant width. Equations (3.1) have been studied extensively for many years, even dating back to Euler's original work on motion of a rigid body. In a geophysical

context, however, their derivation dates back to the work of [McGoldrick, 1965] for studying the resonance of capillary-gravity waves. Shortly afterwards, while worthy of praise for its pioneering influence, at its heart it was criticised for its misinterpretation of secular growth terms and is failure to account for modulation in space as well as time. This was later made rigorous by the variational principle used in [Simmons, 1969], itself a modification of a previous Lagrangian formulation by [Whitham, 1965] and [Luke, 1967]. The elegance of this new derivation greatly simplified the interaction coefficients involved, allowing proof of the local conservation of wave energy and momentum. Naturally, this original work then allowed others to derive interaction equations for a host of other systems, including stratified fluids [Ball, 1964], barotropic Rossby waves [Ripa, 1981], and the development of resonant theory accounting for three- and four-wave interactions in plasmas [Boyd and Turner, 1978]. An excellent account of this history, including an outline of early experiments to identify resonance in actual physical systems, can be found in A. D. D. Craik's exceptional monograph on wave interactions and fluid flows [Craik, 1988].

Due to the prevalence and importance of mode coupling in physical systems, it is no wonder that solutions to equations (3.1) have been studied in a wide variety of different fields. To date, the majority of this work concerns itself with the exactly resonant case. Earliest examples date back to light waves in a nonlinear dielectric [Armstrong et al., 1962], electronics [Jurkus and Robson, 1960], and of course, fluid mechanics [Bretherton, 1964]. While the first of these two references give fully comprehensive accounts of how these solutions can be constructed in terms of Jacobi elliptic functions, the latter gave only asymptotic solutions but did account briefly for the effect of detuning. More recently, corresponding explicit formulae for a linear combination of the phases of each mode, the so-called dynamical phase, were obtained in [Bustamante and Kartashova, 2011] for the exactly resonant case. This was shown to have a remarkable effect on both the energy transfer, interaction timescales and variability in amplitudes of the system [Bustamante and Kartashova, 2009a]. We have also seen this system given a novel mechanical interpretation based on a spring pendulum [Lynch and Houghton, 2004; Lynch, 2003], with the thought being that some intuition as to the dynamics of more complicated systems, such as planetary waves, may be understood from simpler examples. This resurgence may be accounted for by the relatively new line of thinking underlying mesoscopic and discrete wave turbulence.

Certainly in the exactly resonant case, this work encompasses everything that is effectively known about the dynamics of the isolated triad. However, there are

certain exceptional cases when we see an explosive breakdown of solutions occurring in finite time. Implicit in our reduction of equations (3.1) to canonical form was that we could always assign the unstable mode to have a negative coefficient. As identified by [Cairns, 1979] this is not always possible in plasmas where the concept of negative wave energies allows the total energy of the system to remain conserved, but for all three modes to increase indefinitely in what is called an 'explosive instability'. This concept was developed analytically by [Craik and Adam, 1979] and [Coppi et al., 1969], where these explosive solutions were determined explicitly in addition to certain limiting cases. We therefore have that the more generalised interaction equations for the exactly resonant case, where we allow the signs of each coefficient to be left indeterminate, can admit both periodic and non-periodic solutions, and admit finite time singularities. This is definitely shown to be the case in the three-layer Kelvin-Helmholtz flow, which supports both explosive and periodic types. While explicit formulae detailing the solutions for the detuned triad, including analysis of when this explosive instability occurs [Craik, 1988], no in-depth study has been done to date that characterises fully this solution in terms of the strength of detuning. This chapter attempts to remedy this issue, determining boundedness, variability and periodicity of these solutions explicitly in terms of detuning.

As we have seen in the preceding chapter, system (3.1) admits a canonical Hamiltonian representation in the exactly resonant case. In fact, a large class of nonlinear dispersive PDEs can be recast in terms of Hamilton's equations, which then naturally transfers to more general clusters of arbitrary size and connectivity provided we consider only exactly resonant interactions [Bustamante and Kartashova, 2009b]. Here, they considered three different types of small cluster - the triad, kite and butterfly - consisting of three, four and five modes respectively. While the triad and kite are completely integrable, the same can only be said for certain configurations of the remaining butterfly. Historically, we find that the question of whether a certain Hamiltonian system is integrable to be intimately connected with the three-wave resonance equations, dating back to some of the the first work on the inverse scattering method. As a nonlinear analogue to the Fourier transform, it provides a way of solving certain nonlinear PDEs, as first applied to the Korteweg-de Vries equation [Gardner et al., 1974]. It was noted in [Moser, 1975] that this equation, as well other seemingly unrelated but explicitly solvable problems, are related simply through the fact that they all admit a Lax Pair. Finding such a pair of operators is essential to solving nonlinear problems of this type, and indeed the three-wave resonance interaction equations. The solution to the (1+1)-dimensions, or two space dimensions, three-wave interactions equations was first proposed by [Zakharov and

Manakov, 1973, 1975], and simultaneously by [Kaup, 1976].

In this chapter, we will reformulate equations (3.1) in terms of this Lax Pair representation. We will show that this provides a systematic approach to calculating all the necessary conservation laws to prove integrability of the detuned triad in the sense that a solution can be constructed explicitly in terms of quadratures. This is an important distinction to make, since often existence of a Lax Pair is thought to imply that a solution can be calculated explicitly, even though multiple counter-examples are known to exist [Chandre and Eilbeck, 2002]. Indeed, we have already shown in the preliminary chapters that both the 2D Euler equation and CHM equation admit a Lax Pair, yet to date no-one has proposed whether an approach exists, such as the inverse scattering techniques applied to the examples above, that can be used to directly integrate either equation for arbitrary initial conditions. Akin to the approach used to solve the exactly resonant triad, we will then re-derive an explicit solution for the amplitudes, which are well-known in the literature, and individual phases of the detuned triad, which appear often neglected. In contrast to the work on the dynamical phase cited above, we will show that this variable no longer remains bounded for sufficiently large detuning. The remaining part of the chapter is devoted to a numerical investigation on the effect of large detuning on the period and variation in amplitudes for the detuned triad. We will show that even for fixed constants of motion, the detuning plays a dominant role in the underlying evolution of the system, allowing us to set both the amplitudes of each mode and the period arbitrarily small. However, we fail to find an instance of whether the detuning produces the same kind of 'explosive instability' as mentioned above, with the solution remaining bounded for all values of detuning.

3.1 The Lax Pair

Lax Pairs for the N-wave interaction equations have been extensively studied, applied across a multitude of different domains and boundary conditions. As we have stated above, their attractiveness lies in how they form the basis of various different inverse scattering techniques, and so are fundamental to constructing an explicit solution to our problem. Lax pairs for the general N-wave problem have been proposed in [Pelloni and Pinotsis, 2009] and [Menyuk et al., 1982]. To account for the addition of detuning, the Lax Pairs constructed in these references needs to be modified, which has the effect of making each operator in the pair explicitly time-dependent. However, as shown in the second of these references, they still provide a practical means by which we can construct constants of motion for equations (3.1) in

a systematic fashion, removing the element of guess work that usually accompanies such a task.

To construct these conservation laws we use the isospectral property of the Lax Pair formalism. To remind the reader, we define a Lax Pair as a pair of one-parameter, once differentiable operators $L(t)$ and $A(t)$, mapping a Hilbert space onto itself, which satisfy compatibility relation

$$L_t = [A, L]. \tag{3.2}$$

Here, the operator $[\cdot, \cdot]$ denotes the commutator. P. D. Lax showed that $L(t)$ is smoothly unitarily equivalent to $L(0)$ if and only if there exists an anti-Hermitian operator $A(t)$, which together with $L(t)$ forms a Lax Pair [Lax, 1968]. By definition, smoothly unitarily equivalent means there is a family of unitary once differentiable operators $g(t)$, with $g(0) = \mathrm{Id}$, such that $L(t) = g(t)L(0)g^{-1}(t)$. Since $L(t)$ and $L(0)$ are equivalent, it means that their eigenvalues must be identical, and so constant for all $t \geq 0$. The proof of this result is constructive as it gives $g(t)$ explicitly in terms of the solution to the initial value problem $g_t(t) = A(t)g(t)$, $g(0) = \mathrm{Id}$.

Let us assume that B_1, B_2 and B_3 are complex functions of time only. The Lax pair for the canonical form of the detuned triad is given by the two time-dependent operators:

$$L(t) = \frac{i}{2}\begin{pmatrix} 0 & -5B_3\mathrm{e}^{-i\delta t} & -3B_2\mathrm{e}^{i\delta t} \\ 5B_3^*\mathrm{e}^{i\delta t} & 0 & -4B_1^*\mathrm{e}^{i\delta t} \\ 3B_2^*\mathrm{e}^{-i\delta t} & 4B_1\mathrm{e}^{-i\delta t} & 0 \end{pmatrix} + \frac{D}{Z}, \tag{3.3}$$

and

$$A(t) = \frac{Z}{2}\begin{pmatrix} 0 & -B_3\mathrm{e}^{-i\delta t} & B_2\mathrm{e}^{i\delta t} \\ B_3^*\mathrm{e}^{i\delta t} & 0 & -2B_1^*\mathrm{e}^{i\delta t} \\ -B_2^*\mathrm{e}^{-i\delta t} & 2B_1\mathrm{e}^{-i\delta t} & 0 \end{pmatrix}. \tag{3.4}$$

The constants Z and δ are assumed to be real with the latter corresponding to the resonance width. Here we have defined the real diagonal matrix $D = \mathrm{diag}\{d_1, d_2, d_3\}$, with non-zero entries that must satisfy the linear system

$$\begin{cases} d_3 - d_2 = -2\delta, \\ d_3 - d_1 = 3\delta, \\ d_1 - d_2 = -5\delta. \end{cases} \tag{3.5}$$

This system does in fact possess infinitely many solutions, and as such the Lax

pair for the detuned triad is not unique. However, choosing one of these solutions guarantees that the compatibility condition for $L(t)$ and $A(t)$ is equivalent to the dynamical system for the detuned triad given in equation (3.1).

3.1.1 Conservation Laws

Rather than calculating each eigenvalue explicitly, we can simply read off each constant of motion directly from the coefficients of the characteristic polynomial for L. Calculating this polynomial gives

$$\begin{aligned} p(\lambda) &= \det(L - \lambda I) \\ &= -\lambda^3 + \frac{\lambda^2}{Z}(d_1 + d_2 + d_3) + \lambda\left[\frac{I_1}{4} - \frac{1}{Z^2}(d_1d_2 + d_1d_3 + d_2d_3)\right] + \frac{d_1d_2d_3}{Z^3} - I_2, \end{aligned} \tag{3.6}$$

where because each d_j is constant, we have found the two new conservation laws:

$$I_1 = 16|B_1|^2 + 9|B_2|^2 + 25|B_3|^2, \tag{3.7}$$

$$I_2 = 15\Im\left\{B_1B_2B_3^*\mathrm{e}^{i\delta t}\right\} + \frac{1}{4Z}\left[16d_1|B_1|^2 + 9d_2|B_2|^2 + 25d_3|B_3|^2\right]. \tag{3.8}$$

Other invariants often cited in the literature revolve around the idea of constructing what appears to be an infinite number of conservation laws

$$V_n = \mathrm{tr}(L^n) = \sum_i \lambda_i^n,\ n \in \mathbb{N}, \tag{3.9}$$

by virtue that any function of any combination of eigenvalues for L must also be conserved. While each may be functionally independent for an infinite dimensional system, this is certainly not the case here. In fact we can calculate each V_n using a third order linear recursion relationship, which we will now demonstrate. Using the definition of V_n given above we have that

$$V_1V_{n+1} = V_{n+2} + (\lambda_1\lambda_2 + \lambda_1\lambda_3 + \lambda_2\lambda_3)V_n - \det(L)V_{n-1}. \tag{3.10}$$

We can read both the V_1 coefficient and the determinant directly from the characteristic polynomial. Explicitly this gives

$$V_{n+2} = V_1V_{n+1} - \left[\frac{1}{Z^2}(d_1d_2 + d_1d_3 + d_2d_3) - \frac{I_1}{4}\right]V_n + \left[\frac{d_1d_2d_3}{Z^3} - I_2\right]V_{n-1}. \tag{3.11}$$

All that remains is to calculate the first three terms to seed this recurrence relation. We find that

$$V_1 = \frac{1}{Z}(d_1 + d_2 + d_3), \tag{3.12}$$

$$V_2 = \frac{1}{Z^2}(d_1^2 + d_2^2 + d_3^2) + \frac{1}{2}I_1, \tag{3.13}$$

$$V_3 = \frac{1}{Z^3}(d_1^3 + d_2^3 + d_3^3) - 3I_2 + \frac{3}{4Z}(d_1 + d_2 + d_3)I_1. \tag{3.14}$$

It follows that all higher order values of V_n can be expressed in terms of I_1 and I_2. As such, this method proves fruitless in determining any genuinely new invariants for the system.

As we will see in the following section, to show that the detuned triad is locally integrable it is sufficient to have the two conservation laws I_1 and I_2 and to find a Jacobi last multiplier, courtesy of the $(N-2)$-integrability theorem. However, one final integral is still needed if we want to fully solve the system, which we can derive using the symmetry in equation (3.1) with respect to a relabelling of B_1 and B_2. This suggests that

$$J = \frac{|B_1|^2 - |B_2|^2}{2} \tag{3.15}$$

must also be conserved, which is trivial to check by differentiating J explicitly. If we now substitute J and I_1 into I_2 we uncover the simplified form

$$I = 2Z\Im\left\{B_1 B_2 B_3^* \mathrm{e}^{i\delta t}\right\} - \frac{\delta}{2}\left(|B_1|^2 + |B_2|^2\right), \tag{3.16}$$

as well as the pseudo-energy given by

$$E = |B_3|^2 + \frac{|B_1|^2 + |B_2|^2}{2}. \tag{3.17}$$

We call this the pseudo-energy to distinguish between the actual energy of the triad, before we re-scaled each complex amplitude. In the case when $\delta = 0$ we recognise I as the Hamiltonian for the exactly resonant triad. If we remove the quadratic term, system (3.1) is equivalent to Hamilton's equations

$$i\dot{B}_j = \frac{\partial H}{\partial B_j^*},\ j = 1, 2, 3, \tag{3.18}$$

together with their complex conjugates, but with time-dependent Hamiltonian

$$H = 2Z\Im\left\{B_1 B_2 B_3^* \mathrm{e}^{i\delta t}\right\}, \tag{3.19}$$

which is clearly no longer conserved by the dynamics.

3.1.2 Ancillary System

As an alternative approach to solving system (3.1) one might consider trying to compute the family of unitary transformations $g(t)$ directly. In fact, we know that since $L(t)$ is Hermitian, it admits an orthonormal basis of eigenvectors that can be used to diagonalise $L(t)$. Each non-zero entry of this diagonal matrix would consist of the real-valued eigenvalues of $L(t)$, which we know to be constant through the isospectral property detailed above. Computing these eigenvectors directly, we would have $g(t)$ explicitly in terms of each B_j. However, this is ultimately fruitless if we want explicit formulae detailing the evolution of each amplitude and their phases. Instead, one could consider solving the initial value problem

$$g_t(t) = A(t)g(t),\ g(0) = I_3, \tag{3.20}$$

where I_3 represents the 3×3 identity matrix. Doing so would give the solution to the original problem as

$$L(t) = g(t)L(0)g^{-1}(t). \tag{3.21}$$

This gives the following dynamical system for the evolution of each column of $g(t)$:

$$\begin{cases} \dot{g}_1 = \dfrac{Z}{2}\left(g_3 B_2 \mathrm{e}^{i\delta t} - g_2 B_3 \mathrm{e}^{-i\delta t}\right), \\ \dot{g}_2 = \dfrac{Z}{2}\mathrm{e}^{i\delta t}\left(g_1 B_3^* - 2g_3 B_1^*\right), \\ \dot{g}_3 = \dfrac{Z}{2}\mathrm{e}^{-i\delta t}\left(2g_2 B_1 - g_1 B_2^*\right), \end{cases} \tag{3.22}$$

which must be solved subject to the three different initial conditions corresponding to $g(0) = I_3$. The fact that the detuned triad admits an explicit solution, and that each eigenvector could be computed algebraically, suggests that this system is fully solvable. However, solving this ancillary system without knowing these solutions beforehand seems difficult as the only readily available conservation law appears to be

$$|g_1|^2 + |g_2|^2 + |g_3|^2 = 1, \tag{3.23}$$

which is just an expression that each column of $g(t)$ must be normalised.

3.2 Solution to the detuned triad

With the exactly resonant triad, we can know that system (3.1) can be reduced to a four-dimensional, volume preserving one, and so integrability follows trivially using any two conservation laws, such as E and J found above, for example. However, for $\delta \neq 0$, this system is now non-autonomous, suggesting that we might need three conservation laws, together with a Jacobi multiplier, to satisfy the necessary conditions for the $(N-2)$-integrability theorem. This is because we can extend any non-autonomous system to an autonomous one by treating time itself as a dependent variable at the cost of one extra degree of freedom. However, writing each mode in terms of its phase-amplitude representation $B_j = C_j \exp(i\varphi_j)$, $j = 1, 2, 3$, with $C_j \in \mathbb{R}$ and $\varphi_j \in \mathbb{R}$ we have

$$\dot{B}_j = \left(\dot{C}_j + iC_j\dot{\varphi}_j\right) \mathrm{e}^{i\varphi_j}.$$

Using these new variables, we can still reduce system (3.1) to a four-dimensional, volume preserving one

$$\begin{cases} \dot{C}_1 = ZC_2C_3\cos\varphi, \\ \dot{C}_2 = ZC_1C_3\cos\varphi, \\ \dot{C}_3 = -ZC_1C_2\cos\varphi, \\ \dot{\varphi} = \dfrac{1}{2}\left(I + \dfrac{\delta}{2}(C_1^2 + C_2^2)\right)\left(C_3^{-2} - C_2^{-2} - C_1^{-2}\right) + \delta. \end{cases} \tag{3.24}$$

The variable φ is called the dynamical phase. It now differs from its usual definition through the addition of a δ-dependent term to become $\varphi = \varphi_1 + \varphi_2 - \varphi_3 + \delta t$. By using this variable, each individual phase, φ_j, $j = 1, 2, 3$ becomes 'slave' to the dynamical phase and the three different amplitudes; their solution can only be obtained after we have found the solution for each remaining variable. Since the Jacobi multiplier is trivially constant, we can now apply the $(N-2)$-integrability theorem with any two of the conservation laws found in the preceding section. In fact, we know three functionally independent conservation laws and so integrability follows trivially without even having recourse to use this theorem.

Using the three conservation laws, E, J and I, together with the order reduction above, suggests that system (3.24) has a one-dimensional representation. The first step is to define the variable

$$u(t) = \frac{C_1^2 + C_2^2}{2}, \tag{3.25}$$

which when differentiated, we get

$$\frac{\mathrm{d}u}{\mathrm{d}t} = 2Z\Re\left\{B_1B_2B_3^*\mathrm{e}^{i\delta t}\right\}. \tag{3.26}$$

The choice of this variable is then made clear: since the invariant I is naturally written in terms of u and the imaginary part of its derivative, we have that

$$\left[\frac{\mathrm{d}u}{\mathrm{d}t}\right]^2 + (I+\delta u)^2 = 4Z^2C_1^2C_2^2C_3^2. \tag{3.27}$$

Using the remaining conservation laws we can evaluate the right-hand side of this equation in terms of u alone. For instance, we know that both

$$u^2 - J^2 = C_1^2C_2^2, \tag{3.28}$$

and trivially,

$$E - u = C_3^2. \tag{3.29}$$

The choice of J over the standard Manley-Rowe invariants is also highlighted the by the simplicity of relationship (3.28). Finally, so as to make the dependence on δ explicit we introduce the re-scaled Hamiltonian for the exactly resonant triad,

$$G(t) = \Im\left\{B_1B_2B_3^*\right\}. \tag{3.30}$$

As you recall, this is not conserved, but allows us to write $I(t) = 2ZG(0) - \delta u(0)$. Finally, we can remove the explicit dependence on Z by rescaling both time, $\tau = 2|Z|t$, and the detuning parameter, $\delta = 2Z\bar{\delta}$. Combining each of these, we arrive at the one-dimensional particle representation

$$\left[\frac{\mathrm{d}u}{\mathrm{d}\tau}\right]^2 + \left[G_0 + \bar{\delta}(u-u_0)\right]^2 + (u-E)(u^2-J^2) = 0 \tag{3.31}$$

This is precisely the statement that the total energy of the particle trapped within a cubic potential is conserved. To solve this system we need to find the roots of this cubic potential, which if we now expand and make the linear transformation

$$v = u + \frac{1}{3}(\bar{\delta}^2 - E), \tag{3.32}$$

gives the reduced cubic form

$$\left[\frac{\mathrm{d}v}{\mathrm{d}\tau}\right]^2 = -(v^3 + pv + q). \tag{3.33}$$

Here we have defined the two constants

$$\begin{cases} p = -\dfrac{1}{3}\left[(\bar{\delta}^2 - E)^2 + 3(2\bar{\delta}^2 u_0 - 2\bar{\delta}G_0 + J^2)\right], \\ q = \dfrac{(\bar{\delta}^2 - E)}{27}\left[2(\bar{\delta}^2 - E)^2 + 9(2\bar{\delta}^2 u_0 - 2\bar{\delta}G_0 + J^2)\right] + EJ^2 + (G_0 - \bar{\delta}u_0)^2. \end{cases} \tag{3.34}$$

Let us define the cubic potential appearing in equation (3.33) by $P(v) = v^3 + pv + q$. Roots of this cubic determine the boundedness of the solution $v(t)$. Returning to our one-dimensional particle representation, if P admits three real roots, then depending on the initial conditions, the particle is trapped, oscillating between two consecutive roots of this cubic potential. The other option is that only one real root exists. Here the motion is no longer bounded and we see a finite-time singularity develop. This is identical to the 'explosive instability' witnessed in [Coppi et al., 1969].

For this cubic to admit three real roots, we require that both $p \leq 0$, and for the discriminant

$$D(p, q) = -\frac{1}{2}q\left(\frac{3}{|p|}\right)^{\frac{3}{2}} \tag{3.35}$$

to have absolute value less than or equal to one. In the exactly resonant case when $\delta = 0$ we find that

$$p = -\frac{1}{3}\left[E^2 + 3J^2\right],$$

which is trivially negative for all initial conditions. It is relatively simple to prove the corresponding condition for the discriminant in this case. However, what can be said for $\bar{\delta}$ generally. As we will see, the fact that the pseudo-energy is constant does not necessarily imply that each individual amplitude must also remain bounded.

3.2.1 The case when $P(v)$ admits three real roots

Let us assume that the cubic $P(v)$ admits three real roots, which we call β_k for $k = 1, 2, 3$. These roots have an elegant trigonometric representation as given by

[Nickalls, 2006]. If we define $\theta \in [0, \pi]$ by $\cos\theta = D$, then these roots are given by

$$\begin{cases} \beta_1 = \sqrt{\frac{4}{3}|p|}\cos\left(\frac{\theta}{3}\right), \\ \beta_2 = -\sqrt{\frac{4}{3}|p|}\cos\left(\frac{\theta}{3} + \frac{\pi}{3}\right), \\ \beta_3 = -\sqrt{\frac{4}{3}|p|}\cos\left(\frac{\theta}{3} - \frac{\pi}{3}\right), \end{cases} \tag{3.36}$$

which we have written in the order $\beta_1 > \beta_2 > \beta_3$. Once we have found these three roots, it is relatively straightforward to integrate equation (3.33) using any of the standard references such as [Abramowitz and Stegun, 1965]. We find that

$$v(t) = -(\beta_1 - \beta_2)\,\mathrm{sn}^2\left(|Z|\sqrt{\beta_1 - \beta_3}\,t - t_0 \,\middle|\, m\right) + \beta_1, \tag{3.37}$$

where the Jacobi elliptic function $\mathrm{sn}(\,\cdot \mid m)$ is defined in terms of a parameter called the modulus,

$$m = \frac{\cos\left(\frac{\theta}{3} + \frac{\pi}{6}\right)}{\cos\left(\frac{\theta}{3} - \frac{\pi}{6}\right)}. \tag{3.38}$$

The value of the constant t_0 can be computed explicitly in terms of the incomplete elliptic integral of the first kind:

$$t_0 = sF\left(\arcsin\left(\sqrt{\frac{v(0) - \beta_1}{\beta_2 - \beta_1}}\right) \,\middle|\, m\right), \tag{3.39}$$

where we have defined the constants $v(0) = \frac{1}{3}\left(C_1(0)^2 + C_2(0)^2 - C_3(0)^2 + \bar{\delta}^2\right)$ and $s = \mathrm{sgn}\left(Z\Re\left\{B_1(0)B_2(0)B_3^*(0)\right\}\right)$. Since $\mathrm{sn}^2(u \,|\, m)$ is periodic in u with period $2K(m)$, where $K(m)$ is the complete elliptic integral of the first kind, we have that $v(t)$ must be likewise periodic. Calculating this period we find that

$$T = \frac{\sqrt{2}K(m)}{|Z||p|^{\frac{1}{4}}\sqrt{\cos\left(\frac{\theta}{3} - \frac{\pi}{6}\right)}}. \tag{3.40}$$

Solutions for the squared amplitudes

Now that we have an explicit solution for $v(t)$, we can uncover a solution for each of the amplitudes through the conservation laws E and J. We have that

$$\begin{cases} C_1(t)^2 = v(t) + \frac{1}{3}(E - \bar{\delta}^2) + J, \\ C_2(t)^2 = v(t) + \frac{1}{3}(E - \bar{\delta}^2) - J, \\ C_3(t)^2 = -v(t) + \frac{1}{3}(\bar{\delta}^2 + 2E). \end{cases} \tag{3.41}$$

Because each of these squared-amplitudes must be positive, we find the following bound on the largest root, β_1:

$$\frac{1}{3}\left(\bar{\delta}^2 - E\right) - |J| \leq \beta_1 \leq \frac{1}{3}\left(\bar{\delta}^2 + 2E\right). \tag{3.42}$$

Similar bounds can be found for the remaining two roots. We have plotted this solution in figures (3.1(a)) and (3.1(b)) for two different values of detuning.

Solutions for the individual phases

All that remains is to calculate the solution for each of the individual phases of B_j, $j = 1, 2, 3$. Using the same phase-amplitude representation we saw in the derivation of the reduced system (3.24), we have that

$$\begin{cases} \dot{\varphi}_1 = -\frac{1}{2}\frac{I + \delta u(t)}{u(t) + J}, \\ \dot{\varphi}_2 = -\frac{1}{2}\frac{I + \delta u(t)}{u(t) - J}, \\ \dot{\varphi}_3 = +\frac{1}{2}\frac{I + \delta u(t)}{u(t) - E}. \end{cases} \tag{3.43}$$

Since $v(t)$ and hence $u(t)$ is known explicitly, each of these differential equations can be integrated, providing a solution in terms of the incomplete elliptic integral of the third kind, $\Pi(n; z \,|\, m)$. First we simplify notation by introduction the function $\omega(t) = \text{am}\left(|Z|\sqrt{\beta_1 - \beta_3}\, t - t_0 \,|\, m\right)$, known as the Jacobi amplitude. Let us also define the three constants, called the elliptic characteristics, by

$$n_j = \frac{\beta_1 - \beta_2}{\beta_1 + (E - \bar{\delta}^2)/3 + c_j}, \; j = 1, 2, 3, \tag{3.44}$$

where $c_1 = J$, $c_2 = -J$ and $c_3 = -E$. The solution for the three phases is given by

$$\varphi_j(t) = \frac{s_j}{2}\left[\delta t + \frac{n_j(I-\delta c_j)}{m|Z|(\beta_1-\beta_3)^{\frac{3}{2}}}\Pi\left(n_j;\omega(t')\,\middle|\,m\right)\Big|_{t'=0}^{t'=t}\right] + \varphi_j(0), \tag{3.45}$$

where we must choose $s_1 = s_2 = -1$ and $s_3 = +1$, representing the different signs present in equations (3.43). While each of the amplitudes are periodic, their phases are clearly not. This can be identified in figures (3.1(c)) and (3.1(d)).

Solution for the dynamical phase

For the exactly resonant triad, it was shown in [Bustamante and Kartashova, 2009b] that the dynamical phase remains confined to one of the intervals $[n\pi,(n+1)\pi]$, $n \in \mathbb{Z}$, where the choice of interval depends on the initial conditions. An explicit solution was found for $\varphi(t)$ that avoids evaluating each individual phase as detailed above. The significance of the dynamical phase was highlighted in [Bustamante and Kartashova, 2009a] where it was shown to significantly affect the timescales of energy transfer and variability in the individual amplitudes of each mode. With this in mind, we now find a solution for the dynamical phase that takes in account the effect of non-zero detuning.

As was noted in the references above, we cannot simply rearrange the conservation law I and solve to find $\sin\varphi$. This is because the inverse-sine function is ill-defined on any of the intervals $[n\pi,(n+1)\pi]$. Instead, we can re-write the equation of motion for C_3 as

$$\cot\varphi = -\frac{1}{I+\delta u}\frac{\mathrm{d}}{\mathrm{d}t}\left(C_3^2\right). \tag{3.46}$$

The derivative on the right-hand side of this equation can be found explicitly by differentiating the result given in equations (3.41). We obtain

$$\cot\varphi = -2|Z|m\,(\beta_1-\beta_3)^{\frac{3}{2}}\,\frac{\operatorname{sn}\,\operatorname{cn}\,\operatorname{dn}\left(|Z|\sqrt{\beta_1-\beta_3}\,t-t_0\,|\,m\right)}{I+\delta u}, \tag{3.47}$$

where we have defined the function $\operatorname{sn}\,\operatorname{cn}\,\operatorname{dn}(u\,|\,m) = \operatorname{sn}(u\,|\,m)\operatorname{cn}(u\,|\,m)\operatorname{dn}(u\,|\,m)$ to simplify notation. We immediately identify a problem with this solution since it is only well-defined if $|I+\delta u(t)| > 0$ for all $t \geq 0$. This is clearly not an issue with the exactly resonant triad since $\delta = 0$. For sufficiently small δ this solution remains correct, provided we define the inverse-cotangent as mapping to the correct interval. For larger δ, this condition no longer holds, and a singularity develops

at the times when $\varphi(t)$ moves between the intervals $[n\pi, (n+1)\pi]$. The solution still remains T-periodic provided we take $\varphi(t)$ mapping to the interval $[0, 2\pi]$ with periodic boundary conditions. We have plotted these two different types of solution for the dynamical phase in figures (3.1(e)) and (3.1(f)).

3.2.2 The case when only one root of $P(v)$ is real

Let us assume that $P(v)$ admits one real root, β_1, and a pair of complex conjugate roots, $\beta_2 = \beta_3^*$. This case corresponds to the 'explosive instability' mentioned in [Craik and Adam, 1979], and can occur in physical systems such as those modelling three-layer fluid flow in plasmas where the concept of negative energy is used.

Without expressing each of the roots explicitly, equation (3.33) now reads

$$\left[\frac{\mathrm{d}v}{\mathrm{d}\tau}\right]^2 = -(v-\beta_1)(v^2 - 2\Re\{\beta_2\}v + |\beta_2|^2). \tag{3.48}$$

We can still reduce this differential equation by a sequence of transformations to recover a solution in terms of one of the Jacobi elliptic functions. For instance, in this case we use a Moebius transformation of the form

$$w = \frac{a - \beta_1 + v}{a + \beta_1 - v},$$

where $a > 0$ is set by

$$a^2 = \beta_1^2 - 2\Re\{\beta_2\}\beta_1 + |\beta_2|^2. \tag{3.49}$$

With some routine manipulation we uncover the solution

$$v_s(t) = -a\tan^2\left(\frac{1}{2}\mathrm{am}\left(2|Z|\sqrt{a}\;t - u \mid m_s\right)\right) + \beta_1. \tag{3.50}$$

where m_s is the elliptic modulus given by

$$m_s = \frac{a + \beta_1 - \Re\{\beta_2\}}{2a}. \tag{3.51}$$

Here we have used the s-subscript to distinguish between this case, where a singularity develops, and the previous one. It is trivial to show that $0 < m_s < 1$ as required. The constant u can be calculated explicitly as

$$u = sF\left(2\arctan\left(\sqrt{\frac{\beta_1 - v(0)}{a}}\right) \;\middle|\; m_s\right), \tag{3.52}$$

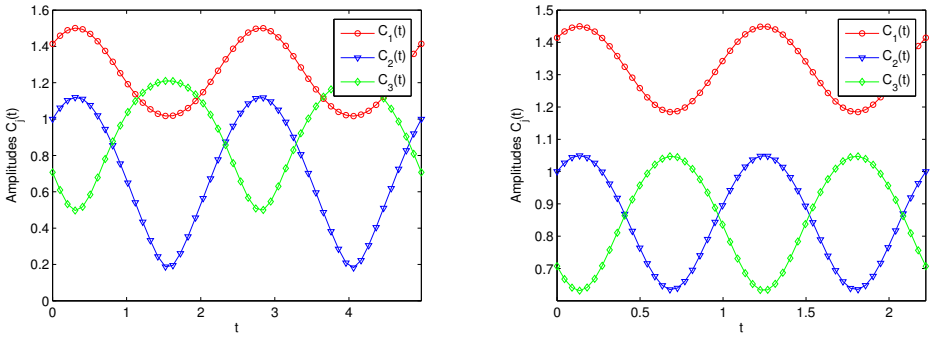

(a) Amplitudes, $\delta = 1$

(b) Amplitudes, $\delta = 5$

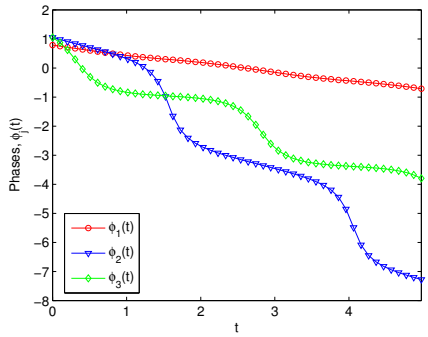

(c) Phases, $\delta = 1$

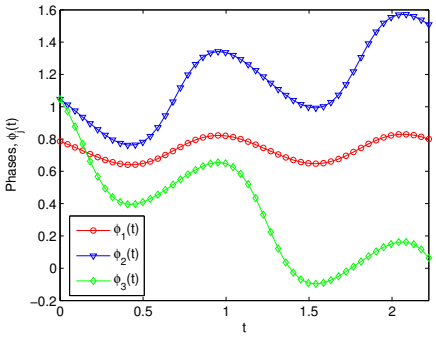

(d) Phases, $\delta = 5$

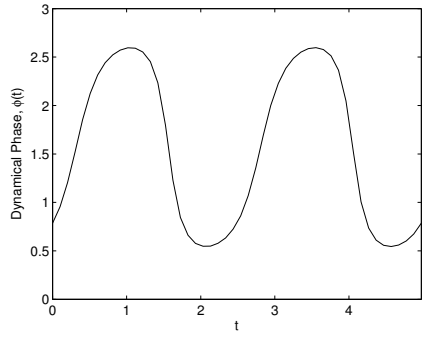

(e) Dynamical Phase, $\delta = 1$

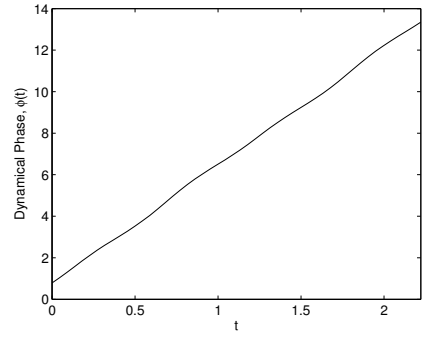

(f) Dynamical Phase, $\delta = 5$

Figure 3.1: Solutions for the individual amplitudes, phases and dynamical phases for two different levels of detuning δ. We have chosen initial conditions $E = 2$, $u_0 = \frac{3}{2}$, $J = \frac{1}{2}$, $\varphi(0) = \frac{\pi}{4}$ and $Z = 1$. Individual phases cease to be monotonic for larger detuning, and the dynamical phase no longer remains bounded. We also see the period and variability in amplitudes decreasing as well.

where the values of s and $v(0)$ are the same as above.

The solution for the amplitudes given in equation (3.41) still holds, which means that each amplitude diverges simultaneously whenever

$$t_n = \frac{2(2n-1)K(m)+u}{2|Z|\sqrt{a}},\ n \in \mathbb{Z}. \tag{3.53}$$

For the very same reason, however, this means that when calculating the pseudo-energy directly from equation (3.17), this quantity remains constant by the virtue that each time-dependent term cancels. This way we can still have a situation where the total wave energy remains conserved, but where each amplitude in a triad of modes can diverge simultaneously, as corroborated by [Coppi et al., 1969]. All that remains to show therefore, at least numerically, is that this case is completely redundant for arbitrary initial conditions and for all values of detuning.

3.3 Numerical study into the effect of detuning

The goal of this section is two-fold: first, we want to show that for arbitrary initial conditions and for all values of detuning, the explosive instability mentioned above never occurs; and second, we want to characterise the limiting behaviour of the solution when the detuning becomes large. Both are important in their own right. However, the second gives us some insight into the collective role of resonance broadening when we consider the wave system as a whole. For instance, whether the dynamics of small clusters with sufficiently large resonance broadening can be neglected, which is one of the principle arguments behind discrete wave turbulence theory.

Let us now consider the first of these points. Building a case to support this assertion relies on proving two key arguments. Namely, that $p(\bar{\delta}) < 0$ for all $\bar{\delta} \in \mathbb{R}$, and that $|D(p,q)| < 1$ for all $\bar{\delta} \in \mathbb{R}$. Both of these statements must also be verified for arbitrary initial conditions.

3.3.1 Parameterising our choice of initial conditions

Before we begin, we present a novel parameterisation of our initial conditions that reduces the problem from one of infinite variability in each J, E and u_0 to one restricted to a domain of finite measure. This makes the problem both easier to visualise and verify numerically. To do this, we introduce two new variables

$$\gamma_1 = \frac{u_0}{E},\ \gamma_2 = \frac{J}{E}. \tag{3.54}$$

These can be considered as being allowed to vary independently, and are restricted to the domains $0 < \gamma_1 < 1$ and $-1 < \gamma_2 < 1$. Moreover, once we have stipulated the value of $C_3(0)^2$, we can find the initial values for the remaining two amplitudes simply by

$$\begin{cases} C_1(0)^2 = C_3(0)^2 \dfrac{\gamma_1 + \gamma_2}{1 - \gamma_1}, \\ C_2(0)^2 = C_3(0)^2 \dfrac{\gamma_1 - \gamma_2}{1 - \gamma_1}. \end{cases} \tag{3.55}$$

For each of these amplitudes to be positive, we must also apply the additional constraint $\gamma_1 \geq |\gamma_2|$. Moreover we observe that we can write G_0^2 purely in terms of

$$G_0^2 = E^3(1 - \gamma_1)(\gamma_1^2 - \gamma_2^2) \sin^2 \varphi(0). \tag{3.56}$$

This has some practical benefit, since $G(t)$ represents the Hamiltonian of the exactly resonant triad. Using this new parameterisation, we know that the choice of u_0 that maximises this Hamiltonian for fixed E can be determined by setting

$$\gamma_1^* = \frac{1}{3}\left(1 + \sqrt{1 + 3\gamma_2^2}\right). \tag{3.57}$$

Once this is done, the global maximum for this Hamiltonian can be found by simply setting $\gamma_2 = 0$ and trivially, $\sin^2 \varphi(0) = 1$.

3.3.2 Proof for $p(\delta) < 0$

We have already shown that $p(0) < 0$ for arbitrary initial conditions. It is also clear to see that for sufficiently large $|\bar{\delta}|$, $p(\bar{\delta})$ must also be negative. What is less clear, however, is what happens for intermediate values of $\bar{\delta}$. Since $p(\bar{\delta})$ is a quartic polynomial in $\bar{\delta}$, if we can show that it admits only two pairs of complex conjugate roots for all choices of initial condition then we are done. Let us write this quartic polynomial, after expanding each term fully and eliminating common factors, as

$$R(x) = x^4 + 2(3u_0 - E)x^2 - 6G_0 x + 3J^2. \tag{3.58}$$

Fortunately, this quartic is already in reduced form with the cubic coefficient being zero. As shown in [Nickalls, 2009], Euler's solution to the quartic equation $R(x) = 0$ relies of finding roots to the resolvent cubic equation

$$z^3 + 4(3u_0 - E)z^2 + 4\left[9u_0^2 - 6u_0 E - 3J^2\right] z - 36G_0^2 = 0. \tag{3.59}$$

It is then relatively straightforward to show that if this resolvent cubic admits three real roots, one being positive and two negative, then $R(x)$ can only have two pairs of complex conjugate roots.

As before with our derivation of equation (3.31), the first step to finding roots of this resolvent cubic is to make the transformation

$$y = z + \frac{4}{3}(3u_0 - E). \tag{3.60}$$

This now gives us the reduced cubic

$$y^3 + p'y + q' = 0, \tag{3.61}$$

except with constants

$$\begin{cases} p' = -\dfrac{4}{3}\left[(3u_0 - E)^2 + 3(E^2 + 3J^2)\right], \\ q' = -\dfrac{4}{27}\Big\{4(3u_0 - E)\left[(3u_0 - E)^2 - 9(E^2 + 3J^2)\right] + 243G_0^2\Big\}. \end{cases} \tag{3.62}$$

We have therefore eliminated one degree of freedom related to the detuning, and reformulated the problem in terms of conditions for p' and q'. These conditions equate to first showing that $p' < 0$ for arbitrary initial values, which is trivial, and finally, showing that the discriminant of the cubic equation given in (3.60) is always bounded in absolute value by one. This discriminant we define by

$$C(p', q') = -\frac{1}{2}q'\left(\frac{3}{|p'|}\right)^{\frac{3}{2}}. \tag{3.63}$$

Once these conditions are shown to hold, we know that the resolvent cubic given in equation (3.59) admits three real roots. The final part is then to show that precisely one of these roots is positive, and the remaining two are negative.

Writing p' and q' in terms of our new variables γ_1 and γ_2 gives

$$C(\gamma_1, \gamma_2, \varphi_0)^2 = \frac{\left[(3\gamma_1 - 1)^3 - 9(3\gamma_1 - 1)(1 + 3\gamma_2^2) + \frac{243}{4}(1 - \gamma_1)(\gamma_1^2 - \gamma_2^2)\sin^2\varphi_0\right]^2}{\left[(3\gamma_1 - 1)^2 + 3(1 + 3\gamma_2^2)\right]^3}. \tag{3.64}$$

When restricted to the domain described above, one can readily verify that C attains its maximum at the three points on the boundary $(\gamma_1, \gamma_2) = (0, 0)$ and $(\gamma_1, \gamma_2) = (1, \pm 1)$, independent of the value of $\varphi(0)$. In all of these cases, the value of this maximum is one, and so immediately we verify that $C(\gamma_1, \gamma_2, \varphi(0))^2 < 1$ for any dynamically accessible choice of γ_1, γ_2 or $\varphi(0)$. As an example, we have plotted the

profile of this discriminant for two different values of $\varphi(0)$ in figure (3.2).

Now we know that $C < 1$ is in fact true, it would imply that the resolvent cubic given in equation (3.59) admits three real roots, which we label z_k for $k = 0, 1, 2$. Since we have that $z_0 z_1 z_2 = 36G_0^2 > 0$, the only possible outcomes are either that they are all positive, or one positive and two negative. All that remains to show, therefore, is that at least one of the z_k is always negative. In fact, we know that we can calculate these roots explicitly: if we define the angle $\alpha \in [0, \pi]$ such that $\cos\alpha = C$, then we have

$$z_k = \frac{4E}{3}\left[\sqrt{(3\gamma_1 - 1)^2 + 3(1 + 3\gamma_2^2)}\cos\left(\frac{\alpha}{3} + \frac{2\pi k}{3}\right) - (3\gamma_1 - 1)\right]. \tag{3.65}$$

If we now consider just the root z_1, we see that it achieves a maximum value of zero at the point $\gamma_1 = \gamma_2 = \alpha = 0$. Since we exclude this point by virtue that it would imply that two of the amplitudes are identically zero, we have that z_1 is strictly negative. We conclude by saying that the quartic equation $R(x) = 0$ has two pairs of complex conjugate roots and so $p(\bar{\delta}) < 0$ for all initial conditions and all values of $\bar{\delta}$.

3.3.3 Numerical evidence for $D(p, q)^2 < 1$

Unfortunately, $D(p, q)$ does not lend itself to the same analytical treatment as we saw for proving $p < 0$. We can, however, still rewrite $D(p, q)$ in terms of two new variables γ_1 and γ_2, making the problem more manageable, except that we have to consider the two extra degrees of freedom corresponding to $\varphi(0)$ and δ. To simplify notation, we first define

$$\begin{cases} \eta_1 = (\delta')^2 - 1, \\ \eta_2 = \gamma_1(\delta')^2 - (\delta')\sqrt{(\gamma_1^2 - \gamma_2^2)(1 - \gamma_1)}\sin\varphi_0 + \frac{1}{2}\gamma_2^2, \end{cases} \tag{3.66}$$

where we have re-scaled the detuning parameter once more to get $\delta' = \bar{\delta}/\sqrt{E}$. We see that η_1 is not independent of η_2 and vice-versa, leaving the problem incompletely defined if we were to use these variables on their own. The problem remains four-dimensional, therefore, where

$$D(\gamma_1, \gamma_2, \delta', \varphi(0))^2 = \frac{\left[\eta_1^3 + 9\eta_1\eta_2 + 27\left(\frac{\gamma_2^2}{2} + \frac{(\eta_2 - \gamma_2^2/2)^2}{2(1+\eta_1)}\right)\right]^2}{\left[\eta_1^2 + 6\eta_2\right]^3}. \tag{3.67}$$

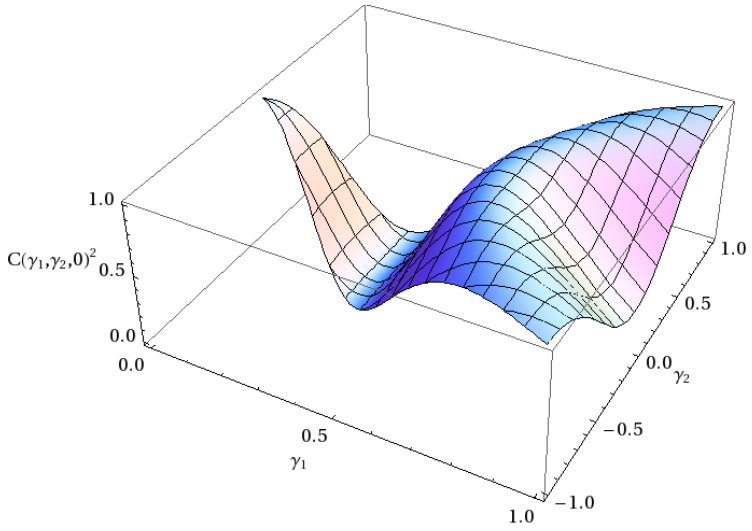

(a) $\varphi(0) = 0$

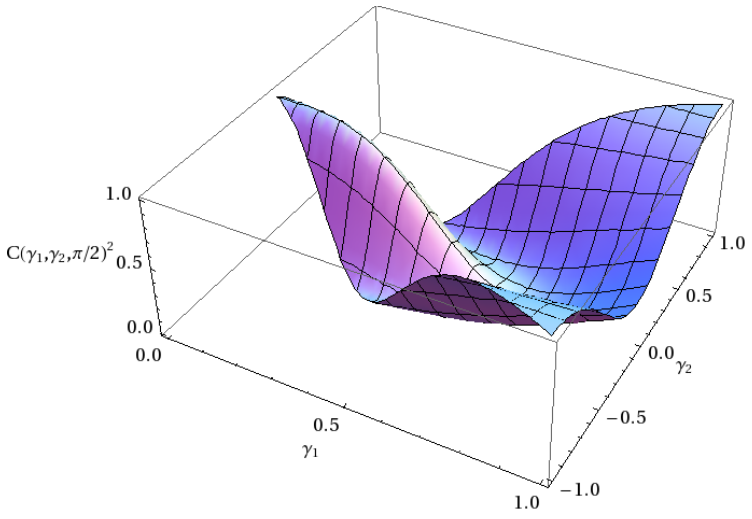

(b) $\varphi(0) = \pi/2$

Figure 3.2: The discriminant $C(\gamma_1, \gamma_2, \varphi(0))$ plotted for two different values of φ_0. We see the appearance of maxima at the points on the boundary $(\gamma_1, \gamma_2) = (0, 0)$ and $(\gamma_1, \gamma_2) = (1, \pm 1)$ where $C(\gamma_1, \gamma_2, \varphi(0))^2 = 1$, independent of the value of $\varphi(0)$.

We have plotted $D(\gamma_1, \gamma_2, \delta', \varphi(0))^2$ for different values of δ in figure (3.3). Since both numerator and denominator are twelfth order polynomials in δ', with identical leading twelfth order coefficients, we see that $D(\gamma_1, \gamma_2, \delta', \varphi(0))^2 \to 1$ uniformly as $|\delta'| \to \infty$. This can already be seen in figure (3.3) for the relatively small value of $\delta' = 2$. We readily identify what appears to be global maxima, independent of either $\varphi(0)$ or δ', when $(\gamma_1, \gamma_2) = (1, \pm 1)$ and $\gamma_1 = \gamma_2 = 0$, with $D^2 = 1$ evaluated at these points.

The limiting behaviour seen here for large $|\delta|$ has a significant effect on the behaviour of the detuned triad. It suggests that for sufficiently large $|\delta|$, we should expect the elliptic modulus to vanish. At this point each Jacobi elliptic function begins to represent its regular trigonometric counterpart. Furthermore, this has direct implications for the both variability in amplitudes and the period of motion, which we will now investigate.

3.3.4 The limiting case when detuning is large

We have already found an explicit expression for the period given by equation (3.40). To calculate the variability in the amplitude of each mode, we define

$$\sigma(p, \theta) = \beta_1 - \beta_2 = 2\sqrt{|p|}\cos\left(\frac{\theta}{3} + \frac{\pi}{6}\right). \tag{3.68}$$

This can be read directly from the solution for $v(t)$ given in equation (3.37). It represents how willingly energy is exchanged between the two passive modes and the unstable B_3 mode. Unlike the period, which we will consider momentarily, σ is so far undetermined in the limit as $|\delta|$ becomes large. To resolve this issue we have plotted σ in figure (3.4a), where we have allowed only J and δ to vary. Surprisingly, we can clearly identify a maximum value at the point $(\delta, J) = (1, 0)$. We should expect resonance broadening to typically diminish the quantity of energy transferred between each mode, but this is clearly not always the case.

Finally we consider how the period responds in the presence of large detuning. Since we know $D \to -1$ uniformly as $|\delta| \to \infty$, we can assume that the elliptic modulus vanishes in this limit. We can therefore make the approximation

$$T \approx \frac{\pi}{|Z||3p|^{\frac{1}{4}}}, \tag{3.69}$$

where we have substituted the values $K(0) = \frac{\pi}{2}$ and $\theta = \frac{\pi}{3}$. Asymptotically we deduce that $T \sim |\delta|^{-1}$ whenever the detuning is sufficiently large. However, this is only half the picture. If we plot the period, as seen in figure (3.4b), we see the

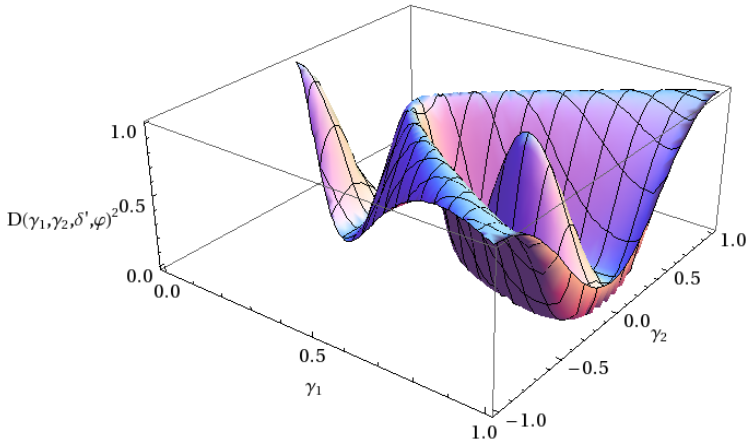

(a) $\delta' = 1/2$

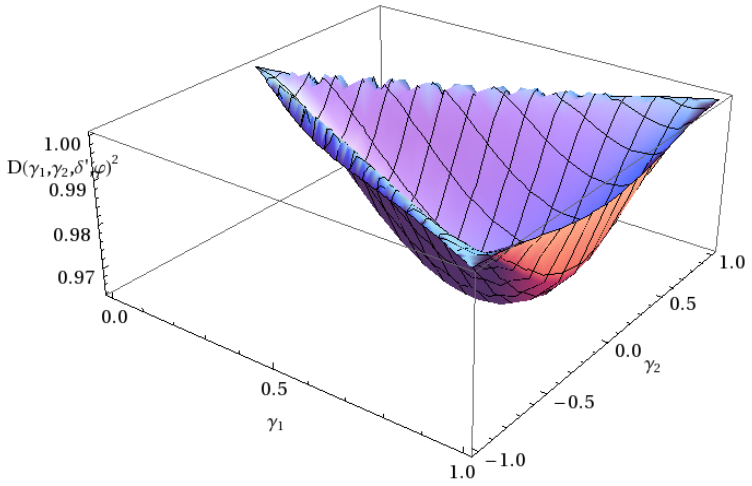

(b) $\delta' = 2$

Figure 3.3: The discriminant $D(\gamma_1, \gamma_2, \delta', \varphi(0))$, showing the behaviour as δ' is increased. Here we have fixed $\varphi(0) = \pi/2$. Maxima can be identified at the boundary points $(\gamma_1, \gamma_2) = (1, \pm 1)$ and $\gamma_1 = \gamma_2 = 0$, which are found to be independent of either δ' or $\varphi(0)$.

creation of a singularity at the same point of interest witnessed for σ. At this isolated value, two of the roots, β_2 and β_3, become identical. This has the effect of setting $m = 1$, which is precisely the point when the elliptic integral K becomes singular. This corresponds to the creation of a homoclinic orbit where we now have solution

$$v(t) = -(\beta_1 - \beta_2)\tanh^2\left(|Z|\sqrt{\beta_1 - \beta_3}\,t - t_0\right) + \beta_1, \tag{3.70}$$

along with new constant

$$t_0 = s\,\text{arctanh}\left(\sqrt{\frac{v(0) - \beta_1}{\beta_1 - \beta_2}}\right). \tag{3.71}$$

We can therefore use the detuning parameter to completely modulate the period of the system, from arbitrarily large to vanishingly small, provided we set $J = 0$.

3.4 Chapter Summary

In this chapter we have provided an in-depth analysis of the evolution of the detuned triad. Using the Lax Pair formalism, we showed that conservation laws for the system can be derived in a systematic and constructive manner. This was necessary since the Hamiltonian of the the exactly resonant case was no longer conserved. Using these conservation laws, integrability followed trivially and we derived explicit solutions for both the amplitudes and individual phases, both in the case when the solution was bounded and to account for the 'explosive instability' referred to in the literature. Through an extensive numerical investigation, we were able to show that for arbitrary initial conditions, and for all values of detuned, this unstable case can be neglected. As a consequence of this analysis we were able to derive reasonable limiting arguments for the period of the motion, as it behaves asymptotically under the limit of large detuning. The most unexpected and welcomed consequence of this work was the discovery of a homoclinic orbit in the presence of non-zero detuning. Here we demonstrated a peak in the variability of amplitudes in the modes, suggesting that near this homoclinic point, the amount of energy exchanged between modes in the triad even surpasses that of the exactly resonant case. We also saw that the period diverged at this point, and we provided an explicit solution for the system in this non-periodic case.

The level of analysis provided in this chapter surpasses that already provided in the literature. Until now we have seen a focus on the integrability of exactly resonant clusters, where these are thought to form the building blocks of understanding

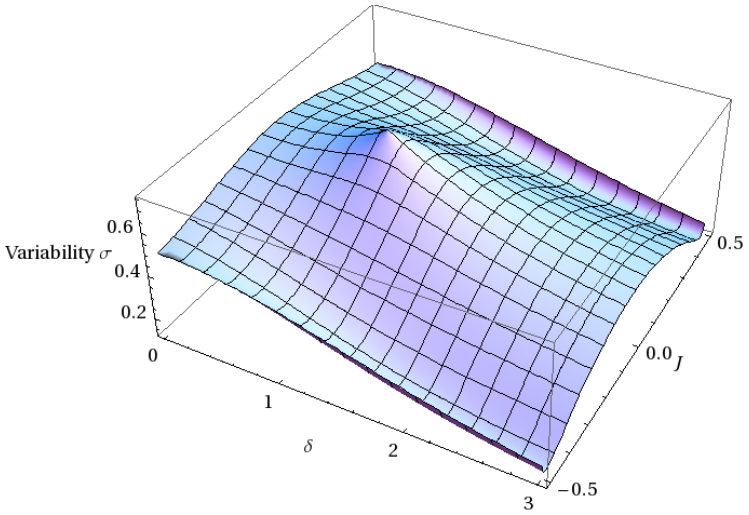

(a) Variability, σ

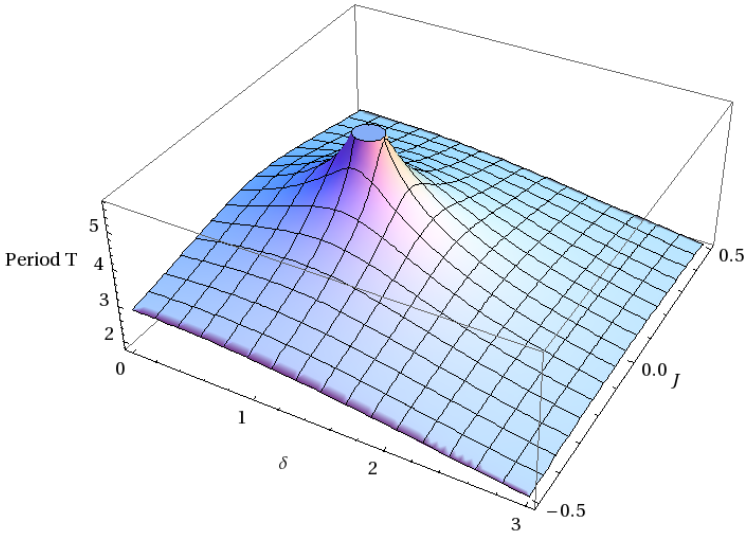

(b) Period, T

Figure 3.4: Analysing the effect of detuning on the period, T, and the variability in the amplitudes, σ. We have fixed $E = 1$, $u_0 = \frac{1}{2}$ and $\varphi(0) = \frac{\pi}{4}$ but allowed the detuning and J to vary. The point $(\delta, J) = (1, 0)$ represents the creation of a homoclinic orbit, where the period becomes singular and σ is maximised.

discrete wave turbulence theory. As we will see towards the end of the thesis, with the discovery of mesoscopic turbulence, quasi-resonant interactions have garnered increasing levels of attention in recent years. In this context, we hope that understanding the significance of detuning applied to smaller, directly integrable systems might provide insight into phenomena that manifests in the wave system as a whole. For instance, we have shown that in some respects the ideas behind discrete wave turbulence are true; if broadening is large, energy exchange between modes rapidly diminishes and can be thought of as small size, small timescale fluctuations around some mean value. Energy therefore remains confined to clusters of modes where the broadening is small. However, we have shown that for intermediate values of detuning energy transfer between quasi-resonant modes can become significant, even greater than the exactly resonant case, and periods of interaction need not be as small as we first thought. We see that quasi-resonant interactions can also be a vehicle to promote interaction between modes, as well as diminish their capacity to transfer energy throughout the system. What is clear, however, is that any study into the dynamics of clusters of interacting modes would be severely undermined if the significance of resonance broadening is not properly accounted for.

Chapter 4

The Forced Triad

So far we have seen how resonant triads form the building blocks for understanding mode coupling in systems of weakly interacting dispersive waves, with quadratic leading order nonlinearity. In the preceding chapter, we discussed how the equations of motion governing the evolution of an isolated triad had been extensively studied, dating back to earlier work on nonlinear optics, plasmas, and atmospheric dynamics. This only emphasises their prevalence in nonlinear systems, being derived simultaneously across three different disciplines. More generally, resonant interactions form the basis of both discrete and statistical wave turbulence. In the latter, energy transfer from large to small scales is thought to be mitigated by resonant interactions to form the onset of an energy cascade. In summary, their importance both theoretically and physically cannot be overstated.

It is somewhat surprising then, given their significance, that almost nothing is known about the dynamics of an isolated triad in the presence of forcing. The purpose of this chapter is to address this issue. We consider the simplest possible forcing: an additive forcing of the unstable mode. We force the unstable, or active mode, since experience with the unforced triad tells us this controls the transfer of energy to the remaining two passive modes. Besides its ubiquity in the study of wave turbulence at both the numerical and analytic level, the addition of forcing to the equations of motion has direct physical meaning in certain applications. In the case of Rossby waves, for example, an additive forcing term in equations (3.1) describes orographic forcing of Rossby waves by an idealised periodic topography [Pedlosky, 1987; Lynch, 2009]. For the swinging spring it would correspond to a periodic oscillation of the point of support. A numerical study [Lynch, 2009] of the forced triad equations suggested that the amplitudes of the modes remain bounded in the presence of forcing, something which is not obvious *a priori*. Elsewhere, these

equations have been studied in the context of random forcing applied to rotating three-dimensional turbulence [Smith and Waleffe, 1999]. As with the previous reference, linear dampening terms were added to each mode. A simple fixed-point analysis of the resulting system revealed a bifurcation point depending on the relative strength of the forcing term; only when the Reynolds number was sufficiently high did the unstable mode exchange energy with the other two, while forcing the passive modes did nothing to promote energy exchange regardless of the magnitude of the forcing term.

In this chapter we provide a detailed study of the properties of an isolated triad in the presence of forcing. The chapter is laid out as follows. We begin in Section 4.1 by writing the equations of the forced triad in the general case and studying their conservation laws. We then specialise in Section 4.2 to studying the case $H = 0$. We prove that the system is generically bounded when $H = 0$ meaning that it is bounded for any choice of initial condition with the exception of a single special initial condition for which the system is unbounded (see Section 4.2.4). We obtain an explicit solution in Section 4.2.3 of the forced triad evolution equations for a particular choice of initial conditions. An explicit solution of the evolution equations in terms of elliptic functions does not seem possible in general, even in the integrable case $H = 0$. Instead, in Section 4.3 we provide formulae for the period and maximum amplitude of the solution which are valid in general. We perform a parametric study of the period and maximum amplitude of the triad as key parameters are varied. Then in Section 4.4, we introduce a novel and accurate scheme for approximating the $H = 0$ dynamics and compare it against numerical solutions of the original system for a variety of initial conditions. Finally, in Section 4.5, we turn our attention to the case $H \neq 0$. We find that the dynamics can be reduced to the one-dimensional motion of a particle in a time-periodic potential. Numerical Poincaré sections of the resulting dynamical system suggest that the dynamics remain bounded when $H \neq 0$ and the motion is generally quasi-periodic although periodic orbits can also be identified. The chapter then ends with a brief summary and conclusions.

4.1 General Forced Triad

Let B_1, B_2 and B_3 be complex functions of time. We assume they satisfy a system of evolution equations derived from the real Hamiltonian

$$H = 2Z\mathrm{Im}\{B_1 B_2 B_3^*\} - 2F\,\mathrm{Im}\{iB_3\}, \tag{4.1}$$

where both F and Z are constant, real parameters. Here, we recognise Z as the interaction coefficient for the exactly resonant triad obtained after scaling the amplitude of each mode. The canonical equations of motion for this system are given by

$$i\dot{B}_j = \frac{\partial H}{\partial B_j^*},\ j = 1, 2, 3 \tag{4.2}$$

along with their complex conjugates. The equations of motion are, therefore,

$$\begin{cases} \dot{B}_1 = ZB_2^* B_3, \\ \dot{B}_2 = ZB_1^* B_3, \\ \dot{B}_3 = -ZB_1 B_2 + iF\,, \end{cases} \tag{4.3}$$

together with their complex conjugates. In this setting, the term 'iF' is originated from a forcing of the so-called 'unstable' mode represented by B_3.

4.1.1 Amplitude-Phase Representation

We write $B_j = C_j \mathrm{e}^{i\varphi_j},\ j = 1, 2, 3$, with $C_j \in \mathbb{R}$ and $\varphi_j \in \mathbb{R}$ to obtain

$$\dot{B}_j = \left(\dot{C}_j + iC_j\dot{\varphi}_j\right)\mathrm{e}^{i\varphi_j}.$$

Under this new representation, the equations of motion (4.3) become

$$\begin{cases} \dot{C}_1 = ZC_2C_3\cos\varphi, \\ \dot{C}_2 = ZC_1C_3\cos\varphi, \\ \dot{C}_3 = -ZC_1C_2\cos\varphi + F\,\sin\varphi_3, \\ \dot{\varphi}_1 = -Z\dfrac{C_2C_3}{C_1}\sin\varphi, \\ \dot{\varphi}_2 = -Z\dfrac{C_1C_3}{C_2}\sin\varphi, \\ \dot{\varphi}_3 = -Z\dfrac{C_1C_2}{C_3}\sin\varphi + \dfrac{F}{C_3}\cos\varphi_3, \end{cases} \tag{4.4}$$

where we have introduced the dynamical phase $\varphi = \varphi_1 + \varphi_2 - \varphi_3$.

4.1.2 Conservation Laws of the General Forced Triad and reductions

The unforced triad (i.e., the case $F = 0$) is known to possess two independent conservation laws that are quadratic in the amplitudes C_j, and one conservation

law which is cubic in the amplitudes. In contrast, the forced triad possesses one quadratic conservation law and one cubic conservation law. These are

$$J = C_1^2 - C_2^2, \tag{4.5}$$

$$H = 2C_3 \left[ZC_1C_2 \sin\varphi - F \cos\varphi_3 \right]. \tag{4.6}$$

Here, H is nothing but the Hamiltonian of the original system (4.3), written in terms of the new variables.

Another important property of the unforced triad is that all the phases φ_1, φ_2 and φ_3 were 'slave' variables, i.e., they were obtainable by quadratures once the solutions for C_1, C_2, C_3 and φ were known. In contrast, in the forced triad only φ_1 and φ_2 are 'slave' variables, and the five real variables C_1, C_2, C_3, φ and φ_3 form the reduced system

$$\begin{cases} \dot{C}_1 = ZC_2C_3 \cos\varphi, \\ \dot{C}_2 = ZC_1C_3 \cos\varphi, \\ \dot{C}_3 = -ZC_1C_2 \cos\varphi + F \sin\varphi_3, \\ \dot{\varphi}_3 = -\dfrac{H}{2C_3^2}, \\ \dot{\varphi} = -ZC_1C_2C_3 \sin\varphi \left(\dfrac{1}{C_1^2} + \dfrac{1}{C_2^2} \right) + \dfrac{H}{2C_3^2}, \end{cases} \tag{4.7}$$

where H is defined as in equation (4.6). Numerical simulations of system (4.7) can be interpreted as either using H as a constant or by explicitly using H as defined in equation (4.6). The accuracy might be sensitive to this choice.

System (4.7) along with the two conservation laws, J and H, is effectively a three-dimensional system and as such it might not be integrable. We notice, however, that the system is volume-preserving, with Jacobi last multiplier

$$\rho = \begin{cases} C_1C_2, & \text{if } H = \text{constant}, \\ C_1C_2C_3, & \text{if } H \text{ is defined as in Eq.(4.6).} \end{cases} \tag{4.8}$$

Reminder: a Jacobi last multiplier, also known as a standard Liouville volume density, is a scalar function $\rho(\mathbf{x})$ of the dependent variables x^a, $a = 1, \ldots, N$, defined by the equation $\nabla \cdot (\rho \mathbf{V}(\mathbf{x})) = 0$, equation to be valid for all values of $\mathbf{x}$, where $\mathbf{V}$ is the right-hand-side of the evolution equations $\dot{\mathbf{x}} = \mathbf{V}(\mathbf{x})$. See either the preliminary section for more details, or [Hojman, 1992; Bustamante and Hojman, 2003; Bustamante and Kartashova, 2011], [Nucci and Leach, 2008] and references

therein.

4.1.3 Integrability of the case $H = 0$

We consider initial conditions for system (4.7) such that $H = 0$. We obtain

$$\begin{cases} \dot{C}_1 = ZC_2C_3\cos\varphi, \\ \dot{C}_2 = ZC_1C_3\cos\varphi, \\ \dot{C}_3 = -ZC_1C_2\cos\varphi + F\,\sin\varphi_3, \\ \dot{\varphi}_3 = 0, \\ \dot{\varphi} = -ZC_1C_2C_3\sin\varphi\left(\dfrac{1}{C_1^2}+\dfrac{1}{C_2^2}\right). \end{cases} \tag{4.9}$$

We notice that the case $C_3 = 0$ is trivially integrable. Assuming that $C_3 \not\equiv 0$, we obtain $H = 0 \Leftrightarrow ZC_1C_2\sin\varphi = F\,\cos\varphi_3$. But, according to the dynamics (4.9), φ_3 is constant, so we derive the new conservation law

$$C_1C_2\sin\varphi = \frac{F\,\cos\varphi_3}{Z}.$$

This new constant, together with $J = C_1^2 - C_2^2$, helps us reduce the system to an effectively two-dimensional volume-preserving and therefore integrable system:

$$\begin{cases} \dot{C}_1 = ZC_2C_3\cos\varphi, \\ \dot{C}_2 = ZC_1C_3\cos\varphi, \\ \dot{C}_3 = -ZC_1C_2\cos\varphi + F\,\sin\varphi_3, \\ \dot{\varphi} = -F\,C_3\cos\varphi_3\left(\dfrac{1}{C_1^2}+\dfrac{1}{C_2^2}\right), \end{cases} \tag{4.10}$$

with φ_3 being constant, together with the conservation laws

$$C_1C_2\sin\varphi = \frac{F\,\cos\varphi_3}{Z}, \tag{4.11}$$

$$C_1^2 - C_2^2 = J, \tag{4.12}$$

and Jacobi last multiplier given by

$$\rho = \begin{cases} C_1C_2, & \text{if } F\cos\varphi_3 = ZC_1C_2\sin\varphi \text{ is used in Eq.(4.10)}, \\ 1, & \text{if } F\cos\varphi_3 = \text{constant is used in Eq.(4.10)}. \end{cases} \tag{4.13}$$

4.2 Generic boundedness of the integrable case $H = 0$

The goal within this section is to establish generic boundedness of the solutions to the integrable system (4.10)–(4.12). By boundedness we mean that the 'energy' $E(t)$ of the system is bounded for all times. The energy is a positive-definite quadratic function of the amplitudes $C_j(t)$:

$$E(t) = \frac{C_1(t)^2 + C_2(t)^2}{2} + C_3(t)^2. \tag{4.14}$$

This quantity is obtained from the kinetic energy of the original wave system and should not be confused with the Hamiltonian H, which is a cubic function of the amplitudes and equal to zero in this case. The time derivative of the energy is obtained using equations (4.10):

$$\begin{aligned} \dot{E}(t) &= C_1(t)\dot{C}_1(t) + C_2(t)\dot{C}_2(t) + 2\,C_3(t)\dot{C}_3(t) \\ &= 2\,F\,\sin\varphi_3\,C_3(t)\,. \end{aligned} \tag{4.15}$$

This result suggests that we use a 'local rescaled time' variable $\tau(t)$ satisfying

$$\frac{\mathrm{d}\tau}{\mathrm{d}t} = C_3(t)\,, \quad \tau(0) = 0\,. \tag{4.16}$$

This time transformation is well defined as long as $C_3(t)$ is not zero. Integrating equation (4.15) we obtain

$$E(t) = E(0) + 2\,\tau\,F\,\sin\varphi_3\,, \tag{4.17}$$

where $\tau = \tau(t)$. We see that proving boundedness of energy is equivalent to proving boundedness of $\tau(t)$.

4.2.1 Establishing boundedness for $J \neq 0$

The conservation law $J = C_1^2 - C_2^2$ naturally suggests a parameterisation of the form:

$$\begin{cases} C_1(t) = \sqrt{J}\,\mathrm{sgn}(C_1(0))\cosh\omega(\tau), \\ C_2(t) = \sqrt{J}\sinh\omega(\tau), \end{cases} \tag{4.18}$$

in the case $J > 0$ and

$$\begin{cases} C_1(t) = \sqrt{-J}\sinh\omega(\tau), \\ C_2(t) = \sqrt{-J}\,\mathrm{sgn}(C_2(0))\cosh\omega(\tau), \end{cases} \tag{4.19}$$

when $J < 0$. Substituting this parameterised solution into equations (4.10) and using equations (4.11), (4.12) and (4.16), we deduce that the function $\omega(\tau)$ must satisfy, regardless of whether J is positive or not,

$$\cosh 2\omega(\tau) = \frac{2}{|J|} R \cosh\left(2Z\tau + \Delta\right), \tag{4.20}$$

where $R > 0$ and $\Delta \in \mathbb{R}$ are constants, related to the initial conditions as follows:

$$R = \sqrt{\left(\frac{J}{2}\right)^2 + \frac{F^2 \cos^2 \varphi_3}{Z^2}}, \tag{4.21}$$

$$R \sinh \Delta = C_1(0)\, C_2(0)\, \cos\varphi(0). \tag{4.22}$$

Substituting the solution for $\omega(\tau)$ into the parameterised forms for $C_1(t)$ and $C_2(t)$ gives the result valid for $J \neq 0$:

$$\begin{cases} C_1(t)^2 = R\, \cosh\left(2Z\tau + \Delta\right) + \dfrac{J}{2}, \\ C_2(t)^2 = R\, \cosh\left(2Z\tau + \Delta\right) - \dfrac{J}{2}. \end{cases} \tag{4.23}$$

The solution for the remaining amplitude $C_3(t)$ is found by using equations (4.14) and (4.17). We get

$$C_3(t)^2 = E(0) + 2F\tau \sin\varphi_3 - R\cosh\left(2Z\tau + \Delta\right), \tag{4.24}$$

and using equation (4.16) we derive the following equation for $\tau(t)$:

$$\left[\frac{\mathrm{d}\tau}{\mathrm{d}t}\right]^2 + R\cosh\left(2Z\tau + \Delta\right) - 2F\tau \sin\varphi_3 = E(0). \tag{4.25}$$

This is precisely the equation for a one-dimensional particle with position $\tau(t)$, total energy $E(0)$, kinetic energy $\left[\frac{\mathrm{d}\tau}{\mathrm{d}t}\right]^2$ and potential energy

$$V(\tau) = R\cosh\left(2Z\tau + \Delta\right) - 2F\tau \sin\varphi_3\,. \tag{4.26}$$

From the fact that $R > 0$ it follows that this potential is in fact attractive: $V''(\tau) > 0$ for all $\tau \in \mathbb{R}$, and $\lim_{\tau\to\pm\infty} V(\tau) = \infty$. It follows that the particle must oscillate about a unique minimum situated at the point

$$\tau_* = -\frac{\Delta}{2Z} + \frac{1}{2Z}\sinh^{-1}\left(\frac{F\sin\varphi_3}{ZR}\right), \tag{4.27}$$

with the motion of $\tau(t)$ being bounded between the two turning points $\tau_{\min} < \tau_{\max}$ defined by the solutions of

$$V(\tau_{\min}) = V(\tau_{\max}) = E(0). \tag{4.28}$$

Since $\tau(t)$ is bounded, we conclude from equations (4.23) and (4.24) that the amplitudes of each mode must also be bounded.

Regarding the evolution of the dynamical phase $\varphi(t)$, equation (4.11) could at first sight be used to to find its solution. However this is not practical because the dynamical phase generically oscillates about $\pi/2$ (modulo $n\pi$) and therefore the inverse sine is multivalued. It is better to integrate directly equation (4.10) for φ using the auxiliary variable $\tau(t)$. The result is: if the initial condition $\varphi(0)$ is in the open interval $(n\pi, (n+1)\pi)$, for some $n \in \mathbb{Z}$, then $\varphi(t)$ remains in that interval and

$$\varphi(t) = \cot^{-1} \frac{ZR \sinh(2Z\tau + \Delta)}{F \cos\varphi_3}\,, \tag{4.29}$$

where the branch is properly selected. In the special case when the constant φ_3 is equal to $(m + 1/2)\pi\,,\ m \in \mathbb{Z}$, then φ is also constant and equal to $\tilde{m}\pi\,,\ \tilde{m} \in \mathbb{Z}\,.$

4.2.2 Formulae for the turning points in terms of new special functions

The turning points $\tau_{\min\,/\,\max}$ of the evolution equation (4.25) are defined by the solutions of the equation $V(\tau) = E(0)$:

$$R\cosh(2Z\tau + \Delta) - 2F\tau\sin\varphi_3 = E(0). \tag{4.30}$$

For physically admissible values of the parameters Z, F and initial conditions R, φ_3, $E(0)$, this equation has either two real solutions or only one real solution. When there is only one real solution, the physical system is "dynamically frozen" at $\tau =$ constant. In order to study a less trivial nonlinear dynamics, it is better to restrict the parameter space so that there are two real solutions, denoted by $\tau_{\min}, \tau_{\max}$, with $\tau_{\min} < \tau_{\max}$.

Let us study the structure of these solutions as functions of the parameters. Notice that if we replaced the hyperbolic cosine in equation (4.30) by an exponential, the solution for $\tau_{\min\,/\,\max}$ would be given in terms of two branches of the product log function $W_k(x)$, a function of one variable. In contrast, in our case such reduction does not get too far: the solution is given in terms of a function of two variables.

Defining the function $\xi(x, y)$ by the implicit equation

$$\cosh \xi = x\, \xi + y\,, \tag{4.31}$$

we look for real solutions $\xi \in \mathbb{R}$. Graphically, we want to find the intersections between two graphs, $\cosh \xi$ and $x\xi + y$, as function of x and y. We see that tangent intersection occurs if in addition to the above equation, $\sinh \xi = x$ holds. Therefore, a relation between the arguments is found in the tangent case: $y = \sqrt{1+x^2} - x \sinh^{-1} x$. Therefore, the condition (of physical origin) to have two solutions is a restriction on the parameter space:

$$y > \sqrt{1+x^2} - x \sinh^{-1} x\,, \quad x \in \mathbb{R}\,. \tag{4.32}$$

With this condition, there will be two real solutions of equation (4.31), denoted

$$\xi_{-1}(x, y) < \xi_0(x, y)\,.$$

With these functions defined, the turning points $\tau_{\min}, \tau_{\max}$ can be obtained via proper rescalings:

$$2Z\, \tau_{\min\,/\,\max} + \Delta = \xi_k \left(\frac{F \sin\varphi_3}{R\, Z}, \frac{E(0)}{R} - \frac{F \sin\varphi_3\, \Delta}{R\, Z} \right)\,, \tag{4.33}$$

where $k = 0$ or -1. In practice, we resort to a numerical algorithm to compute these solutions. It is worth noting however, that condition (4.32) is automatically satisfied for any choice of real initial amplitudes and phases.

4.2.3 An explicit example of bounded motion: $\sin\varphi_3 = 0, J \neq 0$

Continuing with the case $H = 0$, consider now a choice of initial conditions such that $\varphi_3 \in \{0, \pm\pi\}$ and $J \neq 0$. The differential equation for $\tau(t)$, equation (4.25), now reads

$$\left[\frac{\mathrm{d}\tau}{\mathrm{d}t}\right]^2 = E(0) - R\, \cosh\left(2Z\tau + \Delta\right)\,. \tag{4.34}$$

The particle interpretation is simple, given the fact that $E(0) > R$ by virtue of the condition $H = 0$. It turns out that the potential $V(\tau)$, apart from a shift, is a symmetric well and therefore the motion should be bounded. This equation can be explicitly integrated to give an analytical solution for $\tau(t)$ in terms of Jacobi elliptic functions, with modulus $m = \frac{E(0)-R}{E(0)+R} \in (0, 1)$. The procedure is analogous to the one outlined for the detuned triad in the preceding chapter. The result can be checked

directly by substitution into equation (4.34). We obtain the explicit solution

$$2\,Z\,\tau(t) + \Delta = \ln\left(\frac{\left[\mathrm{dn}\left(\frac{2\,K(m)}{T}\,t+u\middle|m\right)-\sqrt{m}\,\mathrm{cn}\left(\frac{2\,K(m)}{T}\,t+u\middle|m\right)\right]^2}{1-m}\right),$$

where $K(m)$ is the complete elliptic integral of the first kind, the period T of the oscillations is defined by

$$T = \frac{2\,K(m)}{Z\,\sqrt{E(0)+R}},$$

and the shift u is defined in terms of the incomplete elliptic integral of the first kind by

$$u = F\left(\frac{C_3(0)}{\sqrt{E(0)-R}}\middle|\,m\right).$$

To see that the above solution for $\tau(t)$ is indeed oscillatory, we compute its time derivative:

$$\frac{\mathrm{d}\tau}{\mathrm{d}t} = \sqrt{E(0)-R}\,\mathrm{sn}\left(\frac{2\,K(m)}{T}\,t+u\middle|\,m\right).$$

With this result, we readily obtain the squares of the amplitudes $C_1(t), C_2(t), C_3(t)$:

$$\begin{cases} C_1(t)^2 = E(0) + \dfrac{J}{2} - (E(0)-R)\,\mathrm{sn}^2\left(\dfrac{2\,K(m)}{T}\,t+u\middle|\,m\right), \\ C_2(t)^2 = E(0) - \dfrac{J}{2} - (E(0)-R)\,\mathrm{sn}^2\left(\dfrac{2\,K(m)}{T}\,t+u\middle|\,m\right), \\ C_3(t)^2 = (E(0)-R)\,\mathrm{sn}^2\left(\dfrac{2\,K(m)}{T}\,t+u\middle|\,m\right). \end{cases} \tag{4.35}$$

We plot these squares in figure 4.1, top panel. Finally, from equation (4.29) we obtain the dynamical phase:

$$\varphi(t) = -\cot^{-1}\left[\frac{Z\,R\,m^{1/2}}{F\,(1-m)\,\cos\varphi_3}\mathrm{cn}\,\mathrm{dn}\left(\frac{2\,K(m)}{T}\,t+u\middle|\,m\right)\right], \tag{4.36}$$

where we have defined $\mathrm{cn}\,\mathrm{dn}(x|m) \equiv \mathrm{cn}(x|m)\,\mathrm{dn}(x|m)$. Depending on the initial value $\varphi(0)$, the dynamical phase remains bounded and oscillates about the value $(n+1/2)\pi$, for some $n \in \mathbb{Z}$. The corresponding plot of the solution for the dynamical phase is shown in figure 4.1, bottom panel.

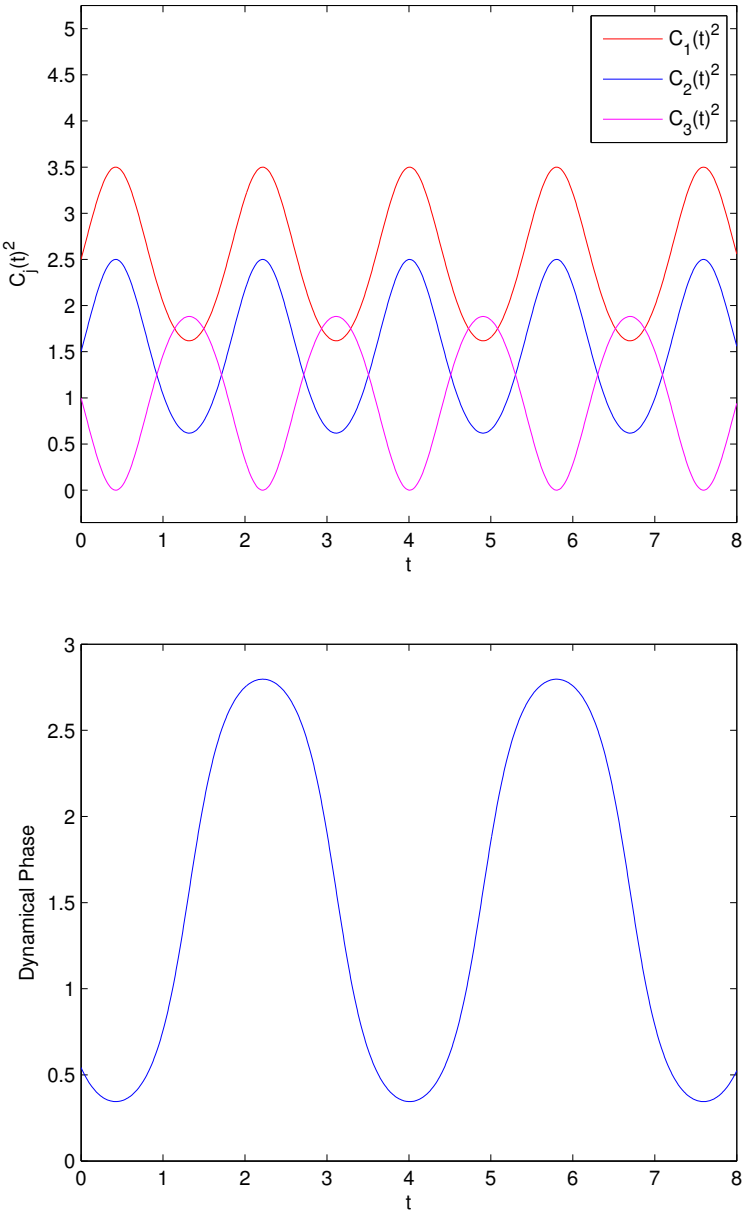

Figure 4.1: Solutions for the square amplitudes (top panel) and dynamical phase (bottom panel) in the explicitly integrable case $H = 0$ and $\varphi_3 = 0$. Choices for parameters and initial conditions: $F = 1$, $Z = 1$, $E(0) = 3$, $J = 1$, and $\varphi(0)$ is obtained from equation (4.36).

4.2.4 The limit $J \to 0$: "almost always" bounded

Always in the case $H = 0$, we have established boundedness of the motion for the case $J \neq 0$ in Section 4.2.1. Using the equations from that Section, it is possible to establish boundedness in the case $J = 0, \cos\varphi_3 \neq 0$, by taking the limit of the $J \neq 0$ equations as $J \to 0$. For example, the auxiliary function $\omega(\tau)$ has a singularity in the limit:

$$\omega(\tau) \approx \frac{1}{2} \log \left[\frac{4|F \cos\varphi_3|}{|J\, Z|} \cosh(2\, Z\, \tau + \Delta) \right] ,$$

but the physical quantities such as amplitudes and phases behave well: in particular, equations (4.23) and (4.29) hold, with the only changes $J = 0$ and $R = \frac{|F \cos\varphi_3|}{|Z|}$.

Let us now consider the case $J = 0$ and $\cos\varphi_3 = 0$. To get there by a limiting procedure of the $J \neq 0$ equations, we need to be more careful. The condition $J = 0$ implies $C_1(t)^2 = C_2(t)^2,\ \forall\, t \geq 0$. For simplicity, we take initial conditions $C_1(0) = C_2(0) \neq 0$ so that $C_1(t) = C_2(t),\ \forall\, t \geq 0$. The condition $\cos\varphi_3 = 0$ along with the conservation law (4.11) then imply that $\sin\varphi(t) = 0,\ \forall\, t \geq 0$. For simplicity we take $\varphi(t) = 0,\ \forall\, t \geq 0$.

Now, equation (4.21) determines $R \approx |J|/2 \to 0$ but equation (4.22) gives a divergent shift: $\Delta \approx \log\left[4C_1(0)^2/|J|\right] \to \infty$. However a consistent limit is obtained for the physical quantities. For example, from equations (4.23) we obtain the amplitudes $C_1(t)^2 \approx C_2(t)^2 \approx C_1(0)^2 \exp(2\, Z\, \tau)$. The evolution equation for τ is still of the form

$$\left[\frac{\mathrm{d}\tau}{\mathrm{d}t}\right]^2 = E(0) - V_{\lim}(\tau)\,, \tag{4.37}$$

but with a new potential $V_{\lim}(\tau) = \lim_{J\to 0} V(\tau)$, which reads

$$V_{\lim}(\tau) = C_1(0)^2 \exp(2\, Z\, \tau) - 2F\, \tau\, \sin\varphi_3. \tag{4.38}$$

As you recall, $\cos\varphi_3 = 0$. We conclude that the new potential $V_{\lim}(\tau)$ is attractive if and only if $\sin\varphi_3 = \mathrm{sgn}\,(Z\, F)$. This gives two separate cases, depending on the initial conditions: a bounded case and an unbounded case.

The bounded sub-case of $J = 0$, $\cos\varphi_3 = 0$

The bounded sub-case is obtained if we set $\sin\varphi_3 = \mathrm{sgn}\,(Z\, F)$. Although there is no simple solution of the system (4.37) in terms of elliptic functions, it is illustrative to obtain explicit expressions for the turning points, and consequently for the maximum and minimum values of the total energy (4.14), in terms of product log functions.

The equations $V_{\lim}(\tau_{\min}) = V_{\lim}(\tau_{\max}) = E(0)$ have solutions

$$\tau_{\min\,/\,\max} = -\frac{E(0)\mathrm{sgn}\,(Z)}{2|F|} - \frac{1}{2Z}W_k\left(-\frac{|Z|C_1(0)^2}{|F|}\exp\left(-\frac{E(0)|Z|}{|F|}\right)\right), \qquad (4.39)$$

where $k \in \mathbb{Z}$ denotes the different branches of the product log function $W_k(z)$, also known as the Lambert W-function. Notice that the argument of W_k appearing above is strictly negative in this case, restricted to the interval $[-1/e, 0]$, with the lower bound being obtained only when $C_3(0) = 0$. Since we require real solutions, we are limited in choice to the two branches W_0 and W_{-1}.

Substituting these expressions for the turning points into equation (4.17), we find the maximum and minimum values of the total energy of the system:

$$E_{\min\,/\,\max} = -\frac{|F|}{|Z|}W_k\left(-\frac{|Z|C_1(0)^2}{|F|}\exp\left(-\frac{E(0)|Z|}{|F|}\right)\right), \qquad (4.40)$$

where we take $k = 0$ for the minimum energy and $k = -1$ for the maximum.

The unbounded sub-case of $J = 0$, $\cos\varphi_3 = 0$

The unbounded sub-case is obtained if we set $\sin\varphi_3 = -\mathrm{sgn}\,(Z\,F)$. In this case, the potential $V_{\lim}(\tau)$ in equation (4.38) has a slope of fixed sign. Depending on the initial conditions, the motion can have one turning point but then the variable $Z\,\tau(t)$ will tend to $-\infty$ in the asymptotic way $Z\,\tau(t) \approx -|Z\,F|\,t^2$, so that the corresponding amplitudes' squares will behave as $C_3(t)^2 \approx 4\,F^2\,t^2$, $C_1(t)^2 = C_2(t)^2 \approx K\,e^{-|Z\,F|\,t^2}$, corresponding to unbounded growth of the forced mode and fast decay of the other two modes.

4.3 Periods and Maximum amplitudes: parametric study

Having established for $H = 0$ the general integrability of equations (4.7) and the boundedness of the solution for almost all initial conditions (with the exception of one sub-case), we turn our attention to two important physical questions:

(i) How does the physical period of oscillation depend on the parameters Z, F and on the initial conditions J, φ_3, $E(0)$ of the problem?

(ii) How do the upper and lower bounds on the total energy of the system behave as a function of the parameters Z, F and the initial conditions?

4.3.1 Summary of analytic results

Before embarking on a numerical parametric study of the behaviour of the physical period and maximum energy, it is useful to try to answer the above questions in the few sub-cases where an explicit solution has been found:

• In the case $H = 0$, $\sin\varphi_3 = 0$ and $J \neq 0$, as detailed in Section 4.2.3, the full solutions for the amplitudes and phases are available explicitly. In particular, the period of oscillations is given by

$$T = \frac{2\,K(m)}{Z\sqrt{E(0)+R}},$$

where we have defined

$$m = \frac{E(0)-R}{E(0)+R} \in (0,1),\ R = \sqrt{\left(\frac{J}{2}\right)^2 + \frac{F^2}{Z^2}},$$

and $K(m)$ is the complete elliptic integral of the first kind. In this case the total energy (4.14) of the system happens to be constant, equal to $E(0)$. This can be clearly identified in figures (4.2) and (4.3) where the surfaces for maximum and minimum energy coincide on the line given by $\sin\varphi_3 = 0$.

• In the bounded sub-case of $H = 0$, $\cos\varphi_3 = 0$ and $J = 0$, as detailed in Section 4.2.4, although we do not have explicit expressions for the solutions for the amplitudes or even for the period of oscillations, we do have an exact expression for the maximum and minimum values of the total energy, from equation (4.40):

$$E_{\min\,/\,\max} = -\frac{|F|}{|Z|} W_k\left(-\frac{|Z|C_1(0)^2}{|F|}\exp\left(-\frac{E(0)|Z|}{|F|}\right)\right),$$

where we take $k = 0$ for the minimum energy and $k = -1$ for the maximum, and we have assumed for simplicity that $C_1(0) = C_2(0)$ and $\varphi = 0$.

We now ask how these bounds obtained for the energy behave in the limit of arbitrarily large forcing. Recall that the Hamiltonian in the case $\cos\varphi_3 = 0$ reads

$$H = 2ZC_1C_2C_3\sin\varphi.$$

Assuming each amplitude to be non-zero, fixing $H = 0$ means that we have had to set $\varphi = 0$, irrespective of the value of F. Therefore, by choosing appropriate initial

amplitudes/phases so that $J = 0$, $\varphi_3 = \pm\pi/2$ and $H = 0$, we can consider directly the limiting case when F tends to infinity but with fixed initial conditions. Since W_0 is differentiable at zero, we have

$$\lim_{F\to+\infty} E_{\min} = C_1(0)^2.$$

Calculating an equivalent expression for $E_{\max}$, is not quite so straightforward since W_{-1} exhibits a singularity at 0. However, knowing the asymptotic behaviour of $W_{-1}(x)$ as $x \to 0^-$ [DLMF], we find that to leading order as $F \to +\infty$,

$$E_{\max} \approx \frac{|F|}{|Z|} \ln\left(\frac{|F|}{|Z|\, C_1(0)^2}\right) + E(0). \tag{4.41}$$

4.3.2 Numerical study for arbitrary values of J and φ_3

Maximum energy. When neither of the two analytic cases detailed in the above bullet points apply, the two roots $\tau_{\min}$ and $\tau_{\max}$ must be computed numerically from equations (4.33). The resulting values of $E_{\max}$ against varying φ_3 and J under fixed forcing are shown in figure 4.2. The unbounded sub-case as $J \to 0, \cos\varphi_3 = 0$ can clearly be identified. If instead we fix $J > 0$ and allow the strength of the forcing F to vary, we obtain figure 4.3. Here we observe a less-than-quadratic growth in the maximal energy in response to forcing, in a similar fashion as shown in the asymptotic result (4.41).

Period of oscillations. Since we only have an explicit expression for the period when $\sin\varphi_3 = 0$, this too must be calculated numerically. After calculating numerically $\tau_{\max}$ and $\tau_{\min}$, integrating Eq. (4.25) gives the period

$$T = 2\int_{\tau_{\min}}^{\tau_{\max}} \frac{\mathrm{d}u}{\sqrt{E(0) - V(u)}}.$$

This integral can be evaluated numerically, with special care being taken where the integrand has singularities at the two end-points. The results are shown in figures 4.4 and 4.5.

One thing to note with regards to the figures, is that setting $H = 0$ restricts the possible range of parameters that can be taken. The effect of this can be seen in figures 4.3 and 4.5, where forbidden parameter values are indicated by 'hashed' regions at the base of the plot.

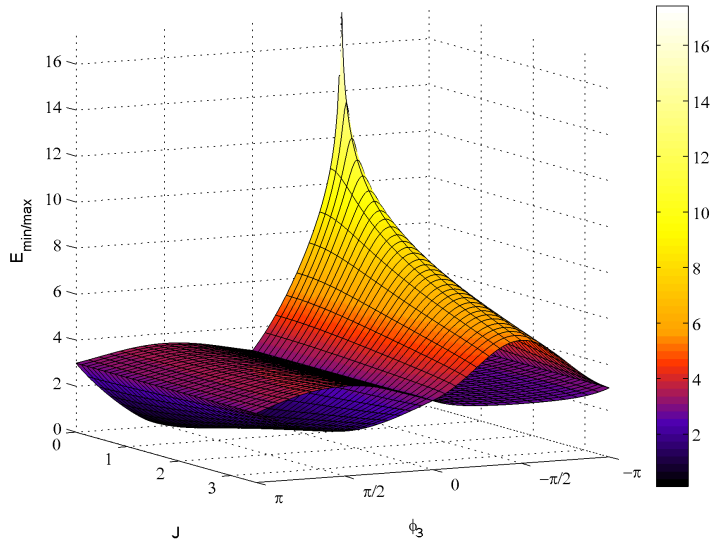

Figure 4.2: $E_{\max}$ and $E_{\min}$ as a function of φ_3 and J. As a choice of parameters and initial conditions, we have fixed $Z = 1$, $E(0) = 3$, $C_3(0) = 1$ and $F = 1$. Values of $C_1(0)$, $C_2(0)$ and $\varphi(0)$ can be found directly from the two conservation laws J and $H = 0$.

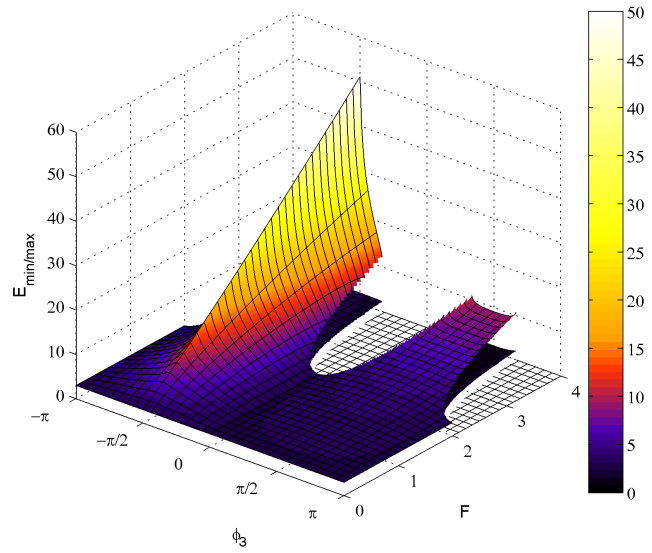

Figure 4.3: $E_{\max}$ and $E_{\min}$ as a function of φ_3 and F. As a choice of parameters and initial conditions, we have fixed $Z = 1$, $E(0) = 3$, $C_3(0) = 1$ and $J = 0.1$. Values of $C_1(0)$, $C_2(0)$ and $\varphi(0)$ can be found directly from the two conservation laws J and $H = 0$.

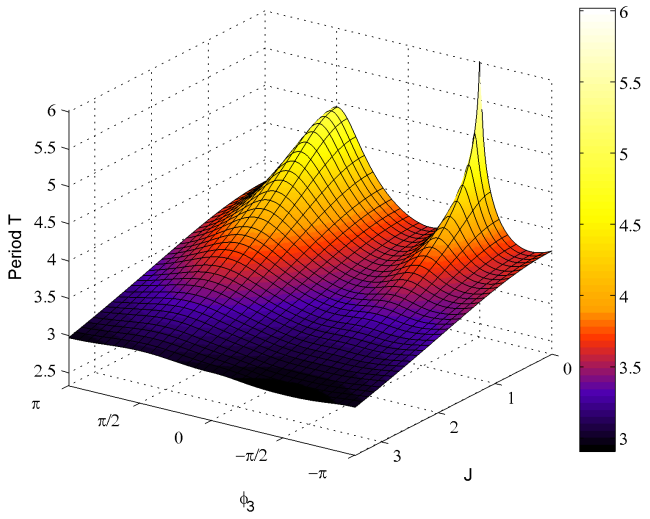

Figure 4.4: Period as a function of φ_3 and J. As a choice of parameters and initial conditions, we have fixed $Z = 1$, $E(0) = 3$, $C_3(0) = 1$ and $F = 1$. Values of $C_1(0)$, $C_2(0)$ and $\varphi(0)$ can be found directly from the two conservation laws J and $H = 0$.

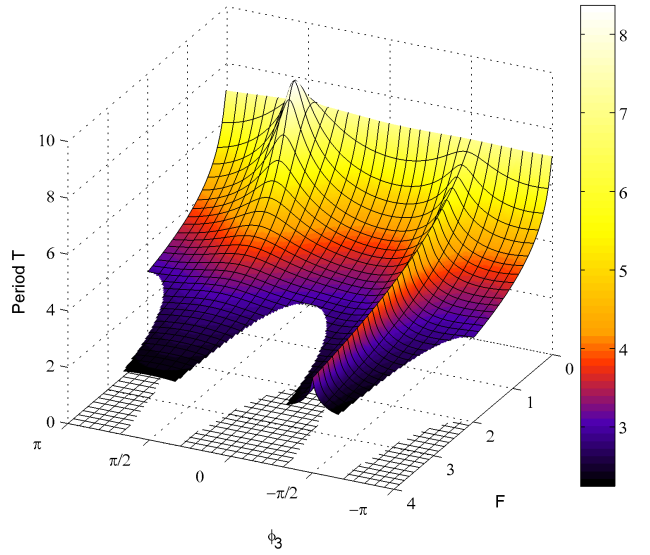

Figure 4.5: Period as a function of φ_3 and F. As a choice of parameters and initial conditions, we have fixed $Z = 1$, $E(0) = 3$, $C_3(0) = 1$ and $J = 0.1$. Values of $C_1(0)$, $C_2(0)$ and $\varphi(0)$ can be found directly from the two conservation laws J and $H = 0$.

4.4 Approximate Solutions in the integrable case $H = 0$

As we have seen in Sec. 4.2, in the integrable case $H = 0$ only certain choices of parameter values lead to explicit formulae for the solution of equation (4.25), in terms of elliptic functions. For other parameter values it is unlikely that such formulae exist and we have to resort to finding an approximate solution for $\tau(t)$. Since the potential $V(\tau) = R\cosh(2Z\tau + \Delta) - 2F\tau\sin\varphi_3$ is attractive, it is possible to approximate this potential by a polynomial in τ. A quartic polynomial is the best compromise between simplicity and accuracy: simplicity in that the resulting approximate evolution equation for $\tau(t)$ can be explicitly integrated, and accuracy in that one can capture nonlinear effects such as the dependence of the period on the parameters of the problem.

The problem is then reduced to compute the coefficients of this approximate potential. A natural place to start would be to obtain these coefficients directly from the fourth-order Taylor expansion of equation (4.25), about the minimum of the potential $\tau = \tau_*$. However, this 'local' approach is doomed because it does not eliminate secular terms, and therefore the solution of the approximate equations differs more and more from the exact solution after each period. Instead, the coefficients of this approximate potential must be chosen by a procedure that takes into account the *global* character of the motion, i.e., the fact that the variable $\tau(t)$ can oscillate with high amplitude.

A quartic polynomial in τ has five free coefficients. We will determine two of them by requesting the approximated potential to have the same turning points as the exact potential. Thus, our approximate system is defined as follows:

$$\left[\frac{\mathrm{d}\tau}{\mathrm{d}t}\right]^2 = (\tau - \tau_{\min})(\tau - \tau_{\max})(\alpha_2\tau^2 + \alpha_1\tau + \alpha_0)\,,$$

where $\tau_{\min}, \tau_{\max}$ are the turning points, defined in equation (4.30), and $\alpha_0, \alpha_1, \alpha_2$, are some unknown coefficients. This approximate system replaces the exact evolution equation (4.25). The remaining three coefficients will be determined by a minimisation procedure of the L^2 norm of the difference between the exact potential and the approximation.

4.4.1 Approximate system, its solution and comparison with numerical simulations of the exact system

In order to determine the unknown coefficients $\alpha_0, \alpha_1, \alpha_2$, we impose a procedure that minimises the L^2 error, globally over the interval $[\tau_{\min}, \tau_{\max}]$. Let us define the

function to be minimised:

$$\Phi(\alpha_0, \alpha_1, \alpha_2) = \frac{1}{2} \int_{\tau_{\min}}^{\tau_{\max}} \left(P(\tau) - E(0) + V(\tau)\right)^2 \, \mathrm{d}\tau, \tag{4.42}$$

where $P(\tau) \equiv (\tau - \tau_{\min})(\tau - \tau_{\max})(\alpha_2\tau^2 + \alpha_1\tau + \alpha_0)$ and $V(\tau)$ is the potential energy, defined in equation (4.26). The function Φ is a positive-definite quadratic function of $(\alpha_0, \alpha_1, \alpha_2) \in \mathbb{R}^3$. It has a single minimum, attained at the point $(\alpha_0, \alpha_1, \alpha_2) = (\alpha_0^*, \alpha_1^*, \alpha_2^*) \in \mathbb{R}^3$. This point is the solution of the linear system

$$\frac{\partial \Phi}{\partial \alpha_j}(\alpha_0^*, \alpha_1^*, \alpha_2^*) = 0\,, \quad j = 0, 1, 2. \tag{4.43}$$

More explicitly, by defining the real coefficients

$$\gamma_j = \int_{\tau_{\min}}^{\tau_{\max}} \tau^j (\tau - \tau_{\min})^2 (\tau - \tau_{\max})^2 \, d\tau, \quad j = 0, \ldots, 4, \tag{4.44}$$

$$\delta_j = \int_{\tau_{\min}}^{\tau_{\max}} \tau^j (\tau - \tau_{\min})(\tau - \tau_{\max})[E(0) - V(\tau)] \, d\tau, \quad j = 0, 1, 2 \tag{4.45}$$

we obtain the system

$$\begin{pmatrix} \gamma_0 & \gamma_1 & \gamma_2 \\ \gamma_1 & \gamma_2 & \gamma_3 \\ \gamma_2 & \gamma_3 & \gamma_4 \end{pmatrix} \begin{pmatrix} \alpha_0^* \\ \alpha_1^* \\ \alpha_2^* \end{pmatrix} = \begin{pmatrix} \delta_0 \\ \delta_1 \\ \delta_2 \end{pmatrix}. \tag{4.46}$$

Each coefficient can be calculated explicitly in terms of elementary functions of $\tau_{\min}$ and $\tau_{\max}$. Since the matrix consisting of all the γ-coefficients is invertible provided we have $\tau_{\min} < \tau_{\max}$, the solution for α_j^* is uniquely determined.

After calculating the coefficients α_j^* for $j = 0, 1, 2$ as outlined above, we return to the approximate nonlinear differential equation

$$\left[\frac{\mathrm{d}\tau}{\mathrm{d}t}\right]^2 = (\tau - \tau_{\min})(\tau - \tau_{\max})(\alpha_2^*\tau^2 + \alpha_1^*\tau + \alpha_0^*)\,. \tag{4.47}$$

Solving this equation for $\tau(t)$ is now a matter of correctly evaluating an elliptic integral. To do this we must first reduce equation (4.47) to Legendre normal form. The method closely follows the approach detailed in [Abramowitz and Stegun, 1965]: the quartic polynomial above is written as a product of two quadratics, $Q_1(\tau) \equiv \alpha_2^*\tau^2 + \alpha_1^*\tau + \alpha_0^*$ and $Q_2(\tau) \equiv (\tau - \tau_{\min})(\tau - \tau_{\max})$. We look for values of λ such that $Q_1 - \lambda Q_2$ is a perfect square of a first-degree binomial in τ. To that end we require

that

$$4(\alpha_2^* - \lambda)(\alpha_0^* - \lambda\tau_{\min}\tau_{\max}) - (\alpha_1^* + (\tau_{\min} + \tau_{\max})\lambda)^2 = 0. \tag{4.48}$$

Solving this quadratic equation for λ we get

$$\lambda_\pm = \frac{-\omega \pm \sqrt{\omega^2 - (\tau_{\max} - \tau_{\min})^2((\alpha_1^*)^2 - 4\alpha_0^*\alpha_2^*)}}{(\tau_{\max} - \tau_{\min})^2}, \tag{4.49}$$

where we have defined

$$\omega = 2\alpha_0^* + \alpha_1^*(\tau_{\max} + \tau_{\min}) + 2\alpha_2^*\tau_{\max}\tau_{\min}. \tag{4.50}$$

Having found λ_+, λ_- we can then write

$$Q_1 - \lambda_- Q_2 = (\alpha_2^* - \lambda_-)\left(\tau + \frac{\alpha_1^* + (\tau_{\max} + \tau_{\min})\lambda_-}{2(\alpha_2^* - \lambda_-)}\right)^2, \tag{4.51}$$

$$Q_1 - \lambda_+ Q_2 = (\alpha_2^* - \lambda_+)\left(\tau + \frac{\alpha_1^* + (\tau_{\max} + \tau_{\min})\lambda_+}{2(\alpha_2^* - \lambda_+)}\right)^2. \tag{4.52}$$

Solving this system for Q_1 and Q_2 we obtain

$$Q_1 = \frac{\lambda_+(\alpha_2^* - \lambda_-)}{\lambda_+ - \lambda_-}(\tau + \alpha)^2 - \frac{\lambda_-(\alpha_2^* - \lambda_+)}{\lambda_+ - \lambda_-}(\tau + \beta)^2, \tag{4.53}$$

$$Q_2 = \frac{\alpha_2^* - \lambda_-}{\lambda_+ - \lambda_-}(\tau + \alpha)^2 - \frac{\alpha_2^* - \lambda_+}{\lambda_+ - \lambda_-}(\tau + \beta)^2, \tag{4.54}$$

where we have defined the two constants

$$\alpha = \frac{\alpha_1^* + (\tau_{\max} + \tau_{\min})\lambda_-}{2(\alpha_2^* - \lambda_-)}, \tag{4.55}$$

$$\beta = \frac{\alpha_1^* + (\tau_{\max} + \tau_{\min})\lambda_+}{2(\alpha_2^* - \lambda_+)}. \tag{4.56}$$

The method will work if and only if $\lambda_\pm$ are real and distinct. Since the coefficients α_j^*, ω, $\tau_{\max}$, $\tau_{\min}$ are all real, this is precisely equivalent to asking that $\omega^2 - (\tau_{\max} - \tau_{\min})^2((\alpha_1^*)^2 - 4\alpha_0^*\alpha_2^*) > 0$. We can restate this inequality in terms of the zeroes τ_+, τ_- of Q_1 and $\tau_{\max}$, $\tau_{\min}$ of Q_2, to find that we must stipulate $(\tau_{\max} - \tau_+)(\tau_{\max} - \tau_-)(\tau_{\min} - \tau_+)(\tau_{\min} - \tau_-) > 0$. Graphically, the latter inequality is equivalent to the statement that the zeroes of Q_1 are either: complex, which necessarily come in conjugate pairs; or real, but where the interval $(\tau_{\min}, \tau_{\max})$ contains either both zeroes of Q_1 or none of them.

We now ask whether it is possible to establish that the method will always work for physically admissible values of the parameters Z, F and initial conditions

R, φ_3, $E(0)$. Let us assume that τ_+, τ_-, the zeroes of Q_1, are real. By looking at the minimisation problem, notice that the potential $V(\tau)$ is convex. Therefore, if any of the zeroes τ_+, τ_- were in $(\tau_{\max}, \tau_{\min})$, then the approximating polynomial $P(\tau) = (\tau - \tau_{\min})(\tau - \tau_{\max})Q_1(\tau)$ would have a zero inside the interval $(\tau_{\max}, \tau_{\min})$, and so $P(\tau)$ would not be concave on $[\tau_{\min}, \tau_{\max}]$. It follows that a deformation of the coefficients α_j could be found so that $\Phi(\alpha_0, \alpha_1, \alpha_2)$ would decrease, thus violating the minimum principle that generated the point α_j^*.

In practice, in numerical applications and for a wide range of parameters we have found that the zeroes of Q_1 are complex (and therefore, conjugate pairs). In this case the method simplifies substantially because the quantities $\lambda_\pm$ satisfy $\lambda_- < 0 < \lambda_+$. So let us assume from here on that this is true. If we now make the substitution $r = (\tau + \alpha)/(\tau + \beta)$, we can reduce equation (4.47) to the normal form

$$\left[\frac{\mathrm{d}r}{\mathrm{d}t}\right]^2 = \frac{\lambda_+(\alpha_2^* - \lambda_-)^2}{(\lambda_+ - \lambda_-)^2}(\beta - \alpha)^2(a^2 + r^2)(r^2 - b^2), \tag{4.57}$$

where a, b are positive parameters defined by

$$a^2 = \max\left\{-\frac{(\alpha_2^* - \lambda_+)}{(\alpha_2^* - \lambda_-)}, -\frac{\lambda_-(\alpha_2^* - \lambda_+)}{\lambda_+(\alpha_2^* - \lambda_-)}\right\}, \tag{4.58}$$

$$b^2 = -\min\left\{-\frac{(\alpha_2^* - \lambda_+)}{(\alpha_2^* - \lambda_-)}, -\frac{\lambda_-(\alpha_2^* - \lambda_+)}{\lambda_+(\alpha_2^* - \lambda_-)}\right\}. \tag{4.59}$$

For physically sensible solutions (i.e., $\tau(t) \in \mathbb{R}$) we must choose the branch $r(t)^2 > b^2$ for all $t \geq 0$. We obtain, in terms of the Jacobi elliptic function,

$$r(t) = b\ \mathrm{nc}\left(\frac{4K(m_0)}{T_0}t + u_0 \middle| m_0\right), \tag{4.60}$$

defined by the physical period,

$$T_0 = \frac{2K(m_0)}{|Z||\beta - \alpha|\left[\frac{\lambda_+\alpha_1^*(\alpha_2^* - \lambda_-)^2}{(\lambda_+ - \lambda_-)^2}(a^2 + b^2)\right]^{\frac{1}{2}}}, \tag{4.61}$$

and elliptic modulus

$$m_0 = \frac{a^2}{a^2 + b^2}. \tag{4.62}$$

The value of the shift u_0 can be found directly in terms of the incomplete elliptic integral of the first kind:

$$u_0 = s_1 F\left(\arccos\left(\frac{b(\Delta + \beta)}{\Delta + \alpha}\right) \middle| m_0\right), \tag{4.63}$$

with $s_1 \in \{-1, +1\}$ being given by

$$s_1 = \operatorname{sgn}\left(ZC_3(0)(\beta - \alpha)\right). \tag{4.64}$$

Undoing the transformations applied to τ we finally uncover the solution

$$\tau(t) = \frac{b\beta - \alpha \operatorname{cn}\left(\frac{4K(m_0)}{T_0}t + u_0 \middle| m_0\right)}{\operatorname{cn}\left(\frac{4K(m_0)}{T_0}t + u_0 \middle| m_0\right) - b}. \tag{4.65}$$

Approximate expressions for the squares of the amplitudes $C_j(t)^2$ are obtained directly from equations (4.23) and (4.24), and the dynamical phase is obtained from equation (4.29). Plugging the solution (4.65) of our approximate system, into these expressions, we generate plots that can be compared with the numerical solutions of the original system (4.10). The results, shown in figures 4.6(a) to 4.6(d), show excellent agreement. We have validated numerically, for a wide range of choices of parameters, the following condition of boundedness of the approximate solution (4.65): $b > 1$ or, equivalently, $\alpha_2^* < 0$.

4.5 Boundedness when $H \neq 0$: Analytical evidence and Poincaré sections

When the Hamiltonian is non-zero, we have no *a priori* guarantee over integrability of the forced triad system, due to the system's formal equivalence to an autonomous volume-preserving 3-dimensional system of first order equations. If we try to reduce the forced triad system to an explicit 3-dimensional system we face yet another difficulty: the generic appearance of coordinate singularities, as exemplified in equations (4.4) at $C_1C_2 = 0$.

Fortunately, we can solve this difficulty completely and simplify matters considerably through an intelligent choice of variables. The procedure works only when $H \neq 0$, and is based on the observation that φ_3 is monotonic and so it becomes a proxy for time. Let us define the new variables,

$$p = \Re\{B_1B_2\},\ q = \Im\{B_1B_2\}, \tag{4.66}$$

with $\varphi_3 = \operatorname{Arg} B_3$ as before. Using the conservation law J, we observe that

$$\left(|B_1|^2 + |B_2|^2\right)^2 - J^2 = 4|B_1|^2|B_2|^2,$$

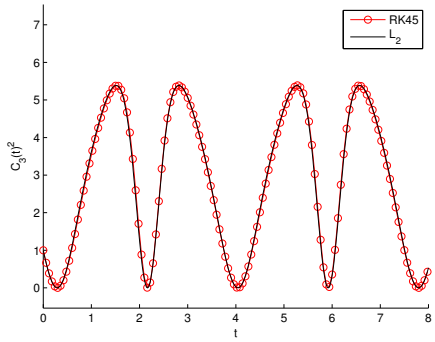

(a) $C_3(t)^2$ with $F = 1$

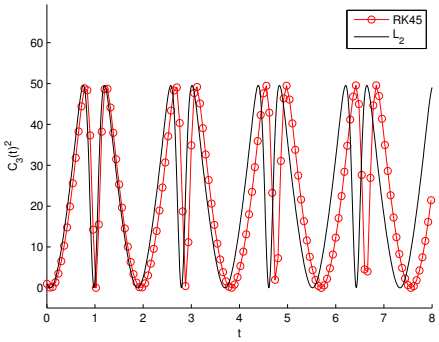

(b) $C_3(t)^2$ with $F = 10$

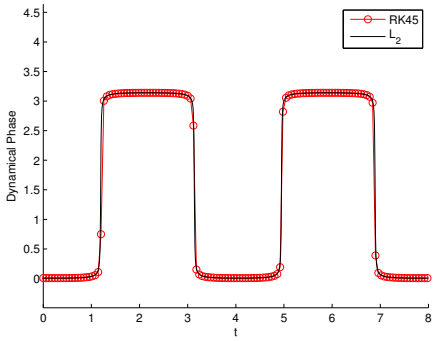

(c) $\varphi(t)$ with $F = 1$

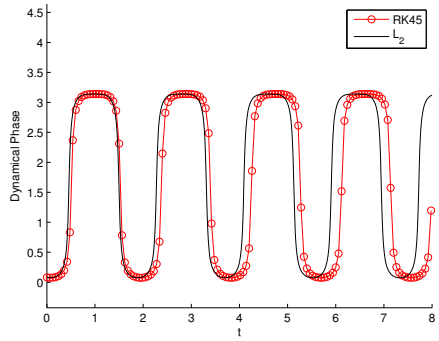

(d) $\varphi(t)$ with $F = 10$

Figure 4.6: Comparison of the L^2-method approximate solutions for the square amplitudes and dynamical phase. The corresponding numerically generated Runge-Kutta solutions are also included as a direct comparison against different forcing strengths. Choices for parameters: $\varphi_3(0) = -0.99\frac{\pi}{2}$, $E(0) = 3$, $J = 1$, $Z = 1$ and $\varphi(0)$ determined by setting $H = 0$.

and rewriting the right-hand term $|B_1|^2|B_2|^2 = p^2 + q^2$, we derive the remarkable formula

$$|B_1|^2 + |B_2|^2 = \sqrt{J^2 + 4(p^2 + q^2)}. \tag{4.67}$$

Differentiating the new variables (p, q, φ_3) with respect to time we obtain, after straightforward computations, the following three-dimensional system:

$$\begin{cases} \dot{p} = Z\sqrt{J^2 + 4(p^2 + q^2)}|B_3|\cos\varphi_3, \\ \dot{q} = Z\sqrt{J^2 + 4(p^2 + q^2)}|B_3|\sin\varphi_3, \\ \dot{\varphi_3} = -\dfrac{H}{2|B_3|^2}, \end{cases} \tag{4.68}$$

where the amplitude $|B_3|$ is a simple function of (p, q, φ_3) and the Hamiltonian H, which now reads

$$H = 2Z|B_3|\left[\left(q - \frac{F}{Z}\right)\cos\varphi_3 - p\sin\varphi_3\right]. \tag{4.69}$$

In this representation, we see that the angle φ_3 is not only monotonically increasing or decreasing depending on H, but can also be read directly as the slope of the parametric curve $(p(t), q(t))$. This follows simply from the relation

$$\frac{\mathrm{d}q}{\mathrm{d}p} = \tan\varphi_3.$$

Furthermore, we see from this new representation of H given in equation (4.69), that the condition for $|B_3|$ to remain finite is equivalent to the statement that the cross-product between the tangent vector, $(\dot{p}, \dot{q})$ and the off-centre radius vector $(p, q - F/Z)$ must remain non-zero. In essence, $(\dot{p}, \dot{q}) \times (p, q - F/Z)$ must point out of the plane.

Using this equivalence it makes sense to shift the origin of (p, q) coordinates and define a new pair of variables (r, ϕ) such that $p = r\cos\phi$ and $q = F/Z + r\sin\phi$, or

$$r^2 = (q - F/Z)^2 + p^2, \tag{4.70}$$

$$\tan\phi = \frac{q - F/Z}{p}. \tag{4.71}$$

Differentiating these expressions with respect to time gives the following system:

$$\begin{cases} \dot{r} = \dfrac{H}{2r}\sqrt{J^2 + 4(p^2+q^2)}\cot\left(\phi - \varphi_3\right), \\ \dot{\phi} = -\dfrac{H}{2r^2}\sqrt{J^2 + 4(p^2+q^2)}, \\ \dot{\varphi_3} = -\dfrac{2Z^2r^2}{H}\sin^2\left(\phi - \varphi_3\right). \end{cases} \tag{4.72}$$

The Hamiltonian now reads

$$H = 2Z|B_3|r\sin\left(\phi - \varphi_3\right). \tag{4.73}$$

Note here how both ϕ and φ_3 are monotonic functions in time, decreasing for $H > 0$ and increasing otherwise. We can go further by showing that their difference, $\theta \equiv \phi - \varphi_3$, must be bounded for all time. For instance, with the Hamiltonian now written in terms of these new variables, we can see that either $\sin\theta > 0$ when $ZH > 0$, or, $\sin\theta < 0$ when $ZH < 0$. Without loss of generality, we therefore know that θ must remain confined to one of the following intervals:

$$\begin{cases} \theta \in (0, \pi) & \text{if } ZH > 0; \\ \theta \in (-\pi, 0) & \text{if } ZH < 0. \end{cases}$$

These bounds cannot be saturated, otherwise we violate the assumption $H \neq 0$. Since we know the variable ϕ to be monotonic, it becomes a natural choice for our new 'time', letting us derive the new system

$$\begin{cases} \dfrac{\mathrm{d}r}{\mathrm{d}\phi} = -r\cot\theta, \\ \dfrac{\mathrm{d}\theta}{\mathrm{d}\phi} = 1 - \dfrac{4Z^2r^4\sin^2\theta}{H^2\sqrt{J^2 + 4(p^2+q^2)}}, \end{cases} \tag{4.74}$$

which is non-autonomous, but one where the 'time'-dependence appears only in the $J^2 + 4(p^2+q^2)$ term. Writing this term in these latest variables reads

$$J^2 + 4(p^2+q^2) = 4\left[\left(r + \frac{F\sin\phi}{Z}\right)^2 + c(\phi)^2\right], \tag{4.75}$$

where we have defined the ϕ-dependent, positive function $c(\phi)$ according to

$$c(\phi)^2 = \frac{J^2}{4} + \frac{F^2\cos^2\phi}{Z^2}. \tag{4.76}$$

4.5.1 Novel one-dimensional particle interpretation.

One may ask what is gained by these successive transformations. After all, this newest version of the system appears to offer little improvement over the original one written in terms of the variables p and q. Surprisingly, however, this new system has a novel one-dimensional particle interpretation similar to that obtained in the $H = 0$ case described earlier. If we make one final transformation $h(\phi) = r(\phi)^{-1}$, we derive the one-dimensional particle representation:

$$\frac{\mathrm{d}^2 h}{\mathrm{d}\phi^2} + h = \frac{2Z^2}{H^2 h^3 \sqrt{\left(h^{-1} + \frac{F\sin\phi}{Z}\right)^2 + c(\phi)^2}}. \tag{4.77}$$

This can be interpreted as a driven harmonic oscillator, with driving force that is 2π-periodic in ϕ but also dependent on the position h. Alternatively, we can write the system in terms of a potential $V(h, \phi)$:

$$\ddot{h} + V_h(h, \phi) = 0,$$

where the 'dot' now denotes derivative with respect to ϕ, and subscripts denote partial derivatives. Integrating equation (4.77) with respect to h, we evaluate this potential to be of the form,

$$\begin{aligned} V(h,\phi) = \frac{h^2}{2} + \frac{2Z^2}{H^2}\sqrt{\left(h^{-1} + \frac{F\sin\phi}{Z}\right)^2 + c(\phi)^2} \\ - \frac{2ZF\sin\phi}{H^2}\mathrm{arsinh}\left(\frac{h^{-1} + \frac{F\sin\phi}{Z}}{c(\phi)}\right) + f(\phi), \end{aligned} \tag{4.78}$$

where $f(\phi)$ is a yet to be determined function that is dependent on ϕ only. This potential is attractive for all values of ϕ, from which it follows that the solution must at least be bounded for finite 'time'.

The important question that remains is whether the solution remains bounded for all time. Our analytical work is in progress, based on Levi's theory [Levi, 1991], and will be reported elsewhere. Our numerical studies suggest that the answer is positive. We present now the evidence.

4.5.2 Poincaré sections.

Due to the periodic nature of the forcing term, we define a Poincaré map, $P : S \to S$, where $S = \mathbb{R}_{>0} \times \mathbb{R}$ is the set of initial conditions of the form $(h(0), h_\phi(0))$, and the

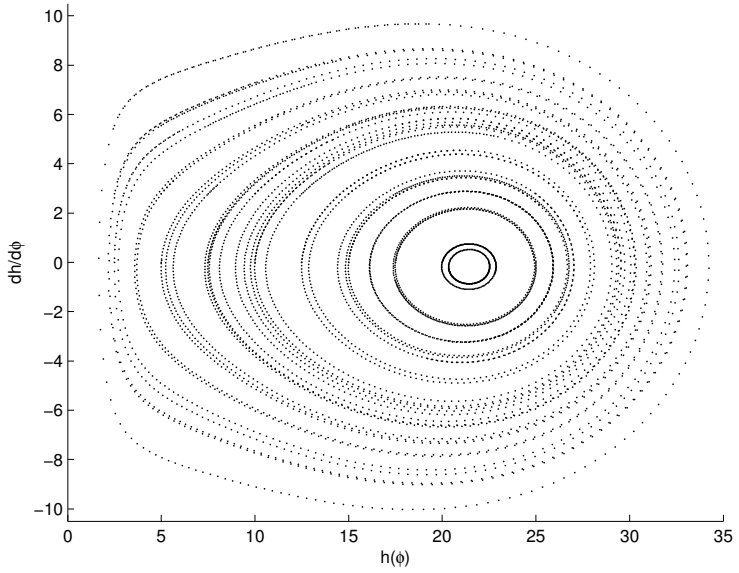

(a) $H = 0.1$

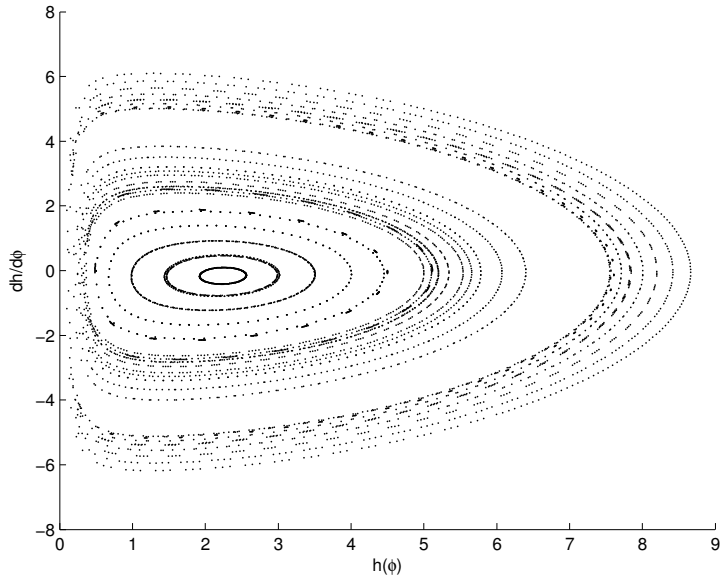

(b) $H = 1$

Figure 4.7: Poincaré sections produced for varying values of H. Here we have fixed the values of $Z = 1$, $J = 1$ and $F = 1$ in both panes. Closed invariant curves can clearly be identified in each figure.

transverse section is given by $\phi_n = 2n\pi$ corresponding to $H < 0$, and $\phi_n = -2n\pi$ if $H > 0$, taking $n \in \mathbb{N}_0$. Successive iterations of the map P are then defined through the equation

$$P^n(h(0), h_\phi(0)) = (h(\phi_n), h_\phi(\phi_n)), \;\; n \in \mathbb{N}_0. \tag{4.79}$$

Examples of some numerically generated Poincaré sections are given in figure 4.7. There is clearly no chaotic behaviour in the system, with the motion being quasi-periodic in nature, restricted to clearly visible closed invariant curves. Each of these curves is in fact a loop, suggesting that the motion remains bounded indefinitely. Furthermore, since the map is continuous when restricted to each of these one-dimensional loops, Brouwer's fixed-point theorem guarantees the existence of at least one fixed-point. It therefore follows that the system contains infinitely many periodic orbits, with period 2π in ϕ, one of which can clearly be identified on the line $h_\phi = 0$ where these loops converge to a point.

4.6 Chapter Summary

We have presented an in-depth analysis of the triad equations driven by external forcing, equations (4.3). We obtained a complete understanding of the dynamics when the Hamiltonian is zero by using conservation laws to reduce equations (4.3) to the one-dimensional motion of a particle in a time-independent potential. In this case, the dynamics are integrable for all initial conditions, and bounded for almost all initial conditions with a single exception provided by the special initial condition discussed in Sec. 4.2.4. Along the way, we presented several new explicit solutions, analytic formulae for the period and maximum energy of the motion and a novel scheme for approximating the dynamics when an explicit solution seems beyond reach. Our results for the case $H \neq 0$ are more qualitative and based on reducing the problem to the one-dimensional motion of a particle in an attractive time-periodic potential. Finite-time boundedness is thus established. Poincaré sections of the dynamics provide strong empirical evidence that the amplitudes remain bounded at all times, by a constant that depends on the initial conditions only, in the case $H \neq 0$. These amplitudes are typically quasi-periodic although periodic orbits also exist.

It is perhaps useful to discuss why the case $H = 0$ is so special. Mathematically, the case $H = 0$ leads to integrability directly as we showed in Section 4.1.3. Physically, there is a coincidence of two different effects that lead to integrability separately. Firstly, there is a phase-locking effect that follows from the fact that the Hamiltonian, being a nonlinear function of the phases and amplitudes, depends "lin-

early" on the amplitude $C_3(t)$ of the unstable mode, in the sense that $H = C_3 \times \frac{\partial H}{\partial C_3}$. In this case it follows that the time derivative of the phase $\varphi_3(t)$ is proportional to the value of the Hamiltonian. Therefore when the Hamiltonian is zero the phase φ_3 becomes a constant. Secondly, there is a "partial initial-condition memory loss" effect consisting of the fact that the Hamiltonian is zero when the amplitude C_3 is equal to zero (this is more general than being "linear" in C_3), and therefore in the case $H = 0$ the amplitude of the unstable mode $C_3(t)$ is allowed to vanish (see, e.g., equation 4.6)). In such a situation, generically, any given non-zero initial condition for C_3 will eventually lead to $C_3(T) = 0$ in a finite time T, due to the dynamics (in fact, this is true in our case $H = 0$, for almost all initial conditions, with the only exception of the unbounded sub-case). This means that generically the choice of initial condition for the amplitude $C_3(t)$ is irrelevant, being equivalent to a time-shifted case of the initial condition $C_3 = 0$. Therefore, the case $H = 0$ is degenerate in the sense that it reduces by an extra unit the dimension of the space of initial conditions, thus rendering the system closer to integrability.

Throughout the introduction we mentioned a multitude of physical systems, from nonlinear optics to plasmas, where resonantly interacting waves prominently feature. It is, however, unsurprising that the main consequences fall within the context of geophysical fluid dynamics. For instance, there has been much discussion, both theoretical and experimental, on the role topographical forcing plays for the onset of the extratropical intraseasonal oscillation [Dehai, 1998; Marcus et al., 1994]. Going back even earlier, the work in [McEwan et al., 1972] studied how the steady-state solution consisting of more than one triad responds to one mode undergoing continuous forcing. Deriving different interaction equations from the ones presented here, the work in [Cree and Swaters, 1991] examined how topographical forcing induces a detuning effect on the resonance conditions. Whereas closer to the work presented in this paper, the use of additive forcing has been directly applied to modelling the resonant interactions among equatorial waves in the presence of a periodic heat source [Raupp and Dias, 2009]. In this last paper, similar interaction equations to our own are derived but only studied numerically. This seems like a general feature across much of the literature in this area, which emphasises the consequences of our own work in providing explicit results pertaining to the integrability of models of this type.

Broadly speaking, our results illustrate two important points which are likely to have relevance beyond the particular problem studied in this article. The first is that, as illustrated by our boundedness results, the addition of forcing to a nonlinear wave system does not necessarily provide a continual source of energy for the

system. This should provide pause for thought for researchers interested in performing numerical simulations of wave turbulence (where a constant source of energy is often desirable in order to compare with theory) since such simulations are often performed by adding an external forcing term to a Hamiltonian wave equation. Our results are particularly relevant in situations when a deterministic forcing protocol is adopted. Having said that, many turbulence simulations adopt a stochastic forcing protocol. A study of the triad equation with stochastic forcing, along the lines of the work presented in [Milewski et al., 2002], while likely to be illuminating is beyond the scope of the present work. The detailed understanding of the deterministic case presented here would, however, be an essential first step. The second general lesson to be drawn from this work is the importance of phases in understanding the dynamics of resonantly interacting nonlinear waves. Since the dynamics of phases are often more difficult to obtain theoretically, they are often somewhat under-emphasised. Our results present some of the most striking examples yet of how varying an initial phase can result in completely different behaviour.

Chapter 5

The Kinematics of Nonlinear Resonance Broadening

There are currently two paradigms of thinking when it comes to tackling systems of nonlinear interacting dispersive waves. The first, and comparatively most recent of the two, devotes its attention to understanding the integrability of small clusters of modes, typically say consisting of three and four modes, deriving analytical solutions for these reduced dimensionality systems. We categorise these regular, discretised systems under the name of Discrete Wave Turbulence (DWT). The second considers when we have large sets, possibly infinite in the continuum limit, of interacting modes, exhibiting some sense of collective randomness that can be well described by statistical theory. While the first of these regimes is applicable when some measure of the overall nonlinearity, or energy, in the system is small, perhaps with a few modes dominating statistically over the rest, the second falls under the remit of what is called Statistical Wave Turbulence (SWT). Intuitively, we know that increasing the dimensionality of the wave system must introduce some sense of randomness, as we move between the DWT and SWT regimes. However, what is unexpected is that we can observe systems that exhibit both statistical and discrete layers of wave turbulence, mutually coexisting at the same time. This new type of turbulence has been given the title of mesoscopic wave turbulence, and it is here that quasi-resonant interactions are thought to be crucial.

We have therefore categorised two different generic types of wave turbulence, and a third, which is simply an intermixing of the two. One question to ask is whether it is possible to categorise when precisely a wave system inhabits each of these three regimes. First, we consider SWT and its underlying assumptions. Discovered by Hasselmann and Zakharov independently, [Hasselmann, 1962] and

[Zakharov and Filonenko, 1967] respectively, SWT was thought to represent the complete understanding of weakly nonlinear wave systems. In fact, for infinitely sized systems, it is known to be asymptotically exact [Nazarenko, 2011; Newell and Rumpf, 2011]. Central to this theory are the assumptions of weak nonlinearity, randomness of phases and an infinite box limit. This statistical regime is thought to be characterised by asking that the degree of resonance broadening, Ω, is far greater than the spacing between individual modes

$$\Omega \gg (\partial\omega/\partial k)2\pi/L, \tag{5.1}$$

where L is the box size in the case of periodic boundary conditions [Kartashova, 2009]. An inertial interval (k_0, k_1) is assumed, where energy is conserved, and dissipation suppresses nonlinear dynamics for $k \gg k_1$. The wave system is then thought to be adequately described by kinetic equations and their corresponding stationary solutions, known as Kolmogorov-Zakharov (KZ) energy spectra, defined across this inertial interval [Zakharov et al., 1992]. When $k \ll k_0$, the dynamics are thought to be attributed to finite-size effects, captured by some low-dimensional, chaotic dynamical system that can be considered separately. For discrete systems however, it is now established that independent clusters of exactly resonant modes can leave a readily identifiable signature way within this inertial interval, with organised structures being recognised across the entire spectrum [Kartashova, 2006]. Here it was suggested that increasing the amplitude of this system allows energy to spread to other modes in a selective way governed by 'channels' of quasi-resonant interactions. Due to the fact that these two layers of turbulence can occur simultaneously, the author of this reference called this phenomenon 'laminated turbulence'. Further evidence of this coexistence of regimes was found in numerical simulations of capillary waves [Pushkarev and Zakharov, 2000] and for surface gravity waves [Zakharov et al., 2005], where the now more commonly used expression 'mesoscopic turbulence' was first coined.

Some attempts have been made to attempt to modify the standard moment closure approach at the heart of SWT that may account for these discrepancies. For instance, when we first encountered the idea of quasi-resonant interactions in section 2.1.4, it is argued that they could be used to resolve what is thought to be an issue of consistency with the derivation of the kinetic equations at the heart of SWT [Lvov et al., 2011]. The addition of quasi-resonant interactions into SWT as a concept is not unique to this reference. It has been applied in the context of gravity waves, and corroborates the idea that two evolutionary timescales must exist in our wave

system: a fast one where quasi-resonant interactions dominate, and then slower resonant interactions follow [Janssen, 2003]. The resulting kurtosis in the wave action is thought to agree well with the occurrence of freak waves in the system. Similar arguments have been proposed elsewhere to suggest that only recently there is now a shift of view that stresses any complete description of dispersive wave systems must take account the influence of quasi-resonant interactions [Bustamante and Hayat, 2012; Connaughton et al., 2010].

On the other hand, we can suitably classify DWT according to two different kinds of interaction. As we have seen, these correspond to exact resonances, where $\Omega = 0$, and quasi-resonances, where instead we consider

$$0 < \Omega \lesssim (\partial\omega/\partial k)2\pi/L. \tag{5.2}$$

The gaps in the KZ-spectra we discussed above, are then shown to correspond to the discrete dynamics of exact and quasi-resonant clusters [Kartashova, 2009]. Classifying the two prominent types of turbulent regime does in fact present what can only be described as a 'gap'. Here, we can find a situation where the broadening satisfies neither condition (5.2) or (5.1). The existence of this gap was first suggested by [Nazarenko, 2007] in the context of MHD wave turbulence, and was promptly categorised as mesoscopic wave turbulence. Here a very nice analogy was made with self-organised-criticality, which ties in nicely with the percolation result of this chapter we will explore later. When this system was exposed to a certain kind of external forcing, it was found that both regular and kinetic regimes statistically alternate with time [Nazarenko, 2006]. The transition between these two regimes can be characterised in terms of avalanche-like behaviour when the resonance broadening becomes of the same order as the spacing between modes.

We note that the existence of these generic three types of turbulence has been corroborated elsewhere in the literature. The mesoscopic regime, for example, has being identified experimentally for gravity wave turbulence in a laboratory flume [Denissenko et al., 2007]. Various experiments have detected the persistent pattern attributed to DWT in gravity water waves [Hammack and Henderson, 2003], [Hammack et al., 2005], as well as being used to describe interseasonal oscillations in the Earth's atmosphere [Kartashova and Lvov, 2007]. However, in certain physical situations, such as found in a tidal channel, only SWT is found to be observable [Grant et al., 1962]. The idea of implementing some tuneable parameter to induce a transition between the DWT and SWT regimes has also been suggested, applying an underlying current to capillary water waves whose vorticity dictate whether

three-wave resonances exist or otherwise [Constantin and Kartashova, 2009]. An excellent summary of current the current theory and methodology behind discrete and mesoscopic wave turbulence can be found in [Kartashova et al., 2010].

The question that remains therefore, is what precisely are the roles played by resonant and quasi-resonant interactions in the full description of mesoscopic wave turbulence. It is only relatively recently, that a new approach has been proposed with the very specific objective of validating through direct numerical simulation many of the quantitative and qualitative theoretical results underlying SWT. A key milestone here being the observation of Kolmogorov-type spectra corresponding to not only the direct, but also inverse cascade [Annenkov and Shrira, 2006b]. The key to this approach is that instead of expressing our wave field in terms of discrete, regular grids of Fourier harmonics, it builds a solution using a large ensemble of what are referred to as 'wave packets' [Annenkov and Shrira, 2001]. Much like the approach of DWT, each of these packets consists of clusters of resonant interactions supplemented by a neighbourhood of quasi-resonantly interacting modes. Each wave packet is endowed with a randomly chosen initial phase, with individual modes contained with each packet evolving according to the full underlying evolutionary equation, otherwise known as the Zakharov equation. Aside from showing strong numerical agreement with much of what underlies SWT, it further corroborates the existence of multiple evolutionary timescales and has even brought into question the significance of exactly resonant interactions in the evolution of the wave field [Annenkov and Shrira, 2006a]. If proven to be rigorous, one could hope this approach might form the foundation of any unified description of wave turbulence that covers each of the three regimes mentioned above: it combines both an account of the full dynamics governing clusters of resonantly and quasi-resonantly interacting modes, in a way that corroborates much of the quantitative and qualitative predictions behind SWT.

The idea of connecting criticality and quasi-resonance is not a new subject. For capillary waves, it has been demonstrated that no exactly resonant clusters can exist, and so a local low boundary for resonance broadening can be found [Kartashova, 2007]. Even when the number of modes tends to infinity, this boundary may in fact be strictly non-zero and so suggests that a critical level of broadening is required that must be in excess of this boundary so quasi-resonant interactions can occur. A different approach is to consider a specific mode, [Pushkarev, 1999], or indeed a group of modes defined within some small initial region [Lvov et al., 2006; Connaughton et al., 2001], and then partition the remaining modes of the system into those that lie within some allowed resonance width of our chosen set

of modes, and those that do not. In both cases, only if the resonance broadening was above some critical value do we see additional quasi-resonant modes become permissible. In terms of a kinematic view of the system, we see that some critical level of broadening is required to allow the onset of an energy cascade. This falls neatly in line with the concept of 'frozen turbulence' as observed by [Pushkarev, 1999] and [Tanaka and Yokoyama, 2004] in the context of capillary waves.

The aim of this chapter is to expand further upon this notion of criticality, except now applied to the dispersion relationship associated with the Charney-Hasagawa-Mima (CHM) equation. Rather than follow the same procedure in the literature, producing what are known as 'cascade trees' described above, we look to characterise the connectedness of the entire system of modes as dictated by some prescribed level of resonance broadening. For this particular dispersion relationship, we will show that the quasi-resonant conditions can be solved analytically and that the solution can appear degenerate for critical values of detuning. This allows us to deduce global bounds on when the system becomes saturated, which in essence, describes when all modes form part of one 'percolating' cluster through the entire system. In fact, we will show that the size of the largest cluster depends critically on the level of resonance broadening, and at this critical point we observe a peak in the total number of distinct clusters. Numerically, we will show that there exists a region of large scale modes that prove resilient to joining this cluster, corresponding to results in the literature based on wave-turbulence boundaries and the generation of zonal flow and jets. Finally, we will show that this critical behaviour is not unique to just the CHM dispersion relationship, and can be applied to other systems where three interactions are thought to dominate, such as those described by power-law dispersion relationships. The thought is then that it may be possible to marry the three different regimes of turbulence with this concept of criticality. In particular, broadening less than this critical point would suggest that DWT should apply, until the onset of criticality where mesoscopic turbulence appears. At saturation, no discreteness should be present and so the system is aptly described by SWT.

5.1 Solving the Detuned Resonance Conditions for the CHM Dispersion Relationship

Throughout this chapter, we will only consider wave systems where three-wave interactions are thought to dominate the underlying nonlinear dynamics. A perfect example of this is found in the CHM equation, which admits a cubic Hamiltonian and so only three-wave interactions are permissible. Generally speaking, however,

dissipative nonlinear wave systems admit a Hamiltonian expanded as series of terms involving interactions of an increasing number of waves. In certain systems it is possible to show that some of these terms are identically zero, such as three-wave interactions in gravity waves at large scales. However, in most physical systems, three and four wave interactions remain prominent. By retaining only those interactions which solve the quasi-resonance conditions below we generate a kinematic interpretation of the system. One where we have distinguished between modes that should dominate the evolution of the system by courtesy of having some small finite resonance width. As you recall, this quasi-resonance condition is given by

$$\begin{cases} k_3 = k_1 + k_2, \\ |\omega(k_3) - \omega(k_1) - \omega(k_2)| \leq \Omega. \end{cases} \tag{5.3}$$

where $\Omega \geq 0$ is real and corresponds to the degree of resonance broadening as described above. As such the detuning corresponds to a perturbation in the frequency space only. The anisotropic dispersion relationship for the CHM equation is given by

$$\omega(k) = -\frac{\beta k_x}{k^2 + F}. \tag{5.4}$$

Here we take the two real and positive non-dimensional parameters F and β to be positive. Their meaning in the context of geophysical fluid dynamics has already been outlined in the preliminary chapter.

The objective is that for fixed $k_3 \in \mathbb{R}^2$, can we define explicitly the corresponding set of $k_1,\ k_2 \in \mathbb{R}^2$ that solve these conditions. When $\Omega = 0$, an explicit form of the resonant manifold is known and already well-documented [Longuet-Higgins et al., 1967]. The idea is then to generalise the method outlined in this reference to account for both arbitrary $F > 0$ and for the introduction of resonance broadening. Instead of a one-dimensional closed and bounded curve, what we will find is that the shape of the two-dimensional region defined by equation (5.3), which we will denote $\mathcal{R}$, is sensitively dependent on the level of resonance broadening. For instance, we will show both how the region $\mathcal{R}$ remains well-behaved in some respects, remaining bounded and representing what could be considered a 'thickening' of the exactly resonant manifold. However, some levels of broadening may present a singularity where the solution set becomes unbounded, enclosing the formation of two, three or possible even four disjoint, bounded but open regions, where the conditions above do not hold.

5.1.1 Explicit solution for the detuned manifold

The approach is to consider the one-dimensional solution curve corresponding to a fixed instance of δ, where $|\delta| < \Omega$, that solves

$$\omega(k_3) - \omega(k_1) - \omega(k_2) = \delta, \tag{5.5}$$

still keeping the relationship $k_3 = k_1 + k_2$. We define these solution curves as the detuned manifold corresponding to a particular value of the resonance width, δ. This parameter can also naturally be called the detuning. Solutions to full quasi-resonant conditions can then be found by integrating over all $|\delta| < \Omega$, with the boundary to $\mathcal{R}$ defined by setting $\delta = \pm\Omega$. To begin, let us substitute the explicit form of the dispersion relationship for the CHM equation into the equality given by equation (5.5). We get

$$\begin{aligned} &k_{1x}(k_2^2 + F)(k_3^2 + F) + k_{2x}(k_1^2 + F)(k_3^2 + F) - k_{3x}(k_1^2 + F)(k_2^2 + F) \\ &\quad = \frac{\delta}{\beta}(k_1^2 + F)(k_2^2 + F)(k_3^2 + F). \end{aligned} \tag{5.6}$$

Since $k_3 = k_1 + k_2$, it follows that the vectors $\mathbf{0}$, k_1, k_2 and k_3 must form a parallelogram whose diagonals bisect at the point $\frac{1}{2}k_3$. We can therefore write both k_1 and k_2 in terms of an additional vector k_0 defined along one of these diagonals such that

$$\begin{cases} k_1 = \frac{1}{2}(k_3 + k_0), \\ k_2 = \frac{1}{2}(k_3 - k_0). \end{cases} \tag{5.7}$$

If we were to consider fixed values of k_3, we would effectively reduce the problem to a two-dimensional one, since the solution can be fully described in terms of the wavenumber k_0. We now substitute these new expressions for k_1 and k_2 into equation (5.6), which removes one more degree of freedom, and deal with each side separately. First, the right-hand-side is the simplest to calculate, which after some routine algebra gives

$$\text{RHS} \equiv \frac{\delta(k_3^2 + F)}{16\beta}\left[k_3^4 + k_0^4 + 2k_0^2k_3^2 + 16F^2 + 8F(k_0^2 + k_3^2) - 4(k_{0x}k_{3x} + k_{0y}k_{3y})^2\right]. \tag{5.8}$$

The left-hand-side is a little more involved, but after simplifying we find

$$\begin{aligned} \text{LHS} \equiv &\frac{1}{16}k_{3x}\left[3k_3^4 - k_0^4 + 2k_0^2k_3^2 + 4F(3k_3^2 - k_0^2) + 4(k_{0x}k_{3x} + k_{0y}k_{3y})^2\right] \\ &- \frac{1}{2}k_{0x}(k_3^2 + F)(k_{0x}k_{3x} + k_{0y}k_{3y}). \end{aligned} \tag{5.9}$$

In both of these expressions, we have introduced the notation $k_j = (k_{jx}, k_{jy})$ to distinguish between each component. Re-writing the problem in terms of the polar co-ordinates

$$k_j = r_j \left(\cos\theta_j, \sin\theta_j\right), \; j = 0, 1, 2, 3, \tag{5.10}$$

the left-hand-side becomes

$$\begin{aligned} \text{LHS} = &\frac{1}{16} r_3 \cos\theta_3 \left[3r_3^4 - r_0^4 + 4F(3r_3^2 - 2r_0^2)\right] \\ &+ \frac{1}{8} r_3 r_0^2 \Big[2(r_3^2 + F)\sin\theta_3 \sin 2\phi - (r_3^2 + 2F)\cos\theta_3 \cos 2\phi\Big]. \end{aligned} \tag{5.11}$$

Here, we have defined the new angle $\phi = \theta_0 - \theta_3$ and applied the identity

$$\cos\theta_0 \cos\phi = \frac{1}{2}\left[\cos(2\phi + \theta_3) + \cos\theta_3\right]. \tag{5.12}$$

For the remaining side we derive the expression

$$\text{RHS} \equiv \frac{\delta(r_3^2 + F)}{16\beta}\Big[r_3^4 + r_0^4 + 16F^2 + 8F(r_0^2 + r_3^2) - 2r_0^2 r_3^2 \cos 2\phi\Big]. \tag{5.13}$$

Say that we now fix our choice for k_3. Equating both sides would now give a quadratic equation in r_0^2 as a function of the new angle ϕ. Roots of this quadratic equation, provided that they were both real and positive, would then define our solution for this particular choice of k_3 and δ. After some routine manipulation we are left with

$$\gamma r_0^4 + 2r_0^2\Big[\gamma(4F - r_3^2\cos 2\phi) + 2r_3\cos(2\phi + \theta_3)\Big] + \left(r_3^2 + 4F\right)^2\left[\gamma - \frac{4r_3\cos\theta_3}{r_3^2 + 4F}\right] = 0, \tag{5.14}$$

where for the sake of brevity we have introduced the new parameter

$$\gamma = \frac{r_3\cos\theta_3}{r_3^2 + F} + \frac{\delta}{\beta}. \tag{5.15}$$

The value of this parameter can be allowed to vary independently as a function of δ alone and corresponds neatly to $\gamma = \left(\delta - \omega(k_3)\right)/\beta$. Naively one might expect that allowing some degree of resonance broadening would result in a 'thickening' of the solution set $\mathcal{R}$. However, as we will now show, changing this value of γ results in a complex array of different behaviour.

Assuming $\gamma \neq 0$, we now have an explicit solution to equation (5.14) and

therefore, the resonance conditions as well. We get

$$r_0(\phi)^2 = \frac{-B(\phi) \pm \Delta(\phi)^{\frac{1}{2}}}{\gamma}, \tag{5.16}$$

written in terms of the two ϕ-dependent functions,

$$B(\phi) = \gamma(4F - r_3^2 \cos 2\phi) + 2r_3 \cos(2\phi + \theta_3), \tag{5.17}$$

and the discriminant

$$\Delta(\phi) = B(\phi)^2 + (r_3^2 + 4F)^2 \left(\frac{4r_3 \cos\theta_3}{r_3^2 + 4F} - \gamma \right) \gamma. \tag{5.18}$$

At this stage it makes sense to write $B(\phi)$ in terms of two new constants, independent of ϕ, an amplitude D and angle α, which are defined by

$$D^2 = r_3^2\gamma^2 - 4r_3\gamma\cos\theta_3 + 4, \tag{5.19}$$

and

$$\tan 2\alpha = \frac{2\sin\theta_3}{2\cos\theta_3 - r_3\gamma}, \ |\alpha| \leq \tfrac{\pi}{4}. \tag{5.20}$$

Note that since here we take the definition of $\arctan(x)$ mapping to the interval $\left[-\frac{\pi}{2}, \frac{\pi}{2}\right]$, we need to ensure that the correct sign is present when substituting α to solve $D\cos 2\alpha = 2\cos\theta_3 - r_3\gamma$ and $D\sin 2\alpha = 2\sin\theta_3$. To do so, we simply take $\alpha \to \alpha + \frac{\pi}{2}$ if $2\cos\theta_3 - r_3\gamma \leq 0$. We now have that

$$B(\phi) = 4F\gamma + r_3 D\cos(2\phi + 2\alpha). \tag{5.21}$$

This has two distinct advantages over the previous form for B: first, we can now identify the angle α that determines the lines of symmetry for each of the boundaries of the region $\mathcal{R}$, and hence their orientation; and secondly, we can readily read off both the maximum and minimum values attained by the discriminant $\Delta(\phi)$. The latter of these will be useful in obtaining bounds of the resonance broadening used in characterising the general shape of $\mathcal{R}$.

5.1.2 Degenerate cases and the exactly resonant manifold

The solution for $r_0(\phi)$ poses some interesting questions. For instance, we have yet to consider the case when $\gamma = 0$, neither have we considered what happens in the other situation when the discriminant is zero, namely when we set $\gamma = 4r_3\cos\theta_3/(r_3^2+4F)$.

For peace of mind, it also makes sense to check that setting $\delta = 0$ recovers the form of the exact manifold found in the literature [Longuet-Higgins et al., 1967]. We treat each of these questions case-by-case as follows.

i) First, let us see what happens in the exactly resonant case by taking $\delta = 0$. Assuming $\cos\theta_3 \neq 0$, the quadratic equation given by equation (5.14) then simplifies considerably to become

$$r_0^4 + 2r_0^2\bar{B}(\phi) - 3r_3^2(r_3^2 + 4F) = 0, \tag{5.22}$$

where we have defined

$$\bar{B}(\phi) = 4F + (r_3^2 + 2F)\sec 2\alpha \cos(2\phi + 2\alpha). \tag{5.23}$$

The definition of α found in equation (5.20) still applies here, but reduces to

$$\tan 2\alpha = \frac{2(r_3^2 + F)\tan\theta_3}{r_3^2 + 2F}. \tag{5.24}$$

In this instance, the now simplified quadratic equation always has positive real roots for any value of ϕ, which are given by

$$r_0^2 = -\bar{B}(\phi) + \sqrt{\bar{B}(\phi)^2 + 3r_3^2(r_3^2 + 4F)}. \tag{5.25}$$

This corresponds exactly with the one-dimensional closed manifold given in the literature cited above. This solution proves useful as a reference point when plotting the solutions to the various quasi-resonant conditions given throughout figures (5.1(a)) - (5.1(d)).

ii) We now examine what happens in the degenerate case when $\gamma = 0$. This corresponds to $\delta = \omega(k_3)$ and we quickly see that the detuned manifold no longer remains bounded. Here, equation (5.14) reduces to a linear one in r_0^2 with solution

$$r_0^2 = \frac{\cos\theta_3(r_3^2 + 4F)}{\cos(2\phi + \theta_3)}. \tag{5.26}$$

Again, let us assume that $\cos\theta_3 \neq 0$. We now have that r_0^2 is only positive provided we choose ϕ such that

$$\frac{\cos\theta_3}{\cos(2\phi + \theta_3)} > 0.$$

We readily see that $r_0(\phi)$ diverges precisely when $2\phi+\theta_3 = (2n+1)\frac{\pi}{2}$, where $n \in \mathbb{Z}$. An example of this case is shown in figure (5.1(b)).

iii) Finally, let us consider what happens when we take $\gamma = 4r_3\cos\theta_3/(r_3^2+4F)$. In this case equation (5.14) gives both the trivial solution $r_0 = 0$ and

$$r_0^2 = -\frac{2}{\gamma}\Big[4F\gamma + r_3 D\cos(2\phi+2\alpha)\Big]. \tag{5.27}$$

For this to be positive we require that $\gamma B(\phi) < 0$, which could potentially restrict our range of viable ϕ for a solution to exist depending on our choice of k_3. One particular instance of this case is shown in figure (5.1(c)), where the boundary of $\mathcal{R}$ intersects itself within the exactly resonant manifold.

From these three cases, we can clearly see that the shape of the detuned manifold depends dramatically on this choice of γ: in case (i) the manifold was well-defined for all values of ϕ with the manifold forming a closed curve in this case, whereas in case (ii), this manifold is only defined for a limited range of ϕ, becoming no longer bounded. Case (iii) in fact touches upon the third type of behaviour, where we find that the solution for r_0 remains valid only for a limited range of ϕ, which is dependent on our choice of k_3. Under these conditions, a point of transition emerges where the manifold self-intersects and two disjoint closed curves begin to form.

5.1.3 Calculating bounds on detuning

From these three cases, a natural question to ask is whether we can define the behaviour of the detuned manifold completely for all values of γ. As an aside, we will show that the manifold is only well-defined for a finite range of γ, which we can calculate explicitly provided $F > 0$. In the case when $F = 0$, the detuned manifold is found to exist for any value of δ. Tackling this question comes in the form of two propositions.

Proposition 1: Let us define the set Γ_1 as all γ such that the following conditions hold:

$$\begin{cases} 0 < \gamma < \dfrac{4r_3\cos\theta_3}{r_3^2+4F}, \text{ if } \cos\theta_3 > 0; \\ \dfrac{4r_3\cos\theta_3}{r_3^2+4F} < \gamma < 0, \text{ if } \cos\theta_3 < 0. \end{cases} \tag{5.28}$$

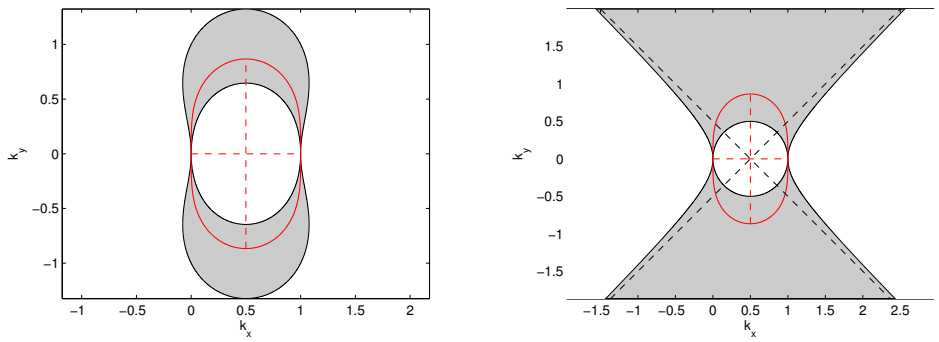

(a) $\Omega = 0.5$ (b) $\Omega = 1$

(c) $\Omega = 3$ (d) $\Omega = 5$

Figure 5.1: Solutions to the resonance conditions with varying degrees of broadening $\Omega = 0.5$. The solution set $\mathcal{R}$ is shaded in grey, calculated by solving the boundary curves for corresponding values of γ. Here we have fixed the wavenumber $k_3 = (1, 0)$ along with parameters $F = 0$ and $\beta = 1$. For comparison, the exactly resonant manifold is plotted in red with axes of symmetry described by the red dashed lines.

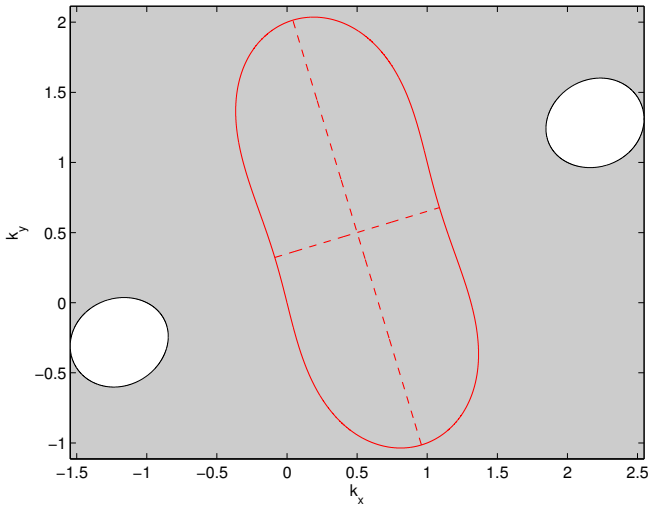

Figure 5.2: Solution to the resonance conditions with broadening $\Omega = 0.5$. The detuned manifold within the exactly resonant manifold no longer exists for this value of detuning, as guaranteed by *Proposition 1*. Here we have set $k_3 = (1, 1)$ and $\beta = F = 1$.

Then the solution r_0 to equation (5.16) is both real and uniquely defined for all values of ϕ if and only if $\gamma \in \Gamma_1$.

Proof: First let us show that if $\gamma \in \Gamma_1$ then $r_0(\phi)$ has only one real solution for all values of ϕ. Using these conditions, the discriminant $\Delta(\phi)$ is clearly positive and trivially, $\Delta(\phi) > B(\phi)^2$ for all values of ϕ. This proves that r_0^2 must be real-valued. Uniqueness follows simply now, where the choice of sign present in equation (5.16) must be taken to be positive when $\gamma > 0$, and the negative otherwise.

We now deal with the converse statement. Expanding $\Delta(\phi)$ and grouping terms of the same power in γ gives the alternate expression

$$\begin{aligned}\Delta(\phi) = &-4r_3^2\cos^2\phi(4F + r_3^2\sin^2\phi)\gamma^2 + 4r_3^2\cos^2(2\phi+\theta_3) \\ &+ 8r_3\cos\phi\Big[4F\cos\theta_0 + r_3^2\sin\phi\sin(2\phi+\theta_3)\Big]\gamma.\end{aligned} \tag{5.29}$$

Let us now suppose we take ϕ such that $\cos\phi = 0$, $\Delta(\phi)$ simplifies giving the two

solutions, $r_0^2 = -(r_3^2 + 4F)$ and

$$r_0^2 = \frac{r_3^2 + 4F}{\gamma^2}\left(\frac{4r_3\cos\theta_3}{r_3^2+4F} - \gamma\right)\gamma. \tag{5.30}$$

Clearly, only this second solution can be positive provided that $\gamma \in \Gamma_1$. We have therefore shown that only for $\gamma \in \Gamma_1$ can the detuned manifold be uniquely defined for all values of ϕ and thus guaranteed to form a single closed and bounded curve. These conditions cannot be extended to include the two end-points in (5.28) as detailed in the three examples given above and so this concludes the proof.

Let us now assume that $\gamma \notin \bar{\Gamma}_1$, which are all points not in the closure of Γ_1. In this case we now have that $\Delta(\phi) \leq B(\phi)^2$ for all values of ϕ. There are now ultimately two possibilities: either, $\gamma B(\phi) > 0$ in which there exists no real solutions to equation (5.16); or, $\gamma B \leq 0$ whereby two real, possibly distinct, solutions now exist. We therefore have two conditions set on ϕ that must be satisfied simultaneously for the detuned manifold to exist, namely, that $\gamma B(\phi) \leq 0$ and $\Delta(\phi) \geq 0$. Let us deal with the first of these two conditions. If you recall from the notation above, we have that

$$\gamma B(\phi) = 4F\gamma^2 + r_3\gamma D\cos(2\phi + 2\alpha). \tag{5.31}$$

For there to at least exist one value of ϕ for which this is negative, we require that $r_3 D \geq 4F|\gamma|$. Since both sides of this inequality are positive, this is precisely equivalent to asking that

$$\gamma^2\left(r_3^4 - 16F^2\right) - 4r_3^3\gamma\cos\theta_3 + 4r_3^2 \geq 0. \tag{5.32}$$

The discriminant for this quadratic can be easily calculated and comes to

$$-16r_3^2\left(r_3^4\sin^2\theta_3 - 16F^2\right), \tag{5.33}$$

which is negative only when $r_3^2|\sin\theta_3| \geq 4F$. If this were the case, then it is trivial to see that $r_3 D \geq 4F|\gamma|$ for any values of γ. Otherwise, we need to define the two bounds

$$\gamma_{1,\pm}^* = \frac{2r_3}{r_3^4 - 16F^2}\left(r_3^2\cos\theta_3 \pm \sqrt{16F^2 - r_3^4\sin^2\theta_3}\right). \tag{5.34}$$

If $r_3^2|\sin\theta_3| < 4F$ and $r_3^2 > 4F$ then we must stipulate that either $\gamma \leq \gamma_{1,-}^*$ and $\gamma \geq \gamma_{1,+}^*$. If, however, we have that $r_3^2|\sin\theta_3| < 4F$ and $r_3^2 < 4F$ then we must take $\gamma_{1,-}^* \leq \gamma \leq \gamma_{1,+}^*$. Finally, we consider when $r_3^2 = 4F$. The inequality defined in

(5.32) is now solved simply by taking γ such that

$$1 - r_3\gamma\cos\theta_3 \geq 0. \tag{5.35}$$

Once these conditions for γ have been met, it now becomes trivial to find the values of ϕ that satisfy the inequality $\gamma B(\phi) \leq 0$. For instance, if $\gamma > 0$, then we take

$$\begin{cases} \phi^* \leq \phi + \alpha \leq \pi - \phi^*, \\ \pi + \phi^* \leq \phi + \alpha \leq 2\pi - \phi^*, \end{cases} \tag{5.36}$$

whereas if $\gamma < 0$, then,

$$\begin{cases} -\phi^* \leq \phi + \alpha \leq \phi^*, \\ \pi - \phi^* \leq \phi + \alpha \leq \pi + \phi^*, \end{cases} \tag{5.37}$$

where we have defined

$$\phi^* = \frac{1}{2}\arccos\left(-\frac{4F\gamma}{r_3 D}\right),\ \phi^* \in \left[0, \tfrac{\pi}{2}\right]. \tag{5.38}$$

This leaves just the final inequality $\Delta(\phi) \geq 0$. We now restrict ϕ to the intervals defined by (5.36) and (5.37) so as to ensure that $\gamma B(\phi) \leq 0$. Once limited to these intervals, $\Delta(\phi)$ attains a minimum value of

$$\Delta_{\min} = \gamma(r_3^2 + 4F)^2\left(\frac{4r_3\cos\theta_3}{r_3^2 + 4F} - \gamma\right). \tag{5.39}$$

As you would expect, when $\gamma \notin \bar{\Gamma}_1$ we must also have $\Delta_{\min} < 0$. In this case, it therefore follows that the restrictions placed on γ to guarantee $\gamma B \leq 0$ are not alone always sufficient to ensure that $\Delta(\phi) \geq 0$. If instead we were to calculate the maximum attained by $\Delta(\phi)$ we would find that

$$\Delta_{\max} = (4F|\gamma| - r_3 D)^2 + \Delta_{\min}. \tag{5.40}$$

A necessary condition for there to exist ϕ such that both $\gamma B(\phi) \leq 0$ and $\Delta(\phi) \geq 0$ would be then to ask that $\Delta_{\max} \geq 0$. Expanding $\Delta_{\max}$ fully, this is equivalent to

$$2FDr_3|\gamma| \leq -2F(r_3\gamma - \cos\theta_3)^2 + r_3^2 + 2F\cos^2\theta_3. \tag{5.41}$$

As functions of γ, the left-hand-side of this equation is always positive, obtaining its minimum of zero when $\gamma = 0$. The right-hand-side, however, is a parabola which becomes negative for sufficiently large $|\gamma|$. Additionally, we know that when $\gamma = 0$,

this side of the inequality evaluates to r_3^2, which is strictly positive. We therefore know that there must be at least two values of γ for which both sides are equal. In fact, squaring each side and grouping terms of similar power in γ gives the following quadratic equation:

$$4F\left(r_3^2 + 4F\sin^2\theta_3\right)\gamma^2 - 8Fr_3\cos\theta_3\gamma - r_3^2 = 0, \tag{5.42}$$

which has two real roots given by

$$\gamma_{2,\pm}^* = \frac{r_3}{r_3^2 + 4F\sin^2\theta_3}\left(\cos\theta_3 \pm \sqrt{1 + \frac{r_3^2}{4F}}\right). \tag{5.43}$$

Clearly, we have that $\gamma_{2,-}^* < 0 < \gamma_{2,+}^*$, with both roots being undefined for $F = 0$. Here, the inequality found in (5.41) holds trivially with $r_3^2 \geq 0$. We have therefore proven the following proposition:

Proposition 2: Let us assume that $F > 0$ and that $\gamma \notin \bar{\Gamma}_1$. Additionally, let us define the set Γ_2 according to the following conditions:

$$\Gamma_2 = \begin{cases} \mathbb{R}, & \text{if } r_3^2|\sin\theta_3| \geq 4F; \\ \mathbb{R}\setminus\left(\gamma_{1,-}^*, \gamma_{1,+}^*\right), & \text{if } r_3^2|\sin\theta_3| < 4F,\ r_3^2 > 4F; \\ \left[\gamma_{1,+}^*, \gamma_{1,-}^*\right], & \text{if } r_3^2|\sin\theta_3| < 4F,\ r_3^2 < 4F; \\ \left(-\infty, r_3^{-1}\sec\theta_3\right], & \text{if } r_3^2 = 4F,\ \cos\theta_3 > 0; \\ \left[r_3^{-1}\sec\theta_3, \infty\right), & \text{if } r_3^2 = 4F,\ \cos\theta_3 < 0. \end{cases} \tag{5.44}$$

The two end-points $\gamma_{1,\pm}^*$ are defined according to equation (5.34). Furthermore, let us also define the interval $\Gamma_3 = \left[\gamma_{2,-}^*, \gamma_{2,+}^*\right]$, where $\gamma_{2,\pm}^*$ is given by equation (5.43). For $\gamma \in (\Gamma_2 \cap \Gamma_3) \setminus \bar{\Gamma}_1$, there exist ϕ such that both the positive and negative-root solutions found in equation (5.16) are real. In this case, the detuned manifold is formed by two disjoint closed curves.

Note that this proposition can be readily extended to the case when $F = 0$, since we have both $\Delta_{\max} \geq 0$ and $\gamma B \leq 0$ holding trivially for any value of γ. Therefore, $F = 0$ offers a unique case where the detuned manifold is well-defined for any value of δ. Furthermore, this proposition does not guarantee that for certain choices of k_3, that $\Gamma_2 \cap \Gamma_3$ is not the empty set. However, it does suggest that when $F > 0$, there exists only a finite range of accessible γ where the solution to the detuned resonance conditions exist.

To cement the ideas presented in these two propositions we will go through two simple examples. First, let us consider when $k_3 = (1, 0)$, $F = 0$ and $\beta = 1$. Since $F = 0$ we know that the detuned manifold is defined for all values of γ, or equivalently, for all values of δ. This corresponds to the complete solution set $\mathcal{R}$ not covering the entire plane, with gaps appearing however small, for any choice of broadening, Ω. For small resonance broadening, we simply see a thickening of the exactly resonant manifold as seen in figure (5.1(a)). The area bounded by this region diverges as we approach the value $\Omega = 1$, or equivalently as we approach $\gamma = 0$, as seen in figure (5.1(b)). We easily calculate $\Gamma_1 = (0, 4)$, and observe that when $\gamma = 4$, the detuned manifold contained within the exactly resonant manifold now self-intersects at the point $(\frac{1}{2}, 0)$. At this point, corresponding to $\Omega = 3$, the region $\mathcal{R}$ now covers the entire plane except for two disjoint regions external to the exactly resonant manifold,and the figure-of-eight structure within, as seen in figure (5.1(c)). Finally, increasing the resonance broadening further, four small disjoint regions form, which shrink but always persist for any value of Ω. This is shown in figure (5.1(d)).

As a final example, let us consider what happens when we choose $F > 0$ and $\theta_3 \neq 0$. To that end, let us choose $k_3 = (1, 1)$ and $F = \beta = 1$. Here, we have that $\sin\theta_3 = 1/\sqrt{2}$, and so it follows that $r_3^2|\sin\theta_3| < 4F$ and $r_3^2 < 4F$. Furthermore, since F is non-zero we can calculate the two sets Γ_2 and Γ_3 and thus $(\Gamma_2 \cap \Gamma_3) \setminus \bar{\Gamma}_1$. We find that

$$\Gamma_2 \cap \Gamma_3 = \left[-\tfrac{\sqrt{3}-1}{4}, \tfrac{\sqrt{7}-1}{3}\right], \tag{5.45}$$

and so,

$$(\Gamma_2 \cap \Gamma_3) \setminus \bar{\Gamma}_1 = \left[-\tfrac{\sqrt{3}-1}{4}, 0\right), \tag{5.46}$$

since $4r_3\cos\theta_3/(r_3^2 + 4F) = \frac{2}{3}$. Summarising, we therefore have that for $0 < \gamma < \frac{2}{3}$, the detuned manifold forms a single closed curve, becoming unbounded as γ tends to 0. When $-\frac{\sqrt{3}-1}{4} \leq \gamma < 0$, two disjoint closed curves form, disappearing to a point as gamma nears the left end-point of this interval. This can be seen in figure (5.2) for the illustrative value of $\Omega = 0.5$, where the detuned manifold that should appear contained within the exactly resonant manifold is no longer defined. Beyond these two intervals, no solution for the detuned manifold exists, and so the region $\mathcal{R}$ occupies the entire plane. It therefore follows that only a finite level of resonance broadening is required for this particular choice of k_3 to become quasi-resonant with all wavenumbers in the system..

5.1.4 Asymptotic analysis for near critical values of detuning

As we have just discovered, the existence of this divergent point in the detuned manifold has some strong implications for how the modes within the wave system interact. If indeed a kinematic consideration of the system is correct, it would suggest that only a finite level of resonance broadening is required before the majority of modes in our system begin to interact quasi-resonantly. We will now show in fact, that it is entirely possible to compute analytically the area of our solution set $\mathcal{R}$ bounded by the detuned manifold, which we know to be well-defined whenever γ satisfies the conditions of *Proposition 1*. Asymptotically we can then show precisely how this region diverges as the value of detuning approaches the critical point corresponding to $\gamma = 0$. This is especially insightful since for a particular choice of k_3, the number of modes thought to be interacting quasi-resonantly with k_3 is proportional to the size of this region.

Keeping in mind the factor of $\frac{1}{2}k_0$ appearing in equation (5.7), the area encompassed by the detuned manifold is given by

$$A = -\pi F + \frac{1}{8|\gamma|}\int_{-\pi}^{\pi} \sqrt{\Delta(\phi)}\ \mathrm{d}\phi. \tag{5.47}$$

We now need to determine the behaviour of this integral as $|\gamma| \to 0$. Let us write this integral out explicitly, exploiting the periodicity of $\Delta(\phi)$, to get

$$4\int_{0}^{\pi/2} \sqrt{\left(4F\gamma + r_3 D\cos 2\phi\right)^2 + c(\gamma)^2}\ \mathrm{d}\phi, \tag{5.48}$$

where we have defined

$$c(\gamma)^2 = (r_3^2 + 4F)^2\left(\frac{4r_3\cos\theta_3}{r_3^2+4F} - \gamma\right)\gamma. \tag{5.49}$$

If we now assume that the conditions of *Proposition 1* hold, we can take $c(\gamma)$ to be both real and positive, with $c(0) = 0$. It follows that in the case $\gamma = 0$, this integral can be evaluated directly as $8r_3$, which means that formally A is infinite at this point. In fact, it is fairly trivial to show, by considering minima and maxima of the integrand, that the following bounds must hold for all values of γ:

$$\frac{\pi c(\gamma)}{4|\gamma|} < A + \pi F < \frac{\pi}{4|\gamma|}\sqrt{\left(4F|\gamma| + r_3 D\right)^2 + c(\gamma)^2}. \tag{5.50}$$

Asymptotically, this lower limit diverges like $|\gamma|^{-1/2}$, whereas for the upper limit, we have simply that $|\gamma|^{-1}$ as $|\gamma| \to 0$.

In fact, we can evaluate the integral appearing in the expression for A explicitly, giving an answer written in terms of the complete forms of the three different kinds of elliptic integrals. There are multiple approaches to reducing our elliptic integral A into standard form, such as for instance, found in either [Byrd and Friedman, 1954] or [Abramowitz and Stegun, 1965]. However, the algebra, while not necessarily sophisticated, can be complicated and so we leave the derivation to the Appendix. Here, we simply state the result. First, let us define the two γ-dependent constants

$$a = \frac{4F\gamma}{r_3 D},\ b = \frac{c(\gamma)}{r_3 D}, \tag{5.51}$$

so that

$$A = -\pi F + \frac{r_3 D}{2|\gamma|} \int_0^{\frac{\pi}{2}} \sqrt{(a + \cos 2\phi)^2 + b^2}\ \mathrm{d}\phi. \tag{5.52}$$

Let us denote this simplified integral by I. If we were then to make the transformation $x = a + \cos 2\phi$, we would find that

$$I = \frac{1}{2} \int_{a-1}^{a+1} \frac{x^2 + b^2}{\sqrt{(a + 1 - x)(x - a + 1)(x^2 + b^2)}}\ \mathrm{d}x. \tag{5.53}$$

This is clearly recognisable as an elliptic integral. To evaluate this integral we need to define the two real constants λ_1 and λ_2 such that

$$\lambda_{1,2} = \frac{1}{2}\left[a^2 + b^2 - 1 \pm \sqrt{(a^2 + b^2 - 1)^2 + 4b^2}\ \right], \tag{5.54}$$

which we label so as to respect $\lambda_1 < 0 < \lambda_2$. The result is then simply

$$\frac{I}{\sqrt{\lambda_2 - \lambda_1}} = E(m) + (1 - n)\ \Pi(n|m) - K(m), \tag{5.55}$$

where we have introduced the two new parameters known as the modulus, m, and characteristic, n, defined by

$$m = \frac{\lambda_1}{\lambda_1 - \lambda_2},\ n = \frac{1 + \lambda_1}{\lambda_1 - \lambda_2}. \tag{5.56}$$

We immediately verify that $0 \leq m < 1$ and $n < 0$ for all values of $a, b \in \mathbb{R}$. The three functions $K(m)$, $E(m)$ and $\Pi(n|m)$ defined in terms of these new quantities are known as the complete elliptic integrals of the first, second and third kind respectively.

While this formula is explicit, there are certain numerical issues that prove problematic when evaluating these transcendental functions numerically, especially

the elliptic integral of the third kind where the additional parameter n presents its own difficulties. However, under some reasonable assumptions we can simplify this expression for I. For instance, if we assume that the conditions within *Proposition 1* were to hold, then this would be sufficient to ensure that

$$|\gamma| < \frac{4r_3|\cos\theta_3|}{r_3^2 + 4F}. \tag{5.57}$$

Since typically we are interested in discrete wavenumbers, we have that γ must be comparatively small. In the limit as $|\gamma| \to 0$, the characteristic n is likewise small. Using the fact that $\Pi(0|m) = K(m)$, the solution given in equation (5.55) can therefore be approximated by

$$I \approx \sqrt{\lambda_2 - \lambda_1}E(m). \tag{5.58}$$

Notice that this limiting argument lacks any formal rigour since as $|\gamma| \to 0$, $m \to 1$ and $K(m)$ develops a singularity at this value. However, near this singularity, $E(m)$ has a convergent series [DLMF], which to first order reads

$$E(m) = 1 + \frac{1}{2}(1-m)\left[\ln\left(\frac{1}{1-m}\right) - \frac{1}{2} - 2\ln 2\right] + O\left((1-m)^2\right). \tag{5.59}$$

Substituting this expression, we therefore have the following asymptotic approximation for A:

$$A \approx -\pi F + \frac{r_3 D\sqrt{\lambda_2 - \lambda_1}}{4|\gamma|}\left[2 + (1-m)\ln\left(\frac{1}{1-m}\right)\right]. \tag{5.60}$$

The accuracy of this approximation is shown figure (5.3), accompanied by the exact solution for A derived from taking the value of I found in equation (5.55). For comparison, we have included the two bounds computed in equation (5.50), as well as the numerically evaluated result for A calculated using quadratures. As you would expect, the result obtained using quadratures and the analytical answer are exactly the same within numerical tolerance. The asymptotic approximation competes favourably well across all values of γ, where the domain is defined by the conditions set in *Proposition 1*. The solution diverges almost identically with the upperbound, which we know diverges like $|\gamma|^{-1}$.

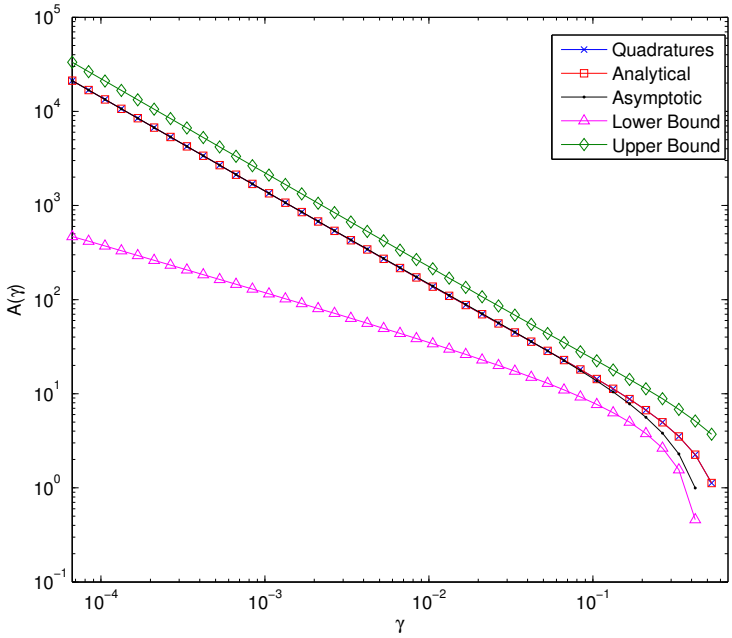

Figure 5.3: Area contained within the detuned resonance manifold calculated as a function of γ. Here we have taken $k_3 = (1, 1)$, $F = 1$ and $\beta = 1$. The domain of γ is defined by the conditions set within *Proposition 1*. For comparison, the analytical solution is compared with the numerically computed result obtained by quadratures. As expected, these are almost exactly identical within numerical tolerance. Lower and upper bounds obtained in equation (5.50) are also included. The asymptotic solution given in equation (5.60) compares favourably across all values of γ.

5.2 Critical Phenomena and the CHM Dispersion Relationship

So far we have shown that locally, that is for each wavenumber, there is some critical value of broadening where the detuned manifold no longer remains bounded. At this point, the mode becomes quasi-resonant with a set of modes comparable in size to the entire system. We have also shown that increasing the resonance broadening and eventually there is some finite limit where the mode is allowed to interact with all modes in the system, at least for $F > 0$. If we now spectrally truncate our wave system, this divergent behaviour for each mode suggests that there is a lower bound of broadening required for all modes to act quasi-resonantly with each other. It is obvious that by increasing the broadening, Ω, will lead to both an increase in the total number of quasi-resonant clusters, but that some of these clusters must also merge together. In a loose analogy with percolation, we ask whether a dominant large cluster emerges at some critical value of Ω. Accompanying this question, we ask how the total number of clusters behaves around this critical value, and whether we can determine how this critical point scales as a function of both the system size and other physically relevant parameters such as F and β. If such a critical point does exist and if the kinematic representation of the wave system is truly representative of the actual dynamics, then DWT is only applicable below this critical value, and that the transition may be more abrupt than initial suspected.

We will now review the motivation and details behind how we construct a network of discrete quasi-resonantly interacting modes for a given level of broadening, Ω. As you recall, we argued that most dispersive wave systems admitted harmonic solutions of the form

$$\psi(x, y, t) = A_k(t) \cos(k_x x + k_y y - \omega(k)t), \tag{5.61}$$

where the amplitude A_k is real, and $\omega(k)$ is the dispersion relationship defined by the wave system itself. These wave solutions depend on the domain and boundary conditions of the system. For the CHM equation, we showed that it can be written in the interaction form,

$$\frac{\partial \phi_k}{\partial t} = \frac{1}{2} \sum_{k_1+k_2=k} T(k, k_1, k_2) \phi_{k_1} \phi_{k_2} \mathrm{e}^{i\delta(k,k_1,k_2)t}, \tag{5.62}$$

where $\delta(k, k_1, k_2) = \omega(k) - \omega(k_1) - \omega(k_2)$ represents the finite resonance width. Each of these new variables, ϕ_k, represent a particular type of plane wave solution called a

Rossby wave. We argued that averaged over long stretches of time, triads of modes that have small resonance width should dominate the dynamics. In reality, however, we showed that near resonant interactions can be comparatively just as significant on relatively short timescales, corresponding to what appears as a 'broadened' delta function in the generalised kinetic equation describing the evolution of the wave action.

We can now build a kinematic overview of the system by exhaustively listing all triplets of wavenumbers that satisfy the quasi-resonant conditions given by equation (5.3). We count these triplets as the smallest cluster available, but each wavenumber could appear in more than one instance of our list, and so generates even larger clusters. Once this is done, a reduced dynamical system can be derived for network of quasi-resonant clusters from the full system given by equation (5.62). This spectral truncation serves to capture the dynamics at least on a sufficiently short time scale if the nonlinearity is weak. There are some practical considerations to consider. Since we can only deal with finite system sizes numerically, we introduce a cut-off wavenumber, M, for which we consider only wavenumbers such that $|k_x|, |k_y| \leq M$. Additionally, we know that for real fields ψ, each wave must satisfy $\phi_{-k} = \phi_k^*$, where $(\cdot)^*$ denotes complex conjugation. We can therefore halve the number of modes in our system, which also avoids the issue of introducing superfluous connections between modes representing k and the conjugate $-k$. We need also remove the degenerate wavenumbers where $k_x = 0$. Here the dispersion relationship is likewise zero, and these zonal modes can be shown to be exactly resonant with an arbitrary number of modes: for instance, any triplet of the form

$$k_1 = (m, n),\ k_2 = (-m, n),\ k_3 = (0, 2n),\ m, n \in \mathbb{Z},$$

is an exactly resonant solution. Finally, we eliminate any clusters where the interaction coefficient, $T(k, k_1, k_2)$, is zero for obvious reasons. This leaves the following set of modes forming the vertices of our quasi-resonant network:

$$V = \left\{ (k_x, k_y) \in \mathbb{Z}^2 \;\middle|\; 1 \leq k_x \leq M,\ -M \leq k_y \leq M \right\}, \tag{5.63}$$

where without loss of generality we have taken $L_x = L_y = 2\pi$. Our set of edges are then clearly defined as above by the clustering induced through the quasi-resonant conditions. In practice, this is done in the most basic computational way, simply by brute force enumeration of each possible triad in our system, although computationally more elegant and efficient methods exist for certain dispersion relationships, such as those based on q-class decomposition [Kartashova, 1998].

There are two measures of interest when building this cluster network. First, in an analogy with percolation theory, we are interested in the density of the largest cluster, ρ, which is simply the number of modes in the largest cluster normalised by the system size, $|V| = M(2M+1)$. The second is the total number of clusters, which we normalise by the maximum number of possible isolated clusters, or $\lfloor |V|/3 \rfloor$. This acts as an unsophisticated measure of the total complexity of the system.

5.2.1 Approximating the saturation value

In the previous section, for each wavenumber we proved the existence of a critical value of resonance width corresponding to $\gamma = 0$, where the detuned manifold diverges. We then showed asymptotically how the solution set $\mathcal{R}$ diverged as the broadening increased to include this critical value of γ. We concluded that at this point, a quasi-resonant cluster formed of size comparable to the size of V. Once one mode has hit this critical value, it is clear that the system should be close to saturation, which we call the point when $\rho = 1$. Since V is finite, we only need to know the minimum critical value over all wavenumbers in the system to estimate the actual saturation value, and so we get

$$\Omega_{sat} \approx \min_{k \in V} |\omega(k)|. \tag{5.64}$$

The reasons this is not an exact value are encoded in *Proposition 2*. Even when the broadening is in excess of this critical point for each mode, gaps in the k-space still remain, forming the complement of $\mathcal{R}$. Using *Propososition 2* we can calculate the minimum value of resonance broadening required for a particular mode to become quasi-resonant with all other modes in V. Minimising this value over all modes in the system would then yield an upperbound on Ω_{sat}. However, equation (5.64) proves easier to implement numerically and does well to represent to the true saturation value for large system sizes. This can be seen in figure (5.4).

5.2.2 Critical resonance broadening

While we have shown that locally each mode exhibits some sense of critical behaviour described above, can the same be said about the system as a whole. In fact we can, by plotting the density ρ and total number of clusters for a given level of broadening. The results can be seen in figures (5.4) and (5.5) respectively, for varying system sizes but fixed $F = \beta = 1$. As you would expect, ρ is a strictly monotonic function of Ω. Critical values of broadening can clearly be identified, which we call Ω^*. The position of this critical point then decreases with system size as you would expect, since large

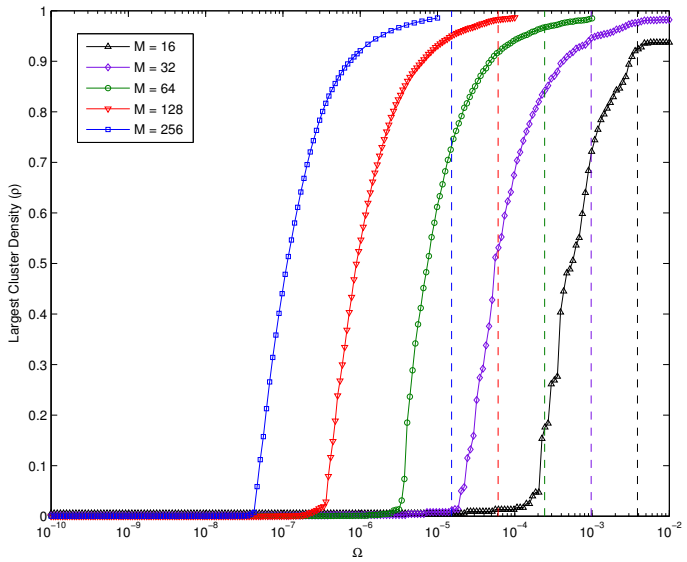

Figure 5.4: The density of the largest quasi-resonant cluster, ρ, plotted as a function of resonance broadening Ω and varying system sizes, M. Here we have fixed $F = \beta = 1$. A critical value of broadening, Ω^*, emerges whose value decreases as a function of system size. The approximate values of Ω_{sat} as described by equation (5.64) are shown as dashed vertical lines.

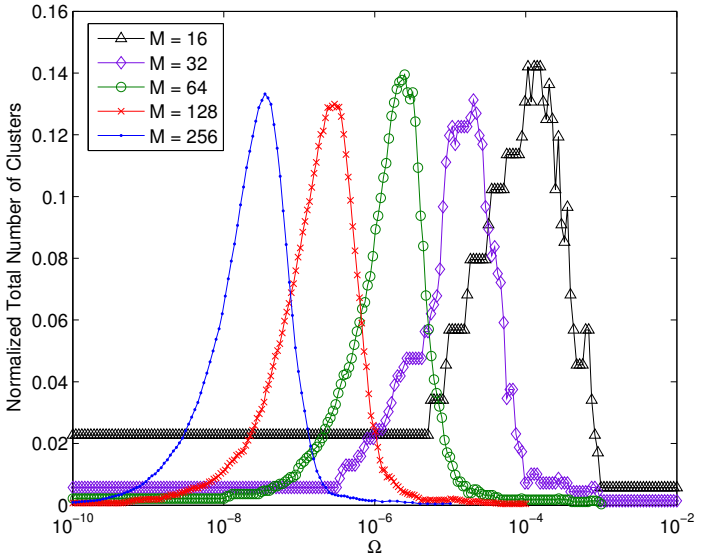

Figure 5.5: The normalised total number of clusters, N, plotted as a function of Ω and varying system sizes, M. Here, we have fixed $F = \beta = 1$. Global maxima of N correspond to the same values of critical detuning found for ρ. The values of these maxima appear invariant to system size subject to finite-size system effects for small M.

system sizes permit the possibility of additional connections between clusters not available for smaller cut-off sizes. However, the profile of ρ seems relatively invariant to changes in M, except for a shift suggesting some simple scaling involved. For comparison, if we now calculate how the total number of clusters vary over the same range of Ω, we obtain figure (5.5). Here, we have that for sufficiently large M, the same critical values of Ω^* correspond to global maxima in the total number of clusters. The existence of this maxima suggests that initially, for small values of Ω, only small isolated clusters begin to form. Upon reaching this critical value in detuning, these clusters begin to merge and consume new quasi-resonant clusters at far more substantial rate than the creation of new ones until one large cluster begins to dominate. Although this cluster formation is deterministic, the 'noise' appears from the competition between the creation of new clusters and coalescence of existing ones, resulting in a fluctuation of total numbers. However, the normalised maximum number of clusters appears independent of M.

Numerically, calculating the maxima of the total number of clusters offers a more direct way of obtaining Ω^*, especially for large system sizes where the critical transition is more abrupt. For smaller system sizes, we need to account for some

degree of uncertainty in Ω^*, which cannot be obtained from any standard statistical techniques since the underlying behaviour is deterministic. Instead, we average the position of all local maxima appearing above a certain threshold to narrow the range where we are certain this critical point is located. Here we take this threshold as half the global maxima, for example. Using this approach, we can therefore see how Ω^* scales with system size, which we have plotted in figure (5.6). We see that the value of F becomes redundant for large M. This is to be expected since for sufficiently large k, the significance of F is diminished by the dominating effect of the k^2 term in the denominator of the dispersion relation. Each of the curves converge to the straight line indicated by the scaling

$$\Omega^* \sim M^{-\sigma_1}, \tag{5.65}$$

with exponent $\sigma_1 = 3.00\ (2.97, 3.03)$ to 3 s.f., where 95% confidence intervals are given in parentheses, obtained by bias-corrected bootstrapping. However, this does not suggest that in the continuum limit, where M tends to infinity, we should see the creation of relatively large exactly resonant clusters. For instance, setting $F = 1$, even with system sizes in excess of $M = 200$, the largest exactly resonant cluster consists of just five modes.

Since we know that for sufficiently large system sizes Ω^* scales invariant to F, can we also say the same about the profiles for ρ and N. These are plotted in figures (5.7) & (5.8) and show almost identical curves across several different orders of F. Only for $F = 10^4$ do we see any discrepancy, appearing identical in shape but only shifted. Near the critical value, ρ appears linear in $\log \Omega$, and so suggests the following scaling

$$\rho \sim \log \left(\frac{\Omega}{\Omega^*} \right)^{\sigma_2} \tag{5.66}$$

where the new scaling exponent, σ, is independent of M and F for sufficiently large systems. This exponent should also be independent of β for reasons we outline below. Setting $M = 1000$ and $F = 1$, we calculated $\sigma_2 = 1.25\ (1.22, 1.30)$ to 3 s.f., where 95% confidence intervals are given in parentheses obtained using bias-corrected bootstrapping.

Each of these scaling exponents should be in fact independent of β, which can readily be identified from the resonance conditions given in equation (5.3). Since the dispersion relationship is linear in β, it can be factorized to obtain new conditions

$$|\bar{\omega}(k_3) - \bar{\omega}(k_1) - \bar{\omega}(k_2)| \leq (\Omega/\beta), \tag{5.67}$$

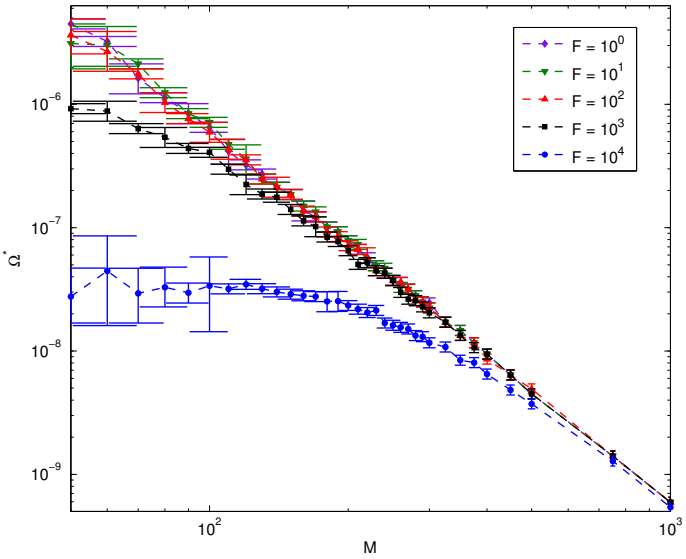

Figure 5.6: The critical values of broadening, Ω^*, plotted against system size and for varying values of F. Here, we have fixed $\beta = 1$. Error bars haven been included, which are calculated by considering the positions of local maxima in N above a certain threshold. For large system sizes, Ω^* converges to the same curve for all values of F. We observe the scaling $\Omega^* \sim M^{-\sigma_1}$, where numerically we find that $\sigma_1 = 3.00\ (2.97, 3.03)$, with 95% confidence intervals are shown in brackets.

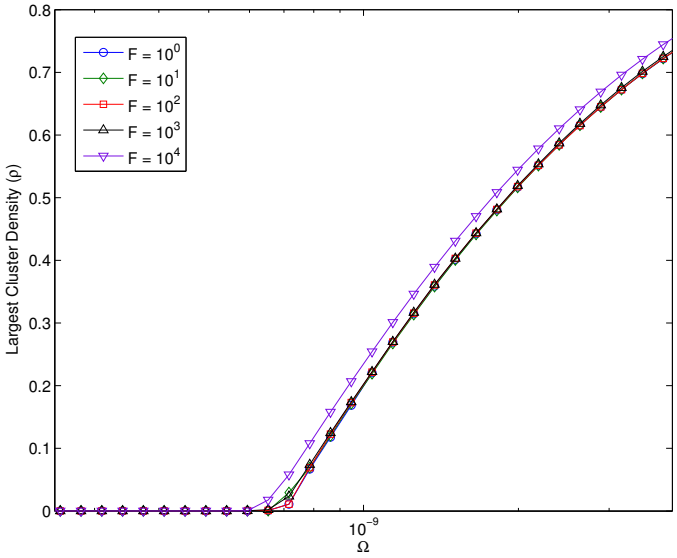

Figure 5.7: The density of the largest cluster, ρ, plotted against Ω near the critical point. Here we have fixed $M = 1000$, but allowed F to vary. The profiles appear identical except for a slight discrepancy with $F = 10^4$.

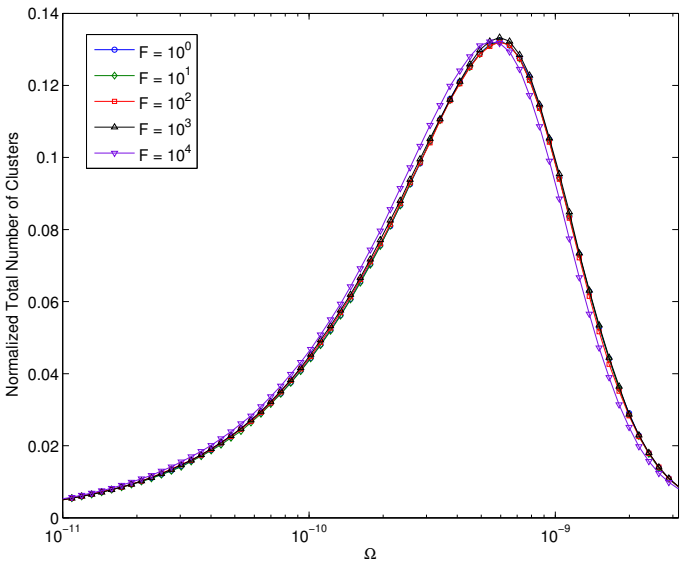

Figure 5.8: Total number of clusters, N, plotted against Ω near the critical point. Here we have fixed $M = 1000$, but allowed F to vary.

where our rescaled dispersion relationship reads

$$\bar{\omega}(k) = -\frac{k_x}{k^2 + F}. \tag{5.68}$$

This means we derive a new effective resonance broadening Ω/β, which suggests that β should only appear multiplicatively in the scaling for Ω^*. Namely, we should find that

$$\Omega^* = c\beta M^{-\sigma_1}, \tag{5.69}$$

where M is sufficiently large and c is some constant independent of both β and F.

5.2.3 Resilience at large scales

So far we looked locally at each mode, assessing a particular mode's proclivity to form quasi-resonant interactions with the rest of the modes in the system. However, in effect this is only half the picture; while we have characterised how the largest cluster grows, we have neglected to ask which modes remain isolated, resilient to forming part of any cluster, even triads. This is addressed in figure (5.9), where we have coloured each mode according to the minimal amount of resonance broadening required for this mode to join a cluster of any size. In essence, the modes resilient to quasi-resonant clustering. Rather than appearing homogeneous and random, we see

the appearance of definite structure: the formation of region at large-scales reluctant to form any quasi-resonant connections, and a larger encompassing, circular region containing modes with a strong propensity to cluster. Additionally, we see a narrow large-scale region of exactly resonant modes, accumulating near the $k_x = 0$ axis.

The existence of these resilient large scales modes is not a new idea, where it has already been suggested that the inherent anisotropy of Rossby waves can be attributed to the formation of zonal flows and jets [Vallis, 2006]. In this reference, a wave-turbulence boundary could be computed explicitly by comparing the CHM dispersion relationship directly against the inverse of the eddy-turnover time. Clearly, no explicit connection with quasi-resonance is made in this argument, but this boundary appears identical in position and shape as the region found above. It is then argued that inside this region Rossby waves dominate, but with a frequency incommensurate with that of the surrounding turbulence. While energy will cascade to large scales, it is argued that this mismatch of frequency prevents energy crossing the boundary, and it gets directed towards to $k_x = 0$ axis, where we see a higher proportion of exactly resonant modes. Furthermore, this phenomena was shown to compare favourably with direct numerical simulation, where this empty energy region could be clearly identified. We therefore have that the kinematic view of quasi-resonant interactions could both distinguish between the DWT, mesoscopic and SWT regimes, and correlate with explicit examples of known turbulent phenomena.

5.3 Critical Phenomena and the Power-Law Dispersion Relationship

So far we have shown that criticality is a prominent feature both within the resonance conditions for individual modes, and as part of the system as a whole. One obvious concern that needs addressing is that this type of behaviour may be unique to the dispersion relationship attributed to the CHM equation. After all, the CHM equation exhibits an array of properties relatively unique among different types of wave systems. For instance, there exists a well-known non-canonical Hamiltonian description of the CHM equation across a range of domains and varying boundary conditions. For details see either, [Weinstein, 1983], [Sueyoshi and Iwayama, 2007] or [Swaters, 1999] for a description of Hamiltonian fluid dynamics as the precursor to stability theory. Furthermore, the CHM equation carries some weak concept of integrability, possessing a Lax Pair, and hence an infinite hierarchy of conservation laws to match [Li, 2003]. We therefore need to apply the same techniques and

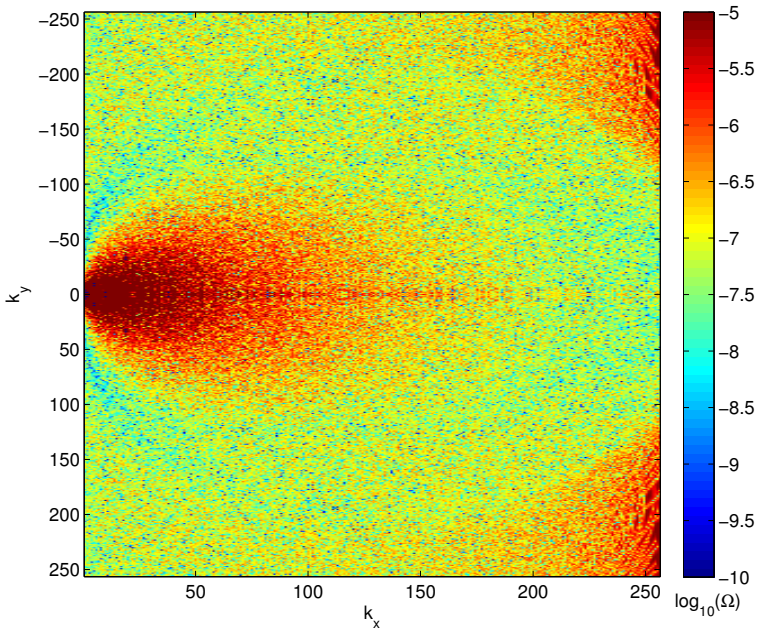

Figure 5.9: The minimal value of broadening required for a particular mode to become a member of any cluster of any size. We see the appearance of a definite structure: large scales seem resilient to forming quasi-resonant connections, requiring a comparatively greater level of broadening to do so, while exactly resonant modes tend to dominate within some circular region. Finite-size effects also take place in the corners of this region, where the corresponding detuned manifolds extend beyond the confines of the boundaries. Otherwise, we also see a significant number of exactly resonant modes at large-scale and near the $k_x = 0$ axis. These modes are responsible for the creation of zonal flow.

analyses as before but to the power law dispersion relationship, $\omega(k) = k^\alpha$, to test whether this concept of criticality is a general component of systems where three-wave interactions dominate.

Unfortunately, for general α, no explicit solution to the quasi-resonant conditions (5.3) exists. We do know however, that in certain cases no exactly resonant three-wave interactions can occur. This was proven in [Kartashova, 1998] in the context of capillary waves in rectangular domains with periodic boundary conditions. However, even without solving the quasi-resonance conditions explicitly as before, we can still mathematically classify the shape of the detuned manifold depending on the value of α. We will see that the characteristic shape of this manifold can be described in two distinct ways, as well as being explicitly solvable for when $\alpha = 1$ and $\alpha = 2$. The first of these marks an interesting transition point, defining whether the problem is convex or otherwise. Interestingly, when $\alpha = 2$ we see degenerate behaviour only when we consider the collective behaviour across all the modes in the system, where just one large percolating cluster exists for all values of resonance broadening.

5.3.1 Calculating bounds on detuning

Our goal is to produce something akin to propositions one and two above, except applied to the power-law dispersion relationship. This is possible even when we know that generally, no explicit solution exists for this type of system. We proceed at first in an almost identical fashion as before by fixing k_3 and then asking which wavenumbers k_1, k_2 satisfy the quasi-resonance condition

$$\omega(k_3) - \omega(k_1) - \omega(k_2) = \delta,$$

where we have chosen some $\delta \in \mathbb{R}$ such that $|\delta| < \Omega$. One-dimensional solution sets to this problem form what we call the detuned manifold for a particular choice of the resonance width, δ. This can also be naturally described as the detuning parameter. The complete solution to the problem is then found by integrating over all $|\delta| < \Omega$, forming the two-dimensional solution set that we call $\mathcal{S}$ to distinguish between this and the previous example. Again, we write write k_1 and k_2 in terms of a new variable k_0, such that

$$\begin{cases} k_1 = \frac{1}{2}(k_3 + k_0), \\ k_2 = \frac{1}{2}(k_3 - k_0), \end{cases}$$

and define a new γ, which is no longer dependent on β, by $\gamma = \omega(k_3) - \delta$. For $\delta = 0$, we readily identify the trivial solution $k_0 = \frac{1}{2}k_3$, which we disregard since this means one of k_1 or k_2 must be zero. Explicitly, the new resonance condition now reads

$$2^\alpha \gamma = (k_3 + k_0)^\alpha + (k_3 - k_0)^\alpha . \tag{5.70}$$

If we introduce the polar co-ordinates

$$k_j = r_j \left(\cos\theta_j, \sin\theta_j\right), \ j = 0, 1, 2, 3,$$

and the new angle $\phi = \theta_0 - \theta_3$, we can reformulate the problem in terms of finding roots of some positive function:

$$2^\alpha \gamma = g(r_0, \phi), \tag{5.71}$$

where we have defined

$$g(r_0, \phi) = \left[(r_0 + r_3\cos\phi)^2 + r_3^2 \sin^2\phi\right]^{\frac{\alpha}{2}} + \left[(r_0 - r_3\cos\phi)^2 + r_3^2\sin^2\phi\right]^{\frac{\alpha}{2}} . \tag{5.72}$$

This new function $g(r_0, \phi)$ is π-periodic in ϕ, corresponding to the fact that the problem is invariant to a relabelling of k_1 and k_2. This means that the detuned manifold has two axes of symmetry: one about the angle $\theta_0 = \theta_3$ and one when $\theta_0 = \theta_3 \pm \pi/2$.

The equation given in (5.71) can only be solved explicitly in a few cases: either when $\cos\phi = 0$ and α can take any value; $\alpha = 1$, where the manifold becomes degenerate in the limiting case of $\delta \to 0$; or the final degenerate case, $\alpha = 2$ where the manifold is well-defined for individual modes but collectively all modes form one percolating cluster. In the first of these cases, we find that

$$r_0^2 = \left(2^{\alpha-1}\gamma\right)^{\frac{2}{\alpha}} - r_3^2, \tag{5.73}$$

which is a valid solution provided that the right-hand side is positive. This requirement places additional constraints on the the range of detuning, dependent on r_3 and α, for a solution $r_0(\phi)$ defined by equation (5.71) to exist. As we will now show, these bounds can be computed explicitly for any value of α and are in fact optimal.

First we consider $g(r_0, \phi)$ as a function of ϕ only. Differentiating with respect

to ϕ gives

$$\frac{\partial g}{\partial \phi} = \alpha r_0 r_3 \sin\phi \Big\{ \left[(r_0 - r_3\cos\phi)^2 + r_3^2\sin^2\phi\right]^{\frac{\alpha-2}{2}} - \left[(r_0 + r_3\cos\phi)^2 + r_3^2\sin^2\phi\right]^{\frac{\alpha-2}{2}} \Big\}. \tag{5.74}$$

Clearly, this derivative is zero for $\sin\phi = 0$. From the factor in parentheses, the second set of zeros are found by setting $\cos\phi = 0$. We therefore have that

$$g\left(r_0, (2n+1)\pi/2\right) = 2\left[r_0^2 + r_3^2\right]^{\frac{\alpha}{2}}, \tag{5.75}$$

$$g\left(r_0, n\pi\right) = |r_0 + r_3|^\alpha + |r_0 - r_3|^\alpha, \tag{5.76}$$

where $n \in \mathbb{Z}$, correspond to the maxima and minima, respectively, of the function $g(r_0, \phi)$. A solution to the detuned resonance condition, equation (5.71), exists therefore, if we can find some value of r_0 for which

$$|r_0 + r_3|^\alpha + |r_0 - r_3|^\alpha \leq 2^\alpha\gamma \leq 2\left[r_0^2 + r_3^2\right]^{\frac{\alpha}{2}}. \tag{5.77}$$

This is always possible provided the minimum of equation (5.76), as a function of r_0, is less than $2^\alpha\gamma$. Calculating this minimum explicitly, we find the following bounds on δ:

$$\begin{cases} \delta \leq 0, & \text{if } \alpha \leq 1; \\ \delta \leq r_3^\alpha\left(1 - 2^{1-\alpha}\right), & \text{if } \alpha > 1. \end{cases} \tag{5.78}$$

5.3.2 Characterising the shape of the detuned manifold

There are essentially two distinguishing cases to consider, marked by whether or not the function $g(r_0, \phi)$ is convex. In addition to these, there are two specific examples of when the detuned manifold can be computed analytically, namely when $\alpha = 1$ and $\alpha = 2$.

The case $\alpha > 1$

We now focus on characterising the shape of the detuned manifold in the case $\alpha > 1$. The point $\alpha = 1$ is critical since it defines the transition between $g(r_0, \phi)$ being convex or otherwise. First, by differentiating once with respect to r_0 we find that

$$\frac{\partial g}{\partial r_0} = \alpha\Big\{(r_0 - \cos\phi)\left[(r_0 - \cos\phi)^2 + r_3^2\sin^2\phi\right]^{\frac{\alpha-2}{2}} + (r_0 + \cos\phi)\left[(r_0 + \cos\phi)^2 + r_3^2\sin^2\phi\right]^{\frac{\alpha-2}{2}}\Big\}. \tag{5.79}$$

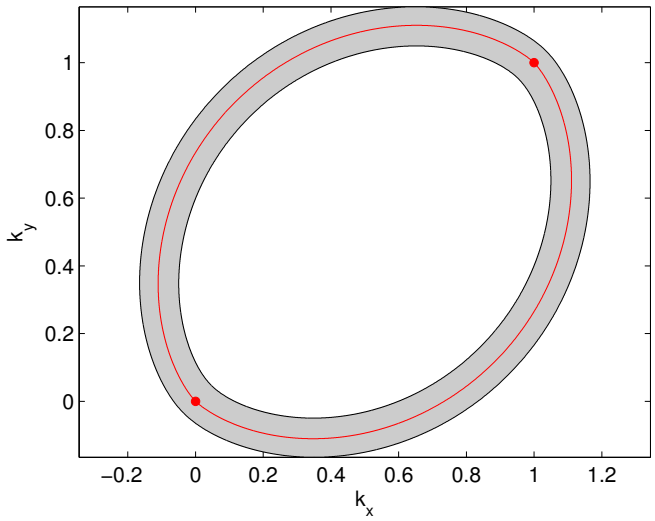

Figure 5.10: Solution to the quasi-resonance conditions for the power-law dispersion relationship with $k_3 = (1, 1)$, $\alpha = 3/2$ and broadening $\Omega = 0.1$. For $\alpha > 1$ the exactly resonant manifold forms a continuous closed curve, with the trivial solution $k_1 = 0$ and $k_2 = k_3$ indicated by the small red circles. $\mathcal{S}$ corresponds to a thickening of this manifold.

This has one of what could possibly be multiple zeros at the point $r_0 = 0$. If we differentiate again, we get

$$\begin{aligned}\frac{\partial^2 g}{\partial r_0^2} = \alpha\Big\{ &\left[(\alpha-1)(r_0-\cos\phi)^2 + r_3^2\sin^2\phi\right]\left[(r_0-\cos\phi)^2 + r_3^2\sin^2\phi\right]^{\frac{\alpha-2}{2}} \\ &+ \left[(\alpha-1)(r_0+\cos\phi)^2 + r_3^2\sin^2\phi\right]\left[(r_0+\cos\phi)^2 + r_3^2\sin^2\phi\right]^{\frac{\alpha-4}{2}}\Big\},\end{aligned} \tag{5.80}$$

which, by virtue of each term being positive, is also strictly positive for all values of r_0 provided that $\alpha \geq 1$. This is sufficient to show that $g(r_0, \phi)$ is a convex function of r_0 with a unique minimum situated at the point $r_0 = 0$. It follows that if $g(0, \phi) > 2^\alpha \gamma$ then equation (5.71) has a unique solution $r_0(\phi)$ for all values of ϕ. This condition is precisely the same as detailed in equation (5.78). In this case, we therefore have that the detuned manifold is described by a single closed curve. An example of this behaviour is included in figure (5.10), taking $k_3 = (1, 1)$ and $\alpha = 3/2$. The upper bounds on detuning for this example is $\delta \leq 2^{3/4}(1 - 2^{-1/2})$, where the manifold contracts to the point $(1/2, 1/2)$ as δ approaches this upper limit. The corresponding solution set $\mathcal{S}$ therefore corresponds to a neat thickening of the exactly resonant manifold and so can be thought of as non-degenerate.

The case $\alpha < 1$

Unfortunately, since $g(r_0, \phi)$ is no longer a convex function in r_0, which suggests that $r_0(\phi)$ may be multivalued for certain values of δ. In terms of computing the detuned manifold numerically, it is actually simpler to consider the inverse function $\phi(r_0)$ in this case. This is because we can find bounds on r_0 by solving numerically the interval of values for which the inequality given in equation (5.77) must hold. Since $g(r_0, \phi)$ is a monotonic function in ϕ when restricted to the separate intervals $[n\pi/2, (n+1)\pi/2]$, where $n \in \mathbb{Z}$, there exists a unique solution $\phi(r_0)$ for each separate interval. It follows that since we need only consider $\phi \in [-\pi, \pi]$, there are four branches of solution for $\phi(r_0)$, dictated by the symmetry of the manifold discussed earlier.

We can continue this analysis further by noting that there is a unique value of delta for which the lower bound on r_0 can be zero: namely, when the stationary points of $g(r_0, \phi)$ coincide at the point $r_0 = 0$, and $g(0, n\pi/2) = 2^\alpha \gamma$. This happens precisely when

$$\delta = r_3^\alpha (1 - 2^{1-\alpha}), \tag{5.81}$$

which is less than zero since $\alpha < 1$. At this point the four branches of the solution $\phi(r_0)$ intersect. If δ is less than this value, the detuned manifold is formed by one continuous closed curve. However, taking δ greater gives two disjoint curves, each enclosing either the point $\mathbf{0}$ or the point k_3. It is easy to show that the only exactly resonant solutions for when $\alpha < 1$ are the trivial ones when we take either k_1 or k_2 equal to zero. We therefore have that when we initially start to increase the broadening, Ω, the set $\mathcal{S}$ first consists of two isolated regions around the points $\mathbf{0}$ and k_3. Eventually these two regions intersect when Ω is increased to the value given by equation (5.81). This behaviour is shown in figure (5.11), where we have chosen $k_3 = (1, 1)$ and $\alpha = 0.5$.

The case $\alpha < 1$ is a contentious for the very reason that it admits only trivial exact resonances between three-waves. For example, in the case of gravity waves, we have that $\alpha = \frac{1}{2}$ when k is small. Since no exactly resonant three-wave interactions exist, formally we should ignore them and consider four-wave interactions or greater.

The explicitly solvable case of $\alpha = 1$

If $\alpha = 1$ then the function $g(r_0, \phi)$ is still a convex function of r_0 with a unique minimum situated at the point $r_0 = 0$. It follows that for equation (5.71) to have any solution we would need to stipulate that $g(0, \phi) \leq 2\gamma$, which is precisely equivalent to asking that $\delta \leq 0$. In fact, in this case we can calculate this solution explicitly to

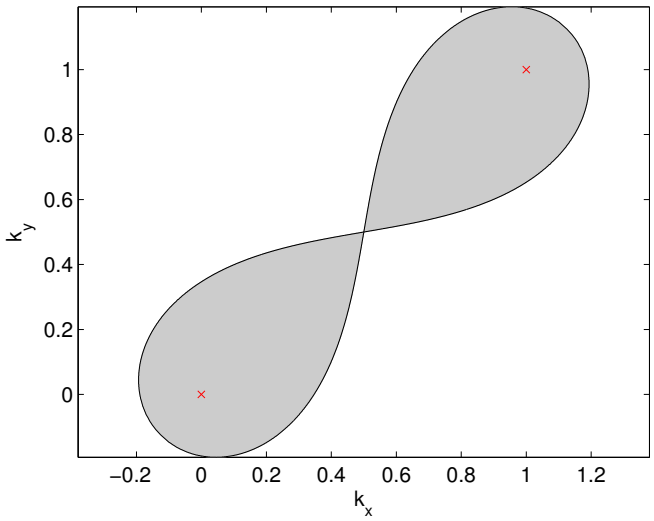

Figure 5.11: The detuned manifold for $k_3 = (1, 1)$, $\alpha = 0.5$ and broadening set to $\Omega = 0.5$. In this case, the solution set $\mathcal{S}$ corresponds to two disjoint regions surrounding the points $\mathbf{0}$ and k_3. However, when $\Omega = 2^{1/4}(1 - 2^{1/2})$ these two regions intersect at the point $(1/2, 1/2)$. No exactly resonant manifold exists for this value of α, except the trivial solution $\mathbf{0}$ and k_3, indicated by the red crosses.

get

$$r_0 = |r_3 - \delta| \left[\frac{(r_3 - \delta)^2 - r_3^2}{(r_3 - \delta)^2 - r_3^2 \cos^2 \phi} \right]^{\frac{1}{2}}. \tag{5.82}$$

Clearly, $\delta < 0$ immediately implies that r_0 is both real and positive for all values of ϕ, and so the detuned manifold forms one continuous closed curve. The final matter to consider is when $\delta = 0$, corresponding to the exactly resonant case. We have that $r_0 = 0$ at all points, even when $\cos \phi = 0$. This means that the only non-trivial exactly resonant solutions for $\alpha = 1$ is the solution $k_1 = k_2 = \frac{1}{2}k_3$. The full solution set $\mathcal{S}$ simply expands around these exactly resonant points, forming one simply-connected region. This behaviour is shown in figure (5.12).

The degenerate case of $\alpha = 2$

In this case the solution to equation (5.71) is readily solvable. We find that

$$r_0^2 = r_3^2 - 2\delta, \tag{5.83}$$

which is independent of ϕ. The detuned manifolds are therefore simply circles of radius $\frac{1}{2}\sqrt{r_3^2 - 2\delta}$, centred at the point $\frac{1}{2}k_3$. While $\mathcal{S}$ behaves well under broadening

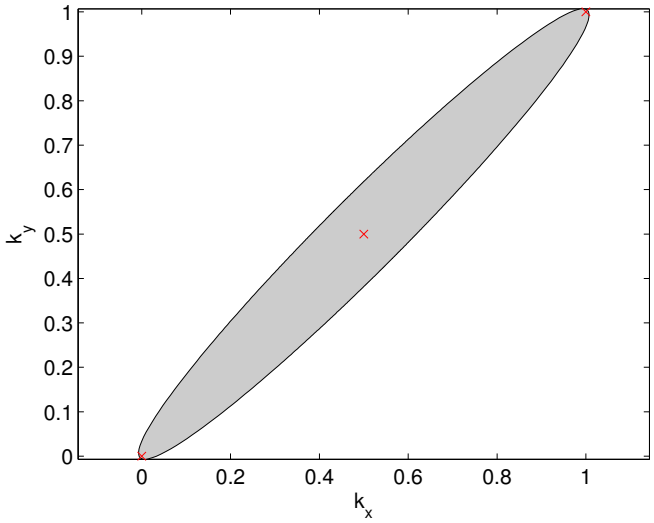

Figure 5.12: The detuned manifold for $k_3 = (1, 1)$, $\alpha = 1$ and broadening set to $\Omega = 0.01$. In this case, the solution set $\mathcal{S}$ encloses the solution to the exactly resonant conditions formed by the trivial points $\mathbf{0}$ and k_3 as well as the solution $k_1 = k_2 = \frac{1}{2}k_3$, indicated by the red crosses.

for any particular choice of mode, the system collectively does not. Here we can generate arbitrarily many exactly resonant solutions of the form

$$k_3 = (m, n),\ k_1 = (m, 0),\ k_2 = (0, n),\ m, n \in \mathbb{R}.$$

The modes of the form k_1 and k_2 above therefore serve as a connecting point for any other mode that shares either k_1 or k_2's nonzero value. It follows that large clusters are immediately present in the system before we add any broadening, or even consider non-trivial solutions that are not of this type.

5.3.3 Critical Phenomena

We have already seen that unlike the CHM case, the detuned manifold for the power-law dispersion relationship exhibits no divergent behaviour, nor is it explicitly solvable. While we were able to calculate explicit bounds for the detuning, δ, because of this lack of degeneracy it becomes a non-trivial matter if we want to predict anything about the criticality of the entire wave system, such as estimating the saturation point for the resonance broadening, for example. Regardless, we will now show that the same notion of criticality present in the CHM equation is readily transferable to other systems characterised by different dispersion relationships.

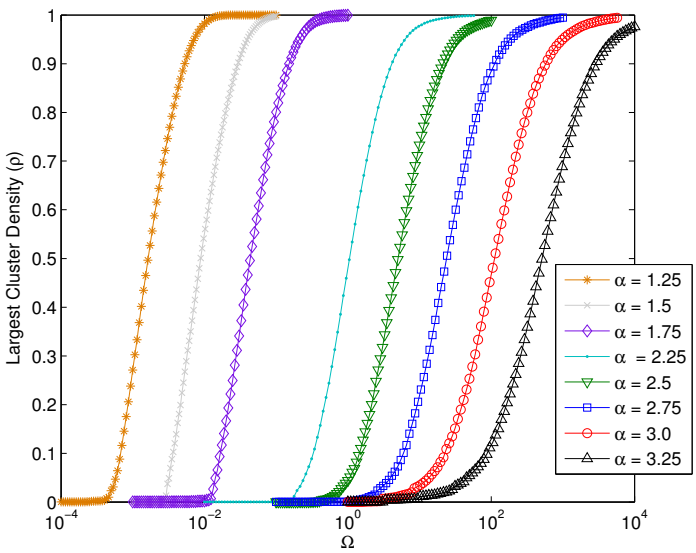

Figure 5.13: Density of the largest cluster plotted against the value of resonance broadening Ω, where we have allowed the exponent α to vary but fixed the system size $M = 512$. A critical point Ω^* can be identified, marked by the onset of a sudden growth in the density. This transition is more abrupt for $\alpha < 2$.

The motivation and clustering algorithm described previously still applies here, except we include modes where $k_x = 0$. Because no interaction coefficient is given, we only omit clusters that have the trivial solution $k_1 = (0, 0)$ and $k_2 = k_3$, or vice-versa, as well removing complex-conjugate copies of each mode, assuming the solution to our wave system is real. If our domain is rectangular, with sides of length 2π, and assuming that periodic boundary conditions apply, we therefore have the same set of vertices V, but with the addition of

$$\{k \in \mathbb{Z}^2 \mid k_x = 0,\ 1 \leq k_y \leq M\}.$$

Our edge set is still generated using brute force computation, by checking all triplets of wave numbers in our set of vertices, along with their negative counterparts, against the resonance conditions stipulated in equation (5.3).

Let us first consider how the density of the largest cluster depends on the exponent α. For the reasons we have cited above in the preceding section, we ignore the case $\alpha < 1$ since it has already been established that four-wave interactions dominate in this regime. As you can see from figure (5.13), some resemblance of critical phenomena still exists for $\alpha < 2$, with the transition appearing less abrupt α greater than this value. Furthermore, even relatively small changes in α corresponds

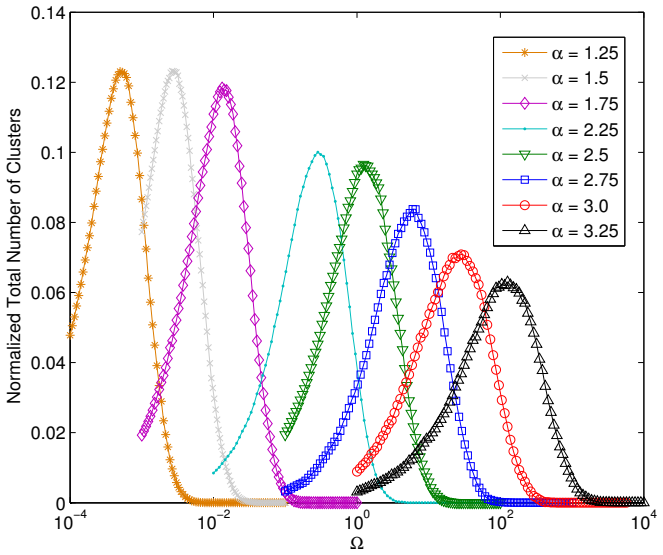

Figure 5.14: The normalised total number of clusters plotted against broadening Ω, shown for different values of the exponent α but where we have fixed the system size $M = 512$. The positions of the maxima correlate to the existence of a critical point, Ω^* within the system.

to changes in this critical point over a range of different orders. Still, this critical point remains, and can be more readily identified from the normalised total number of clusters as seen in figure (5.14). Each maxima is seen to correspond with the position of these critical points. We still therefore see the same kind of process underlying the formation of this large 'percolating' cluster; smaller quasi-resonant clusters form, initially independent, until some critical level of broadening is required for connections to form between them. However, the maximum total number of clusters diminishes for larger α, suggesting that relatively fewer smaller clusters are required before sufficient connections are made for the system to begin saturating.

For all values of α it appears that the critical transition is the most abrupt when $\alpha = \frac{3}{2}$. This particular example has received substantial analysis due to its connection with capillary waves, and for its significance in terms of number theory. For instance, efficient algorithms based on the q-class decomposition method have been developed [Kartashova and Kartashov, 2007], and generalisations of the Thue-Siegel-Roth theorem can be used to prove that a lower boundary on Ω must exist before quasi-resonances begin to form [Kartashova, 2007]. The existence of this boundary can be attributed to this abrupt transition, which we have highlighted in figure (5.15) against varying system sizes. By inspection, we see the same kind of

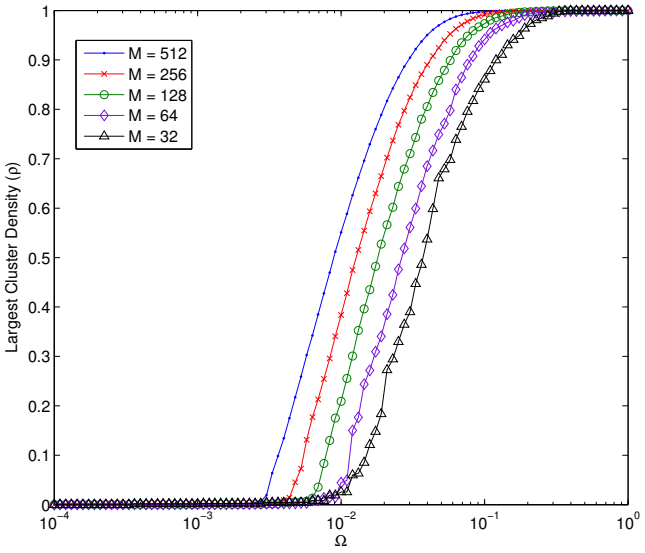

Figure 5.15: Density of the largest cluster plotted against resonance broadening Ω, where $\alpha = \frac{3}{2}$ and the system size M is allowed to vary. Here the onset of the growth in the largest cluster appears atypically abrupt when compared to other values of α, suggested by the existence of a definite lower bound on Ω before quasi-resonant interactions can occur.

scaling dependent on system size, $\Omega^* \sim M^{-\sigma_3}$, as detected with the CHM equation although additional computation would be required to make this concrete.

5.4 Chapter Summary

We began this chapter by arguing that resonance broadening played a critical role in categorising the wave system according to three different types of turbulent regime - the discrete, the kinetic and the mesoscopic. The idea was the to marry each of these different regimes with a kinematic overview of the wave system generated by solving the quasi-resonance conditions for the CHM dispersion relationship. We showed that these conditions could be solved explicitly in this case, exhibiting a divergent point where a given choice of mode can become quasi-resonant with a set of modes comparable to the size of the system. This allowed us to predict the amount of resonance broadening required for the system to be saturated, drawing a connection between the localised behaviour at each mode and the collective behaviour across the system. Numerically we showed a critical point of resonance broadening exists, marked by the onset of growth in one large cluster and maxima in total number of

independent clusters. Additionally, we demonstrated how this critical point scaled with system size and proposed a scaling argument for the growth in the largest cluster around this point. Finally, we argued that this critical phenomena is not unique to wave systems governed by the CHM dispersion relationship. Indeed, even though we proved the power-law dispersion relationship presents no localised sense of criticality, the full system observes the same hallmarks of criticality as found in the CHM case.

It must be stressed that while it is appealing to draw connections between the onset of the quasi-resonant energy cascade and percolation theory, it would be incorrect to do so for the very reason that no stochasticity is present in the kinematic approach presented here. Furthermore, the behaviour around the critical point does not scale with the typical $\rho \sim (\Omega - \Omega^*)^\sigma$ present in most types of critical phenomena within the realms of percolation theory. What we can suggest however, is that we have readily identified a point where DWT seems applicable. Namely, this is when we can identify that the resonance broadening is below this critical point. Above this point, as large clusters begin to appear, it is not hard to imagine that this defines the onset of mesoscopic turbulence, where broadening is small enough for some clusters to remain independent, but with the introduction of dominant cluster introducing some element randomness. When the system saturates, we therefore have the SWT regime, where no element of discreteness can be detected.

Chapter 6

Mutual Information and the Detection of Resonant Clusters

Since the pioneering work of [Phillips, 1960], much of what followed was dedicated either to developing a theoretical basis for resonant interactions in different physical systems, or validating this theory experimentally. With the latter, much of this work was based on idealised assumptions surrounding simplistic topography, for example, and is usually limited in scale. For instance, [McGoldrick, 1970] managed to completely track the resonant interactions of capillary-gravity waves from their inception to extinction through viscous dissipation, but their experimental set up was limited to a simple rectangular box whose dimensions measured no greater than a few metres. This was later corroborated experimentally by [Banerjee and Korpel, 1982], but again on even a smaller scale than the first reference. Both of these experiments managed to show that the generated waveforms were well represented by linear theory, including the effects of viscosity. Similar successes were replicated for stratified fluids in the context of long and short internal gravity waves [Koop and Redekopp, 1981]. Still, this kind of experimental setting remains idealised. The main question we will be asking in this chapter is whether there exist statistical techniques that can isolate the signature of resonant clusters either in simulated models of realistic scope and complexity, or directly from data generated from real-world examples. This is very much the converse of what we have considered up until this point, where we have motivated the study of resonance through a perturbation style analysis of the underlying equations of motion for our wave system in question.

Apart from the small scale experimental investigations detailed above, this concept of directly inferring the signature of interacting waves is relatively a new one. Some of the simplest statistical techniques revolve around the idea of decon-

structing the data in terms of its wavenumber-frequency spectrum [Wheeler and Kiladis, 1999]. Essentially, after some standard pre-processing techniques to filter out the effects of background fluctuations, we apply a Fourier transform to the data first spatially with respect to the longitudinal direction and then afterwards, applied with respect to time. This has been done to great effect, for instance, in identifying the signatures of equatorially trapped Rossby and Kelvin waves in the Pacific ocean from TOPEX/POSEIDON satellite altimetry data for Sea Surface Height (SSH) [Wakata, 2007; Shinoda et al., 2009]. The signature of these waves then appear as a spectral peak in the data, which neatly aligns to the expected dispersion relationship of these waves predicted from some underlying wave theory. As in the case of the last of these references, prominent peaks along these curves can then be attributed to interactions between different waves, such as those between tropical instability waves and Rossby waves.

Another prominent statistical technique centres around the idea of Principal Component Analysis (PCA), and its extension to both spatially and time dependent data known as Empirical Orthogonal Function (EOF) decomposition [Preisendorfer and Mobley, 1988]. Put simply, the idea is that these orthogonal functions can deconstruct the data into eigenvectors representing spatial patterns that maximise variance, along with principal components describing how the amplitude of these eigenfunctions evolve with time [Hogg et al., 2006]. As shown in this reference, this technique can be used to great effect in determining the dominant modes underlying often rich and complex dynamical flows. In this instance it was shown that in a coupled ocean-atmosphere quasi-geostrophic model, one can detect one dominant interdecadal mode in oceanic variability that would then control the timescales over which principal modes in the atmosphere would evolve. These techniques have been applied elsewhere to similar effect. For example, [White, 2000] proposes that the use of Complex Empirical Orthogonal Function (CEOF) analysis can be used to infer a simple analytical model for the coupling of Rossby waves in the Indian Ocean based on geophysical data generated throughout years from 1970 to 1998. This model then captures the reasons why Rossby waves propagate slower than expected for free Rossby waves. Elsewhere, this has been applied to coupled climate models to explain periodicity in variations of the Antarctic Intermediate Water [Santoso, 2004], and how CEOF can extract the signature of dominant resonant modes in the variability of the climate over the tropical ocean [Yang et al., 2004].

While these PCA techniques are shown to work effectively in isolating dominant modes within a system, the real question is whether we can infer correlations between them. In an analogy to how we constructed a network of resonant or

quasi-resonant clusters, we can compare this against an inferred network of interacting modes measured directly from the correlations between them. In terms of the CEOF analysis above, this has only been briefly touched upon by [Farneti, 2007]. Here the author identified a clear coupling between a baroclinic Rossby wave and a barotropic atmospheric wave in the same kind of coupled ocean-atmopshere model detailed above. This was achieved through the linear statistical technique known as Canonical Correlation Analysis, but only after the data had been deconstructed in terms of its CEOFs. The question is now can we generalise this approach to cover a more generalised notion of network structure underpinning the evolution of the system, and whether there are any inherent limitations in use linear statistical techniques such as CCA. Moreover, if we could sensibly reformulate such a problem in terms of the language of graph theory, we would gain access to a new way of characterising our system, using techniques and theory all ready well established across other disciplines.

While it is certainly true that the abstract concepts of graph theory has been applied to all manner of disciplines, from the study of social networks [Newman et al., 2002], to modelling disease transmission [Keeling and Eames, 2005], the idea of a 'climate network' was first introduced by [Tsonis and Roebber, 2004]. Here it was proposed that the climate can be be thought of as being represented by a grid of interacting, but individual in their own right, set of dynamical systems. As an example, the NCEP/NCAR reanalysis of the global 500-hPa dataset was considered, which gives the height of this pressure value at regularly spaced points of longitude an latitude across Earth's surface sampled at monthly intervals throughout the years from 1950 to 2004. Each point therefore represented a node in a climate network, whose edges were defined simply by thresholding the pairwise correlation coefficient between nodes. This concept was developed further in [Tsonis et al., 2006] and [Tsonis et al., 2008], where it was shown that the global climate network actually consisted of two coupled subnetworks, with the tropics and extra-tropics being characteristically fully connected or scale-free in nature, respectively. This was achieved simply by measuring the area-weighted connectivity of each node. It was suggested that this scale-free structure provided a way of guaranteeing stability by allowing any localised fluctuations to rapidly diffuse throughout the system. It was also shown that the appearance of super-nodes, that is nodes of substantially higher connectivity, corresponded to known patterns of circulation the atmosphere. Elsewhere, we have seen this approach applied to comparing the relative stabilities of El Niño and La Niña based on surface temperature data [Tsonis and Swanson, 2008], and understanding to what extent El Niño affects other climate regions [Gozolchiani

et al., 2008].

To date, most of these references use the linear correlation coefficient to define edges when constructing this climate network. As a statistical measure of correlation itself, CCA is known to be uncompetitive compared to other method when dealing with small sample sets [Bretherton et al., 1992]. In this case, we also see several different PCA based techniques, such as those using EOF decomposition, exhibiting bias. There are additional issues when dealing with these classically linear methods as they only typically uncover details about spatially localised interactions [Donges et al., 2009a]. Here, this issue was resolved by quantifying energy transmission across the network by introducing a concept of 'betweeness', where a given vertex is given a value according to how frequently it appears in all shortest paths across the entire network. Furthermore, it introduces the idea of using mutual information to determine statistical interdependence between nodes. When compared with a linear measure, such as the Pearson correlation coefficient, the underlying climate network was found to differ significantly on a global scale, indicative of the mutual information being better suited in determining nonlinear interactions between nodes. This is elaborated upon in greater detail by [Donges et al., 2009b].

What is surprising is that to date no connections between discrete wave turbulence and the construction of these climate networks has ever been made. This is peculiar since discrete wave turbulence offers a natural way to kinematically describe a wave system in terms of networks of quasi-resonantly interacting waves, rather than the above way of defining nodes in terms of fixed reference points in space. The aim of this chapter is to therefore determine whether mutual information can be sensibly used to infer the relative strength of interactions between waves, and more importantly, whether we see a correspondence with the strength of these interactions and the amount of broadening between modes. In doing so, it will provide a way of connecting the kinematic overview of turbulent systems discovered in the preceding chapter, with the actual dynamics of quasi-resonantly interacting waves.

The outline of this chapter is as follows. First we need to define mutual information, discuss its properties and how it can be calculated numerically from the time series of two different variables. We will then apply this technique to measure correlations in wave amplitudes for the CHM equation, but where dissipation has been added through a hyper-viscous term applied at small scales. For certain parameter values we know this equation admits an exactly resonant triad, with each mode in the triad being uncharacteristically large scale in nature. This allows us to choose an initial condition where all the energy is isolated in this triad alone. By

varying the amplitude of this triad, we will then show that we can effectively tune the resonance broadening, or equivalently the strength of nonlinearity in interaction between the triad and surrounding modes. We will show that mutual information effectively captures this increased broadening, with a corresponding decrease in pairwise mutual information between modes in the triad, and in the total correlation of triad itself. Furthermore, we will show that the triad continues to remain strongly correlated for significantly long integration times, even when compared to the correlation between surrounding quasi-resonant three-wave interactions. We will then show that the mutual information is sensitive enough to detect subtle qualitative changes in the dynamics of the principal resonant triad. We argue that these changes correspond to precisely when the nonlinear broadening becomes sufficient enough for additional quasi-resonant connections to form between the isolated triad and surrounding modes.

6.1 Mutual Information

Much of the analysis contained within this chapter will be based around the concept of the mutual information between two random variables, and its generalisation to multivariate distributions known as the 'total correlation'. Broadly speaking, the mutual information tells us the redundancy in information between two variables; that is, given the average amount of information we known about one variable, what does this tell us about the state of the other. More formally, say that X_1 and X_2 are two discrete random variables then the mutual information $I(X_1; X_2)$ is defined as [MacKay, 2003]:

$$I(X_1; X_2) = \sum_{x_1 \in \mathcal{X}_1} \sum_{x_2 \mathcal{X}_2} p(x_1, x_2) \log \left(\frac{p(x_1, x_2)}{p(x_1)p(x_2)} \right). \tag{6.1}$$

Equivalently, this is known as the Kullback-Leibler divergence between the joint distribution $p(x_1, x_2)$ and the independent distribution $p(x_1)p(x_2)$. Typically, the logarithm is taken base 2, giving the mutual information in units of bits, although this is often left ambiguous. Some of the key properties of the mutual information are:

(i) symmetry, $I(X_1, X_2) = I(X_2, X_1)$;

(ii) non-negativity, $I(X_1, X_2) \geq 0$;

(iii) $I(X_1; X_2) = 0$ iff X_1 and X_2 are independent.

This last property is significant as it suggests that the mutual information offers a means to measure the statistical correlation between two random variables. To this end, it has already been exploited for determining global dependence in financial time series among different stock market indices [Dionisio et al., 2004], and as we have already suggested, as a method for determining transport patterns in climate data [Donges et al., 2009b].

There are two significant points of contention often encountered when using mutual information. The first is found when dealing with continuous random variables, where it can be shown that $0 \leq I(X_1; X_2) \leq +\infty$ and so the mutual information may be unbounded. This is because an equivalent definition for the mutual information is often given in terms of the joint entropy of X_1 and X_2:

$$I(X_1; X_2) = H(X_1) + H(X_2) - H(X_1, X_2), \tag{6.2}$$

where

$$H(X_1, X_2) = -\sum_{x_1 \in \mathcal{X}_1} \sum_{x_2 \in \mathcal{X}_2} p(x_1, x_2) \log p(x_1, x_2), \tag{6.3}$$

with analogous definitions given for the two marginal entropies. It can be shown that these individual entropies can diverge in the continuous case even though the mutual information remains well-defined. Often we find that a suitable transformation is used to rescale he mutual information so that it lies in the interval $[0, 1]$, thus bringing it in line with the standard linear correlation coefficient so that an absolute measure of correlation can be provided [Dionisio et al., 2004]. The second is that the mutual information is that it is not a true 'metric' in the sense that it fails to satisfy the triangle inequality. Several entropy based invariants have been proposed elsewhere that correct this problem [Granger et al., 2004]. As we will see, neither of these issues pose a problem in this chapter, as we only a require to measure only the *relative* correlation between sets of different discrete random variables, neither is it necessary to use a strict metric.

One measure that generalises this concept of mutual information to account for larger sets of random variables is called 'total correlation' [Watanabe, 1960]. Its definition appears as a natural extension to the one above: given a set of N discrete random variables $\{X_1, \ldots, X_N\}$, the total correlation $C(X_1, \ldots, X_N)$ is defined as

$$C(X_1, \ldots, X_N) = \sum_{x_1 \in \mathcal{X}_1} \cdots \sum_{x_N \in \mathcal{X}_N} p(x_1, \ldots, x_N) \log \left(\frac{p(x_1, \ldots, x_N)}{p(x_1) \cdots p(x_N)} \right). \tag{6.4}$$

In a similar fashion as before, we can write this in terms of a combination of marginal and joint entropies:

$$C(X_1, \ldots, X_N) = \left[\sum_{i=1}^{N} H(X_i)\right] - H(X_1, \ldots, X_N). \tag{6.5}$$

In effect, we therefore see the total correlation as the redundancy in information between the total information assuming each variable is independent, the first term, compared to the actual information contained within the complete set of variables. If they were truly independent, then this total correlation would be zero. Similar to the mutual information, this measure can be seen as the Kullback-Leibler divergence between the joint and independent distributions, and as such is guaranteed to be non-negative.

For discrete random variables, the total correlation is guaranteed to be bounded and is maximised when one of the variables is redundant to all the others. This concept of redundancy falls perfectly in line with the idea of clustering, suggesting that we can group variables by removing extraneous degrees of freedom in the system. One example we have already seen is where equations of motion for the detuned triad can be reduced to a one-dimensional system. Elsewhere, this idea of inferring structure has been used to develop algorithms for learning Bayesian networks [Cheng et al., 2002], and as a method for highlighting structure to help visualise data [Jakulin and Bratko, 2003].

6.1.1 Methods for estimating mutual information

The question is once we have sampled from our random variables, how do we estimate the mutual information, or indeed, the total correlation between them. There are several approaches often cited in the literature of varying levels of sophistication, each having their own advantages and disadvantages [Moddemeijer, 1999]. The three prominent approaches in the literature include: histogram-based estimators, with either equidistant or equiprobable cells [Darbellay and Vajda, 1999]; the use of kernel density estimators to calculate the underlying joint and marginal distributions [Moon et al., 1995]; and finally, a k-nearest neighbours approach [Kraskov et al., 2004]. While the last of these has been praised for its accuracy and favourable bias, it relies on the assumption that each of the samples has been generated independently. For samples drawn from a dynamical system, this assumption does not hold if the trajectories are suitably regular. The second of these estimators suffers from the problem that they rely on the correct choice of parameters to work successfully.

Finally, the use of histogram-based estimators are computationally the simplest and conceptually the easiest to understand. However, they suffer from issues of bias, variance and robustness.

Certain approaches have been suggested to solve some of these issues, such as those where the additional correlations between samples in a time series can be beneficial in estimating mutual information provided they are treated correctly [Galka et al., 2006]. However, often these more sophisticated approaches are computationally more expensive. If we were to measure the pairwise mutual information, or even the total correlation across all triplets of variables and this set is comparatively large, then the amount of computation involved grows explosively with the size of this set. This leaves the histogram-based estimator as the only viable approach, but where the cells are equidistant rather than equiprobable in size. A similar argument was adopted in [Donges et al., 2009b] for the construction of climate networks, where it was stressed that it was not necessary to accurately determine the mutual information, but rather correctly estimate the relative mutual information between different clusters of nodes. The point is that this approach remains credible provided that the error is systematic and equally applied across all measurements.

6.2 Measuring correlations from Direct Numerical Simulation of the CHM equation

As you recall, the theory of discrete wave turbulence suggests that for systems of weakly nonlinear dispersive waves, energy transfer between modes should be chiefly governed by resonant interactions. This motivates the idea behind studying clusters of exactly resonant modes and their corresponding dynamical systems; the understanding is that these reduced dynamical systems are sufficient alone to capture the underlying dynamics of the entire wave system. In the preceding chapter we then saw how increasing the nonlinearity, which we argued was equivalent to increasing the resonance broadening between modes, induced the onset of a percolating cluster of quasi-resonantly interacting modes. At this point, the system is no longer suitably describe by these reduced resonant clusters, and its behaviour becomes more random in nature. We had therefore married the idea of this critical behaviour with the onset of statistical wave turbulence. We ask now whether we can capture this transition through Direct Numerical Simulation (DNS) of the CHM equation. Using these nonlinear measures of correlation we have described above, can we measure this breakdown in correlation between exactly resonant clusters as broadening becomes sufficient enough for energy to be exchanged through quasi-resonant interactions.

6.2.1 Scale Invariance and Controlling Nonlinearity

Throughout the thesis we have used the CHM equation as our archetypal dispersive wave system, courtesy of its quadratic nonlinearity and application to a variety of physical systems. Including the effects of dissipation, this equation now reads

$$\frac{\partial}{\partial t}(\Delta\psi - F\psi) + \partial(\psi, \Delta\psi) + \beta\frac{\partial}{\partial x}\psi = \mu(-\Delta)^n\psi. \tag{6.6}$$

As we have seen, ignoring this hyper-viscosity term on the right-hand-side and assuming that we have doubly-periodic boundary conditions, we can express the stream function ψ in terms of its Fourier series, whose coefficients ψ_k evolve according to an infinite dimensional system. Writing this system in terms of its interaction form, $\phi_k = \psi_k \exp(i\omega_k t)$, we find that

$$\frac{\partial\phi_k}{\partial t} = \frac{1}{2}\sum_{k_1+k_2=k} T(k, k_1, k_2)\phi_{k_1}\phi_{k_2}\mathrm{e}^{i\delta(k,k_1,k_2)t}, \tag{6.7}$$

where $\delta(k, k_1, k_2) = \omega(k) - \omega(k_1) - \omega(k_2)$ represents the finite resonance width. We saw how each propagating plane wave ϕ_k is itself a solution to the CHM equation, called either drift or Rossby wave depending on the context.

Let us now consider the scaling transformation

$$\bar{\phi}_k(\tau) = A\phi_k(t), \tag{6.8}$$

where A is some arbitrary real constant and $\tau = A^{-1}t$ represents our re-scaled time. Using this new variable we derive the system

$$\frac{\partial\bar{\phi}_k}{\partial\tau} = \frac{1}{2}\sum_{k_1+k_2=k} T(k, k_1, k_2)\bar{\phi}_{k_1}\bar{\phi}_{k_2}\mathrm{e}^{i\delta(k,k_1,k_2)A\tau}. \tag{6.9}$$

This is almost identical to the equation above except we have re-scaled all of the resonance widths by a constant factor. It follows that clusters of exactly resonant modes, that is for those where $\delta(k, k_1, k_2) = 0$ for each triad of modes in the cluster, the corresponding dynamical systems are invariant under this scaling transformation. In effect, the amplitude A allows us to regulate the degree of broadening in the system and hence the nonlinearity: if A is small then the detuning between modes is likewise small and so clusters should remain isolated. The consequence of this is that initial conditions of inherently small nonlinearity dramatically lengthen the timescale over which interactions can occur.

The idea is that we can use this value of A to parameterise our initial con-

ditions when we integrate the full CHM equation given in equation (6.7). Setting $F = 1$, we know that the CHM equation admits an exactly resonant triad with wave numbers $k_1 = (1, -4)$, $k_2 = (1, 2)$ and $k_3 = k_1 + k_2 = (2, -2)$. We now localise the majority of the initial within just these three modes, along with their complex conjugates. We can then tune the amount of broadening in the system by varying A, controlling the transfer of energy through quasi-resonant interactions to the surrounding modes. For sufficiently small A we should see this energy remaining confined to just the isolated triad, with a small loss to surrounding modes through finite nonlinearity. The fact that the energy cascade cannot initialise gives this phenomena the name "frozen turbulence" [Pushkarev, 1999].

6.2.2 Parameterising the initial conditions

First though, we need to find a way of parameterising the initial conditions for the isolated triad in a sensible way. Fortunately, we can do this using the results from the chapter on the detuned triad. After appropriate re-scalings of each complex variable ϕ_k and assuming that the nonlinearity is sufficiently small, the dynamical system governing this isolated triad is given by

$$\begin{cases} \dot{B}_1 = ZB_2^* B_3, \\ \dot{B}_2 = ZB_1^* B_3, \\ \dot{B}_3 = -ZB_1 B_2, \end{cases} \tag{6.10}$$

where B_3 represents the unstable mode corresponding to k_3 since $k_2^2 < k_3^2 < k_1^2$. As we have seen, the evolution of this system is completely determined once we have specified the the value of the pseudo-energy E, plus the two additional parameters γ_1 and γ_2 and a value for the initial condition of the dynamical phase $\varphi(0)$. Given a solution $B_j(t)$, $j = 1, 2, 3$, the scale invariance property derived above means that

$$b_j(\tau) = AB_j(t),\ j = 1, 2, 3,$$

forms an infinite family of solutions parameterised by $A \neq 0$. Each of these solutions inherits the rescaled conservation laws $\mathcal{J} = A^2 J$, $\mathcal{E} = A^2 E$, as well as the Hamiltonian

$$\mathcal{I}^2 = 4Z^2\mathcal{E}^3(\gamma_1^2 - \gamma_2^2)(1 - \gamma_1)\sin^2\varphi(0). \tag{6.11}$$

We immediately see that γ_1 and γ_2 must remain independent of A, and likewise for the ratio $\mathcal{I}^2/\mathcal{E}^3$ provided we fix the initial value $\varphi(0)$. Fixing these three values and an initial reference value for E completely defines the evolution of our re-scaled

system once we have specified the amplitude A.

6.2.3 Methodology

We proceed by numerically integrating equation (6.7) with the addition of the hyper-viscosity acting to dissipate small scales. Since for each of the wave-numbers in the isolated triad we have that $k^2 < 20$, we spectrally truncate this equation by introducing the cut-off $|k_x|$, $|k_y| < 32$. Initial conditions were chosen by localising the majority of the energy in the isolated triad setting $\gamma_1 = 0.4$, $\gamma_2 = 0.2$ and $\varphi(0) = \frac{\pi}{2}$ with reference energy $E = 10^{-4}$. All other modes in the system were set to have randomised phases, but with a fixed energy of 1.0×10^{-8}, where this value corresponds to the actual energy $(k^2 + F)|\phi_k|^2$ and not the pseudo-energy defined after re-scaling each variable. System (6.7) was then integrated to a total time of $20T$, where T is the characteristic period of the isolated triad as given by equation (3.40). This was found to be sufficient to allow us to deduce any statistically meaningful measures of total correlation and mutual information, but before the point energy loss from the system becomes significant through the effects of dissipation. The time over which we integrate is therefore not fixed, but depends on the nonlinearity A. Due to the scaling properties mentioned above, small values of A therefore result in substantially longer run times.

The mutual information and total correlation was then estimated using the amplitudes $|\phi_k(t)|$ of each wave. To remove inducing any additional correlations through using fixed initial conditions, the first $2T$ of any trajectory was discarded. We used the naive histogram method to estimate each of the joint and marginal distributions, using 100 identically sized cells between the minima and maxima attained by each trajectory, itself consisting of 1000 regularly sampled points. Since we know that the dynamics are sufficiently regular, we use linear interpolation to calculate the crossing times between each cell. Thus, each distribution corresponds to the total time throughout the course of the simulation that the trajectory remains in each cell. We calculate the 95% confidence intervals by running several instances of the same initial conditions, with random background fluctuations, and then using bias-corrected bootstrapping to quantify the error. Due to the long run time for small values of nonlinearity, we are restricted to taking 20 samples for $1 < A < 10$, but this is value is increased to 50 whenever $A \geq 10$.

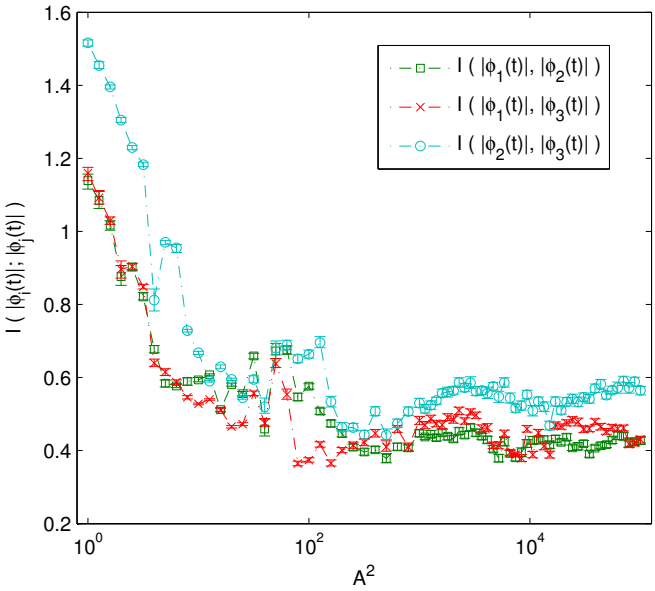

Figure 6.1: Mutual information calculated between three modes in the isolated triad as a function of the amplitude A. This isolated triad is formed by the three modes $k_1 = (1, -4)$, $k_2 = (1, 2)$ and $k_3 = k_1 + k_2$. Initial conditions are chosen by setting $\varphi(0) = \frac{\pi}{2}$, $\gamma_1 = 0.4$ and $\gamma_2 = 0.2$. We have set a reference energy of $E = 10^{-4}$.

6.2.4 Detecting the resonant signature

We know when the resonance broadening is small, the isolated triad should evolve according to the spectrally truncated system given by equation (6.10), at least initially. If this is true, because the system is explicitly integrable, we have induced a level of redundancy that should mean that the total correlation is maximised. As we increase the broadening and this isolated cluster forms quasi-resonant connections with other modes in the system, this triad loses coherence as its motion becomes less regular. We therefore expect both the total correlation and mutual information to decrease in this case. As we continue to increase the amount of broadening, or equivalently A, and the motion becomes more random the question is whether each mode effectively becomes independent, and similarly does the total correlation vanish to zero. Particularly, we ask whether the signature of the resonant cluster remains in this statistical case.

The mutual information between the three modes in the isolated triad is plotted in figure (6.1) as a function of A. We see that the mutually information rapidly decreases across all modes as we increase the nonlinearity, indicating that the triad itself begins to lose cohesion as the modes begin to interact quasi-resonantly

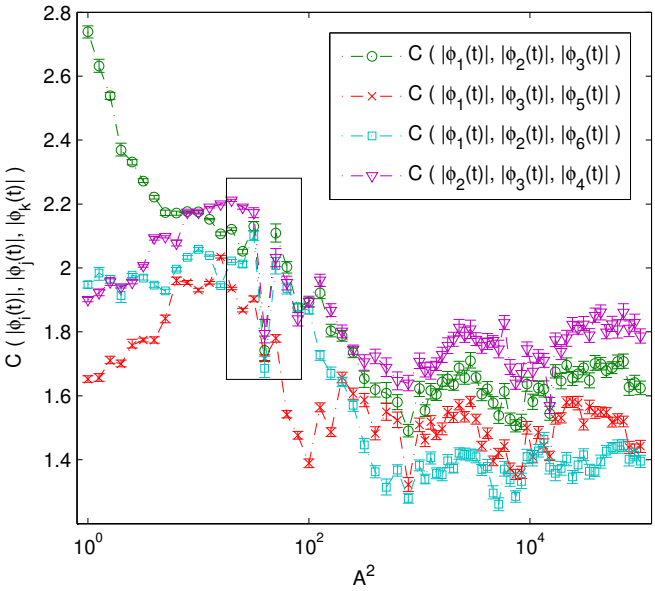

(a) Total Correlation

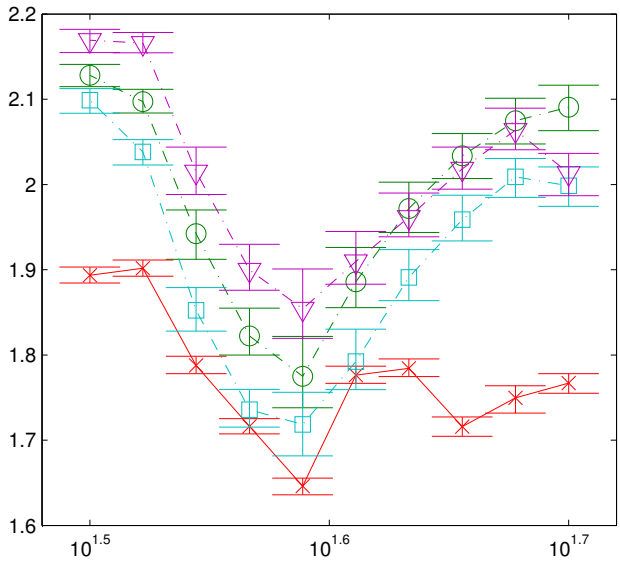

(b) Magnified Section

Figure 6.2: The total correlation of the isolated exactly resonant triad, and of surrounding quasi-resonant triads, as a function of the amplitude A. This isolated triad is formed by the three modes $k_1 = (1, -4)$, $k_2 = (1, 2)$ and $k_3 = k_1 + k_2$. The surrounding quasi-resonant triads are formed by combinations of two of these modes, plus the modes $k_4 = k_2 + k_3$, $k_5 = k_1 + k_3$ and $k_6 = k_1 - k_2$. We have magnified a section of the plot where there is abrupt change in total correlation. Initial conditions are chosen by setting $\varphi(0) = \frac{\pi}{2}$, $\gamma_1 = 0.4$ and $\gamma_2 = 0.2$. We have set a reference energy of $E = 10^{-4}$.

with the surrounding modes. They do not become completely independent however, with the mutual information appearing to tend to a constant value. This suggests that correlations between modes in the resonant triad still persist even when the strength of the nonlinearity is strong.

We can compare how resilient this resonant signature is by comparing the total correlation with that of the surrounding quasi-resonant, three-wave interactions. Since the majority of the energy is initially localised to the isolated triad, we know that any significant three-wave resonant interaction must consist of at least two of the modes from this exactly resonant cluster. One mode is not sufficient, otherwise we see that the right-hand-side of equation (6.7) must vanish. At least initially, we see that energy must transfer to the three modes $k_4 = k_2 + k_3$, $k_5 = k_1 + k_3$ and $k_6 = k_1 - k_2$. We now have six modes of interest in total, so rather than considering the fifteen possible pairwise interactions, we use the four different triads as the basis of calculating the total correlation. This can be seen in figure (6.2(a)). Here, we see that for $A < 10$, the resonant triad appears the most correlated, decaying almost linearly on the semi-log scale. For the same amplitude, we see the surrounding quasi-resonant triads becoming maximally correlated and then diminishing to what appears to be a near constant value. Importantly, the quasi-resonant triad formed by the three-modes k_2, k_3 and k_4 now becomes the most dominant. However, the exactly resonant triad still persists for large nonlinearity, rather than becoming completely uncorrelated.

This behaviour confirms the idea that A effectively controls the resonance broadening between the modes. Initially, the total correlation of the exactly resonant triad evolves independently, with only minimal transfer to the surrounding modes. As we increase the amount of broadening, the immediate surrounding modes begin to become correlated with two of the modes which formed part of the resonant triad. We see a peak value in this correlation, before broadening becomes significant enough for additional modes to begin interfering with the underlying dynamics of the six modes described above. Correlation begins to decrease at this point before settling at constant value. What is significant is that we have found evidence to suggest that quasi-resonant triads can appear more correlated than exactly resonant ones. Even for relatively small nonlinearity, it may be unwise to assume that the magnitude of detuning and correlation are synonymous, or even proportional.

6.2.5 Correlation Anomaly

When measuring the total correlation we see a momentary and abrupt change in both the resonant triad, and surrounding quasi-resonant triads, when $A \approx 10^{1.6}$.

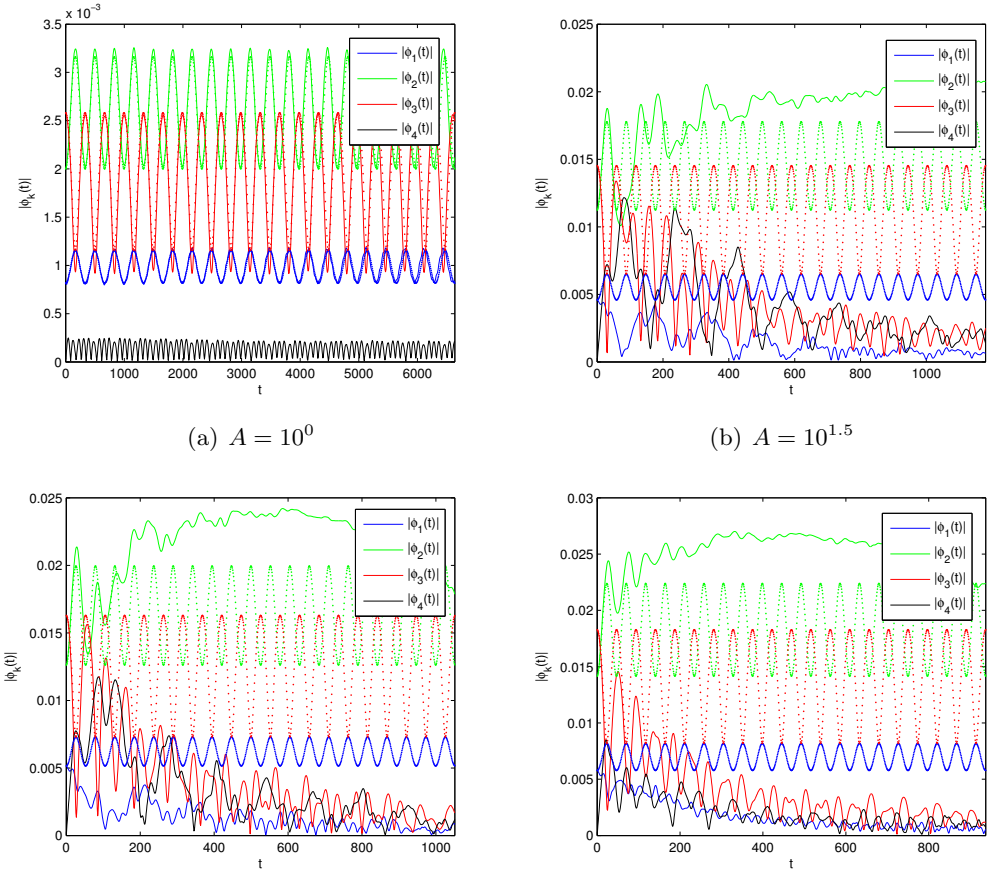

(a) $A = 10^0$ (b) $A = 10^{1.5}$

(c) $A = 10^{1.6}$ (d) $A = 10^{1.7}$

Figure 6.3: Sample trajectories of the amplitudes of three modes in the isolated, exactly resonant triad as function of A. This isolated triad is formed by the three modes $k_1 = (1, -4)$, $k_2 = (1, 2)$ and $k_3 = k_1 + k_2$. The trajectory of the nearby quasi-resonant mode $k_4 = k_2 + k_3$ is included to monitor energy transfer from the isolated triad. For comparison, we have included the solution of the dynamical system (6.10) given by dotted lines. Values of A correspond to the anomaly identified in figure (6.2). Initial conditions are chosen by setting $\varphi(0) = \frac{\pi}{2}$, $\gamma_1 = 0.4$ and $\gamma_2 = 0.2$, with reference energy $E = 10^{-4}$.

We have highlighted this phenomena in figure (6.2(b)) where we have magnified the corresponding section of the plot. This is not just an isolated point, but acts as a continuous deformation in the parameter A. The question is whether this anomaly corresponds to a qualitative change in the underlying dynamics. To investigate, we have plotted some sample trajectories in figure (6.3), choosing three values of A located at and around this anomaly. For comparison we have also shown that for a value of $A = 1$, the dynamics of the isolated triad correspond to the solutions of the system (6.10). While qualitatively the behaviour of the two modes k_2 and k_3 remain unaffected at this point, this is not the case for the two modes k_1 and k_4. We see a transition where the characteristic timescale for these two modes dramatically shortens. Oscillations become more rapid and the variability in the amplitudes of these two modes decreases. This may suggest that these modes are beginning to form additional quasi-resonant interactions with other modes in the system. For instance, where the dynamics of these modes are now governed by the formation of an even larger quasi-resonant cluster, which suppresses energy transfer to these modes. We saw this briefly when discussing the detuned triad in the limit when broadening becomes large.

6.3 Chapter Summary

This chapter provided a precursory look into how the use statistical measures, such as total correlation and mutual information, can be used detect the signature of resonant interactions from direct numerical simulation of the CHM equation. We demonstrated that the nonlinearity of the system can be tuned simply by changing the energy contained within a single isolated triad. Using mutual information to measure pairwise correlations between modes within the triad, we showed that for small nonlinearity these correlations were initially strong and then diminished in strength as we increased the amplitude of the system. However, these correlations persisted even in the presence of large nonlinearity. It is the more generalised notion of total correlation, however, which can be extended to measure correlations between sets of modes, that can effectively measure the breakdown of cohesion in the isolated triad. This breakdown occurs through the onset of mode coupling between the isolated triad and the surrounding quasi-resonant modes. We demonstrated that broadening progressively activates these modes, until these surrounding quasi-resonant modes also lose coherence as even larger clusters begin to form. We remarked that some quasi-resonant clusters may even in fact appear more correlated than those that are exactly resonant. This puts into question the belief that in some

way the broadening of the cluster and its correlation are one and the same thing. Finally, we demonstrated that total correlation is a subtle enough measure to detect qualitative changes in the underlying dynamics of quasi-resonant clusters. This was marked by an abrupt and anomalous change in this measure that affected not only the exactly resonant triad, but the surrounding quasi-resonant clusters as well.

It is perhaps due to the precursory approach adopted in this chapter, that some outstanding issues undoubtably remain. For some it might appear unsettling that apparently no physical meaning can really be attached to mutual information as it is used here. Indeed, the naive histogram approach we have applied here acts only as a proxy for mutual information; the relatively regular dynamics of the small interacting cluster we used as a toy example throughout this chapter are not amenable to any of the more sophisticated implementations of mutual information that require independence of sampling, for example. Say we were able to apply this technique to a fully evolved, turbulent wave system, one where we knew SWT was appropriate, it would still be difficult to relate the quantity of mutual information to a physical property of the system. What is important, however, is that it offers a nonlinear measure of the relative strength of interactions between modes. In this regard, it may even be difficult to even relate it to other statistical measures of correlation used throughout the literature, most of which are either linear or rely on a PCA-type approach. Where it may be physically meaningful, however, is that both the mutual information and total correlation between modes for sufficiently large levels of nonlinear appear constant. If this is not an artefact of either the method employed or limited timescale used, it could have interesting implications for the statistical modelling of random interactions between modes in either mesoscopic or fully statistical turbulent regimes. Specifically, it would seem to tell us that these interactions must be modelled in such a way that the pairwise mutual information between modes must agree with this constant value.

The significance of this work is that it marries together two concepts that so far have remained disconnected: that of the 'climate network', in the context of real-world data driven problems connected with turbulence; and with the theoretical study of the kinematics of nonlinear resonance broadening as it appears in the theory of wave turbulence. As such, it extends upon this first naïve network approach, which to date has only been used to detect localised transport, confirming already known circulation patterns in the atmosphere. Here, we have developed a technique that has the potential to measure actual correlation between clusters of resonant and quasi-resonant modes in fully-realised turbulent systems. As we have seen throughout this thesis, understanding the onset of resonance broadening and generation of

quasi-resonant interactions is in turn crucial to understanding discrete and statistical wave turbulence. As such it provides a way of validating these principles in both more realistic settings, from real data for example, and direct numerical simulation of fully turbulent systems. This is the direction this work needs to take. So far, we have only looked at a very idealised and small scale system, with localised energy confined to one isolated, exactly resonant triad at large scales. Applying forcing at these scales, truly randomising the initial conditions, and allowing the system to reach quasi-stationarity will be a true test of whether total correlation, or even mutual information, can infer any meaningful about underlying dynamical network of interacting modes.

Chapter 7

Conclusions

Throughout the course of this thesis, we have studied the dynamics, kinematics and statistics of three-wave interactions in models of geophysical flows. In particular, we considered models described by spatially extended, nonlinear dispersive wave systems, such as those appearing across a variety of different physical applications, covering multiple scientific disciplines. We demonstrated how resonance interactions formed a crucial component of these systems, and how the phenomenon nonlinear resonance broadening is paramount to the characterisation of three different branches of wave turbulence theory. These being formed by the discrete description of isolated, independently evolving and exactly resonant clusters; the classical statistical description of wave turbulence, which is asymptotically exact in the infinite box and weakly nonlinear limit; and the mesoscopic regime, which because of the discreteness inherited from finite sized systems, actually consists of an amalgamation of both these two extremes. The principal aim of this thesis therefore, was to understand the process by which nonlinear broadening induces a transition between these three different turbulent regimes.

We proceeded by considering a variant of the isolated, exactly resonant triad, created through the addition of non-zero detuning to the system. Since the exactly resonant version is completely integrable, with explicit solutions known for both the amplitudes and phases, we asked how the presence of broadening would affect this. Using a Lax pair representation for the detuned triad, we demonstrated how this could be used in a precise and systematic way for calculating invariants for the system. Explicit solutions could then be readily calculated and compared with the exactly resonant case. For sufficiently large values of detuning, we demonstrated that each of the phases need no longer be monotonic, with the dynamical phase being no longer confined to one bounded interval as it was before. In this limit, we

found a vanishing asymptotic limit for the period of motion, and concluded that variations in the amplitudes must likewise diminish. We therefore showed that for large detuning, energy exchange between modes becomes almost insignificant, with any temporal correlation between them only happening on vanishingly small scales. This corroborates the existing idea of discrete wave turbulence; that energy exchange is at its most efficient between sets of modes having zero or only slight amounts of detuning. What is perhaps surprising, however, is that we showed intermediate levels of detuning can actually promote energy transfer between modes for certain choices of initial conditions, even surpassing that of the exactly resonant case. At this point, we showed that the period diverged through the creation of a homoclinic orbit, and so argued that broadening can in fact be used to tune the period of the system from vanishingly small to arbitrarily large.

We then focused our attention on another variant of the isolated triad, which we called the forced triad, where we applied a constant, additive forcing term to the unstable mode. In contrast with the detuned triad, while the system still retained a canonical Hamiltonian structure, it was only shown to be explicitly integrable corresponding to the case when Hamiltonian was zero. An explicit solution for this system could be then only be derived for very restricted set of initial conditions. We did however show that generally speaking, the motion appeared to be bounded, even when the Hamiltonian was non-zero. We demonstrated this by introducing a novel-one dimensional particle representation for the system, described by a particle trapped in a time-dependent, attractive potential. When the Hamiltonian was zero, this potential was found to be no longer time-dependent and so could be exploited to provide analytic formulae for the periods and maximal energies, even providing a novel scheme for approximating the dynamics of the system when no explicit solution was available. For the case when the Hamiltonian was non-zero, it was possible to prove finite-time boundedness for solutions. By analysing Poincareé sections of the dynamics, we managed to find instances when the motion could be both periodic and quasi-periodic depending on the initial conditions. We argued that the general boundedness of the system had important implications in terms of the ad hoc introduction of external forcing used in the numerical simulation of wave turbulence. Particularly, that certain types of forcing need not act to supply a continual source of energy to the system. Furthermore, this system provides a striking example of how changing initial conditions for the phases alone can lead to qualitatively different behaviour for the system. This has important implications in the study of resonant and quasi-resonant dynamics in general, suggesting that the phases cannot be simply neglected as is often the case with studies of this type.

The novel type of phenomenon observed with the detuned triad then naturally promoted a more detailed investigation into the kinematics of nonlinear resonance broadening. Using the archetypal example of the CHM equation used throughout this thesis, we were able to characterise analytically how the set of quasi-resonantly interacting modes, corresponding to just one triad, developed under increased levels of broadening. We found that while it was certainly true that for small values of broadening, we observe a subtle 'thickening' of the exactly resonant manifold, for larger values, this idea became very misleading. We saw that this solution set in fact diverges for a finite, critical value of broadening. Through a series of propositions, we showed that this divergent behaviour naturally leads to the idea that only a finite range of broadening is actually required for a single mode to become quasi-resonantly connected with all modes in the system, regardless of its size. We showed that the set of modes generated by triads sharing quasi-resonant modes does in fact have very natural network based interpretation. By numerically investigating how broadening affects the connectivity of this network, we managed to show the existence of a percolation-like transition, where a single dominant cluster begins to emerge. This was true independent of the dispersion relationship used, both the for CHM equation, which we know exhibits this critical behaviour in the detuned manifold, and for a more general class of power-law dispersion relationships where no such behaviour provably exists. We argue that this phenomenon is therefore typical for a host of different dispersive wave systems, even those that do not admit any resonant clusters, as seen in the context of capillary waves. If this is the case, it suggests that the percolation phenomenon uncovered here could be used to characterise the three different types of fundamental regimes found in the theory of wave turbulence.

Up to this point, we had only considered a kinematic overview into the effect of nonlinear resonance broadening. The question we then asked was whether the view developed here is actually representative of the true underlying dynamics between interacting modes. By direct numerical simulation of the CHM equation, we showed that the generation of quasi-resonantly excited modes can in fact be detected using the statistical measures of total correlation and mutual information. We did this by confining all the energy in the wave system to just one isolated triad, which we could then tune to affect a corresponding change in the nonlinearity. We showed that the breakdown in cohesion of the isolated triad could actually be detected through loss of correlation, met with an increasing measure of correlation in the surrounding sets of quasi-resonant modes. Even when the system begins to become progressively nonlinear, the signature of these resonant and quasi-resonant clusters

was shown to persist. However, we observed that quasi-resonant clusters may in fact appear more correlated than those that were exactly resonant, thus dispelling any idea that correlation between modes and their degree of broadening are not necessarily equivalent. Finally, we argued that total correlation may in fact be a subtle enough measure to detect qualitative changes in the dynamics of interacting modes, which could correlate to the onset of even larger clusters being formed as the broadening is increased.

While the work presented in this final chapter is only in its infancy, its potential is already clear. First, as we have mentioned it provides a mechanism by which we can actually quantitatively measure the effect of nonlinear broadening, as it induces correlations between quasi-resonantly interacting modes. This factor is critical for any further numerical study into role of nonlinear resonance broadening. Secondly, it provides away to infer the signature of resonant and quasi-resonant interactions in fully-realised turbulent systems. This is central to the now emerging topic of mesoscopic wave turbulence; it provides a way of detecting whether regular dynamics actually exist among the background fluctuations of the statistical regime, and if so, between which modes. Without doubt, this is a computationally involved task for systems of physically realistic scale. It involves at least a pairwise computation of the mutual information between every mode in the system, and this is before we even consider enumerating over all possible triads. At least however, when combined with the kinematic description of turbulence considered in this thesis, it might at least provide a way in to this complex, and difficult, emerging field.

Appendix A

Explicit form for the area enclosed by the detuned manifold

We present here the reduction to standard form of the elliptic integral A found in the chapter on quasi-resonances. If you recall, we defined the two γ-dependent constants

$$a = \frac{4F\gamma}{r_3 D},\ b = \frac{c(\gamma)}{r_3 D}, \tag{A.1}$$

so that

$$A = -\pi F + \frac{r_3 D}{2|\gamma|} \int_0^{\frac{\pi}{2}} \sqrt{(a + \cos 2\phi)^2 + b^2}\ \mathrm{d}\phi. \tag{A.2}$$

We named this simplified integral I. If we now make the transformation $x = a + \cos 2\phi$, we find that

$$I = \frac{1}{2} \int_{a-1}^{a+1} \frac{x^2 + b^2}{\sqrt{(a + 1 - x)(x - a + 1)(x^2 + b^2)}}\ \mathrm{d}x. \tag{A.3}$$

This is clearly recognisable as an elliptic integral. Let us define

$$y^2 = (a + 1 - x)(x - a + 1)(x^2 + b^2), \tag{A.4}$$

which is positive for $a - 1 \leq x \leq a + 1$. This can be factorized as the product of two quadratic polynomials, $y^2 = Q_1 Q_2$, where

$$Q_1 = x^2 + b^2, \tag{A.5}$$

$$Q_2 = -x^2 + 2ax + 1 - a^2. \tag{A.6}$$

The next step is to find two real constants λ_1 and λ_2 such that $Q_1 - \lambda_j Q_2$ is a perfect square, which is done by choosing λ_j such that the discriminant of this quantity is zero. We find that

$$\lambda_{1,2} = \frac{1}{2}\left[a^2 + b^2 - 1 \pm \sqrt{(a^2+b^2-1)^2 + 4b^2}\,\right], \tag{A.7}$$

labelling each of these constants so as to respect $\lambda_1 < 0 < \lambda_2$. We therefore have that

$$Q_1 - \lambda_1 Q_2 = (1+\lambda_1)\left(x - \frac{a\lambda_1}{1+\lambda_1}\right)^2, \tag{A.8}$$

$$Q_1 - \lambda_2 Q_2 = (1+\lambda_2)\left(x - \frac{a\lambda_2}{1+\lambda_2}\right)^2. \tag{A.9}$$

It is now a simple case of solving this system for Q_1 and Q_2 to find that

$$Q_1 = \frac{\lambda_2(1+\lambda_1)}{\lambda_2 - \lambda_1}(x-\alpha)^2 - \frac{\lambda_1(1+\lambda_2)}{\lambda_2-\lambda_1}(x-\beta)^2, \tag{A.10}$$

$$Q_2 = \frac{1+\lambda_1}{\lambda_2-\lambda_1}(x-\alpha)^2 - \frac{1+\lambda_2}{\lambda_2-\lambda_1}(x-\beta)^2 \tag{A.11}$$

where we have defined the two constants

$$\alpha = \frac{a\lambda_1}{1+\lambda_1},\ \beta = \frac{a\lambda_2}{1+\lambda_2}. \tag{A.12}$$

It is fairly trivial to show that $1+\lambda_1 > 0$ for all values of $a, b \in \mathbb{R}$. Written more concisely, we therefore have $Q_1 \equiv A_1(x-\alpha)^2 + B_1(x-\beta)^2$ and $Q_2 \equiv A_2(x-\alpha)^2 - B_2(x-\beta)^2$, where each A_j and B_j is strictly positive.

Now that we have found this alternate form for y^2, the next stage is to make the substitution $t = (x-\beta)/(x-\alpha)$. This gives

$$\frac{\mathrm{d}x}{y} = \frac{1}{\beta-\alpha}\frac{\mathrm{d}t}{\sqrt{(A_1+B_1t^2)(A_2-B_2t^2)}}, \tag{A.13}$$

where t is lies within the two roots of Q_2, specifically $-\sqrt{A_2/B_2} \le t \le \sqrt{A_2/B_2}$. For brevity, let us define this new quartic in t appearing inside the radical by

$$s^2 = (A_1+B_1t^2)(A_2-B_2t^2). \tag{A.14}$$

Lastly, we need to find the inverse of this substitution to evaluate I in terms of t.

We calculate

$$x = \frac{\alpha - \beta}{t - 1} + \alpha, \tag{A.15}$$

from which it follows that

$$2(\beta - \alpha)I = (\alpha^2 + b^2) \int \frac{\mathrm{d}t}{s(t)} + 2\alpha(\alpha - \beta) \int \frac{\mathrm{d}t}{(t-1)s(t)} + (\alpha - \beta)^2 \int \frac{\mathrm{d}t}{(t-1)^2 s(t)}. \tag{A.16}$$

Here, each of the integrals are to be evaluated between the two roots of Q_2 defined above. The first two of these integrals are complete elliptic integrals of the first and third kind respectively. However, the third can be reduced further using integration by parts to a combination of all three kinds of elliptic integral. To do this, note that after repeated decomposition using partial fractions, we have that

$$\frac{\mathrm{d}}{\mathrm{d}t}\left[(t-1)^{-1}s(t)\right] = \frac{1}{(t-1)^2 s(t)} + \frac{B_1 + B_2}{(t-1)s(t)} + B_1 B_2 \frac{1 - t^2}{s(t)}. \tag{A.17}$$

If we now integrate with respect to t between the two limits $-\sqrt{A_2/B_2}$ and $\sqrt{A_2/B_2}$ we have that

$$\int \frac{\mathrm{d}t}{(t-1)^2 s(t)} = -(B_1 + B_2) \int \frac{\mathrm{d}t}{(t-1)s(t)} + B_1 B_2 \int \frac{t^2 - 1}{s(t)}\, \mathrm{d}t. \tag{A.18}$$

We can now evaluate each of these integrals in turn, using any of the standard references mentioned above. We find that

$$\int \frac{\mathrm{d}t}{s(t)} = \frac{2}{\sqrt{A_1 B_2 + A_2 B_1}}\, K(m), \tag{A.19}$$

$$\int \frac{\mathrm{d}t}{(t-1)s(t)} = \frac{2B_2}{(A_2 - B_2)\sqrt{A_1 B_2 + A_2 B_1}}\, \Pi(n|m), \tag{A.20}$$

$$\int \frac{t^2 \mathrm{d}t}{s(t)} = \frac{2\sqrt{A_1 B_2 + A_2 B_1}}{B_1 B_2}\, E(m) - \frac{2A_1}{B_1\sqrt{A_1 B_2 + A_2 B_1}}\, K(m). \tag{A.21}$$

Here, we have introduced two new parameters known as the modulus, m, and characteristic, n, defined by

$$m = \frac{\lambda_1}{\lambda_1 - \lambda_2},\ n = \frac{1 + \lambda_1}{\lambda_1 - \lambda_2}. \tag{A.22}$$

We immediately verify that $0 \leq m < 1$ and $n < 0$ for all values of $a, b \in \mathbb{R}$. The three functions $K(m)$, $E(m)$ and $\Pi(n|m)$ defined in terms of these parameters are known as the complete elliptic integrals of the first, second and third kind respectively.

Substituting these integrals we derive the result

$$\begin{aligned}(\beta-\alpha)\sqrt{A_1B_2+A_2B_1}I &= (\alpha-\beta)^2(A_1B_2+A_2B_1)\ E(m)\\ &+\left[\alpha^2+b^2-B_2(\alpha-\beta)^2(A_1+B_1)\right]\ K(m)\\ &+\frac{(\alpha-\beta)B_2}{A_2-B_2}\left[2\alpha-(B_1+B_2)(\alpha-\beta)\right]\ \Pi(n|m).\end{aligned} \tag{A.23}$$

Surprisingly, this expression simplifies dramatically when rewriting each coefficient back in terms of λ_1 and λ_2. Using the two relationships $\lambda_1\lambda_2 = -b^2$ and $(1+\lambda_1)(1+\lambda_2) = a^2$, we get

$$\frac{I}{\sqrt{\lambda_2-\lambda_1}} = E(m) + (1-n)\ \Pi(n|m) - K(m). \tag{A.24}$$

It appears that this is a new result, certainly not appearing either in the definitive tabulated reference on elliptic integrals [Byrd and Friedman, 1954], nor is this result given when using any of the standard automatic integrators such as *Mathematica*.

Bibliography

Rafail V. Abramov and Andrew J. Majda. Discrete approximations with additional conserved quantities: Deterministic and statistical behavior. *Methods Appl. Anal*, 10(2):151–190, 2003.

M. Abramowitz and I. A. Stegun. *Handbook of Mathematical Functions: With Formulas, Graphs, and Mathematical Tables*. Applied mathematics series. Dover Publications, 1965. ISBN 9780486612720.

S. Y. Annenkov and V. I. Shrira. Numerical modelling of water-wave evolution based on the zakharov equation. *Journal of Fluid Mechanics*, 449:341–371, 2001. doi: 10.1017/S0022112001006139.

S. Y. Annenkov and V. I. Shrira. Role of non-resonant interactions in the evolution of nonlinear random water wave fields. *Journal of Fluid Mechanics*, 561:181–207, 2006a. ISSN 1469-7645. doi: 10.1017/S0022112006000632.

S. Y. Annenkov and V. I. Shrira. Direct numerical simulation of downshift and inverse cascade for water wave turbulence. *Phys. Rev. Lett.*, 96:204501, 2006b. doi: 10.1103/PhysRevLett.96.204501.

J. A. Armstrong, N. Bloembergen, J. Ducuing, and P. S. Pershan. Interactions between Light Waves in a Nonlinear Dielectric. *Phys. Rev.*, 127(6):1918–1939, 1962.

V. I.. Arnol'd and M. Levi. *Geometrical Methods in the Theory of Ordinary Differential Equations*. Grundlehren Der Mathematischen Wissenschaften. Springer-Verlag GmbH, 1988. ISBN 9780387966496.

V. I. Arnol'd, K. Vogtmann, and A. Weinstein. *Mathematical Methods of Classical Mechanics*. Graduate Texts in Mathematics. Springer, 1989. ISBN 9780387968902.

O. Babelon, D. Bernard, and M. Talon. *Introduction to Classical Integrable Systems*. Cambridge Monographs on Mathematical Physics. Cambridge University Press, 2003. ISBN 9780521822671.

A. M. Balk. A new invariant for rossby wave systems. *Physics Letters A*, 155(1):20 – 24, 1991. doi: 10.1016/0375-9601(91)90501-X.

A. M. Balk, S. V. Nazarenko, and V. E. Zakharov. New invariant for drift turbulence. *Physics Letters A*, 152:276 – 280, 1991. doi: 10.1016/0375-9601(91)90105-H.

Alexander M. Balk and Francois van Heerden. Conservation style of the extra invariant for rossby waves. *Physica D: Nonlinear Phenomena*, 223(1):109 – 120, 2006. doi: 10.1016/j.physd.2006.08.020.

F. K. Ball. Energy transfer between external and internal gravity waves. *Journal of Fluid Mechanics*, 19(03):465–478, 1964. doi: 10.1017/S0022112064001550.

P. P. Banerjee and A. Korpel. Subharmonic generation by resonant three-wave interaction of deep-water capillary waves. *Physics of Fluids*, 25(11):1938–1943, 1982. doi: 10.1063/1.863682.

J. Barrow-Green. *Poincaré and the Three Body Problem*. Number v. 2 in History of Mathematics, V. 11. American Mathematical Society, 1997. ISBN 9780821803677.

R. Beals and D. H. Sattinger. On the complete integrability of completely integrable systems. *Communcations in Mathematical Physics*, 138:409–436, 1991.

T. Brooke Benjamin. Impulse, flow force and variational principles. *IMA Journal of Applied Mathematics*, 32(1-3):3–68, 1984. doi: 10.1093/imamat/32.1-3.3.

Lucio Berrone and Hector Giacomini. Inverse jacobi multipliers. *Rendiconti del Circolo Matematico di Palermo*, 52:77–130, 2003. doi: 10.1007/BF02871926.

A. Bihlo. A tutorial on hamiltonian mechanics. Available online at ftp://ftp.meteo.physik.uni-muenchen.de/public/craig/bihlo_COSTMunich.pdf, 2011.

A. V. Bolsinov and A. T. A. Fomenko. *Integrable Hamiltonian Systems: Geometry, Topology, Classification*. Taylor & Francis Group, 2004. ISBN 9780415298056.

G. Boole. *A treatise on differential equations*. New York : Chelsea Pub. Co., 5th edition, 1959.

T. J. M. Boyd and J. G. Turner. Three- and four-wave interactions in plasmas. *Journal of Mathematical Physics*, 19(6):1403–1413, 1978. doi: 10.1063/1.523842.

Christopher S. Bretherton, Catherine Smith, and John M. Wallace. An intercomparison of methods for finding coupled patterns in climate data. *Journal of Climate*, 5(6):541–560, 1992.

F. P. Bretherton. Resonant interactions between waves. the case of discrete oscillations. *Journal of Fluid Mechanics*, 20(03):457–479, 1964. doi: 10.1017/S0022112064001355.

M. D. Bustamante and U. Hayat. Complete classification of discrete resonant Rossby/drift wave triads on periodic domains. *ArXiv e-prints*, 2012.

M. D. Bustamante and E. Kartashova. Effect of the dynamical phases on the nonlinear amplitudes' evolution. *Europhys. Lett.*, 85(3):34002, 2009a.

M. D. Bustamante and E. Kartashova. Dynamics of nonlinear resonances in hamiltonian systems. *Europhys. Lett.*, 85(1):14004, 2009b.

Miguel D. Bustamante and Sergio A. Hojman. Lagrangian structures, integrability and chaos for 3d dynamical equations. *Journal of Physics A: Mathematical and General*, 36(1):151, 2003.

Miguel D. Bustamante and Elena Kartashova. Resonance clustering in wave turbulent regimes: Integrable dynamics. *Communications in Computational Physics*, 10:1211–1240, 2011.

P. F. Byrd and M. D. Friedman. *Handbook of elliptic integrals for engineers and physicists*. Grundlehren der mathematischen Wissenschaften. Springer, 1954.

R. A. Cairns. The role of negative energy waves in some instabilities of parallel flows. *Journal of Fluid Mechanics*, 92(01):1–14, 1979. doi: 10.1017/S0022112079000495.

C. Chandre and J. C. Eilbeck. Does the existence of a lax pair imply integrability? Available online at http://www.cns.gatech.edu/people/chandre/Articles/Lax-Pair.pdf, 2002.

J. G. Charney. On the scale of atmospheric motions. *Geofys. Publ.*, 17:3–17, 1948.

Jule G. Charney and John G. DeVore. Multiple flow equilibria in the atmosphere and blocking. *Journal of the Atmospheric Sciences*, 36(7):1205–1216, 1979.

Jie Cheng, Russell Greiner, Jonathan Kelly, David Bell, and Weiru Liu. Learning bayesian networks from data: An information-theory based approach. *Artificial Intelligence*, 137:43 – 90, 2002. doi: 10.1016/S0004-3702(02)00191-1.

C. Connaughton, B. Nadiga, S. V. Nazarenko, and B. E. Quinn. Modulational instability of Rossby and drift waves and the generation of zonal jets. *J. Fluid Mech.*, 654:207–231, 2010.

Colm Connaughton, Sergey Nazarenko, and Andrei Pushkarev. Discreteness and quasiresonances in weak turbulence of capillary waves. *Phys. Rev. E*, 63:046306, 2001. doi: 10.1103/PhysRevE.63.046306.

A. Constantin and E. Kartashova. Effect of non-zero constant vorticity on the nonlinear resonances of capillary water waves. *EPL (Europhysics Letters)*, 86(2): 29001, 2009.

B. Coppi, M. N. Rosenbluth, and R. N. Sudan. Nonlinear interactions of positive and negative energy modes in rarefied plasmas (i). *Annals of Physics*, 55(2):207 – 247, 1969. doi: 10.1016/0003-4916(69)90178-X.

A. D. D. Craik. *Wave Interactions and Fluid Flows*. Cambridge Monographs on Mechanics and Applied Mathematics. Cambridge University Press, 1988. ISBN 9780521368292.

A. D. D. Craik and J. A. Adam. 'explosive' resonant wave interactions in a three-layer fluid flow. *Journal of Fluid Mechanics*, 92(01):15–33, 1979. doi: 10.1017/S0022112079000501.

Warren C. Cree and Gordon E. Swaters. On the topographic dephasing and amplitude modulation of nonlinear Rossby wave interactions. *Geophys. Astrophys. Fluid Dynamics*, 61:75–99, 1991.

G. A. Darbellay and I. Vajda. Estimation of the information by an adaptive partitioning of the observation space. *Information Theory, IEEE Transactions on*, 45 (4):1315 –1321, 1999. doi: 10.1109/18.761290.

Luo Dehai. Topographically forced three-wave quasi-resonant and non-resonant interactions among barotropic Rossby waves on an infinite beta-plane. *Advances in Atmospheric Sciences*, 15(1), 1998.

Petr Denissenko, Sergei Lukaschuk, and Sergey Nazarenko. Gravity wave turbulence in a laboratory flume. *Phys. Rev. Lett.*, 99:014501, 2007. doi: 10.1103/PhysRevLett.99.014501.

Qinghua Ding, Eric J. Steig, David S. Battisti, and Marcel Küttel. Winter warming in west antarctica caused by central tropical pacific warming. *Nature Geoscience*, 4:398–403, 2010.

Andreia Dionisio, Rui Menezes, and Diana A. Mendes. Mutual information: a measure of dependency for nonlinear time series. *Physica A: Statistical Mechanics and its Applications*, 344:326 – 329, 2004. doi: 10.1016/j.physa.2004.06.144.

DLMF. NIST Digital Library of Mathematical Functions. http://dlmf.nist.gov/, Release 1.0.5 of 2012-10-01, 2012. URL `http://dlmf.nist.gov/`. Online companion to Olver et al. [2010].

J. F. Donges, Y. Zou, N. Marwan, and J. Kurths. The backbone of the climate network. *EPL (Europhysics Letters)*, 87(4):48007, 2009a.

J. F. Donges, Y. Zou, N. Marwan, and J. Kurths. Complex networks in climate dynamics. *The European Physical Journal - Special Topics*, 174:157–179, 2009b. doi: 10.1140/epjst/e2009-01098-2.

A. I. Dyachenko, A. O. Korotkevich, and V. E. Zakharov. Decay of the Monochromatic Capillary Wave. *J. Exp. Theor. Phys. Lett.*, 77:477–481, 2003.

Riccardo Farneti. Coupled interannual rossby waves in a quasigeostrophic ocean–atmosphere model. *Journal of Physical Oceanography*, 37(5):1192–1214, 2007. doi: 10.1175/JPO3061.1.

Andreas Galka, Tohru Ozaki, Jorge Bayard, and Okito Yamashita. Whitening as a tool for estimating mutual information in spatiotemporal data sets. *Journal of Statistical Physics*, 124:1275–1315, 2006. doi: 10.1007/s10955-006-9131-x.

S. Galtier, S. V. Nazarenko, A. C. Newell, and A. Pouquet. Anisotropic turbulence of shear-alfvén waves. *The Astrophysical Journal Letters*, 564(1):L49, 2002.

Clifford S. Gardner. Korteweg-de vries equation and generalizations. iv. the korteweg-de vries equation as a hamiltonian system. *Journal of Mathematical Physics*, 12(8):1548–1551, 1971. doi: 10.1063/1.1665772.

Clifford S. Gardner, John M. Greene, Martin D. Kruskal, and Robert M. Miura. Korteweg-devries equation and generalizations. vi. methods for exact solution. *Communications on Pure and Applied Mathematics*, 27(1):97–133, 1974. doi: 10.1002/cpa.3160270108.

Boris Gershgorin, Yuri V. Lvov, and David Cai. Interactions of renormalized waves in thermalized fermi-pasta-ulam chains. *Phys. Rev. E*, 75:046603, 2007. doi: 10.1103/PhysRevE.75.046603.

A. E. Gill. The stability on planetary waves on an infinite beta-plane. *Geophys. Fluid Dyn.*, 6:29–47, 1974.

A. Gozolchiani, K. Yamasaki, O. Gazit, and S. Havlin. Pattern of climate network blinking links follows el niño events. *EPL (Europhysics Letters)*, 83(2):28005, 2008.

Izrail Solomonovich Gradshteĭn, Iosif Moiseevich Ryzhik, Alan Jeffrey, and Daniel Zwillinger. *Table of Integrals, Series, And Products*. Academic Press, 2007.

K.F. Graff. *Wave Motion in Elastic Solids*. Dover Books on Engineering Series. Dover Publ., 1975. ISBN 9780486667454.

C. W. Granger, E. Maasoumi, and J. Racine. A dependence metric for possibly nonlinear processes. *Journal of Time Series Analysis*, 25(5):649–669, 2004. doi: 10.1111/j.1467-9892.2004.01866.x.

H. L. Grant, R. W. Stewart, and A. Moilliet. Turbulence spectra from a tidal channel. *Journal of Fluid Mechanics*, 12(02):241–268, 1962. doi: 10.1017/S002211206200018X.

Joseph L. Hammack and Diane M. Henderson. Experiments on deep-water waves with two-dimensional surface patterns. *Journal of Offshore Mechanics and Arctic Engineering*, 125(1):48–53, 2003. doi: 10.1115/1.1537725.

Joseph L. Hammack, Diane M. Henderson, and Harvey Segur. Progressive waves with persistent two-dimensional surface patterns in deep water. *Journal of Fluid Mechanics*, 532:1–52, 2005. doi: 10.1017/S0022112005003733.

J. Harris, C. Connaughton, and M. D. Bustamante. Percolation transition in the kinematics of nonlinear resonance broadening in Charney-Hasegawa-Mima model of Rossby wave turbulence. *ArXiv e-prints*, 2012.

Jamie Harris, Miguel D. Bustamante, and Colm Connaughton. Externally forced triads of resonantly interacting waves: Boundedness and integrability properties. *Communications in Nonlinear Science and Numerical Simulation*, 17(12):4988–5006, 2012a. doi: dx.doi.org/10.1016/j.cnsns.2012.04.002.

Akira Hasegawa and Kunioki Mima. Pseudo-three-dimensional turbulence in magnetized nonuniform plasma. *Physics of Fluids*, 21(1):87–92, 1978. doi: 10.1063/1.862083.

K. Hasselmann. On the non-linear energy transfer in a gravity-wave spectrum part 1. general theory. *Journal of Fluid Mechanics*, 12(04):481–500, 1962. doi: 10.1017/S0022112062000373.

K. Hasselmann. A criterion for nonlinear wave stability. *Journal of Fluid Mechanics*, 30:737–739, 1967.

Andrew Mc C. Hogg, William K. Dewar, Peter D. Killworth, and Jeffrey R. Blundell. Decadal variability of the midlatitude climate system driven by the ocean circulation. *Journal of Climate*, 19(7):1149–1166, 2006. doi: 10.1175/JCLI3651.1.

S. A. Hojman. A new conservation law constructed without using either lagrangians or hamiltonians. *Journal of Physics A: Mathematical and General*, 25(7):L291, 1992.

W. Horton and A. Hasegawa. Quasi–two–dimensional dynamics of plasmas and fluids. *Chaos*, 4(2):227–251, 1994.

Aleks Jakulin and Ivan Bratko. Quantifying and visualizing attribute interactions. *CoRR*, cs.AI/0308002, 2003.

Peter A. E. M. Janssen. Nonlinear four-wave interactions and freak waves. *Journal of Physical Oceanography*, 33(863-884), 2003.

A. Jurkus and P. N. Robson. Saturation effects in a travelling-wave parametric amplifier. *Proceedings of the IEE - Part B: Electronic and Communication Engineering*, 107(32):119 –122, 1960. doi: 10.1049/pi-b-2.1960.0087.

B. Karasözen. Poisson integrators. *Mathematical and Computer Modelling*, 40(11–12):1225–1244, 2004. doi: 10.1016/j.mcm.2005.01.015.

E. Kartashova. Wave resonances in systems with discrete spectra. In V.E. Zakharov, editor, *Nonlinear Waves and Weak Turbulence*, volume 182 of *AMS Translations 2*, pages 95–130. American Mathematical Society, 1998.

E. Kartashova. Model of laminated wave turbulence. *JETP Letters*, 83:283–287, 2006. doi: 10.1134/S0021364006070058.

E. Kartashova. Exact and quasi-resonances in discrete water-wave turbulence. *Physical Review Letters*, 98(21):214502–4, 2007.

E. Kartashova. Discrete wave turbulence. *EPL (Europhysics Letters)*, 87(4):44001, 2009.

E. Kartashova and A. Kartashov. Laminated wave turbulence: generic algorithms II. *CiCP (Communications in Computational Physics)*, 2(4):783–794, 2007.

E. Kartashova and V. S. L'vov. Cluster dynamics of planetary waves. *EPL (Europhysics Letters)*, 83(5):50012, 2008.

E. Kartashova and V. Lvov. A model of intra-seasonal oscillations in the Earth atmosphere. *Physical Review Letters*, 98(19):198501–4, 2007.

E. Kartashova and G. Mayrhofer. Cluster formation in mesoscopic systems. *Physica A: Statistical Mechanics and its Applications*, 385(2):527 – 542, 2007. doi: 10.1016/j.physa.2007.07.035.

E. Kartashova and A. Shabat. Computable Integrability. Chapter 1: General notions and ideas. Technical Report 05-07, RISC Report Series, University of Linz, Austria, 2005.

E. Kartashova, V. Lvov, S. Nazarenko, and I. Procaccia. Towards a Theory of Discrete and Mesoscopic Wave Turbulence. Technical report, RISC Report Series, University of Linz, Austria, 2010.

D. Kaup. A perturbation expansion for the zakharov–shabat inverse scattering transform. *SIAM Journal on Applied Mathematics*, 31(1):121–133, 1976. doi: 10.1137/0131013.

Matt J Keeling and Ken T.D Eames. Networks and epidemic models. *Journal of The Royal Society Interface*, 2(4):295–307, 2005. doi: 10.1098/rsif.2005.0051.

C. G. Koop and L. G. Redekopp. The interaction of long and short internal gravity waves: theory and experiment. *Journal of Fluid Mechanics*, 111:367–409, 1981. doi: 10.1017/S0022112081002425.

Alexander Kraskov, Harald Stögbauer, and Peter Grassberger. Estimating mutual information. *Phys. Rev. E*, 69:066138, 2004. doi: 10.1103/PhysRevE.69.066138.

M. Kundu and D. Bauer. Nonlinear resonance absorption in the laser-cluster interaction. *Phys. Rev. Lett.*, 96:123401, 2006. doi: 10.1103/PhysRevLett.96.123401.

Tom Lachlan-Cope and William Connolley. Teleconnections between the tropical pacific and the amundsen-bellinghausens sea: Role of the el niòo/southern oscillation. *J. Geophys. Res.*, 111(D23):D23101, 2006. doi: 10.1029/2005JD006386.

Peter D. Lax. Integrals of nonlinear equations of evolution and solitary waves. *Communications on Pure and Applied Mathematics*, 21(5):467–490, 1968. doi: 10.1002/cpa.3160210503.

V. Lerichev and G. Reznik. Two-dimensional rossby soliton: an exact solution. *Rep. U.S.S.R. Acad. Sci*, 231(5):1077–1079, 1976.

M. Levi. Quasiperiodic motions in superquadratic time-periodic potentials. *Commun. Math. Phys.*, 143:43–83, 1991.

Yanguang (Charles) Li. A lax pair for the two dimensional euler equation. *Journal of Mathematical Physics*, 42(8):3552–3553, 2001. doi: 10.1063/1.1378305.

Yanguang (Charles) Li. Chaos in pdes and lax pairs of euler equations. *Acta Applicandae Mathematicae*, 77:181–214, 2003. doi: 10.1023/A:1024024001070.

Yanguang (Charles) Li. Ergodic isospectral theory of the lax pairs of euler equations with harmonic analysis flavour. *Proceedings of the American Mathematical Society*, 133(9):2681–2687, 2005.

M. S. Longuet-Higgins, A. E. Gill, and K. Kenyon. Resonant interactions between planetary waves [and discussion]. *Proceedings of the Royal Society of London. Series A. Mathematical and Physical Sciences*, 299(1456):120–144, 1967. doi: 10.1098/rspa.1967.0126.

J. C. Luke. A variational principle for a fluid with a free surface. *Journal of Fluid Mechanics*, 27(02):395–397, 1967. doi: 10.1017/S0022112067000412.

V. S. L'vov and S. Nazarenko. Discrete and mesoscopic regimes of finite-size wave turbulence. *Phys. Rev. E*, 82:056322, 2010. doi: 10.1103/PhysRevE.82.056322.

V. S. L'vov, Yu. L'vov, A. C. Newell, and V. Zakharov. Statistical description of acoustic turbulence. *Phys. Rev. E*, 56:390–405, 1997. doi: 10.1103/PhysRevE.56.390.

Yuri V. Lvov, Sergey Nazarenko, and Boris Pokorni. Discreteness and its effect on water-wave turbulence. *Physica D: Nonlinear Phenomena*, 218(1):24 – 35, 2006. ISSN 0167-2789. doi: 10.1016/j.physd.2006.04.003.

Yuri V. Lvov, Kurt L. Polzin, and Naoto Yokoyama. Resonant and near-resonant internal wave interactions. *Journal of Physical Oceanography*, 42(5):669–691, 2011. doi: 10.1175/2011JPO4129.1.

P. Lynch. Resonant Rossby Wave Triads and the Swinging Spring. *Bull. Am. Met. Soc.*, 84:605–616, 2003.

P. Lynch. On resonant Rossby-Haurwitz triads. *Tellus A*, 61(3):438–445, 2009.

P. Lynch and C. Houghton. Pulsation and precession of the resonant swinging spring. *Physica D*, 190(1-2):38 – 62, 2004.

Peter Lynch. Resonant motions of the three-dimensional elastic pendulum. *Intl. J. Nonlin. Mech*, 37:345–367, 2001.

Peter Lynch. Hamiltonian methods for geophysical fluid dynamics: An introduction. IMA, University of Minnesota, Preprint 1838, 2002.

Peter Lynch. Supplement to resonant rossby wave triads and the swinging spring. *Bulletin of the American Meteorological Society*, 84(5):616–616, 2003. doi: 10.1175/BAMS-84-5-Lynch.

D. J. C. MacKay. *Information Theory, Inference and Learning Algorithms*. Cambridge University Press, 2003. ISBN 9780521642989.

J.M. Manley and H.E. Rowe. Some general properties of nonlinear elements-part i. general energy relations. *Proc. IRE*, 44(7):904 –913, 1956.

S. L. Marcus, M. Ghil, and J. O. Dickey. The extratropical 40-day oscillation in the UCLA General Circulation Model. Part I: Atmospheric angular momentum. *Journal of the Atmospheric Sciences*, 51(11):1431 – 1446, 1994.

A. D. McEwan, D. W. Mander, and R. K. Smith. Forced resonant second-order interaction between damped internal waves. *Journal of Fluid Mechanics*, 55(4): 589–608, 1972.

Lawrence F. McGoldrick. Resonant interactions among capillary-gravity waves. *Journal of Fluid Mechanics*, 21(02):305–331, 1965. doi: 10.1017/S0022112065000198.

Lawrence F. McGoldrick. An experiment on second-order capillary gravity resonant wave interactions. *Journal of Fluid Mechanics*, 40(02):251–271, 1970. doi: 10.1017/S0022112070000162.

Robert I. McLachlan. Explicit lie-poisson integration and the euler equations. *Phys. Rev. Lett.*, 71:3043–3046, 1993. doi: 10.1103/PhysRevLett.71.3043.

C. R. Menyuk, H. H. Chen, and Y. C. Lee. Integrable hamiltonian systems and the lax pair formalism. *Phys. Rev. A*, 26:3731–3733, 1982. doi: 10.1103/PhysRevA.26.3731.

Paul A. Milewski, Esteban G. Tabak, and Eric Vanden-Eijnden. Resonant wave interaction with random forcing and dissipation. *Studies in Applied Mathematics*, 108(1):123–144, 2002. doi: 10.1111/1467-9590.01427.

Robert M. Miura, Clifford S. Gardner, and Martin D. Kruskal. Korteweg-de vries equation and generalizations. ii. existence of conservation laws and constants of motion. *Journal of Mathematical Physics*, 9(8):1204–1209, 1968. doi: 10.1063/1.1664701.

R. Moddemeijer. A statistic to estimate the variance of the histogram-based mutual information estimator based on dependent pairs of observations. *Signal Processing*, 75(1):51 – 63, 1999. doi: 10.1016/S0165-1684(98)00224-2.

Young-Il Moon, Balaji Rajagopalan, and Upmanu Lall. Estimation of mutual information using kernel density estimators. *Phys. Rev. E*, 52:2318–2321, 1995. doi: 10.1103/PhysRevE.52.2318.

Nobuhito Mori and Peter A. E. M. Janssen. On kurtosis and occurrence probability of freak waves. *Journal of Physical Oceanography*, 36(7):1471–1483, 2006. doi: 10.1175/JPO2922.1.

P. J. Morrison. Poisson brackets for fluids and plasmas. *Mathematical Methods in Hydrodynamics and Integrability in Dynamical Systems*, 1982.

P. J. Morrison. Hamiltonian description of the ideal fluid. *Rev. Mod. Phys.*, 70: 467–521, 1998. doi: 10.1103/RevModPhys.70.467.

Philip J. Morrison and John M. Greene. Noncanonical hamiltonian density formulation of hydrodynamics and ideal magnetohydrodynamics. *Phys. Rev. Lett.*, 45: 790–794, 1980. doi: 10.1103/PhysRevLett.45.790.

J Moser. Three integrable hamiltonian systems connected with isospectral deformations. *Advances in Mathematics*, 16(2):197 – 220, 1975. doi: 10.1016/0001-8708(75)90151-6.

S. Nazarenko. *Wave Turbulence*. Lecture Notes in Physics. Springer, 2011. ISBN 9783642159411.

S. Nazarenko and B. Quinn. Triple cascade behaviour in quasigeostrophic and drift turbulence and generation of zonal jets. *Phys. Rev. Lett.*, 103, 2009.

Sergey Nazarenko. Sandpile behaviour in discrete water-wave turbulence. *Journal of Statistical Mechanics: Theory and Experiment*, 2006(02):L02002, 2006.

Sergey Nazarenko. 2D enslaving of MHD turbulence. *New Journal of Physics*, 9(8): 307, 2007.

A. C. Newell and B. Rumpf. Wave turbulence. *Ann. Rev. Fluid Mech.*, 43(1):59–78, 2011.

M. E. J. Newman, D. J. Watts, and S. H. Strogatz. Random graph models of social networks. *Proceedings of the National Academy of Sciences of the United States of America*, 99(Suppl 1):2566–2572, 2002. doi: 10.1073/pnas.012582999.

R. W. D. Nickalls. Viète, descartes and the cubic equation. *The Mathematical Gazette*, 90(518):203–208, 2006.

R. W. D. Nickalls. The quartic equation: invariants and euler's solution revealed. *The Mathematical Gazette*, 93(526):66–75, 2009.

M. C. Nucci and P. G. L. Leach. The Jacobi last multiplier and its applications in mechanics. *Physica Scripta*, 78(6):065011, 2008.

F. W. J. Olver, D. W. Lozier, R. F. Boisvert, and C. W. Clark, editors. *NIST Handbook of Mathematical Functions*. Cambridge University Press, New York, NY, 2010. Print companion to DLMF.

J. Pedlosky. *Geophysical fluid dynamics, 2nd Ed.* Springer, New York, 1987.

B. Pelloni and D. A. Pinotsis. Boundary value problems for the n-wave interaction equations. *Physics Letters A*, 373(22):1940 – 1950, 2009. doi: 10.1016/j.physleta.2009.03.064.

O. M. Phillips. On the dynamics of unsteady gravity waves of finite amplitude part 1. the elementary interactions. *Journal of Fluid Mechanics*, 9(02):193–217, 1960. doi: 10.1017/S0022112060001043.

R. W. Preisendorfer and C. D. Mobley. *Principal component analysis in meteorology and oceanography*. Developments in atmospheric science. Elsevier, 1988. ISBN 9780444430144.

A. N. Pushkarev. On the kolmogorov and frozen turbulence in numerical simulation of capillary waves. *European Journal of Mechanics - B/Fluids*, 18(3):345 – 351, 1999. doi: 10.1016/S0997-7546(99)80032-6.

A. N. Pushkarev and V. E. Zakharov. Turbulence of capillary waves - theory and numerical simulation. *Physica D: Nonlinear Phenomena*, 135:98 – 116, 2000. doi: 10.1016/S0167-2789(99)00069-X.

Carlos F. M. Raupp and Pedro L. Silva Dias. Resonant wave interactions in the presence of a diurnally varying heat source. *Journal of the Atmospheric Sciences*, 66:3165–3183, 2009.

P. Ripa. On the theory of nonlinear wave-wave interactions among geophysical waves. *Journal of Fluid Mechanics*, 103:87–115, 1981. doi: 10.1017/S0022112081001250.

C. G. Rossby. Relation between variations in the intensity of the zonal circulation of the atmosphere and the displacements of the semi-permanent centers of action. *Journal of Marine Research*, 2(1):38–55, 1939.

R. Salmon. Hamiltonian fluid mechanics. *Ann. Rev. Fluid Mech.*, 20:225–56, 1988.

M. H. Santoso, A.and England. Antarctic intermediate water circulation and variability in a coupled climate model. *Journal of Physical Oceanography*, 34(10): 2160–2179, 2004.

R. L. Seliger and G. B. Whitham. Variational principles in continuum mechanics. *Proceedings of the Royal Society of London. Series A. Mathematical and Physical Sciences*, 305(1480):1–25, 1968. doi: 10.1098/rspa.1968.0103.

Lou Sen-Yue and Li Yi-Shen. Exact solutions of (2+1)-dimensional euler equation found by weak darboux transformation. *Chinese Physics Letters*, 23(10):2633, 2006.

Theodore G. Shepherd. Symmetries, conservation laws, and hamiltonian structure in geophysical fluid dynamics. *Advances in Geophysics*, 32:287 – 338, 1990. doi: 10.1016/S0065-2687(08)60429-X.

T. Shinoda, G. N. Kiladis, and P. E. Roundy. Statistical representation of equatorial waves and tropical instability waves in the pacific ocean. *Atmospheric Research*, pages 27–44, 2009.

W. F. Simmons. A variational method for weak resonant wave interactions. *Proceedings of the Royal Society of London. A. Mathematical and Physical Sciences*, 309(1499):551–577, 1969. doi: 10.1098/rspa.1969.0056.

L. M. Smith and F. Waleffe. Transfer of energy to two-dimensional large scales in forced, rotating three-dimensional turbulence. *Physics of Fluids*, 11(6):1608 – 1622, 1999.

Masakazu Sueyoshi and Takahiro Iwayama. Hamiltonian structure for the charney-hasegawa-mima equation in the asymptotic model regime. *Fluid Dynamics Research*, 39(4):346 – 352, 2007. doi: 10.1016/j.fluiddyn.2006.11.002.

G. E. Swaters. *Introduction to Hamiltonian Fluid Dynamics and Stability Theory*. Chapman & Hall/CRC Monographs and Surveys in Pure and Applied Mathematics. Taylor & Francis, 1999. ISBN 9781584880233.

Mitsuhiro Tanaka and Naoto Yokoyama. Effects of discretization of the spectrum in water-wave turbulence. *Fluid Dynamics Research*, 34(3):199, 2004.

A. A. Tsonis and P. J. Roebber. The architecture of the climate network. *Physica A: Statistical Mechanics and its Applications*, 333(0):497 – 504, 2004. doi: 10.1016/j.physa.2003.10.045.

Anastasios A. Tsonis and Kyle L. Swanson. Topology and predictability of el niño and la niña networks. *Phys. Rev. Lett.*, 100:228502, 2008. doi: 10.1103/PhysRevLett.100.228502.

Anastasios A. Tsonis, Kyle L. Swanson, and Paul J. Roebber. What do networks have to do with climate? *Bulletin of the American Meteorological Society*, 87(5): 585–595, 2006. doi: 10.1175/BAMS-87-5-585.

Anastasios A. Tsonis, Kyle L. Swanson, and Geli Wang. On the role of atmospheric teleconnections in climate. *Journal of Climate*, 21(12):2990–3001, 2008. doi: 10.1175/2007JCLI1907.1.

G. K. Vallis. *Atmospheric and Oceanic Fluid Dynamics*. Cambridge University Press, Cambridge, U.K., 2006.

M. A. Virasoro. Variational principle for two-dimensional incompressible hydrodynamics and quasigeostrophic flows. *Phys. Rev. Lett.*, 47:1181–1183, 1981. doi: 10.1103/PhysRevLett.47.1181.

Y. Wakata. Frequency-wavenumber spectra of equatorial waves detected from satellite altimeter data. *Journal of Oceanography*, 63:483 – 490, 2007.

Satosi Watanabe. Information theoretical analysis of multivariate correlation. *IBM Journal of Research and Development*, 4(1):66 –82, 1960. ISSN 0018-8646. doi: 10.1147/rd.41.0066.

Alan Weinstein. Hamiltonian structure for drift waves and geostrophic flow. *Physics of Fluids*, 26(2):388–390, 1983. doi: 10.1063/1.864174.

M. Wheeler and G. N. Kiladis. Convectively coupled equatorial waves: Analysis of clouds and temperature in the wavenumber–frequency domain. *Journal of the Atmospheric Sciences*, 56(3):374 – 399, 1999.

Warren B. White. Coupled rossby waves in the indian ocean on interannual timescales. *Journal of Physical Oceanography*, 30(11):2972–2988, 2000.

G. B. Whitham. A general approach to linear and non-linear dispersive waves using a lagrangian. *Journal of Fluid Mechanics*, 22(02):273–283, 1965. doi: 10.1017/S0022112065000745.

G.B. Whitham. *Linear and nonlinear waves*. Pure and applied mathematics. Wiley, 1974. ISBN 9780471359425.

Hu Xiao-Rui and Chen Yong. Bäcklund transformations and explicit solutions of (2+1)-dimensional barotropic and quasi-geostrophic potential vorticity equation. *Communications in Theoretical Physics*, 53(5):803, 2010.

Haijun Yang, Zhengyu Liu, and Qiong Zhang. Tropical ocean decadal variability and resonance of planetary wave basin modes. part ii: Numerical study. *Journal of Climate*, 17(8):1711–1721, 2004.

V. E. Zakharov and L. D. Faddeev. Korteweg-de vries equation: A completely integrable hamiltonian system. *Functional Analysis and Its Applications*, 5:280–287, 1971. doi: 10.1007/BF01086739.

V. E. Zakharov and N. N. Filonenko. Energy spectrum for stochastic oscillations of the surface of a liquid. *Soviet Physics Doklady*, 11:881, 1967.

V. E. Zakharov and S. V. Manakov. Resonant interaction of wave packets in nonlinear media. *Soviet Journal of Experimental and Theoretical Physics Letters*, 18: 243, 1973.

V. E. Zakharov and S. V. Manakov. The theory of resonance interaction of wave packets in nonlinear media. *Soviet Journal of Experimental and Theoretical Physics*, 42:842, 1975.

V. E. Zakharov, V. S. L'vov, and G. Falkovich. *Kolmogorov Spectra of Turbulence*. Springer-Verlag, Berlin, 1992.

V. E. Zakharov, A. Korotkevich, A. Pushkarev, and A. Dyachenko. Mesoscopic wave turbulence. *JETP Letters*, 82:487–491, 2005. doi: 10.1134/1.2150867.

V. Zeitlin. Finite-mode analogs of 2d ideal hydrodynamics: Coadjoint orbits and local canonical structure. *Physica D: Nonlinear Phenomena*, 49(3):353 – 362, 1991. doi: 10.1016/0167-2789(91)90152-Y.